OPEN ACCESS

ORIGINAL RESEARCH

Inhibition of G-protein signalling in cardiac dysfunction of intellectual developmental disorder with cardiac arrhythmia (IDDCA) syndrome

Pasquelena De Nittis ,[1] Stephanie Efthymiou,[2] Alexandre Sarre,[3] Nicolas Guex,[4] Jacqueline Chrast,[1] Audrey Putoux,[5] Tipu Sultan,[6] Javeria Raza Alvi,[6] Zia ur Rahman,[6] Faisal Zafar,[7] Nuzhat Rana,[7] Fatima Rahman,[8] Najwa Anwar,[8] Shazia Maqbool,[8] Maha S Zaki ,[9] Joseph G Gleeson ,[10] David Murphy,[2] Hamid Galehdari,[11] Gholamreza Shariati,[12] Neda Mazaheri,[11] Alireza Sedaghat,[13] SYNAPS Study Group, Gaetan Lesca,[14] Nicolas Chatron,[1,14] Vincenzo Salpietro,[2] Marilena Christoforou,[2] Henry Houlden,[2] William F Simonds,[15] Thierry Pedrazzini,[16] Reza Maroofian,[2] Alexandre Reymond[1]

► Additional material is published online only. To view, please visit the journal online (http://dx.doi.org/10.1136/jmedgenet-2020-107015).

For numbered affiliations see end of article.

Correspondence to
Professor Alexandre Reymond, Center for Integrative Genomics, University of Lausanne, Lausanne 1015, Switzerland; alexandre.reymond@unil.ch

Received 19 March 2020
Revised 30 August 2020
Accepted 4 September 2020

To cite: De Nittis P, Efthymiou S, Sarre A, *et al*. *J Med Genet* Epub ahead of print: [please include Day Month Year]. doi:10.1136/jmedgenet-2020-107015

ABSTRACT

Background Pathogenic variants of *GNB5* encoding the β_5 subunit of the guanine nucleotide-binding protein cause IDDCA syndrome, an autosomal recessive neurodevelopmental disorder associated with cognitive disability and cardiac arrhythmia, particularly severe bradycardia.

Methods We used echocardiography and telemetric ECG recordings to investigate consequences of *Gnb5* loss in mouse.

Results We delineated a key role of *Gnb5* in heart sinus conduction and showed that *Gnb5*-inhibitory signalling is essential for parasympathetic control of heart rate (HR) and maintenance of the sympathovagal balance. $Gnb5^{-/-}$ mice were smaller and had a smaller heart than $Gnb5^{+/+}$ and $Gnb5^{+/-}$, but exhibited better cardiac function. Lower autonomic nervous system modulation through diminished parasympathetic control and greater sympathetic regulation resulted in a higher baseline HR in $Gnb5^{-/-}$ mice. In contrast, $Gnb5^{-/-}$ mice exhibited profound bradycardia on treatment with carbachol, while sympathetic modulation of the cardiac stimulation was not altered. Concordantly, transcriptome study pinpointed altered expression of genes involved in cardiac muscle contractility in atria and ventricles of knocked-out mice. Homozygous *Gnb5* loss resulted in significantly higher frequencies of sinus arrhythmias. Moreover, we described 13 affected individuals, increasing the IDDCA cohort to 44 patients.

Conclusions Our data demonstrate that loss of negative regulation of the inhibitory G-protein signalling causes HR perturbations in $Gnb5^{-/-}$ mice, an effect mainly driven by impaired parasympathetic activity. We anticipate that unravelling the mechanism of *Gnb5* signalling in the autonomic control of the heart will pave the way for future drug screening.

INTRODUCTION

Intellectual developmental disorder with cardiac arrhythmia (IDDCA, OMIM (Online Mendelian Inheritance in Man): #617173) is an autosomal recessive neurodevelopmental disorder with onset in early childhood. Inactivating and hypomorphic mutations in the β_5 subunit of guanine nucleotide-binding protein (*GNB5*), respectively, cause severe and mild forms of the disorder.[1] The former is associated with cognitive disability, poor or absent speech and/or severe cardiac arrhythmias. The moderate manifestation of the syndrome, also named language delay and ADHD/cognitive impairment with or without cardiac arrhythmia (LADCI) syndrome (OMIM: #617182), consists of mild intellectual impairment, language delay, attention deficit hyperactivity disorder (ADHD) and, in about half the cases, severe cardiac arrhythmia.[1 2] Some patients with IDDCA also showed retinal dysfunction and nystagmus, epilepsy, hypotonia and gastrointestinal problems.[1–10] The *GNB5* retinopathy is a unique combination of dual retinal signalling defects reminiscent of features of both bradyopsia and rod ON-bipolar dysfunction,[5] while the IDDCA epilepsy is characterised by early seizure onset (~3 months of age) with focal seizures rapidly evolving into epileptic spasms and consequent generalised multifocal discharges.[4]

The heart rate (HR) is established by the sinoatrial node, the pacemaker of the cardiac muscle, and controlled by the autonomic nervous system. This autonomic nervous system consists of two anatomically and functionally distinct divisions: the sympathetic and the parasympathetic branches, whose functions are often antagonistic but work together to maintain balance. In the heart, the postganglionic fibres of the sympathetic trunk stimulate the β-adrenoreceptors, thereby increasing HR and force of contraction. The parasympathetic modulation of the heart is primarily mediated by acetylcholine release, which activates the M_2-muscarinic receptors (M_2R) present on cells innervated by parasympathetic postganglionic neurons, including sinoatrial node cells. The activation of M_2R triggers $G_{i/o}$ subfamily G-proteins, which turn on G-protein-gated

inwardly rectifying K^+ channels (GIRK) resulting in membrane hyperpolarisation and decrease in HR. Regulator of G-protein signalling (RGS) proteins negatively regulate the timing of this M_2R-GIRK signalling. GNB5, a divergent member of the Gβ family, has the unique property of forming complexes with R7-RGS proteins.[11–16] In particular, the GNB5-RGS6 complex is involved in cardiac GIRK deactivation kinetics. *Rgs6*-null mice manifested heart conduction anomalies and hypersensitivity to parasympathomimetics.[17] Zebrafish model defective for *gnb5* gene correspondingly showed reduced heartbeat on reinforced parasympathetic stimulation, eye movement defects and altered swimming behaviour[1] and cardiomyocytes differentiated from human induced pluripotent stem cells (iPSCs) edited to engineer the GNB5-Ser81Leu missense variant associated with LADCI showed a decrease in spontaneous activity on stimulation with carbachol compared with normal cells.[7]

Whereas homozygous *Gnb5*-null mice recapitulated many of the corresponding human disease phenotypes such as learning deficiencies, hyperactivity, impaired motor coordination and perturbed vision,[18–22] a systematic cardiac evaluation has never been performed in a mammalian model. Here, we assessed heart electrophysiology of *Gnb5* mice models. We detected an increased frequency of sinus arrhythmias in $Gnb5^{-/-}$ animals, which have a smaller heart than wild-type and $Gnb5^{+/-}$, but exhibited better cardiac function. $Gnb5^{-/-}$ mice also displayed enhanced parasympathetic sensitivity on stimulation with a cholinergic agonist. Consistent with this, transcriptome profiling of atria and ventricles revealed overexpression of genes involved in cardiac muscle contractility, along with reduced ventricular expression of genes required for development of pacemaker cells in $Gnb5^{-/-}$ mice. Finally, we expanded the number of ascertained IDDCA individuals and the *GNB5* mutational spectrum.

MATERIALS AND METHODS

Enrolment

All affected individuals and their family members were recruited in Pakistan (families R–V), France (family W), Egypt (families X and Y) and Iran (family Z) after signing a written informed consent according to ethical review boards policies. Clinical ascertainment included physical examinations, medical history interviews and specialised consultations by a certified neurologist and cardiologist as appropriate. Venous blood was collected in EDTA for DNA extraction according to standard procedures.

Exome sequencing

Whole-exome sequencing of families R–V and Z was performed by Macrogen, Korea, as described in reference.[23] Briefly, target enrichment was performed with 2 µg genomic DNA using the SureSelectXT Human All Exon Kit version 6 (Agilent Technologies, Santa Clara, California, USA) to generate barcoded whole-exome sequencing libraries. Libraries were sequenced on the HiSeqX platform (Illumina, San Diego, California, USA) with 50× coverage. Quality assessment of the sequence reads was performed by generating QC statistics with FastQC.[24] The filtering strategy included screening for only exonic and donor/acceptor splicing variants. In accordance with the pedigree and phenotype, priority was given to variants rare or absent in public databases (1000 Genomes project, National Heart, Lung, and Blood Institute Exome Variant Server, Complete Genomics 69 and Exome Aggregation Consortium V.0.2).

Trio exome sequencing was performed in proband 37 (family W) and her parents using SeqCap EZ Medexome library preparation kit following manufacturer's recommendations (Roche, Indiana, Indianapolis, USA). Libraries were sequenced on a NextSeq500 (Illumina) at a mean depth coverage of 73× with 93.3% of the target bases above 30×. Genomic alignment against the hg19/GRCh37 assembly and variant calling were, respectively, done with BWAMEM V.0.7.12 and GATK HaplotypeCaller V.3.4 (Broad Institute, Boston, Massachusetts, USA). Only highly confident variants were kept for analysis (total depth >9, alternative allele depth >4, no strand bias, mosaicism >10%). Rare variants were considered as having a frequency of <1% in GnomAD v2 dataset. Whole-exome sequencing of families X and Y was performed as described in Makrythanasis *et al*.[25] Sanger sequencing in each family confirmed the segregation of *GNB5* variants with the phenotype.

Mouse husbandry

The *Gnb5* mouse line was recovered from cryopreserved sperm using in vitro fertilisation. The knockout allele was engineered in a C57BL/6J inbred genetic background by heterozygous deletion of exon 3 in the germline, as previously described.[18 22] Genetically modified animals were born and housed in the Animal Facility of the Centre for Integrative Genomics, under controlled temperature conditions and a 12-hour light–dark cycle with free access to water, normal chow and nest building material. Mouse genomic DNA was extracted from ear biopsies using the hot shot protocol[26] and used for genotyping as described.[22] To prevent the previously documented high mortality of $Gnb5^{-/-}$ pups at weaning,[18] heterozygous breeding couples used to obtain knockout pups were given breeding food pellet enriched for proteins and vitamins (Kliba 3336, extrudate). Additionally, litters including $Gnb5^{-/-}$ pups were fed from 14 to 28 days of age, that is, starting 1 week before weaning, with powdered wet maintenance food (Kliba 3436) in a Petri dish placed directly onto the floor of the cages, an expedient that should provide easier access to the food for the pups.

In vivo transthoracic ultrasound imaging protocol

Transthoracic echocardiography was performed using a 30 MHz probe and the Vevo 2100 Ultrasound machine (VisualSonics, Toronto, Ontario, Canada). A light anaesthesia was achieved with 1%–1.5% isoflurane, maintaining HR at 400–500 beats/min. The mice were placed in decubitus dorsal on a heated 37°C platform to maintain body temperature. The heart was imaged in the 2D mode in the parasternal long-axis view. From this view, an M-mode cursor was positioned perpendicular to the interventricular septum and the posterior wall of the left ventricle, at the level of the papillary muscles. Diastolic and systolic interventricular septa, left ventricular posterior wall thickness and left ventricular internal end-diastolic and end-systolic chamber dimensions were measured. Three separate M-mode images were measured and averaged. Left ventricular fractional shortening and ejection fraction were also calculated. Fractional shortening and ejection fraction were assessed from M-mode based on the percentage changes of left ventricular end-diastolic and end-systolic diameters and volumes, respectively. We used male mice at 9 weeks of age of three different genotypes ($Gnb5^{+/+}$, $Gnb5^{+/-}$ and $Gnb5^{-/-}$).

In vivo electrocardiography measurements

For in vivo electrocardiography monitoring we have subcutaneously implanted biopotential telemetric transponders (ETA-F10, Data Sciences International) allowing continuous monitoring in conscious freely moving animals at 12 weeks of age. The negative electrode was implanted at the top of the right pectoral

muscle, and the positive one was anchored at the level of the last left rib (at about 1 cm of the xiphoid appendix), thus leading to a normal lead II trace. Baseline ECG was recorded 10 days after device implantation, over a period of 86 hours. After 30 min of basal measurements, we injected mice with 0.9% saline solution (intraperitoneal NaCl, 10 mL/kg) as a vehicle control; next, the following compounds were administered one at a time: atropine (PubChem CID: 174174, intraperitoneal, 1 mg/kg), carbachol (PubChem CID: 5831, intraperitoneal 0.1 mg/kg) and in a subset of mice isoprenaline (PubChem CID: 3779, intraperitoneal 4 mg/kg) and atenolol (PubChem CID: 2249, intraperitoneal 2 mg/kg) as well, with a one night interval between each injection. The amounts of isoprenaline and atenolol were chosen after testing 10 doses ranging from 4 µg/kg to 4 mg/kg and 2 µg/kg to 2 mg/kg, respectively. While atropine and carbachol respectively inhibit and activate the parasympathetic system atenolol and isoprenaline respectively block and promote the sympathetic response.

At the end of the experiment, mice were sacrificed by CO_2 inhalation; the heart was digitally imaged both within its thoracic position and after excision. Heart weight was recorded and tibia length was measured to normalise the heart weight to body size. Images were taken by a Leica DCF295 digital colour camera with 3M pixels mounted on a MZ6 stereomiscroscope (Leica, Switzerland). The length of the tibia was measured using a precision calliper after removal from the left leg (without patella nor articular cartilage).

Baseline ECG traces were analysed as follows: 10 min of recording were analysed using ECG-Auto software in shape recognition mode (EMKA Technology, France) every 30 min, during night and day phases. Mean values were reported for each analysed parameter. During pharmacological challenges, ECG recording was analysed continuously, with 10 min steps; thus, one mean of each parameter was calculated every 10 min. On ECG traces we analysed: (1) RR interval (measured at R peak, expressed in millisecond; (2) HR: heart beating rate, calculated as 60/(RR/1000), expressed in beats/min; (3) PR interval (interval between beginning of P wave and R peak, expressed in millisecond); (4) QT duration: duration of the QT complex; (5) QTc (corrected QT, calculated from QT/√(RR/100)[27] (all expressed in millisecond) that allows correction of QT from HR variations).

Temperature and activity were also recorded. Activity was estimated by displacement of the telemetric device from the antennas of the recording plate. This measurement was only used as a qualitative index of mouse activity/movement. Temperature and activity values are mean values of 1-hour interval.

Time-domain heart rate variation (HRV) analysis

Twelve-hour segments of day/night phases were selected from the baseline recording period and analysed separately for the HRV analysis. Specifically, R wave detection was performed and R-R interval time series were obtained. To ensure inclusion of sinus beats only, values not included between R–R intervals±2 SD were excluded as reported in Thireau *et al*.[28] The analysed time-domain HRV parameters, computed using Kubios HRV Standard software V. 3.2.0, were: (1) mean R–R intervals (NN, in millisecond); (2) SD of all normal R–R intervals (SDNN, in millisecond); (3) square root of the mean square differences (RMSSD) between successive normal intervals (in millisecond); and (4) percentage of normal consecutive R–R intervals differing by >*x*ms (pNNx, in %, in this study x=6 ms).

Arrhythmia assessment

Arrhythmias were identified based on ECG trace (RR interval) and counted. Observed arrhythmias were defined as follows: (1) escape atrial beat, with a P wave morphology different from that of the sinus P wave, classified as 'long' and 'short' according to the location of the P wave on the ECG trace (specifically, long was an escape beat whose duration was longer than two normal PP intervals, and short were those escape beats that lasted less than two normal PP intervals); (2) atrioventricular block defined on ECG by more than one P wave for one QRS complex; (3) premature beats; and (4) episodes of tachycardia followed by bradycardia, with HR oscillation between high and low values within a few seconds, independently of other type of arrhythmias.

Statistical tests

Each parameter measured was reported as mean±SD. Standard t-test was used to assess differences between two groups. Analysis of variance tests, followed by Tukey post hoc tests, were also calculated and are displayed. A p value of <0.05 was considered significant, and stars on the plots represent the level of significance (*p≤0.05, **p≤0.01, ***p≤0.001, ****p≤0.0001; p>0.05 was considered not significant).

Transcriptome profiling, data processing and differential expression analysis

A total of 72 RNA sequencing libraries were generated from two heart tissues, atria and ventricles, and three brain regions, cerebellum, hippocampus and cerebral cortex. Both the entire ventricles (left and right) or atria (left and right) were used for the sample processing; therefore, the atrial tissue represents a mixture of heart muscle cells, as well as sinoatrial and atrioventricular cells. The whole cerebellum, the hippocampi from each hemisphere of the brain and the whole cerebral cortex were dissected for RNA extraction. For this experiment, we created a cohort of adult (18 weeks) male mice including 6 *Gnb5*$^{-/-}$, 6 *Gnb5*$^{+/-}$ and 6 *Gnb5*$^{+/+}$ animals. Brain transcriptome was only assessed in *Gnb5*$^{-/-}$ and *Gnb5*$^{+/+}$ animals. Tissue collection and processing procedures were designed to minimise biological and technical variation. Specifically, tissues were dissociated in QIAzol Lysis Reagent (Qiagen) using the gentleMACS Dissociator (Miltenyi Biotec). Cell suspension was used to obtain total RNA. Genomic DNA contamination was removed by digestion with RNase-free Deoxyribonuclease I (Qiagen). RNA concentration and purity were measured by ND-1000 spectrophotometer (Thermo Scientific, Wilmington, North Carolina, USA), and RNA integrity was verified by fragment analyser automated CE system (Advanced Analytical Technologies) according to manufacturer's instructions. Libraries were then prepared with TruSeq Stranded RNA Library Prep Kit (Illumina) and sequenced on multiple lanes of an Illumina HiSeq4000 platform, generating an average of 50M single-end 125-cycle reads for each sample. Quality of sequence was assessed by FastQC V.0.11.4.[24] Purity-filtered reads were adapters-trimmed and quality- trimmed with Cutadapt V.1.8.[29] Reads matching to ribosomal RNA sequences were removed with fastq_screen V.0.11.1. Remaining reads were further filtered for low complexity with reaper V.15–065.[30] Reads were then aligned against *Mus Musculus. GRCm38.92* genome using STAR V.2.5.3a.[31] The number of read counts per gene locus was summarised with htseq-count V.0.9.1[32] using *Mus Musculus.GRCm38.92* gene annotations. Quality of the RNA-seq data alignment was assessed using RSeQC V. 2.3.7.[33] Reads were also aligned to the *Mus Musculus.GRCm38.92* transcriptome using STAR V. 2.5.3a,[31] and the estimation of the isoforms abundance was computed using RSEM V.1.2.31.[34] To assess differential expression between genotypes within each tissue, we compared

Table 1 Overlapping clinical features of individuals with IDDCA and LADCI syndromes

	Individuals with phenotype/ individuals (total n)	Phenotype severity (IDDCA)	Phenotype severity (LADCI)	Phenotype severity (intermediate)
Gender	23F, 21M	15F, 19M	7F, 2M	1F
Clinical examination				
Dysmorphic features	11/44 (25%)	10/34	–	1/1
Congenital malformations	4/44 (9%)	4/34 (heart)	–	–
Neurological manifestations				
Intellectual disability	37/44 (84%)	32/34	4/9	1/1
Speech delay	34/44 (77%)	27/34	6/9	1/1
Hypotonia	33/44 (75%)	29/34	3/9	1/1
Seizures	25/44 (57%)	25/34	–	–
Behavioural disorders	6/44 (14%)	3/34 (ASD)	3/9 (ADHD)	–
MRI anomalies	8/44 (18%)	8/34	–	–
Sleep disturbance	2/44 (5%)	2/34	–	–
Cardiac manifestations				
Sinus sick syndrome	27/44 (61%)	22/34	4/9	1/1
Pacemaker implantation	6/44 (14%)	4/34	1/9	1/1
Ophthalmological findings				
Nystagmus	26/44 (59%)	26/34	–	–
Strabismus	6/44 (14%)	5/34	–	1/1
Retinal disease	14/44 (32%)	14/34	–	–
Gastrointestinal problems				
Pathological gastric reflux	18/44 (41%)	18/34	–	–

Pedigree charts and variants of single individuals are detailed in the corresponding published reports[1–4 6 8–10 81] and in online supplemental figure S1. Detailed phenotypical information of each affected individuals is reported in online supplemental table S1 and supplemental note.
ADHD, attention deficit hyperactivity disorder; ASD, autism spectrum disorder; F, female; IDDCA, Intellectual developmental disorder with cardiac arrhythmia; LADCI, language delay and ADHD/cognitive impairment; M, male.

Gnb5$^{-/-}$ and *Gnb5*$^{+/-}$ ± to wild-type specimens. Data analysis was performed with the R Bioconductor package DESeq2 V.1.14.1.[35] Differentially expressed genes (DEGs) were identified at the Benjamini-Hochberg adjusted $p<0.05$ level, using Wald test under design ~genotype. For gene set enrichment analysis, no direction criterion on fold change was applied. Enriched Gene Ontology (GO) categories were identified using the enrichment analysis package in R/Bioconductor, clusterProfiler,[36] considering only categories with at least 10 and maximum 500 annotated genes. Nominally significant enriched terms were retained for results interpretation.

Western blotting analysis

Tissue lysates, including atria, ventricles, cerebral cortex, cerebellum and hippocampi, were prepared in RIPA buffer (Millipore) supplemented with protease inhibitors (Thermo Fisher Scientific). Tissues were homogenised using the gentleMACS Dissociator (Miltenyi Biotec). After SDS-polyacrylamide gel electrophoresis (SDS-PAGE) and transfer to nitrocellulose membrane, blots were incubated with anti-Gnb5, anti-Rgs7 (both a generous gift from Dr William F Simonds) and anti-Gnb3 (Cell Signalling Technology) antibodies, separately, and with an antiactin antibody (Sigma), used for loading control. Horseradish peroxidase-conjugated anti-rabbit antibody (Santa Cruz) and the ECL chemiluminescence system (Millipore) were used for detection.

RESULTS

Clinical and molecular features of thirteen novel patients with IDDCA

We identified 13 additional IDDCA cases (online supplemental figure S1, table S1 and table 1) through exome sequencing of nine consanguineous families and data aggregation of multiple laboratories and clinical centres via GeneMatcher[37 38] or direct contacts. Consistent with previous reports,[1–10] the carrier of a homozygous *GNB5* missense variant on Ser81 presented with LADCI, the mild form of IDDCA (family W), while the nine individuals with biallelic loss-of-function (LoF) alleles due to truncating or splicing mutations displayed phenotypes corresponding to the severe end of the disease spectrum (families R and S, U and V, and X and Z). The remaining three individuals (families T and Y) carrying novel homozygous missense variants on Gly215 (family T) and on Leu59 (family Y) similarly presented with the severe IDDCA phenotypical spectrum. Clinical features of affected individuals are summarised in table 1 and detailed in the online supplemental note and table S1. The three missense variants (c.644G>A, p.(Gly215Glu), family T, c. 242C>G, p.(Ser81Trp), family W and c.176T>C, p.(Leu59Pro), family Y; transcript NM_006578.3) were not reported before (figure 1). They are predicted by a majority of prediction tools to be likely damaging to protein function (online supplemental table S2) and are absent from GnomAD V.3.[39] To assess possible impact, we modelled these three substitutions using the crystal structure of the GNB5-RGS9 complex[40] and found that each variant could impact the potential binding properties of the GNB5 central pore (p.(Ser81Trp) and p.(Gly215Glu)) or the protein folding (p.(Leu59Pro)) (figure 1A). Specifically, Serine 81 is buried inside a β strand of the first WD40 repeat close to the central pore of the β propeller structure[1 2] where a glycerol molecule is observed in pbi structure 2pbi (figure 1A, top left panel). Reminiscent of the Ser81Leu variant previously documented,[1] a tryptophan at position 81 cannot be accommodated without disrupting the structure and potential binding properties of the pore. Our model suggests that the rearrangements necessary to settle such a bulky sidechain will change the channel characteristics. We have investigated the related rotamers, emphasising the steric

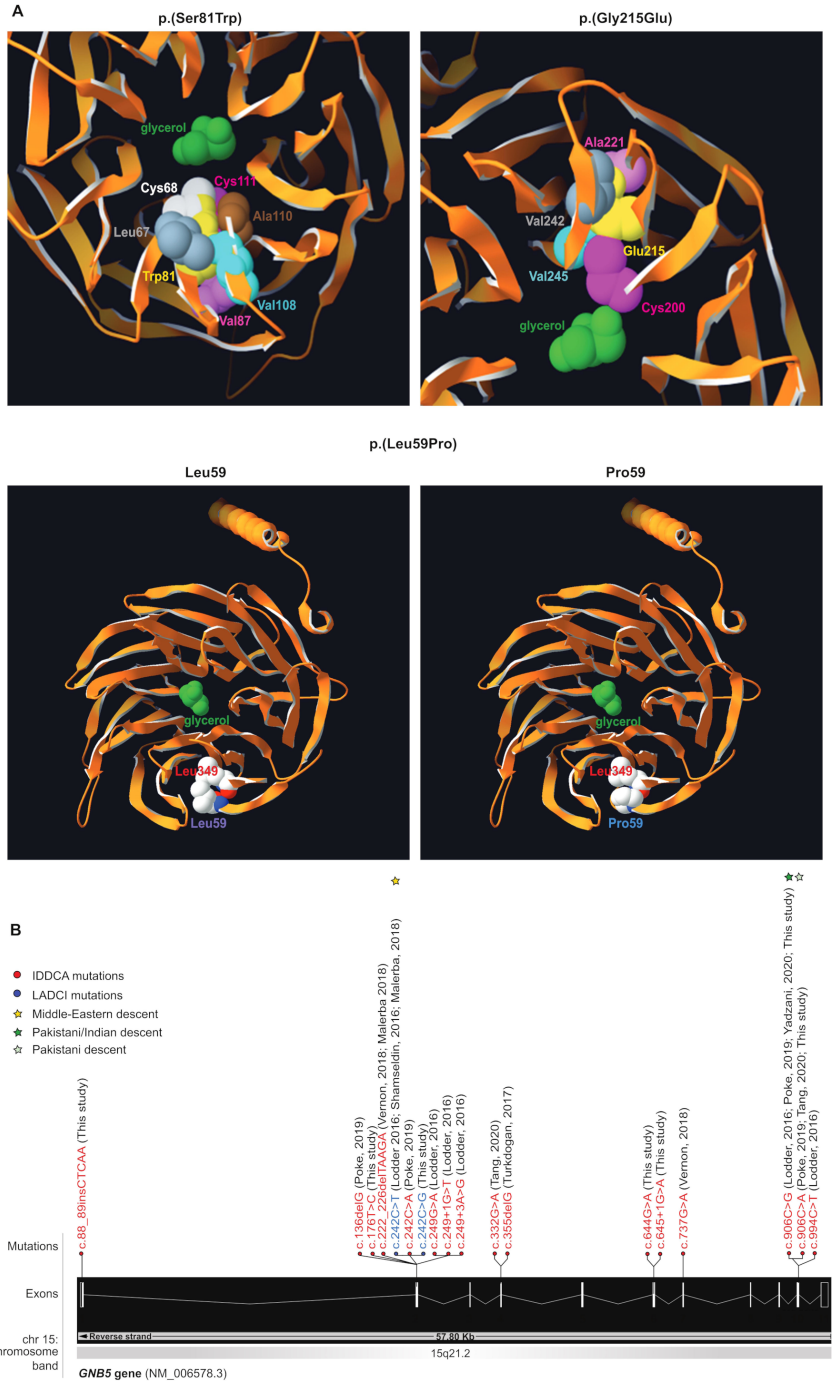

Figure 1 Variants modelling and IDDCA mutational spectrum. (A, top left) Top view of the Gnb5 (orange, PDB entry 2pbi) 3D protein model, showing the mutated Trp81 (yellow) and the glycerol molecule (green) in the centre of the pore. The rearrangements necessary to accommodate a tryptophan residue at position 81 will change the channel characteristics. The rotamer displayed here highlights clashes of Trp81 with Cys68 (white) and Cys111 (magenta). In additional rotamers, the bulky tryptophan sidechain will severely bump into Leu67 (grey), Val87 (pink), Val108 (cyan) and Ala110 (brown). (A, top right) As shown in this view of the beta propeller from above, the 'wild-type' Gly215 (not shown) lays in a beta-sheet, with on top Ala221 (pink), at the bottom Cys200 (magenta), and in front a beta-strand harbouring Val242 (grey) and Val245 (cyan). The presence of Glu215 cannot be tolerated, as it will encroach into one of the residues previously enumerated. Another rotamer shows clashes into Val245 (cyan). Overall, all rotamers may also force the sidechain of Cys200 (magenta) to reorient itself toward the internal part of the channel to provide space to accommodate glutamine at position 215 (yellow). In this position, the Cys200 sidechain will occupy the space dedicated to the glycerol (green), thus changing the properties of the channel. (A, bottom) The Leu59 (purple label, left panel) is positioned closely to the Leu349 residue just above (red label) in an antiparallel beta-sheet. This secondary structure will likely be broken in presence of a proline at that position (blue label, right panel), which in turn will disrupt the protein folding as the proline sidechain will collide into Leu349 (red label). (B) Distribution of the IDDCA published and novel variants along the schematically represented 11 exons of the human *GNB5* gene (transcript NM_006578.3; Ensembl (release 98, September 2019). The variants of IDDCA affected individuals are represented in red (LoF) and the missense LADCI variants in blue. The yellow star marks the variant of Middle Eastern descent, while green stars indicate the amber and ochre variants from the Indian subcontinent (dark green) and of Pakistani descent (light green), respectively. IDDCA, intellectual developmental disorder with cardiac arrhythmia; LADCI, language delay and ADHD/cognitive impairment; LoF, loss of function.

hindrance-induced local rearrangements associated with the tryptophan replacement, whose perturbations were evaluated using the backbone-dependent rotamer library implemented in the Swiss-PdbViewer.[41] Depending on the rotamer, tryptophan 81 will severely encroach with leucine 67, cysteine 68, valine 87, cysteine 111, valine 108 and/or alanine 110 (figure 1A, top left panel).

Pedigree charts and variants of single individuals are detailed in the corresponding published reports[1–4 6 8–10 43] and in (online supplemental figure S1). Detailed phenotypic information of each affected individuals is reported in (online supplemental table S1 and Supplemental Note). Abbreviations are as follows: M: male; F: female, ASD: Autism Spectrum Disorder, ADHD: Attention Deficit Hyperactivity Disorder.

Glycine 215 (figure 1A, top right panel) lies in a beta-sheet, between alanine 221 and cysteine 200. It faces a beta-strand harbouring valine 242 and valine 245. There is not enough space to accommodate the glutamic acid sidechain as it would encroach into one or more sidechains of the above-enumerated residues. All rotamers would also probably force the sidechain of cysteine 200 to reorient itself toward the interior of the channel to accommodate the glutamic acid 215 sidechain. This will infringe on the glycerol molecule space[40] changing the channel characteristics. Additionally, the c.644G>A, p.(Gly215Glu) variant that affects the second to last nucleotide of exon 6 might alter the activity of the donor splice site as well as create cryptic exonic splicing enhancers or silencers according to the NNSplice, NetGene2 and Splicing Finder prediction tools (online supplemental table S2).

Leucine 59 (figure 1A, bottom left panel) is in close contact with leucine 349, and both residues, linked by a hydrogen bond, belong to an antiparallel beta-sheet. A proline at position 59 (figure 1A, bottom right panel) will likely destabilise (break) this hydrogen bond, thus representing a structural conundrum. Locally, the presence of a proline might disrupt the overall protein fold as there will not be enough space to accommodate this residue, its cyclic sidechain clashing into Leu349.

To date a total of 18 pathogenic *GNB5* variants and one homozygous deletion at 15q21.2 encompassing *GNB5* gene have been identified in 44 individuals with IDDCA (online supplemental ffigure 1S 1B and table S1). Suggestive of a founder effect, the eight affected individuals from three families (families E–G) carrying the Ser81Leu variant all originate from Arab countries (Morocco, Algeria and Saudi Arabia). Of note, the Greater Middle East Variome Project[42] (http://igm.ucsd.edu/gme/) did not identify this variant within 2497 individuals. Similarly, the patients from six families (families D, L, P, R, S and V) harbouring the amber nonsense c.906C>G (Tyr302*) variant are from the Indian subcontinent (one from India and five from Pakistan). Another variant modifying the Tyr302 codon in an ochre codon (c.906C>A) was found in two additional Pakistani families (families N and U), suggesting again a possible founder effect. Of note, the same ochre variant was shown to be de novo on the paternal allele of the proband of the Chinese descent family O.[9] The 34 IDDCA individuals present with the severe end of the disease spectrum, which is characterised by severe ID (32 out of 34) with poor or absent speech (27/34), early onset sinus node dysfunction (22/34) with 4/22 who had a pacemaker implanted, variable visual abnormalities (26/34), seizures (25/34), hypotonia (29/34) and gastrointestinal problems (18/34). Additionally, 9/34 individuals showed different types of dysmorphic features (table 1 and online supplemental table 1), and MRI evaluation revealed altered brain structure in 8/34 children, with four having thinner corpus callosum, two having long posterior and hypogenesis of corpus callosum, respectively, one cerebral atrophy and one cerebral and cerebellar cortical atrophy. Three individuals (individual 16, family H; individual 39, family X; and individual 44, Family Z) showed autistic features, and the other two displayed sleep disturbances (individual 27, family N, and individual 29, family P). All severely affected individuals carry either biallelic truncation mutations or biallelic missense variants that probably result in LoF. Nine patients displayed the milder LADCI syndrome and biallelic missense variants at position 81: 4/9 presented with mild ID with 6/9 showing language deficits; 4/9 were noted to have sinus node dysfunction (one of which with pacemaker implantation); and 3/9 were reported with impaired fine motor skills. Behaviorally, 3/9 patients exhibited ADHD. The remaining patient (family J) is compound heterozygous for the LoF p.Asp74Glufs52* and the Ser81Leu variants.[3] She presented with an intermediate manifestation of the symptoms with mild ID accompanied by speech delay, hypotonia and sinus bradycardia (table 1). Like patient 21 from family I who carries the same LoF p.Asp74Glufs52* combined with a different missense, p.(Arg246Gln),[8] she is affected by hearing loss (online supplemental table S1).

Gnb5 knockout mouse cohort

To model the cardiac manifestations occurring in IDDCA syndrome, we used the mouse model knockout for *Gnb5* (*Gnb5*$^{-/-}$), thus mimicking a complete LoF. Whereas ~66% of the pups carrying the homozygous null allele were previously reported to die prior to or at weaning,[18] preweaning mortality was very low in our husbandry setting (see Materials and methods). We experienced only 5%, 11% and 6% of losses in the three cohorts we generated by mating heterozygous parents (figure 2A). We recorded two to eight breeding events during three generations of husbandry with an average litter size of 4–10 pups. The vast majority of preweaning lethality appears to be associated with *Gnb5*$^{-/-}$ as shown by the quasi-Mendelian distribution of genotypes (figure 2A). We longitudinally monitored the body weight of *Gnb5*$^{+/+}$ (wild type), *Gnb5*$^{+/-}$ and *Gnb5*$^{-/-}$ male and female mice from 3 to 46 weeks of age (figure 2C,D). We confirmed previous reports[18 22] that showed that female and male knockout animals are smaller (figure 2B–D) and that heterozygote male mice are heavier (figure 2). Importantly, knockout mice had a smaller heart (figure 2E), even smaller than expected when the heart weight was normalised to the tibia length, a proxy for animal size (figure 2F). During animal handling, no obvious gender differences were observed regarding development, behaviour or other gross phenotypes.

Ultrasound scans pinpointed increased cardiac function in *Gnb5* knockout mice

To characterise the *Gnb5* knockout mouse line at cardiac level, we first performed ultrasound scans in baseline conditions. We used 16 *Gnb5*$^{+/+}$, 8 *Gnb5*$^{+/-}$ and 16 *Gnb5*$^{-/-}$ male mice (9 wo (weeks of age)) and analysed heart morphology and function (see Materials and methods section). Echocardiography confirmed that *Gnb5*$^{-/-}$ animals had smaller hearts, as demonstrated by reduced ventricular chambers both in diastole and systole (figure 3A). Consequently, ventricular volume was also smaller (figure 3B). Estimated left ventricular weight was significantly lower in *Gnb5*$^{-/-}$ compared with *Gnb5*$^{+/-}$ and wild-type (figure 3C). Left posterior ventricular wall and interventricular septum thickness were not substantially modified (online supplemental figure S2A, B). Interestingly, *Gnb5*$^{-/-}$ mice demonstrated improved cardiac function, as judged by increased fractional shortening (figure 3D) and ejection fraction (figure 3E). However, stroke

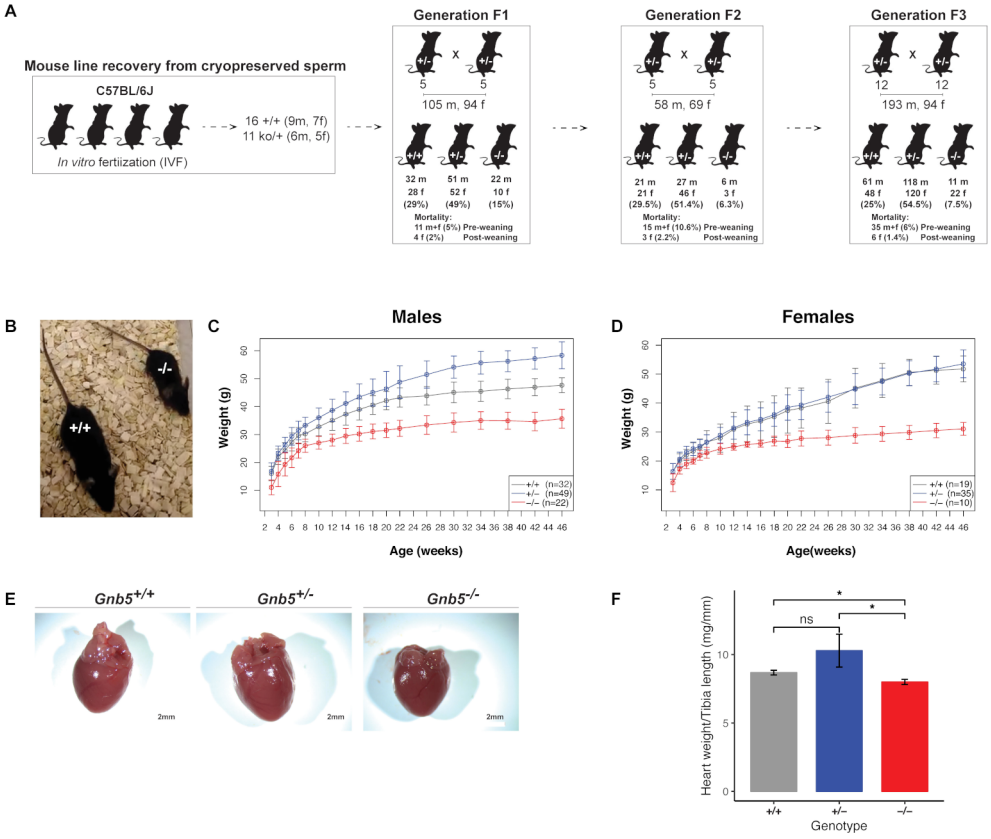

Figure 2 *Gnb5* mouse line features. (A) Mouse mating strategy and gender and genotype distribution over three successive generations. Preweaning and postweaning mortality is reported for each colony. (B) Size of $Gnb5^{+/+}$ and $Gnb5^{-/-}$ mice. (C,D) Body weights profile monitored from 3–46 weeks of age. All mice were weaned on week 3. Data are shown as mean±SD. (C,D) Panels separate body weights according to sex. $Gnb5^{+/+}$ is depicted in grey, $Gnb5^{+/-}$ in blue and $Gnb5^{-/-}$ in red. (E) At sacrifice, neither significant morphology difference nor thoracic position of the heart were observed among groups. (F) Bar plot showing that $Gnb5^{-/-}$ hearts (red, n=16) are smaller compared with the other genotypes ($Gnb5^{+/-}$, blue (n=8) and $Gnb5^{+/+}$, grey (n=16)). Data are shown as mean of the ratio between heart weight and tibia length (used to normalise for animal size)±SEM. Asterisks on the plots represent the level of significance: *p≤0.05, **p≤0.01, ***p≤0.001, ****p≤0.0001; p>0.05 was considered not significant.

volume (figure 3F) and cardiac output (figure 3G) were similar to those measured in wild-type mice. Notably, and unexpectedly, $Gnb5^{+/-}$ have a bigger heart (figure 3A–C) compared with wild type, while their cardiac function remains unchanged (figure 3D–E). Therefore, the increased stroke volume (figure 3F) and cardiac output (figure 3G) reflected an increased volume of blood pumped by the ventricle.

Taken together, these results indicated that $Gnb5^{-/-}$ mouse hearts were smaller than that of the other two genotypes but compensated their smaller size by increased cardiac efficiency.

Loss of functional *Gnb5* determines the onset of sinus arrhythmias

As cardiac arrhythmia in the form of bradycardia and ectopic beats is one of the core symptoms in IDDCA, we examined HRVs in *Gnb5* mouse models with in vivo ECG monitoring. ECG was performed at 12 weeks on the same male mice used for echocardiography. Baseline ECG parameters were not different among $Gnb5^{+/+}$, $Gnb5^{+/-}$ and $Gnb5^{-/-}$ animals, except for HR in knocked-out animals that showed a trend toward higher values (online supplemental figure S2C, minimum and maximum HR values registered in wild-type were 313 and 741 beats/min, while lowest and greatest HR values in knockout were 349 and 744 beats/min, significance varying between p=1.28E-04 and p=0.9971, over 36 daylight time points).

Close inspection of baseline ECG over a 24-hour window allowed the quantification and characterisation of small changes in the intervals between successive heartbeats (RR interval) corresponding to cardiac arrhythmias (Materials and methods). The 24-hour ECGs unearthed a significant increase in arrhythmic events in $Gnb5^{-/-}$ mice compared with heterozygous and wild-type littermates. We counted on average 53 short atrial escape beats in $Gnb5^{+/+}$ and 204 in $Gnb5^{-/-}$ animals over 24 hours (figure 4B–E, p=4.936e-06). Long atrial escape beats (figure 4C–F; 1 vs 117 events, p=7.792e-06) and atrioventricular blocks (figure 4D–G; 0.6 vs 30 events, p=0.04078) were similarly observed significantly more frequently in knockout animals. Few episodes of tachycardia followed by bradycardia and premature beats were also observed in homozygous knockouts.

These results demonstrated that $Gnb5^{-/-}$ mice have a defect at the level of sinus node as well as cardiac conduction anomalies linked to the atrioventricular node. Of note, we did not assess for other anomalies.

Gnb5-deficient mice exhibit higher cholinergic sensitivity and normal sympathetic activity

Human homozygote carriers of *GNB5* pathogenic variants show severe bradycardia at rest with a maximal HR unchanged during exercise. Zebrafish and human cell modelling supported predominantly parasympathetic modulation in the aetiology of

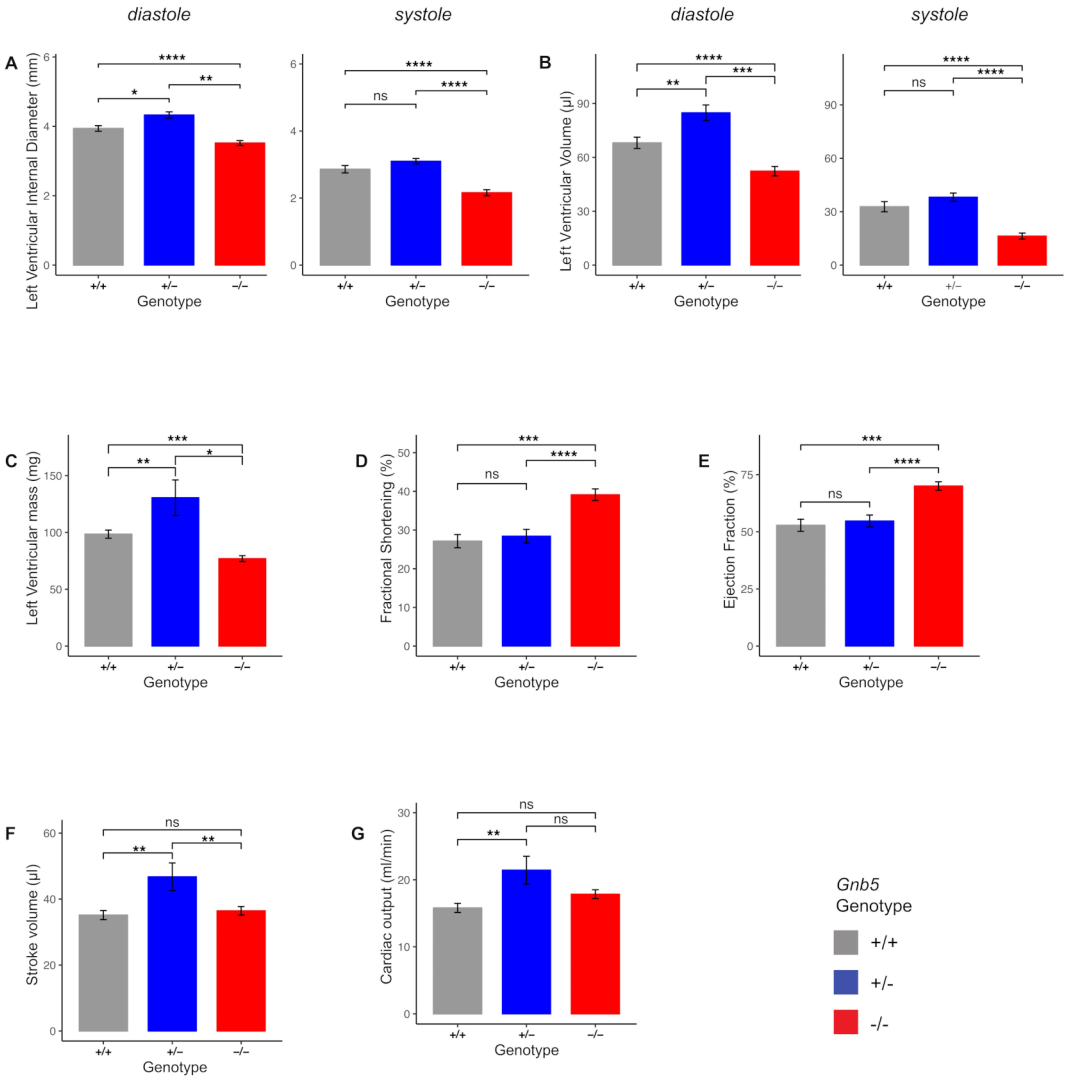

Figure 3 Morphological and functional parameters measured by ultrasound scan in *Gnb5*$^{+/+}$, *Gnb5*$^{+/-}$ and *Gnb5*$^{-/-}$ male mice. (A) Left ventricular internal diameter at diastole (left) and systole (right). (B) Left ventricular volume in diastole (left) and systole (right). (C) Mass of the left ventricle. (D–G) Cardiac function expressed as fractional shortening (D), ejection fraction (E), cardiac output (F) and stroke volume (G). Parameters unchanged between the three genotypes are shown in online supplemental figure S2A,B.

HR disturbances in IDDCA individuals.[1 7] To better assess the possible involvement of the autonomic innervation, we used an in vivo mammalian model system whose physiology is closer to humans. We used ECG telemetry to monitor HR and observed higher HR in baseline conditions (online supplemental figure S2C) possibly reflecting a higher rate of activity of the *Gnb5*$^{-/-}$ mice, as measured qualitatively here and reported previously[22] (online supplemental figure S2D,E), or alternatively differences in the HR regulation.

Parasympathetic blockade with atropine (1 mg/kg) had a positive chronotropic effect; that is, HR increased (HR *Gnb5*$^{+/+}$=690 beats/min±68, HR *Gnb5*$^{+/-}$=700 beats/min±34, HR *Gnb5*$^{-/-}$=758 beats/min±28 ($p_{+/+\ vs.\ +/-}$=0.63, $p_{+/+\ vs\ -/-}$=2.62E-03, $p_{+/-\ vs\ -/-}$=2.38E-03)) (online supplemental figure S3A). In contrast, carbachol administration (0.1 mg/kg) triggered a rapid decrease of the HR in the three groups, with a significant effect in *Gnb5*$^{-/-}$ mice, whose HR dropped until 335 beats/min (HR *Gnb5*$^{+/+}$=448 beats/min±147, HR *Gnb5*$^{+/-}$=415 beats/min±157, HR *Gnb5*$^{-/-}$=335 beats/min±141 ($p_{+/+\ vs\ -/-}$=3E-02; online supplemental figure S3B). HR quickly recovered in all genotypes. The duration of the bradycardia was similar in the three groups (~1 hour). Moreover, since the baseline HR of knockout animals was higher, when expressed in relation to the basal values, the effect of atropine was not different in the three groups of mice ($p_{+/+\ vs\ +/-}$=0.22, $p_{+/+\ vs\ -/-}$=0.07, $p_{+/-\ vs\ -/-}$=0.77; figure 5A), while the carbachol-induced bradycardia was more severe in *Gnb5*$^{-/-}$ (p=1.79E-03, figure 5B).

To mimic the sympathetic response and investigate a possible role of the β-adrenergic response in the heart rhythm perturbations of IDDCA syndrome, we challenged *Gnb5*$^{+/+}$ and *Gnb5*$^{-/-}$ animals with either isoprenaline or atenolol. Injection of the sympathetic agonist isoprenaline (4 mg/kg) resulted in a prolonged (~1 hour) increase of HR, with values comparable in both genotypes (p=0.41, online supplemental figure S3C). HR slowly decreased to baseline; this reduction reached lower than baseline values in *Gnb5*$^{-/-}$ mice (online supplemental figure S3C). However, when expressed in percentage of the baseline, the tachycardia seemed stronger in wild-type (p=0.09, figure 5C).

The sympathetic antagonist atenolol (2 mg/kg) induced a similar decrease of HR in both groups (p=0.73, p=0.22 when compared with baseline (online supplemental figure S3D and figure 5D).

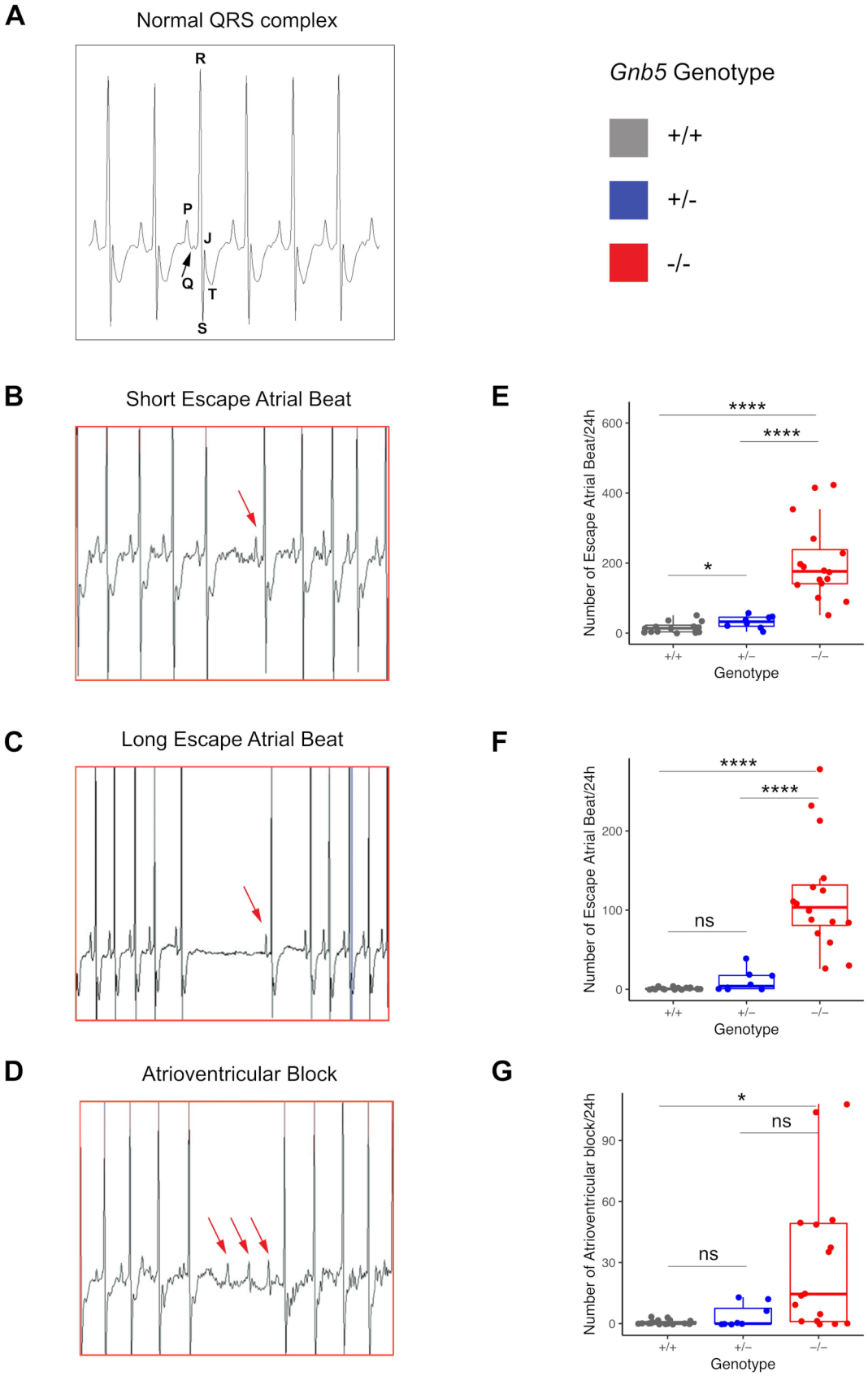

Figure 4 Cardiac arrhythmias recorded in *Gnb5* mouse line. (A) Normal ECG trace recorded in wild-type male mice with the main spikes specified as used in the text. (B,C) *Gnb5*$^{-/-}$ male mice ECG traces showing escape atrial beats classified as short (B) and long (C) and characterised by the occurrence of a late P-wave (red arrow). (D) *Gnb5*$^{-/-}$ male mice ECG trace demonstrating atrioventricular blocks, with more than one P-wave per QRS complex (consecutive red arrows). (E–G) Respective box plots indicating the number of arrhythmias, that is, the number of short (E) and long (F) escape atrial beats and atrioventricular blocks (G) per 24 hours. ns, not significant.

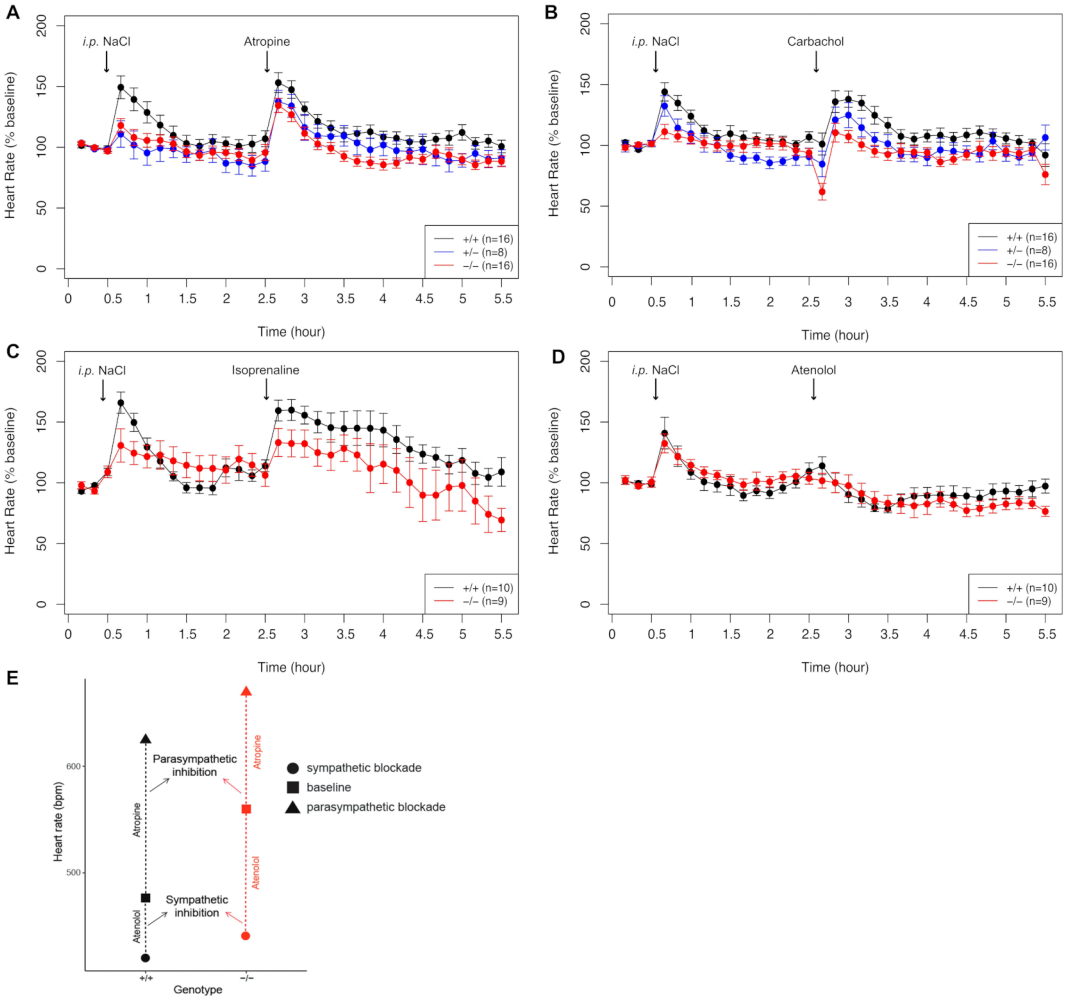

Figure 5 Pharmacological administration of compounds mimicking parasympathetic and sympathetic stimulation. (A) HR monitoring after injection of atropin (intraperitoneal 1 mg/kg). (B) Bradycardia measured in response to carbachol (intraperitoneal 0.1 m/kg). (C) HR variation in response to atenolol (intraperitoneal 2 mg/kg). (D) Increased HR after isoprenaline administration (intraperitoneal 4 mg/kg). Data points are expressed as percentage of the baseline values. (E) Smaller parasympathetic and bigger sympathetic blockade in *Gnb5*$^{-/-}$ mice (red), compared with wild-type littermates (black), indicative of lower parasympathetic and higher sympathetic tones in basal conditions. HR, heart rate.

These results indicate that the *Gnb5*$^{-/-}$ mice bradycardia results from enhanced parasympathetic (cholinergic) stimulation/reflex. Our data also suggest an increased sympathetic activation when animals are under stress, that is, when they are challenged by the injection of drugs.

In contrast to individuals affected with IDDCA, *Gnb5*$^{-/-}$ mice showed a higher HR in baseline conditions (online supplemental figure S2C and S3A-D, first three data points). We hypothesised that such discrepancy could be linked to different autonomic nervous system tone between human and mouse.[43] We therefore analysed the response to the administration of drugs to determine which of the parasympathetic and sympathetic system mostly influences baseline HR. Atropine-mediated parasympathetic inhibition induced an increase in HR with a variation from the baseline, which was smaller in knockout animals than in wild types (figure 5E), pinpointing that the parasympathetic tone is lower in *Gnb5*$^{-/-}$ mice. Conversely, the sympathetic blockade by atenolol induced a greater reduction of the HR in *Gnb5*$^{-/-}$ than control littermates (figure 5E) evocative of the greater sympathetic tone observed in basal conditions. Of note, the control responses mediated by NaCl injection also showed a difference in HR attributable to increased parasympathetic/sympathetic balance; the HR increase, due to the stress caused by the injection and animal handling, was less pronounced in *Gnb5*$^{-/-}$ mice. Our results suggest that higher basal HR in *Gnb5*$^{-/-}$ mice could be due to lower parasympathetic tone and higher sympathetic tone.

To further assess the functioning of cardiac autonomic regulation, we performed time domain analysis of HRV in *Gnb5*$^{+/+}$ and *Gnb5*$^{-/-}$ mice. We measured NN, SDNN, RMSSD and pNN6 during light (day) and dark (night) phases in each genotype. Whereas all parameters differ in the wild-types, the knockouts showed no significant HRV differences between light and dark phases (table 2) confirming that differences in RR intervals (NN), and hence in HR, were greater in *Gnb5*$^{+/+}$ (p_{NN}=1.25E-08, table 2) than in *Gnb5*$^{-/-}$ mice (p_{NN}=0.72, table 2). This suggests abnormal autonomic regulation, in particular via the parasympathetic system in the *Gnb5*$^{-/-}$ mouse. Concordantly, RMSSD, which reflects short-term variations in HR, and pNN6, both measures of the parasympathetic nervous system regulation, were significantly different between night and day in *Gnb5*$^{+/+}$ mice (p_{RMSSD}=4.38E-05, p_{pNN6}=9.71E-06; table 2), while they were almost unchanged in *Gnb5*$^{-/-}$ mice (p_{RMSSD}=0.65, p_{pNN6}=0.9, table 2). Similarly, SDNN that indicates the total autonomic variability, fluctuated in *Gnb5*$^{+/+}$ mice (p_{SDNN}=1.16E-02, table 2) but not in *Gnb5*$^{-/-}$ mice (p_{SDNN}=0.61, table 2) at night.

Table 2 Results of HRV analysis

Genotype	*Gnb5*$^{+/+}$							*Gnb5*$^{-/-}$							*Gnb5*$^{+/+}$ vs *Gnb5*$^{-/-}$	
Night/day	Night			Day			P value	Night			Day			P value	P value	P value
	Mean	SD	SEM	Mean	SD	SEM	Night versus day	Mean	SD	SEM	Mean	SD	SEM	Night versus day	Night	Day
Mean RR (NN)	112.27	10.32	2.66	136.81	13.25	3.31	1.25E-08	110.00	7.45	1.92	111.63	24.18	6.04	0.72	0.21	3.45E-03
SDNN	23.47	3.44	0.89	26.56	5.02	1.25	0.012	24.05	4.16	1.11	23.17	3.31	0.83	0.61	0.94	4.76E-02
RMSSD	4.77	1.74	0.45	6.54	2.10	0.53	4.38E-05	5.05	2.49	0.64	4.69	1.05	0.26	0.65	0.86	9.07E-03
pNN6	13.81	8.96	2.31	24.13	10.49	2.62	9.71E-06	13.33	7.98	2.06	13.21	5.00	1.25	0.90	0.88	7.34E-04

HRV parameters measured in time-domain HRV analysis over 12-hour nocturnal and 12-hour diurnal intervals. Values are reported as mean; SD and SEM were calculated and reported. Standard t-test was used to assess differences between Gnb5$^{+/+}$ and Gnb5$^{-/-}$ groups, as well as for differences between day and night. Description of the parameters used can be found in the Materials and Methods section.
HRV, heart rate variation; NN, mean R–R interval; RMSSD, square root of the mean square difference; SDNN, SD of all normal R–R intervals.

All parameters were significantly reduced during the light phase when comparing *Gnb5*$^{+/+}$ and *Gnb5*$^{-/-}$ mice (p_{NN}=3.45E-03, p_{SDNN}=4.76E-02, p_{RMSSD}=9.07E-03, p_{pNN6}=7.34E-04; table 2).

Taken together, these results demonstrated an impaired autonomic regulation in *Gnb5*$^{-/-}$ mice, in particular a lower modulation of the parasympathetic activity.

Transcriptome analysis of *Gnb5* mice

To explore the transcriptional consequences of *Gnb5* loss in the heart, we profiled the transcriptomes of atria and ventricles of *Gnb5*$^{-/-}$, *Gnb5*$^{+/-}$ and wild-type male mice at 18 weeks of age using RNA-sequencing (RNA-seq) (online supplemental table S3). RNA-seq libraries were sequenced to a median depth of ~50 000 000 single-end reads per samples. Samples clustering (using Poisson model[44]) to define the global relationship among all samples, showed a very clear separation of atria and ventricles (online supplemental figure S4A) as well as of hippocampi, cerebellum and cerebral cortex (online supplemental figure S4B).

Transcripts quantification confirmed that *Gnb5*, the orthologue of *GNB5*, is expressed in the brain (online supplemental figure S5) and cardiac tissues (atria and ventricles; figure 6A,B, top) of adult mice and that its expression levels correlated with gene dosage. We identified 98 significantly DEGs in atria (online supplemental table S4) and 63 in ventricles (online supplemental table S5) applying a false discovery rate method for multiple testing with a 5% threshold. Consistent with the phenotype described in *Gnb5*$^{-/-}$ mice, we found altered expression of genes involved in cardiac muscle contractility, HR regulation and cardiac conduction. Among the upregulated genes falling into these categories in atria were *Npr3* (p=9.71E-04), *Comp* (p=3.7E-05) and *Scn10a* (p=2.88E-02), while downregulated transcripts were *Myh7* (p=1.31E-02), *Lmod2* (p=1.04E-04) and *Agt* (p=7.97E-03) (figure 6A, top). Profiling of the ventricles demonstrated significant upregulation of *Lrrc10* (p=3.91E-02), *Tnnt2* (cardiac troponin, p=2.88E-02), *Scn10a* (p=1.84E-02) and *Drd2* (p=8.28E-04) (figure 6B, top), and reduced expression

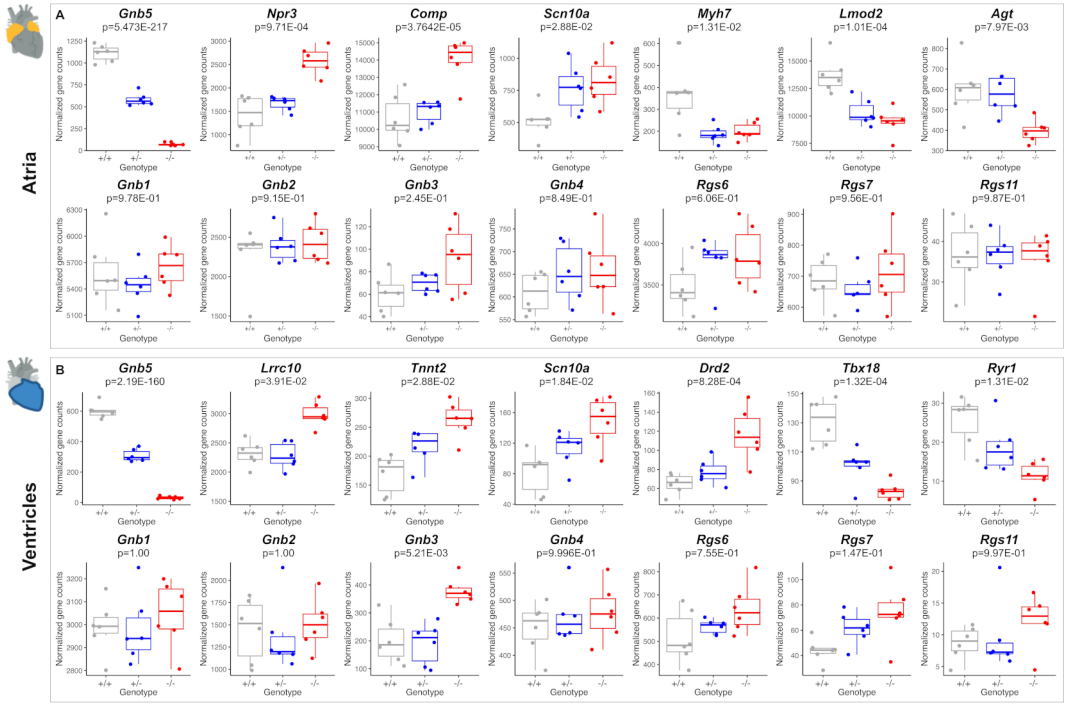

Figure 6 Comparison of transcriptome profiles of atria and ventricles in *Gnb5*$^{+/+}$, *Gnb5*$^{+/}$ and *Gnb5*$^{-/-}$ male mice. (A) Atrial expression profiles of *Gnb5* (top, left) and other DEGs (top Lane); *Gnb* and *Rgs* transcripts quantification in atria (bottom lane). (B) Ventricular expression profiles of *Gnb5* gene (top, left) and other DEGs (top lane); *Gnb* and *Rgs* transcripts quantification in ventricles (bottom). DEG, differentially expressed gene.

of *Tbx18* (p=1.32E-04). Notably, the expression level of *TNNT2* gene was not modified in GNB5-Ser81Leu hiPSC.[7] Correspondingly, nominally enriched gene sets were associated with development of the cardiac conduction system (GO:0003161, online supplemental table S6, S7), regulation of HR (GO:0002027, online supplemental table S6, S7) and cardiac muscle contraction (GO:0060047, GO:0060048; online supplemental table S6, S7). *MYH7* and *TNNT2* encode sarcomeric proteins, essential for contraction and relaxation of the heart muscle, and mutations in these genes have been linked to cardiomyopathy.[45]

Scn10a encodes the voltage-gated sodium channel $Na_v1.8$. Its human orthologue was associated with HR regulation and genome-wide association studies suggested it as a modulator of PR interval duration, that is, atrial conduction time.[46] *Lrrc10* and *Lmod2* are associated with dilated cardiomyopathy in both human and mice[47–50]; while *Lrrc10* functions in the sarcomeric Z-disc and the T-tubule components, involved in muscle contraction,[47] loss of functional *Lmod2* has been linked to short thin filaments and reduction in maximum calcium-activated force production.[48] Rodent ventricular cardiomyocytes are converted into spontaneous firing cells (eg, sinoatrial-node pacemaker cells) by expression of the transcription factor *Tbx18*,[51] whereas a polymorphism in *DRD2* has been associated with motor learning and HR.[52] *RYR1* has a dominant role in muscles contractility, even though it is more prominently associated with skeletal muscle.[53] Common variants in *RYR1* are associated with left ventricular hypertrophy.[54]

Given that (1) *Gnb5* has four paralogous genes, with ~50% sequence identity[55 56]; (2) the respective encoded proteins may have redundant function; (3) the propagation of the Gnb5-mediated signal is controlled by RGS[15 16 57]; and (4) Gnb5 and Rgs (ie, Rgs6 and Rgs7) are coexpressed both at RNA (online supplemental figure S6A,B) and protein levels,[17] we investigated the expression patterns of these two families of genes in our transcriptome profiles to investigate possible compensatory mechanisms. We found significant upregulation of *Gnb3* in ventricles (figure 6B, bottom, p=5.21E-03) and a trend toward increased expression level in atria (figure 6A, bottom, p=0.24). The genes encoding the other Gβ subunits, named *Gnb1*, *Gnb2* and *Gnb4*, did not change expression (figure 6A,B, bottom). In ventricles, the three R7-Rgs expressed in heart, *Rgs6*, *Rgs7* and *Rgs11*, showed a trend towards increased expression when *Gnb5* was knocked out (figure 6B, bottom). Only *Rgs6* showed a similar trend in atria (figure 6A, bottom). $Gnb5^{+/-}$ mice showed no or very subtle changes of their transcriptome compared with controls; we detected only six DEGs in atria (online supplemental table S8) and one in ventricles (online supplemental table S9) beside the engineered *Gnb5*. Profiling Gnb5 protein expression revealed detectable levels in the heart of wild-type mice, along with abundant presence in three brain regions (cortex, cerebellum and hippocampi), while immunoblotting of $Gnb5^{-/-}$ tissues verified the complete absence of the protein (online supplemental figure S6C). Notably, we detected no compensatory changes in either Gnb3 or Rgs7 levels; the two proteins were undetectable in $Gnb5^{-/-}$ atria and ventricles (online supplemental figure S6C). This suggests that Gnb3 protein stability may be decreased and further demonstrates that the physical association with Gnb5 is critical for the stability of the Gnb5/R7-Rgs complex, as previously described for Rgs6.[17] Gnb5 and Rgs7 proteins were enriched in atria compared with ventricles in wild-type mice (online supplemental figure S6C).

We further investigated transcriptome signatures in three brain regions relevant to the IDDCA pathology: the cortex because of its role in higher cognitive function, the hippocampus as it participates in the formation of long-term and spatial memories and the cerebellum for its motor control and language processing. Cerebellar and hippocampal anomalies were documented in *Gnb5* knockout pups.[22] Overall, we observed 206 DEGs in cerebellum, 105 in hippocampus and 48 in cerebral cortex (at false discovery rate (FDR) 5%) (online supplemental table S10-S12). These genes resulted in over-representation of gene ontology (GO) terms involved in regulation of excitatory postsynaptic membrane potential (GO:0060079), regulation of neurotransmitters secretion (GO:0046928), learning (GO:0007612) and synapse organisation (GO:0050808), regulation of inositol 3-phosphate (GO:0014065), regulation of cAMP-mediated signalling (GO:0043951) (in cerebellum, online supplemental table S13); visual perception (GO:0007601), phototransduction (GO:007602), guanylate cyclase activity (GO:0031282) and regulator of signalling receptors (GO:2000272) (in hippocampus, online supplemental table S14); and sensory perception of light stimuli (GO:0050953) and lens development (GO:0002088) (in cortex, online supplemental table S15).

Quantitative RT-PCR and microarray data previously indicated altered expression levels of genes implicated in neuronal development and function, such as down-regulation of *Grid2* (glutamate ionotropic receptor, delta 2) and upregulation of *Synpo* (synaptopodin),[22] as well as increased expression of *Guca1a* and *Guca1b,* calcium-binding protein activating photoreceptor guanylate cyclases. *Guca1a* ($p_{hippocampus}$=1.81E-03) and *Guca1b* ($p_{cerebellum}$=1.56E-302, $p_{hippocampus}$=1.9589E-196, p_{cortex}=2.209E-178) were DEGs in the brain of *Gnb5* knockout mice; they showed significant upregulation (online supplemental figure S5). *Synpo* showed a trend of increased expression in the hippocampus (online supplemental figure S5B, p=0.55).

A subset of additional DEGs included *Grin2a* (p=1.044E-06), *Snca* (p=7.96E-03), *Gnai2* (p=7.79E-03) and *Kcnj2* (p=0.04), in the cerebellum (online supplemental figure S5A), *Hes5* (p=0.04) and *Sox6* (p=0.02) in the hippocampus (online supplemental figure S5B) and *Ntrk3* (p=9.69E-04) and *Cacna2d4* (p=0.03) in the cortex (online supplemental figure S5C). The glutamate-gated ion channel Grin2a protein plays important roles in long-term potentiation and in efficient synaptic transmission. Disruption of this gene is associated with focal epilepsy and speech disorder with or without cognitive disability.[58] *Hes5* and *Sox6* genes, respectively, are a transcriptional repressor and activator, required for the regulation of transition timing of neurogenesis and gliogenesis in mammalian neocortical development[59] and in the normal development of the central nervous system.[60] *Cacna2d4* encodes for a calcium channel whose mutations are associated with retinal dysfunction in human.[61] The expression of transcripts encoding for different Gβ subunits and R7-RGS genes remained unchanged (online supplemental figure S5 A-C, bottom), suggesting that the brain could be less proficient than the heart in compensating dysregulated pathways. Rgs7 protein level was greatly reduced in $Gnb5^{-/-}$ brain, further emphasising the Gnb5/R7-Rgs codependence (online supplemental figure S6C).

DISCUSSION

The advent of high-throughput sequencing allowed identification of the cause of hundreds of Mendelian diseases,[62] in particular those involving intellectual disability.[63] For example, data aggregation of exome sequencing uncovered a link between variants in genes encoding the Gβ subunits of the heterotrimeric G-proteins with a group of neuropsychiatric conditions with cardiac manifestations and ophthalmic pathologies.[1–4 6 8–10 64–79]

Mutations in *GNB5*, encoding the divergent $G\beta_5$ subunit of the guanine–nucleotide binding protein family, were recently shown to be causative of the autosomal recessive IDDCA syndrome. Differently from $G\beta_{1-4}$, $G\beta_5$ forms irreversible dimer with the G-protein γ-like domain[80] present in the R7 regulator group of G-protein signalling proteins (R7 RGS). Dimerisation with $G\beta_5$ is absolutely required for the stability of the R7 RGS proteins[16].

Genotype–phenotype correlation showed that carriers of truncating *GNB5* variants present with the severe form of this syndrome, while missense alleles are associated with milder phenotypical manifestations. Recently, an individual carrying a homozygous deletion spanning three genes, *BCL2L*, *GNB5* and *MYO5C*, was reported to display a phenotype which overlaps significantly with the IDDCA manifestations,[81] further confirming that this phenotype is associated with loss of function of *GNB5*. In this work, we increased the number of reported individuals with IDDCA and associated variants, through identification of nine additional families and five novel causative variants. The core symptoms of IDDCA include cognitive disability, epilepsy, retinopathy and cardiac arrhythmia.[1–10] This is a life-long condition with a risk of sudden death. Six of the seven deceased IDDCA individuals are suspected to have died from a sudden cardiac arrest secondary to an arrhythmia. Although the mutational spectrum of this syndrome has already been partly defined, the overall molecular mechanism by which perturbations of *GNB5* translate into IDDCA phenotypical manifestations remains unclear. Modelling in zebrafish and cardiomyocytes differentiated from human iPSCs provided some initial answers[1 7]; however, we thought that the mouse would be a more appropriate tool to investigate consequences of this human syndromic neurodevelopmental condition. As little was known about possible cardiac conduction anomalies in mice, we characterised both the cardiac phenotype and molecular outcome of knocking-out *Gnb5*. $Gnb5^{-/-}$ animals were smaller and had smaller ventricles, and therefore the chambers would contain less blood as a consequence. However, they exhibited an increase in fractional shortening and ejection fraction, a sign of compensatory cardiac function. The quantity of blood ejected by the ventricles, as defined by the cardiac output and stroke volume, remained unchanged between $Gnb5^{-/-}$ and $Gnb5^{+/+}$ mice, indicating that $Gnb5^{-/-}$ heart has adapted to ensure that it efficiently meets the body's demands for perfusion.

ECG measurements showed that, conversely to IDDCA affected individuals who present with severe bradycardia at rest, $Gnb5^{-/-}$ mice have higher HRs in basal condition, especially during the day, the mouse sleeping phase. Zebrafish knocked-out for all *gnb5a* and *gnb5b* copies present in the fish genome, showed a similar trend of increased basal HR.[1] It is plausible that these differences are linked to a lower parasympathetic tone in fish and rodents compared with humans. Of note, we showed that the parasympathetic and sympathetic tones of $Gnb5^{-/-}$ mice were, respectively, lower and higher than those of controls (figure 5E), thus possibly influencing the basal HR. Whereas we cannot conclude that this higher basal HR is exclusively due to changes in HR regulation as we and others observed an increase in activity of $Gnb5^{-/-}$ mice[21 22] (online supplemental figure S2D), the zebrafish model showed no sign of hyperactivity.[1] In normal conditions, HR is balanced by the synergic interactions between the sympathetic and parasympathetic nervous systems. Our HRV analysis, aimed at assessing such sympathovagal balance, confirmed a reduced modulation of the parasympathetic stimulation in the heart of $Gnb5^{-/-}$ mice (table 2).

ECG recordings additionally revealed a high number of arrhythmias in knockout animals, including escape beats, tachycardia/bradycardia episodes and atrioventricular block. These sinus arrhythmias and conduction problems, reminiscent of arrhythmias observed in IDDCA subjects, further corroborate the involvement of *Gnb5* gene in altered cardiac function and irregular heartbeat. Finally, our mice study showed that *Gnb5*-inhibitory signalling is essential for the parasympathetic control of the HR as suggested by previous studies in other models.[1 7] Knockout mice treated with a parasympathomimetic presented with bradycardia, while injection of an antiparasympathetic drug atropine had the same effect as in wild type. The β-adrenergic activity of $Gnb5^{-/-}$ mice was unaltered, suggesting a normal sympathetic modulation of the cardiac stimulation, and further confirming that the more efficient cardiac function is an adaptation to counteract the reduced size of the $Gnb5^{-/-}$ heart.

Consistent with this observation, transcriptome profiling provided insights into modifications of cardiac contraction properties, along with reduced ventricular expression of genes required for development of pacemaker cells. Instead of specific signals (eg, pacemaker function genes in atria), genes related to heart muscle contraction (eg, *Myh7* and *Lmod2* in atria, *Tnnt2* and *Lrrc10* in ventricles) and conduction system functions (eg, *Agt* and *Npr3* in atria, *Tbx18* in ventricles and *Snc10a* in both) were identified as DEGs in both atria and ventricles in $Gnb5^{-/-}$ animals. These transcriptome alterations may shed light on the mechanisms that result in the pathology of IDDCA. Approaches like single-cell RNA-sequencing combined with the isolation of sinoatrial node cells are warranted to complement our findings in the future. Globally, these data further challenge our study, since we cannot unravel whether the transcriptome modifications are cause or consequence of the augmented contractility. We argue, in line with the aforementioned results, that we are possibly investigating a compensatory mechanism. Interestingly, mice lacking *Gnb5* overexpress *Gnb3*, a gene encoding a different Gβ subunit and involved in the activation of GIRK channels.[82] In contrast to *Gnb1* and *Gnb4* that have a well-documented role in the nervous system,[76 83] *Gnb3*-null mice presented with cardiac manifestations, including slower HRs. However, their isolated hearts responded equivalently to muscarinic receptor-adrenergic and β-adrenergic receptor-stimulations, thus suggesting that *Gnb3* is unlikely to be involved directly in the G-protein signalling controlling heart pacemaker activity.[84] Nonetheless, its higher expression may play a role in coping with the loss of *Gnb5*; further studies are warranted to elucidate such compensatory mechanisms. The expression of *Gnb2* is unchanged in the cardiac tissue of *Gnb5* knockouts; however, it was also linked to heart functions in mouse and human[66 69] with *Gnb2* knockout mice having increased HR, and ECG trace revealing shortened RR and PQ intervals and ST segment (https://www.mousephenotype.org/data/genes/MGI:95784).[85]

The transcriptome data provided molecular data supporting an increased cardiac function of $Gnb5^{-/-}$ mice. It probably results from both a compensatory mechanism, as shown by misexpression of genes involved in cardiac muscle contractility, and an alteration of the expression of genes involved in the regulation of the HR. We also documented transcriptional changes in three brain regions of knockout mice which correlate with the IDDCA neuropsychiatric disease spectrum.

HR regulation by the parasympathetic and sympathetic branches of the autonomic nervous system takes place in the pacemaker cells of the sinoatrial node. While sympathetic modulation increases pacemaker cell firing rate, the vagal parasympathetic activity decreases the HR. Both activities are mediated

by G-protein-coupled signalling on β-adrenergic (sympathetic) and cholinergic M_2 muscarinic (parasympathetic) receptors, respectively. Autonomic innervation is regulated in vivo by RGS proteins. In particular, in the heart, the M_2 receptor signalling is mediated by the Rgs6–Gnb5 complex.[17] As *Gnb5* and *Rgs* genes are coexpressed and as the physical association of the encoded proteins is critical for complex stability, we expected to observe reduced *Rgs* expression levels. In a previous report,[17] no Rgs6 was detected in the atria and in the brain of *Gnb5* knockout mice. Surprisingly, we detected a trend of increased expression of *Rgs* subunits, in particular *Rgs6*, contrary to findings in reference[7] where expression of *RGS6* was not different between GNB5-Ser81Leu and wild-type hiPSCs. These discrepancies may stem from the fact that we are investigating different model systems, that is, mouse tissues versus human cells, as well as by the use of different technologies to detect mRNA abundance; that is, RNA-sequencing versus qRT-PCR and that in case of hiPSCs data were generated from one clone per genotype.

Altogether, our results unveil that potentially compensatory changes occur at a transcriptional level in $Gnb5^{-/-}$ mice through higher expression of *Gnb3* and *Rgs* genes in heart tissues. Additional evidence at protein level did not confirm compensatory changes. The previously cited link between *GNB5* and the R7-RGS *RGS6* and *RGS11* suggests that they are part of the same pathway. Consistent with this hypothesis, the members of a Tunisian family presenting with cataract, mental retardation and microcephaly were carriers of biallelic mutations in *RGS6*[86] . Another unpublished case harbouring mutation in *RGS11* presented with overlapping neuropsychiatric phenotype (Sarah Montgomery, *in litt*). No specific cardiac evaluation is reported in these individuals, but our data suggest that this should be considered. Co-occurrence of neuropsychiatric symptoms with visual and cardiac manifestations could represent a unique combination associated with Gβ and the R7-RGS related proteins. We hypothesise that the disease mechanism responsible for HR perturbations is the reduction or the loss of negative regulation by Rgs6 on the inhibitory $G\beta_5$ signalling, resulting in enhanced parasympathetic activity.

Overall, our work highlights that $Gnb5^{-/-}$ mice not only recapitulate IDDCA's neurological manifestations previously outlined elsewhere[22] but also mimic its cardiac perturbations, especially regarding heart arrhythmias and autonomic nervous system control, allowing for future screening of drugs modulating the parasympathetic branch of the autonomic nervous system, in view of the development of patients' therapy.

WEB RESOURCES

GnomAD: https://gnomad.broadinstitute.org/about

IMPC: http://www.mousephenotype.org/MutationTaster2: http://www.mutationtaster.org/

PolyPhen-2:http://genetics.bwh.harvard.edu/pph2/index.shtml

PROVEAN: http://provean.jcvi.org/index.phpSIFT: http://sift.jcvi.org/

UMD Predictor: http://umd-predictor.eu/

Functional Analysis through Hidden Markov Models V.2.3: http://fathmm.biocompute.org.uk/

Splice Site Prediction by Neural Network (NNSplice): https://www.fruitfly.org/seq_tools/splice.html

NetGene2 server: http://www.cbs.dtu.dk/services/NetGene2/

Human Splicing Finder: http://www.umd.be/HSF/

CADD: https://cadd.gs.washington.edu/

Greater Middle East Variome Project: http://igm.ucsd.edu/gme/

ACCESSION NUMBERS

The RNA-seq data have been deposited in the Gene Expression Omnibus database under accession number GSE156898.

Author affiliations
[1]Center for Integrative Genomics, University of Lausanne, Lausanne, Switzerland
[2]Department of Neuromuscular Disorders, Queen Square Institute of Neurology, University College London, London, UK
[3]Cardiovascular Assessment Facility, University of Lausanne, Lausanne, Switzerland
[4]Bioinformatics Competence Center, University of Lausanne, Lausanne, Switzerland
[5]Service de Génétique, Hopital Femme Mere Enfant, Bron, France
[6]Department of Pediatric Neurology, The Children's Hospital and Institute of Child Health, Lahore, Pakistan
[7]Department of Paediatric Neurology, Children's Hospital and Institute of Child Health, Multan, Pakistan
[8]Department of Developmental-Behavioural Paediatrics, The Children's Hospital and Institute of Child Health, Lahore, Pakistan
[9]Clinical Genetics Department, Human Genetics and Genome Research Division, National Research Centre, Cairo, Egypt
[10]Department of Neuroscience and Pediatrics, Howard Hughes Medical Institute, La Jolla, California, USA
[11]Department of Genetics, Faculty of Science, Shahid Chamran University of Ahvaz, Ahwaz, Iran (the Islamic Republic of)
[12]Department of Medical Genetics, Faculty of Medicine, Ahvaz Jondishapour University of Medical Sciences, Ahvaz, Iran (the Islamic Republic of)
[13]Health Research Institute, Diabetes Research Center, Ahvaz Jundishapur University of medical Sciences, Ahvaz, Iran (the Islamic Republic of)
[14]Service de Genetique, Hospices Civils de Lyon, Lyon, France
[15]Metabolic Diseases Branch/NIDDK, National Institutes of Health, Bethesda, MD, USA
[16]Experimental Cardiology Unit, Department of Cardiovascular Medicine, University of Lausanne, Lausanne, Switzerland

Twitter Pasquelena De Nittis @EDN_88 and Nicolas Chatron @NicoChatron

Acknowledgements We thank the probands and their families for their participation in this study and Jacques S Beckmann for comments. We are grateful to the Genomics Technologies Facility of the University of Lausanne and the Transgenic Core Facility of the EPFL.

Collaborators SYNAPS Study Group: Stanislav Groppa, Blagovesta Marinova Karashova, Wolfgang Nachbauer, Sylvia Boesch, Larissa Arning, Dagmar Timmann, Bru Cormand, Belen Pérez-Dueñas, Jatinder S Goraya, Tipu Sultan, Jun Mine, Daniela Avdjieva, Hadil Kathom, Radka Tincheva, Selina Banu, Mercedes Pineda-Marfa, Pierangelo Veggiotti, Michel D. Ferrari, Arn M. J. M. van den Maagdenberg, Alberto Verrotti, Giangluigi Marseglia, Salvatore Savasta, Mayte García-Silva, Alfons Macaya Ruiz, Barbara Garavaglia, Eugenia Borgione, Simona Portaro, Benigno Monteagudo Sanchez, Richard Boles, Savvas Papacostas, Michail Vikelis, Eleni Zamba Papanicolaou, Efthymios Dardiotis, Shazia Maqbool, Shahnaz Ibrahim, Salman Kirmani, Nuzhat Noureen Rana, Osama Atawneh, George Koutsis, Salvatore Mangano, Carmela Scuderi, Eugenia Borgione, Giovanna Morello, Tanya Stojkovic, Massimo Zollo, Gali Heimer, Yves A. Dauvilliers, Pasquale Striano, Issam Al-Khawaja, Fuad Al-Mutairi, Hamed Sherifa.

Contributors PDN and AR conceived and directed the study. SE, AP, TS, JRA, ZuR, FZ, NR, FR, NA, SM, MSZ, JGG, DM, HG, GS, NM, ASe, GL, NC, VDS, MC, RM and HH recruited the patients, gathered clinical information, prepared samples, and performed whole-exome and mutational analysis. PDN, ASa and JC carried out the other experiments. NG performed structural modeling of GNB5 variants. ASa, TP, PDN and AR designed the mouse experiments. ASa, with the help of PDN, conducted the mouse experiments. PDN and ASa performed statistical analysis and analysed the data. WFS provided Gnb5 knockout mouse model. PDN and AR wrote the manuscript. All authors reviewed and approved the manuscript.

Funding This work was supported by grants from the Swiss National Science Foundation (31003A_182632) and the Jérôme Lejeune Foundation to AR, the MRC (MR/S01165X/1, MR/S005021/1, G0601943), Rosetree Trust, Ataxia UK, MSA Trust, Brain Research UK, Sparks GOSH Charity, Muscular Dystrophy UK (MDUK) and Muscular Dystrophy Association (MDA USA) to HH. The families (R-V and Z) were collected as part of the SYNaPS Study Group collaboration funded by The Wellcome Trust and strategic award (Synaptopathies) funding (WT093205 MA and WT104033AIA). Their assessment was conducted as part of the Queen Square Genomics group at University College London, with support from the National

Institute for Health Research University College London Hospitals Biomedical Research Centre.

Competing interests None declared.

Patient consent for publication Not required.

Ethics approval Maintenance and mouse experimental procedures were approved by institutional and Swiss Federal Veterinary Office (experimental protocol VD3289.c).

Provenance and peer review Not commissioned; externally peer reviewed.

Data availability statement Data are available in a public, open access repository. The RNA-seq data have been deposited in the Gene Expression Omnibus database under accession number GSE156898.

Author note The Twitter account of Pasquelena De Nittis is wrong it is "@elena_denittis"

ORCID iDs
Pasquelena De Nittis http://orcid.org/0000-0001-7144-8425
Maha S Zaki http://orcid.org/0000-0001-7840-0002
Joseph G Gleeson http://orcid.org/0000-0002-0889-9220

REFERENCES

1 Lodder EM, De Nittis P, Koopman CD, Wiszniewski W, Moura de Souza CF, Lahrouchi N, Guex N, Napolioni V, Tessadori F, Beekman L, Nannenberg EA, Boualla L, Blom NA, de Graaff W, Kamermans M, Cocciadiferro D, Malerba N, Mandriani B, Coban Akdemir ZH, Fish RJ, Eldomery MK, Ratbi I, Wilde AAM, de Boer T, Simonds WF, Neerman-Arbez M, Sutton VR, Kok F, Lupski JR, Reymond A, Bezzina CR, Bakkers J, Merla G. GNB5 mutations cause an autosomal-recessive multisystem syndrome with sinus bradycardia and cognitive disability. *Am J Hum Genet* 2016;99:786.
2 Shamseldin HE, Masuho I, Alenizi A, Alyamani S, Patil DN, Ibrahim N, Martemyanov KA, Alkuraya FS. GNB5 mutation causes a novel neuropsychiatric disorder featuring attention deficit hyperactivity disorder, severely impaired language development and normal cognition. *Genome Biol* 2016;17:195.
3 Malerba N, Towner S, Keating K, Squeo GM, Wilson W, Merla G. A NGS-Targeted Autism/ID panel reveals compound heterozygous GNB5 variants in a novel patient. *Front Genet* 2018;9:626.
4 Poke G, King C, Muir A, de Valles-Ibáñez G, Germano M, Moura de Souza CF, Fung J, Chung B, Fung CW, Mignot C, Ilea A, Keren B, Vermersch A-I, Davis S, Stanley T, Moharir M, Kannu P, Shao Z, Malerba N, Merla G, Mefford HC, Scheffer IE, Sadleir LG. The epileptology of GNB5 encephalopathy. *Epilepsia* 2019;60:e121–7.
5 Shao Z, Tumber A, Maynes J, Tavares E, Kannu P, Heon E, Vincent A. Unique retinal signaling defect in GNB5-related disease. *Doc Ophthalmol* 2020;140:273-277.
6 Turkdogan D, Usluer S, Akalin F, Agyuz U, Aslan ES. Familial early infantile epileptic encephalopathy and cardiac conduction disorder: a rare cause of SUDEP in infancy. *Seizure* 2017;50:171–2.
7 Veerman CC, Mengarelli I, Koopman CD, Wilders R, van Amersfoorth SC, Bakker D, Wolswinkel R, Hababa M, de Boer TP, Guan K, Milnes J, Lodder EM, Bakkers J, Verkerk AO, Bezzina CR. Genetic variation in i>i>GNB5i>i> causes bradycardia by augmenting the cholinergic response via increased acetylcholine-activated potassium current (i>Ii>$_{K,ACh}$). *Dis Model Mech* 2019;12. doi:10.1242/dmm.037994. [Epub ahead of print: 09 07 2019].
8 Vernon H, Cohen J, De Nittis P, Fatemi A, McClellan R, Goldstein A, Malerba N, Guex N, Reymond A, Merla G. Intellectual developmental disorder with cardiac arrhythmia syndrome in a child with compound heterozygous GNB5 variants. *Clin Genet* 2018;93:1254–6.
9 Tang M, Wang Y, Xu Y, Tong W, Jin D, Yang X-A. IDDCA syndrome in a Chinese infant due to GNB5 biallelic mutations. *J Hum Genet* 2020;65:627-631.
10 Yazdani S, Badjatiya A, Dorrani N, Lee H, Grody WW, Nelson SF, Dipple KM. Genetic characterization and long-term management of severely affected siblings with intellectual developmental disorder with cardiac arrhythmia syndrome. *Mol Genet Metab Rep* 2020;23:100582.
11 Nini L, Zhang J-H, Pandey M, Panicker LM, Simonds WF. Expression of the Gβ5/R7-RGS protein complex in pituitary and pancreatic islet cells. *Endocrine* 2012;42:214–7.
12 Sánchez-Blázquez P, Rodríguez-Díaz M, López-Fando A, Rodríguez-Muñoz M, Garzón J. The GBeta5 subunit that associates with the R7 subfamily of RGS proteins regulates mu-opioid effects. *Neuropharmacology* 2003;45:82–95.
13 Sondek J, Siderovski DP, gamma-like G. Ggamma-like (GGL) domains: new frontiers in G-protein signaling and beta-propeller scaffolding. *Biochem Pharmacol* 2001;61:1329–37.
14 Witherow DS, Slepak VZ. A novel kind of G protein heterodimer: the G beta 5-RGS complex. *Receptor Channel* 2003;9:205–12.
15 Xie K, Allen KL, Kourrich S, Colón-Saez J, Thomas MJ, Wickman K, Martemyanov KA. Gbeta5 recruits R7 RGS proteins to GIRK channels to regulate the timing of neuronal inhibitory signaling. *Nat Neurosci* 2010;13:661–3.
16 Xie K, Ge S, Collins VE, Haynes CL, Renner KJ, Meisel RL, Lujan R, Martemyanov KA. Gβ5-RGS complexes are gatekeepers of hyperactivity involved in control of multiple neurotransmitter systems. *Psychopharmacology* 2012;219:823–34.
17 Posokhova E, Wydeven N, Allen KL, Wickman K, Martemyanov KA. RGS6/Gβ5 complex accelerates IKACh gating kinetics in atrial myocytes and modulates parasympathetic regulation of heart rate. *Circ Res* 2010;107:1350–4.
18 Chen C-K, Eversole-Cire P, Zhang H, Mancino V, Chen Y-J, He W, Wensel TG, Simon MI. Instability of GGL domain-containing RGS proteins in mice lacking the G protein beta-subunit Gbeta5. *Proc Natl Acad Sci U S A* 2003;100:6604–9.
19 Krispel CM, Chen C-K, Simon MI, Burns ME. Prolonged photoresponses and defective adaptation in rods of Gbeta5-/- mice. *J Neurosci* 2003;23:6965–71.
20 Rao A, Dallman R, Henderson S, Chen C-K. Gbeta5 is required for normal light responses and morphology of retinal on-bipolar cells. *J Neurosci* 2007;27:14199–204.
21 Wang Q, Levay K, Chanturiya T, Dvoriantchikova G, Anderson KL, Bianco SDC, Ueta CB, Molano RD, Pileggi A, Gurevich EV, Gavrilova O, Slepak VZ. Targeted deletion of one or two copies of the G protein β subunit Gβ5 gene has distinct effects on body weight and behavior in mice. *Faseb J* 2011;25:3949–57.
22 Zhang J-H, Pandey M, Seigneur EM, Panicker LM, Koo L, Schwartz OM, Chen W, Chen C-K, Simonds WF. Knockout of G protein β5 impairs brain development and causes multiple neurologic abnormalities in mice. *J Neurochem* 2011;119:544–54.
23 Mencacci NE, Kamsteeg E-J, Nakashima K, R'Bibo L, Lynch DS, Balint B, Willemsen MAAP, Adams ME, Wiethoff S, Suzuki K, Davies CH, Ng J, Meyer E, Veneziano L, Giunti P, Hughes D, Raymond FL, Carecchio M, Zorzi G, Nardocci N, Barzaghi C, Garavaglia B, Salpietro V, Hardy J, Pittman AM, Houlden H, Kurian MA, Kimura H, Vissers LELM, Wood NW, Bhatia KP. De novo mutations in PDE10A cause childhood-onset chorea with bilateral striatal lesions. *Am J Hum Genet* 2016;98:763–71.
24 Andrews S. *FastQC: a quality control tool for high throughput sequence data*, 2010.
25 Makrythanasis P, Maroofian R, Stray-Pedersen A, Musaev D, Zaki MS, Mahmoud IG, Selim L, Elbadawy A, Jhangiani SN, Coban Akdemir ZH, Gambin T, Sorte HS, Heiberg A, McEvoy-Venneri J, James KN, Stanley V, Belandres D, Guipponi M, Santoni FA, Ahangari N, Tara F, Doosti M, Iwaszkiewicz J, Zoete V, Backe PH, Hamamy H, Gleeson JG, Lupski JR, Karimiani EG, Antonarakis SE. Biallelic variants in KIF14 cause intellectual disability with microcephaly. *Eur J Hum Genet* 2018;26:330–9.
26 Truett GE, Heeger P, Mynatt RL, Truett AA, Walker JA, Warman ML. Preparation of PCR-quality mouse genomic DNA with hot sodium hydroxide and tris (HotSHOT). *Biotechniques* 2000;29:52–4.
27 Mitchell GF, Jeron A, Koren G. Measurement of heart rate and Q-T interval in the conscious mouse. *Am J Physiol* 1998;274:H747–51.
28 Thireau J, Zhang BL, Poisson D, Babuty D. Heart rate variability in mice: a theoretical and practical guide. *Exp Physiol* 2008;93:83–94.
29 Martin M. Cutadapt removes adapter sequences from high-throughput sequencing reads. *EMBnet Journal* 2011;17.
30 Davis MPA, van Dongen S, Abreu-Goodger C, Bartonicek N, Enright AJ. Kraken: a set of tools for quality control and analysis of high-throughput sequence data. *Methods* 2013;63:41–9.
31 Dobin A, Davis CA, Schlesinger F, Drenkow J, Zaleski C, Jha S, Batut P, Chaisson M, Gingeras TR. STAR: ultrafast universal RNA-seq aligner. *Bioinformatics* 2013;29:15–21.
32 Anders S, Pyl PT, Huber W. HTSeq--a Python framework to work with high-throughput sequencing data. *Bioinformatics* 2015;31:166–9.
33 Wang L, Wang S, Li W. RSeQC: quality control of RNA-Seq experiments. *Bioinformatics* 2012;28:2184–5.
34 Li B, Dewey CN. RSEM: accurate transcript quantification from RNA-Seq data with or without a reference genome. *BMC Bioinformatics* 2011;12:323.
35 Love MI, Huber W, Anders S. Moderated estimation of fold change and dispersion for RNA-Seq data with DESeq2. *Genome Biol* 2014;15:550.
36 Yu G, Wang L-G, Han Y, He Q-Y. clusterProfiler: an R package for comparing biological themes among gene clusters. *OMICS* 2012;16:284–7.
37 Sobreira N, Schiettecatte F, Boehm C, Valle D, Hamosh A. New tools for Mendelian disease gene identification: PhenoDB variant analysis module; and GeneMatcher, a web-based tool for linking investigators with an interest in the same gene. *Hum Mutat* 2015;36:425–31.

38 Sobreira N, Schiettecatte F, Valle D, Hamosh A. GeneMatcher: a matching tool for connecting investigators with an interest in the same gene. *Hum Mutat* 2015;36:928–30.
39 Karczewski KJ, Francioli LC, Tiao G, Cummings BB, Alföldi J, Wang Q, Collins RL, Laricchia KM, Ganna A, Birnbaum DP. Variation across141,456 human exomes and genomes reveals the spectrum of loss-of-functionintolerance across human protein-coding genes. *bioRxiv* 2019;531210.
40 Cheever ML, Snyder JT, Gershburg S, Siderovski DP, Harden TK, Sondek J. Crystal structure of the multifunctional Gbeta5-RGS9 complex. *Nat Struct Mol Biol* 2008;15:155–62.
41 Guex N, Peitsch MC. SWISS-MODEL and the Swiss-PdbViewer: an environment for comparative protein modeling. *Electrophoresis* 1997;18:2714–23.
42 Scott EM, Halees A, Itan Y, Spencer EG, He Y, Azab MA, Gabriel SB, Belkadi A, Boisson B, Abel L, Clark AG, Alkuraya FS, Casanova J-L, Gleeson JG, Greater Middle East Variome Consortium. Characterization of greater middle Eastern genetic variation for enhanced disease gene discovery. *Nat Genet* 2016;48:1071–6.
43 Kurhanewicz N, Ledbetter A, Farraj A, Hazari M. TRPA1 mediates the cardiac effects of acrolein through parasympathetic dominance but also sympathetic modulation in mice. *Toxicol Appl Pharmacol* 2018;347:104–14.
44 Witten DM. Classification and clustering of sequencing data using a poisson model. *Ann Appl Stat* 2011;5:2493–518.
45 Frey N, Luedde M, Katus HA. Mechanisms of disease: hypertrophic cardiomyopathy. *Nat Rev Cardiol* 2011;9:91–100.
46 Chambers JC, Zhao J, Terracciano CMN, Bezzina CR, Zhang W, Kaba R, Navaratnarajah M, Lotlikar A, Sehmi JS, Kooner MK, Deng G, Siedlecka U, Parasramka S, El-Hamamsy I, Wass MN, Dekker LRC, de Jong JSSG, Sternberg MJE, McKenna W, Severs NJ, de Silva R, Wilde AAM, Anand P, Yacoub M, Scott J, Elliott P, Wood JN, Kooner JS. Genetic variation in SCN10A influences cardiac conduction. *Nat Genet* 2010;42:149–80.
47 Brody MJ, Lee Y. The role of leucine-rich repeat containing protein 10 (LRRC10) in dilated cardiomyopathy. *Front Physiol* 2016;7:337.
48 Pappas CT, Mayfield RM, Henderson C, Jamilpour N, Cover C, Hernandez Z, Hutchinson KR, Chu M, Nam K-H, Valdez JM, Wong PK, Granzier HL, Gregorio CC. Knockout of Lmod2 results in shorter thin filaments followed by dilated cardiomyopathy and juvenile lethality. *Proc Natl Acad Sci U S A* 2015;112:13573–8.
49 Brody MJ, Hacker TA, Patel JR, Feng L, Sadoshima J, Tevosian SG, Balijepalli RC, Moss RL, Lee Y. Ablation of the cardiac-specific gene leucine-rich repeat containing 10 (Lrrc10) results in dilated cardiomyopathy. *PLoS One* 2012;7:e51621.
50 Ahrens-Nicklas RC, Pappas CT, Farman GP, Mayfield RM, Larrinaga TM, Medne L, Ritter A, Krantz ID, Murali C, Lin KY, Berger JH, Yum SW, Carreon CK, Gregorio CC. Disruption of cardiac thin filament assembly arising from a mutation in *LMOD2*: A novel mechanism of neonatal dilated cardiomyopathy. *Sci Adv* 2019;5:eaax2066.
51 Kapoor N, Liang W, Marbán E, Cho HC. Direct conversion of quiescent cardiomyocytes to pacemaker cells by expression of Tbx18. *Nat Biotechnol* 2013;31:54–62.
52 Huertas E, Bühler K-M, Echeverry-Alzate V, Giménez T, López-Moreno JA. C957T polymorphism of the dopamine D2 receptor gene is associated with motor learning and heart rate. *Genes Brain Behav* 2012;11:677–83.
53 Hernández-Ochoa EO, Pratt SJP, Lovering RM, Schneider MF. Critical role of intracellular RyR1 calcium release channels in skeletal muscle function and disease. *Front Physiol* 2015;6:420.
54 Hong K-W, Shin D-J, Lee S-H, Son N-H, Go M-J, Lim J-E, Shin C, Jang Y, Oh B. Common variants in RyR1 are associated with left ventricular hypertrophy assessed by electrocardiogram. *Eur Heart J* 2012;33:1250–6.
55 Watson AJ, Aragay AM, Slepak VZ, Simon MI. A novel form of the G protein beta subunit Gbeta5 is specifically expressed in the vertebrate retina. *J Biol Chem* 1996;271:28154–60.
56 Watson AJ, Katz A, Simon MI. A fifth member of the mammalian G-protein beta-subunit family. Expression in brain and activation of the beta 2 isotype of phospholipase C. *J Biol Chem* 1994;269:22150–6.
57 Xie K, Masuho I, Brand C, Dessauer CW, Martemyanov KA. The complex of G protein regulator RGS9-2 and Gβ(5) controls sensitization and signaling kinetics of type 5 adenylyl cyclase in the striatum. *Sci Signal* 2012;5:ra63.
58 Strehlow V, Heyne HO, Vlaskamp DRM, Marwick KFM, Rudolf G, de Bellescize J, Biskup S, Brilstra EH, Brouwer OF, Callenbach PMC, Hentschel J, Hirsch E, Kind PC, Mignot C, Platzer K, Rump P, Skehel PA, Wyllie DJA, Hardingham GE, van Ravenswaaij-Arts CMA, Lesca G, Lemke JR, GAs group, GRIN2A study group. GRIN2A-related disorders: genotype and functional consequence predict phenotype. *Brain* 2019;142:80–92.
59 Bansod S, Kageyama R, Ohtsuka T. Hes5 regulates the transition timing of neurogenesis and gliogenesis in mammalian neocortical development. *Development* 2017;144:3156–67.
60 Lee KE, Seo J, Shin J, Ji EH, Roh J, Kim JY, Sun W, Muhr J, Lee S, Kim J. Positive feedback loop between Sox2 and SOX6 inhibits neuronal differentiation in the developing central nervous system. *Proc Natl Acad Sci U S A* 2014;111:2794–9.
61 Wycisk KA, Zeitz C, Feil S, Wittmer M, Forster U, Neidhardt J, Wissinger B, Zrenner E, Wilke R, Kohl S, Berger W. Mutation in the auxiliary calcium-channel subunit CACNA2D4 causes autosomal recessive cone dystrophy. *Am J Hum Genet* 2006;79:973–7.
62 Bamshad MJ, Nickerson DA, Chong JX. Mendelian gene discovery: fast and Furious with no end in sight. *Am J Hum Genet* 2019;105:448–55.
63 Vissers LELM, Gilissen C, Veltman JA. Genetic studies in intellectual disability and related disorders. *Nat Rev Genet* 2016;17:9–18.
64 Arno G, Holder GE, Chakarova C, Kohl S, Pontikos N, Fiorentino A, Plagnol V, Cheetham ME, Hardcastle AJ, Webster AR, Michaelides M, UK Inherited Retinal Disease Consortium. Recessive retinopathy consequent on mutant G-protein β subunit 3 (GNB3). *JAMA Ophthalmol* 2016;134:924–7.
65 Endo W, Ikemoto S, Togashi N, Miyabayashi T, Nakajima E, Hamano S-I, Shibuya M, Sato R, Takezawa Y, Okubo Y, Inui T, Kato M, Sengoku T, Ogata K, Hamanaka K, Mizuguchi T, Miyatake S, Nakashima M, Matsumoto N, Haginoya K. Phenotype-Genotype correlations in patients with GNB1 gene variants, including the first three reported Japanese patients to exhibit spastic diplegia, dyskinetic quadriplegia, and infantile spasms. *Brain Dev* 2020;42.
66 Fukuda T, Hiraide T, Yamoto K, Nakashima M, Kawai T, Yanagi K, Ogata T, Saitsu H. Exome reports a de novo GNB2 variant associated with global developmental delay, intellectual disability, and dysmorphic features. *Eur J Med Genet* 2019;103804.
67 Hemati P, Revah-Politi A, Bassan H, Petrovski S, Bilancia CG, Ramsey K, Griffin NG, Bier L, Cho MT, Rosello M, Lynch SA, Colombo S, Weber A, Haug M, Heinzen EL, Sands TT, Narayanan V, Primiano M, Aggarwal VS, Millan F, Sattler-Holtrop SG, Caro-Llopis A, Pillar N, Baker J, Freedman R, Kroes HY, Sacharow S, Stong N, Lapunzina P, Schneider MC, Mendelsohn NJ, Singleton A, Loik Ramey V, Wou K, Kuzminsky A, Monfort S, Weiss M, Doyle S, Iglesias A, Martinez F, Mckenzie F, Orellana C, van Gassen KLI, Palomares M, Bazak L, Lee A, Bircher A, Basel-Vanagaite L, Hafström M, Houge G, Goldstein DB, Anyane-Yeboa K, Ramey LV, C4RCD Research Group, DDD study. Refining the phenotype associated with GNB1 mutations: clinical data on 18 newly identified patients and review of the literature. *Am J Med Genet A* 2018;176:2259–75.
68 Jones HF, Morales-Briceño H, Barwick K, Lewis J, Sanchis-Juan A, Raymond FL, Stewart K, Waugh M-C, Mahant N, Kurian MA, Dale RC, Mohammad SS. Myoclonus-dystonia caused by GNB1 mutation responsive to deep brain stimulation. *Mov Disord* 2019;34:1079–80.
69 Kuß J, Stallmeyer B, Goldstein M, Rinné S, Pees C, Zumhagen S, Seebohm G, Decher N, Pott L, Kienitz M-C, Schulze-Bahr E. Familial sinus node disease caused by a gain of GIRK (G-Protein Activated Inwardly Rectifying K^+ Channel) channel function. *Circ Genom Precis Med* 2019;12:e002238.
70 Laššuthová P, Šafka Brožková D, Neupauerová J, Krůtová M, Mazanec R, Seeman P. Confirmation of the GNB4 gene as causal for Charcot-Marie-Tooth disease by a novel de novo mutation in a Czech patient. *Neuromuscul Disord* 2017;27:57–60.
71 Lohmann K, Masuho I, Patil DN, Baumann H, Hebert E, Steinrücke S, Trujillano D, Skamangas NK, Dobricic V, Hüning I, Gillessen-Kaesbach G, Westenberger A, Savic-Pavicevic D, Münchau A, Oprea G, Klein C, Rolfs A, Martemyanov KA. Novel GNB1 mutations disrupt assembly and function of G protein heterotrimers and cause global developmental delay in humans. *Hum Mol Genet* 2017;26:1078–86.
72 Malerba N, De Nittis P, Merla G. The emerging role of Gβ subunits in human genetic diseases. *Cells* 2019;8. doi:10.3390/cells8121567. [Epub ahead of print: 04 12 2019].
73 Miura S, Morikawa T, Fujioka R, Noda K, Kosaka K, Taniwaki T, Shibata H. A novel missense variant (Gln220Arg) of GNB4 encoding guanine nucleotide-binding protein, subunit beta-4 in a Japanese family with autosomal dominant motor and sensory neuropathy. *Eur J Med Genet* 2017;60:474–8.
74 Peng J, Wang Y, He F, Chen C, Wu L-W, Yang L-F, Ma Y-P, Zhang W, Shi Z-Q, Chen C, Xia K, Guo H, Yin F, Pang N. Novel West syndrome candidate genes in a Chinese cohort. *CNS Neurosci Ther* 2018;24:1196–206.
75 Petrovski S, Küry S, Myers CT, Anyane-Yeboa K, Cogné B, Bialer M, Xia F, Hemati P, Riviello J, Mehaffey M, Besnard T, Becraft E, Wadley A, Politi AR, Colombo S, Zhu X, Ren Z, Andrews I, Dudding-Byth T, Schneider AL, Wallace G, Rosen ABI, Schelley S, Enns GM, Corre P, Dalton J, Mercier S, Latypova X, Schmitt S, Guzman E, Moore C, Bier L, Heinzen EL, Karachunski P, Shur N, Grebe T, Basinger A, Nguyen JM, Bézieau S, Wierenga K, Bernstein JA, Scheffer IE, Rosenfeld JA, Mefford HC, Isidor B, Goldstein DB. Germline de novo mutations in GNB1 cause severe neurodevelopmental disability, hypotonia, and seizures. *Am J Hum Genet* 2016;98:1001–10.
76 Soong B-W, Huang Y-H, Tsai P-C, Huang C-C, Pan H-C, Lu Y-C, Chien H-J, Liu T-T, Chang M-H, Lin K-P, Tu P-H, Kao L-S, Lee Y-C. Exome sequencing identifies GNB4 mutations as a cause of dominant intermediate Charcot-Marie-Tooth disease. *Am J Hum Genet* 2013;92:422–30.
77 Steinrücke S, Lohmann K, Domingo A, Rolfs A, Bäumer T, Spiegler J, Hartmann C, Münchau A. Novel GNB1 missense mutation in a patient with generalized dystonia, hypotonia, and intellectual disability. *Neurol Genet* 2016;2:e106.
78 Szczałuba K, Biernacka A, Szymańska K, Gasperowicz P, Kosińska J, Rydzanicz M, Płoski R. Novel GNB1 de novo mutation in a patient with neurodevelopmental disorder and cutaneous mastocytosis: clinical report and literature review. *Eur J Med Genet* 2018;61:157–60.
79 Vincent A, Audo I, Tavares E, Maynes JT, Tumber A, Wright T, Li S, Michiels C, Condroyer C, MacDonald H, Verdet R, Sahel J-A, Hamel CP, Zeitz C, Héon E, GNB3 Consortium. Biallelic mutations in GNB3 cause a unique form of autosomal-recessive congenital stationary night blindness. *Am J Hum Genet* 2016;98:1011–9.
80 Patil DN, Rangarajan ES, Novick SJ, Pascal BD, Kojetin DJ, Griffin PR, Izard T, Martemyanov KA. Structural organization of a major neuronal G protein regulator, the

RGS7-Gβ5-R7BP complex. *Elife* 2018;7. doi:10.7554/eLife.42150. [Epub ahead of print: 12 12 2018].
81 Sciacca FL, Ciaccio C, Fontana F, Strano C, Gilardoni F, Pantaleoni C, D'Arrigo S. Severe Phenotype in a Patient With Homozygous 15q21.2 Microdeletion Involving *BCL2L10*, *GNB5*, and *MYO5C* Genes, Resembling Infantile Developmental Disorder With Cardiac Arrhythmias (IDDCA). *Front Genet* 2020;11:399.
82 Lei Q, Jones MB, Talley EM, Garrison JC, Bayliss DA. Molecular mechanisms mediating inhibition of G protein-coupled inwardly-rectifying K+ channels. *Mol Cells* 2003;15:1–9.
83 Okae H, Iwakura Y. Neural tube defects and impaired neural progenitor cell proliferation in Gbeta1-deficient mice. *Dev Dyn* 2010;239:1089–101.
84 Ye Y, Sun Z, Guo A, Song L-S, Grobe JL, Chen S. Ablation of the GNB3 gene in mice does not affect body weight, metabolism or blood pressure, but causes bradycardia. *Cell Signal* 2014;26:2514–20.
85 Dickinson ME, Flenniken AM, Ji X, Teboul L, Wong MD, White JK, Meehan TF, Weninger WJ, Westerberg H, Adissu H, Baker CN, Bower L, Brown JM, Caddle LB, Chiani F, Clary D, Cleak J, Daly MJ, Denegre JM, Doe B, Dolan ME, Edie SM, Fuchs H, Gailus-Durner V, Galli A, Gambadoro A, Gallegos J, Guo S, Horner NR, Hsu C-W, Johnson SJ, Kalaga S, Keith LC, Lanoue L, Lawson TN, Lek M, Mark M, Marschall S, Mason J, McElwee ML, Newbigging S, Nutter LMJ, Peterson KA, Ramirez-Solis R, Rowland DJ, Ryder E, Samocha KE, Seavitt JR, Selloum M, Szoke-Kovacs Z, Tamura M, Trainor AG, Tudose I, Wakana S, Warren J, Wendling O, West DB, Wong L, Yoshiki A, MacArthur DG, Tocchini-Valentini GP, Gao X, Flicek P, Bradley A, Skarnes WC, Justice MJ, Parkinson HE, Moore M, Wells S, Braun RE, Svenson KL, de Angelis MH, Herault Y, Mohun T, Mallon A-M, Henkelman RM, Brown SDM, Adams DJ, Lloyd KCK, McKerlie C, Beaudet AL, Bućan M, Murray SA, Consortium IMP, International Mouse Phenotyping Consortium, Jackson Laboratory, Infrastructure Nationale PHENOMIN, Institut Clinique de la Souris (ICS), Charles River Laboratories, MRC Harwell, Toronto Centre for Phenogenomics, Wellcome Trust Sanger Institute, RIKEN BioResource Center. High-Throughput discovery of novel developmental phenotypes. *Nature* 2016;537:508-+:514.
86 Chograni M, Alkuraya FS, Maazoul F, Lariani I, Chaabouni-Bouhamed H. RGS6: a novel gene associated with congenital cataract, mental retardation, and microcephaly in a Tunisian family. *Invest Ophthalmol Vis Sci* 2014;56:1261–6.

Appendix: Consortia and networks involved in this study

Full details are available below.

The Synaptopathies and Paroxysmal Syndromes (SYNaPS) Study Group (http://neurogenetics.co.uk/synaptopathies-synaps/):

Stanislav Groppa, Blagovesta Marinova Karashova, Wolfgang Nachbauer, Sylvia Boesch, Larissa Arning, Dagmar Timmann, Bru Cormand, Belen Pérez-Dueñas, Jatinder S. Goraya,, Tipu Sultan, Jun Mine, Daniela Avdjieva, Hadil Kathom, Radka Tincheva, Selina Banu, Mercedes Pineda-Marfa, Pierangelo Veggiotti, Michel D. Ferrari, Arn M. J. M. van den Maagdenberg, Alberto Verrotti, Giangluigi Marseglia, Salvatore Savasta, Mayte García-Silva, Alfons Macaya Ruiz, Barbara Garavaglia, Eugenia Borgione, Simona Portaro, Benigno Monteagudo Sanchez, Richard Boles, Savvas Papacostas, Michail Vikelis, Eleni Zamba Papanicolaou, Efthymios Dardiotis, Shazia Maqbool, Shahnaz Ibrahim, Salman Kirmani, Nuzhat Noureen Rana, Osama Atawneh, George Koutsis, Salvatore Mangano, Carmela Scuderi, Eugenia Borgione, Giovanna Morello, Tanya Stojkovic, Massimo Zollo, Gali Heimer, Yves A. Dauvilliers, Pasquale Striano, Issam Al-Khawaja, Fuad Al-Mutairi, Hamed Sherifa.

Study Group Members:

Prof Stanislav Groppa

Affiliation: Department of Neurology and Neurosurgery, Institute of Emergency Medicine, Chisinau, Republic of Moldova.

Email: sgroppa@gmail.com

Dr. Blagovesta Marinova Karashova

Affiliation: Department of Paediatrics, Medical University of Sofia, Sofia 1431, Bulgaria

Email: blagovestakarashova@gmail.com

Dr. Wolfgang Nachbauer

Affiliation: Department of Neurology, Medical University Innsbruck, Anichstrasse 35, Innsbruck 6020, Austria

Email: Wolfgang.Nachbauer@i-med.ac.at

Prof. Sylvia Boesch

Affiliation: Department of Neurology, Medical University Innsbruck, Anichstrasse 35, Innsbruck 6020, Austria

Email: sylvia.boesch@i-med.ac.at

Dr. Larissa Arning

Affiliation: Department of Human Genetics, Ruhr-University Bochum, Bochum 44801, Germany

Email: Larissa.Arning@ruhr-uni-bochum.de

Prof. Dagmar Timmann

Affiliation: Braun Neurologische Universitätsklinik Universität Essen, Hufelandstr 55, Essen D-45122, Germany

Email: Dagmar.Timmann-Braun@uni-duisburg-essen.de

Prof. Bru Cormand

Affiliation: Department of Genetics, Universitat de Barcelona, Barcelona 08007, Spain

Email: bcormand@ub.edu

Dr. Belen Pérez-Dueñas

Affiliation: Hospital Sant Joan de Deu, Esplugues de Llobregat 08950, Barcelona, Spain

Email: bperez@sjdhospitalbarcelona.org

Dr Gabriella Di Rosa, MD, PhD

Affiliation: Department of Pediatrics, University of Messina, Messina 98123, Italy

Email: gdirosa@unime.it

Prof. Jatinder S. Goraya, MD, FRCP

Affiliation: Division of Paediatric Neurology, Dayanand Medical College & Hospital, Ludhiana, Punjab 141001, India

Email: gorayajs@gmail.com

Prof. Tipu Sultan

Affiliation: Division of Paediatric Neurology, Children's Hospital of Lahore, Lahore 381-D/2, Pakistan

Email: tipusultanmalik@hotmail.com

Prof Jun Mine

Affiliation: Department of Paediatrics, Shimane University, Faculty of Medicine, Izumo, 693-8501, Japan

Email: jmine@med.shimane-u.ac.jp

Prof. Daniela Avdjieva,

Affiliation: Department of Paediatrics, Medical University of Sofia, Sofia 1431, Bulgaria

Email: davdjieva@yahoo.com

Dr. Hadil Kathom,

Affiliation: Department of Pediatrics, Medical University of Sofia, Sofia 1431, Bulgaria

Email: hadilmk@gmail.com

Prof.Dr Radka Tincheva

Affiliation: Head of Department of Clinical Genetics, University Pediatric Hospital, Sofia 1431, Bulgaria

Email: radka.tincheva@gmail.com

Prof. Selina Banu

Affiliation: Neurosciences Unit, Institute of Child Health and Shishu Shastho Foundation Hospital, Mirpur, Dhaka 1216, Bangladesh

Email: selinabanu17@gmail.com

Prof. Mercedes Pineda-Marfa

Affiliation Servei de Neurologia Pediàtrica, l'Hospital Universitari Vall d'Hebron, Barcelona 08035, Spain

Email: pineda@hsjdbcn.org

Prof. Pierangelo Veggiotti

Affiliation: Unit of Infantile Neuropsychiatry Fondazione

Istituto Neurologico "C. Mondino" IRCCS, Via Mondino 2, Pavia 27100, Italy

Email: pierangelo.veggiotti@unipv.it

Prof. Michel D. Ferrari

Affiliation: Leiden University Medical Center, Albinusdreef 2, Leiden 2333, Netherlands

Email: M.D.Ferrari@lumc.nl

Prof. Alberto Verrotti

Affiliation: University of L'Aquila, L'Aquila, Italy

Email: verrottidipianella@univaq.it

Prof Giangluigi Marseglia

Affiliation: Department of Pediatrics, University of Pavia, IRCCS Policlinico "San Matteo", Pavia 27100, Italy

Email: gl.marseglia@smatteo.pv.it

Dr. Salvatore Savasta

Affiliation: Division of Pediatric Neurology, Department of Pediatrics, University of Pavia, IRCCS Policlinico "San Matteo", Pavia 27100, Italy

Email: S.Savasta@smatteo.pv.it

Dr. Mayte García-Silva

Affiliation: Hospital Universitario 12 de Octubre, Madrid 28041, Spain

Email: mgarciasilva@salud.madrid.org

Dr. Alfons Macaya Ruiz

Affiliation: University Hospital Vall d'Hebron, Barcelona 08035, Spain

Email: amacaya@vhebron.net

Prof. Barbara Garavaglia

Affiliation: IRCCS Foundation, Neurological Institute “Carlo Besta”, Molecular Neurogenetics, 20126 Milan, Italy

Email: segr.neurogenetica@istituto-besta.it

Dr. Eugenia Borgione

Affiliation: Laboratorio di Neuropatologia Clinica, U.O.S. Malattie, Neuromuscolari Associazione OASI Maria SS. ONLUS – IRCCS, Via Conte Ruggero 73, 94018 Troina, Italy

Email: eborgione@oasi.en.it

Dr. Simona Portaro

Affiliation: IRCCS Centro Neurolesi "Bonino Pulejo", SS113, c.da Casazza, 98124 Messina, Italy

Email: simonaportaro@hotmail.it

Dr. Benigno Monteagudo Sanchez

Affiliation: Hospital Arquitecto Marcide, Avenida de la Residencia S/N, Ferrol (A Coruña), 15401 Spain

Email: benims@hotmail.com

Dr. Richard Boles

Affiliation: Courtagen Life Sciences, 12 Gill Street Suite 3700, Woburn, MA 01801 USA

Email: Richard.Boles@courtagen.com

Prof. Savvas Papacostas

Affiliation: Neurology Clinic B, The Cyprus Institute of Neurology and Genetics, 6 International Airport Road, 1683 Nicosia, Cyprus

Email: savvas@cing.ac.cy

Dr. Michail Vikelis

Affiliation: Iatreio Kefalalgias Glyfadas, 8 Lazaraki str, 3rd floor, 16675, Athens, Greece

Email: mvikelis@headaches.gr

Prof Eleni Zamba Papanicolaou

Affiliation: The Cyprus Institute of Neurology & Genetics, Nicosia, Cyprus

Email: ezamba@cing.ac.cy

Dr Efthymios Dardiotis

Affiliation: UNIVERSITY HOSPITAL OF LARISSA, NEUROLOGY Department, Greece

Email: edar@med.uth.gr

Prof Shazia Maqbool

Affiliation: Department of Developmental and Behavioral Pediatrics, CH&ICH, Lahore, Pakistan

Email: drshazimaq@yahoo.com

Prof Shahnaz Ibrahim

Affiliation: Department of Pediatrics and child health, Aga Khan University, Karachi, Pakistan

Email: shahnaz.ibrahim@aku.edu

Prof Salman Kirmani

Affiliation: Department of Paediatrics & Child Health, The Aga Khan University, Karachi , Pakistan

Email: salman.kirmani@aku.edu

Dr. Nuzhat Noureen Rana

Affiliation: Department of Paediatric Neurology, Children Hospital Complex and ICH, Multan, Pakistan

Email: drnuzhatrana@gmail.com

Dr. Osama Atawneh

Affiliation: Hilal Pediatric Hospital Hebron, Hebron West Bank, Palestine

Email: osamaat@gmail.com

Prof George Koutsis

Dr Marianthi Breza

Affiliation: Neurogenetics Unit, Neurology Department, Eginition Hospital, National and Kapodistrian University, Athens, Greece

Email: marianthibr@med.uoa.gr

Prof Salvatore Mangano

Affiliation: Unità di Neuropsichiatria Infantile, AOUP "P.Giaccone" Palermo, Italy

Email: salvatore.mangano@unipa.it

Dr Carmela Scuderi

Affiliation: Associazione Oasi Maria SS, 94018 Troina, Italy

Email: cscuderi@oasi.en.it

Dr Eugenia Borgione

Affiliation: Associazione Oasi Maria SS, 94018 Troina, Italy

Email: eborgione@oasi.en.it

Dr Giovanna Morello

Affiliation: Institute of Neurological Sciences, National Research Council, Mangone, Italy

Email: g.morello@isn.cnr.it

Dr Tanya Stojkovic

Affiliation: Institute of Myology, Hôpital La Pitié Salpêtrière, Paris, France

Email: stojkovic.tanya@aphp.fr

Prof Massimi Zollo

Affiliation: CEINGE, Biotecnologie Avanzate S.c.a.rl., Naples, Italy

Email: massimo.zollo@unina.it

Dr Gali Heimer

Affiliation: University Hospital of Tel Aviv, Tel Aviv, Israel

Email: galih.md@gmail.com

Prof Yves A. Dauvilliers

Affiliation: University Hospital Montpellier, Montpellier, France

Email: ydauvilliers@yahoo.fr

Prof Pasquale Striano

Affiliation: Institute “Giannina Gaslini”, Genova, Italy

Email: strianop@gmail.com

Dr Issam Al-Khawaja

Affiliation: Albashir University Hospital, Amman, Jordan

Email: isamkhawaja61@gmail.com

Dr Fuad Al-Mutairi

Affiliation: King Saud University, Riyadh, Saudi Arabia

Email: almutairifu@NGHA.MED.SA

Prof Hamed Sherifa

Affiliation: Assiut University Hospital, Assiut, Egypt

Email: hamed_sherifa@yahoo.com

Supplemental note: Case Reports

Family R

Family R (**Figure S1, Table 1, Supplementary Table S1**) is a Pakistani family from Lahore. The proband is an 8-month-old boy born from healthy consanguineous parents and with a healthy female sibling. He presented with global developmental delay characterized by intellectual disability (ID), severe hypotonia, and altered speech development. Physical examination of this child revealed respiratory stridor, macrocephaly and failure to thrive. The child has passed away in the last months. Cardiologic assessment was not performed prior.

Family S

Family S (**Figure S1, Table 1, Supplementary Table S1**) is a consanguineous Pakistani family from the Multan region with one affected 15-year-old boy who showed global developmental delay and flexor spasm seizures, kept under control with the administration of Valproic Acid. He was non-verbal and presented impaired verbal understanding too. He was hypotonic with no head control. He was thin, and showed nystagmus and gastric reflux.

Electroencephalogram (EEG) demonstrated modified hypsarrhythmia. Magnetic Resonance Imaging (MRI) revealed hypogenesis of the corpus callosum. He experienced episodes of breath holding spell.

Family T

Family T (**Figure S1, Table 1, Supplementary Table S1**) is a consanguineous Pakistani family from Lahore with two affected daughters. The older sister likely died of cardiac arrest. The younger sister is the proband. At 1.2-year of age, she showed global developmental delay, ID, nystagmus and no neck holding. She did not reach developmental milestones regarding lexical

production and verbal understanding. Holter monitoring revealed signs of sick sinus syndrome, with severe bradycardia at rest and prolonged sinus pauses.

Family U

Family U (**Figure S1, Table 1, Supplementary Table S1**) is a consanguineous Pakistani trio family from Lahore with an affected 1 year-old female child. Of the main IDDCA characteristics, the proband displayed ID, inability to hold her neck, and lack of eye contact. She also presented with Fatty Acid Oxidation disorder. MRI showed cerebral atrophy. Dysmorphic features of this individual included prominent philtral ridges, micrognathia, prominent ears and craniofacial disproportion.

Family V

Family V (**Figure S1, Table 1, Supplementary Table S1**) is a consanguineous Pakistani trio family from Lahore with an affected male child showing severe ID, developmental delay, hypotonia and seizures, kept under control with the administration of Epictam. He had no eye contact, no social smile and did not respond to his name. He presented with nystagmus and some dysmoprhic features (blond hair, frontal bossing, epicanthic folds, small palpebral fissure, depressed nasal bridge, high arched palate). Urinary organic acid and plasma amino acids were normal. Holter monitoring revealed a sinus rhythm with insignificant (<3 sec) sinus pauses.

Family W

Family W (**Figure S1, Table 1, Supplementary Table S1**) is a Tunisian family with one non-dysmorphic affected child and two healthy siblings born to consanguineous parents who are

first cousins. The affected 7-year old girl was born at term and weighed 2.9 kg (with a body height of 49 cm, and head circumference of 35 cm). She was delayed in her early developmental milestones and first walked at 31 months; she remains nonverbal with mild intellectual disability (a formal neuropsychological assessment was not performed). Growth parameters at evaluation (5 yo) include height and weight at 2 SD and head circumference at 3 SD. Neurologically, she demonstrated impaired fine motor skills. Both MRI and EEG failed to show anything abnormal. Electrocardiographic monitoring showed sinus-node dysfunction with sinus bradycardia, and prolonged sinus pauses.

At 21 months, she experienced an unexplained coma after a septic shock subsequent to a digestive tract infection. She also had an episode of pyelonephritis, concluded without complications. She had shorter thumbs, but no history of eye disease, nor gastric problems. Metabolic screening reported plasma amino acids imbalances with higher phenylalanine concentrations. Currently, her fine movements progressed with re-education, and she developed sign language; she is enrolled in a special education class.

Family history revealed a non-verbal paternal uncle with severe cognitive impairment with no diagnosis. Additionally, a maternal aunt, a maternal uncle and the son of another maternal aunt presented with severe neurodevelopmental problems, including speech impairment.

Family X

Family X (**Figure S1, Table 1, Supplementary Table S1**) is a consanguineous family from Egypt with one 2 year-old affected boy and two healthy girls. The parents have had a previously affected child who is now deceased (IV.8, Individual 39, **Figure S1, Supplementary Table S1**); his clinical findings were similar to the proband's phenotype (IV.10, Individual 38, **Figure S1, Supplementary Table S1**). Additionally, three of the couple's pregnancies resulted in

spontaneous miscarriages (IV.4, IV.7 and IV.9, **Figure S1**). Family history showed an affected cousin (IV.1, Individual 40, **Figure S1, Supplementary Table S1).**

The proband is a nonverbal child with severe ID and mild dysmorphic features including prominent forehead, synophrys, downslanting palpebral fissures, depressed nasal root and low-set ears. He presents with severe hypotonia and hyporeflexia; the child cannot use his hands or stand on his feet, and has no head support. MRI showed prominent ventricular system, mild occipitoparietal patchy white matter lesions, indicating dysmyelination. Additionally, the three affected family members presented retinal disease with mild affection of rods and cones functions. They developed epileptic tonic and focal seizures within the first year of life (7 months for individual 38, 1 year for individual 39 and 9 months for individual 40) treated with valproate and levetiracetam. Comprehensive cardiac evaluation was not carried out in the three individuals of these family.

Family Y

Family Y (**Figure S1, Table 1, Supplementary Table S1**) is a consanguineous Egyptian family with one 19-year-old affected girl and one 16-year-old affected boy. Both siblings are nonverbal individuals displaying severe ID, autistic behaviors, severe hypotonia, mild nystagmus and reduced eye pigmentation. Individual 41 (V.I, **Figure S1, Supplementary Table S1**) presents febrile seizures and an abnormal EEG; seizures were treated with valproate and carbamazepine antiepileptic drugs. Her brother (individual 42, V.II, **Figure S1, Supplementary Table S1**) developed generalized tonic-clonic seizures with cyanosis at 1 year of age; he is on valproate, carbamazepine and levetiracetam antiepileptic treatment. On MRI, cortical deep white matter lesions resulting in defective myelination was noticed; additionally, thin dysplastic corpus callosum and abnormal gyral overfolding resembling polymicrogyria were

observed as well in both siblings. The children present with facial dysmorphisms including long hypotonic face, open mouth, arched eyebrows, mild ptosis, prominent upturned nose, long philtrum, thin lips, broad chin and low set ears. Abnormal ECG testing identified sinus arrhythmias and ectopic premature complexes in individual 41 and 42, respectively.

Family Z

Family Z (**Figure S1, Table 1, Supplementary Table S1**) is a family from Iran with two affected cousins born from healthy consanguineous parents who are in turn first cousins. The children are two boys of 8 (IV.1, individual 43, **Figure S1, Supplementary Table S1**) and 6 years (IV.6, individual 44, **Figure S1, Supplementary Table S1**), respectively, both affected by global developmental delay, severe ID, and epilepsy (treated with phenobarbital until 5 years of age for individual 43 and with topiramate, clobazam and orfiril for individual 44). They presented pathological gastric reflux until 1.5-2 years of age, horizontal nystagmus and strabismus. Tandem Mass Spectrometry revealed an unremarkable metabolic workup in Individual 43. Among other features, Individual 43 presented muscle atrophy, while Individual 44 showed behavioral anomalies including laughing and hand stereotypies. Array CGH (Individual 43) and karyotyping (Individual 44) showed no chromosomal abnormalities. Exhaustive cardiac assessment was not performed in individual 43; echocardiography and cardiac examination at birth were normal in individual 44.

Figure S1

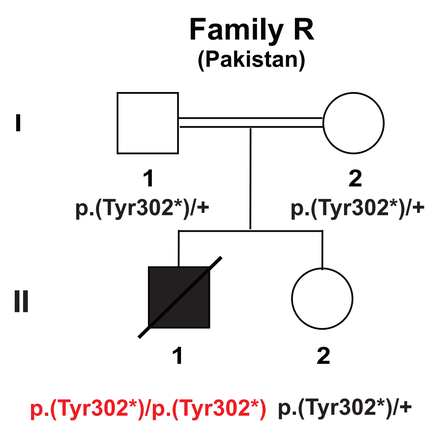

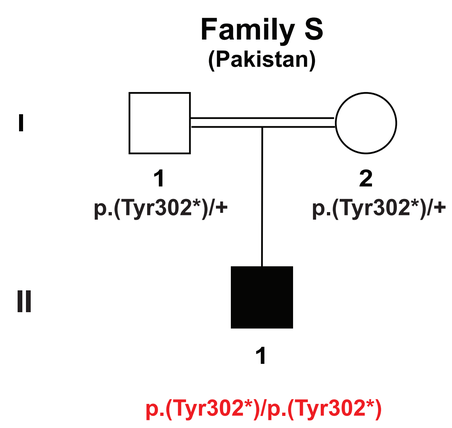

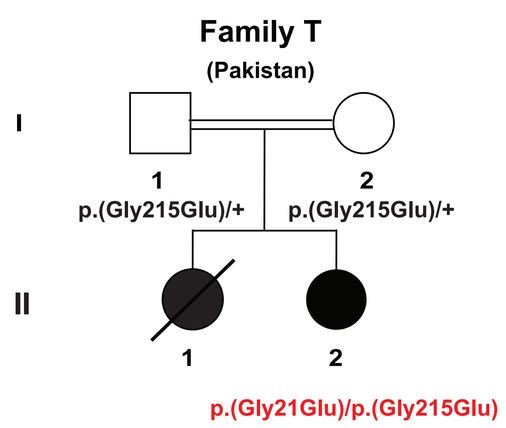

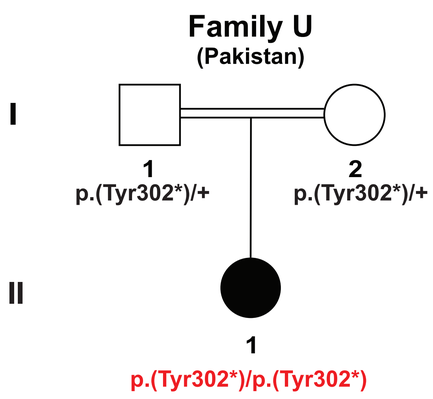

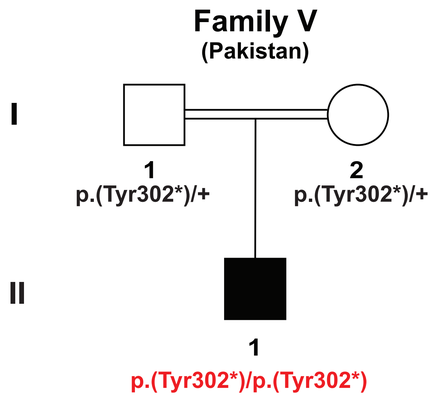

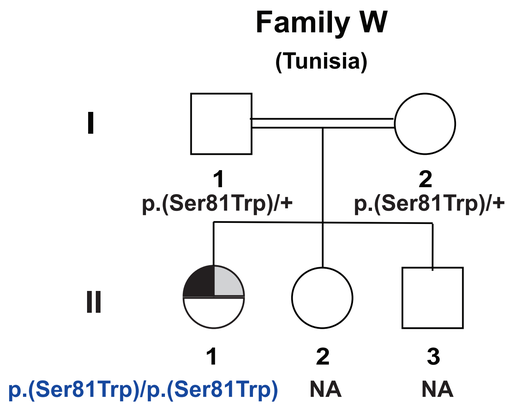

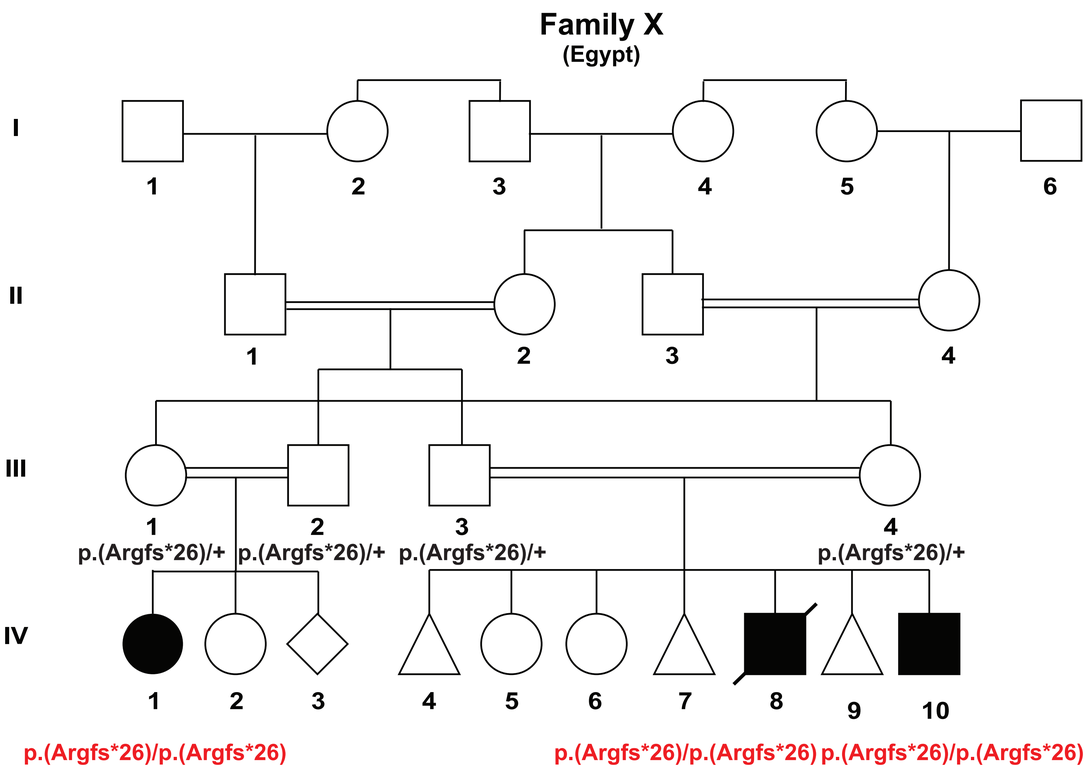

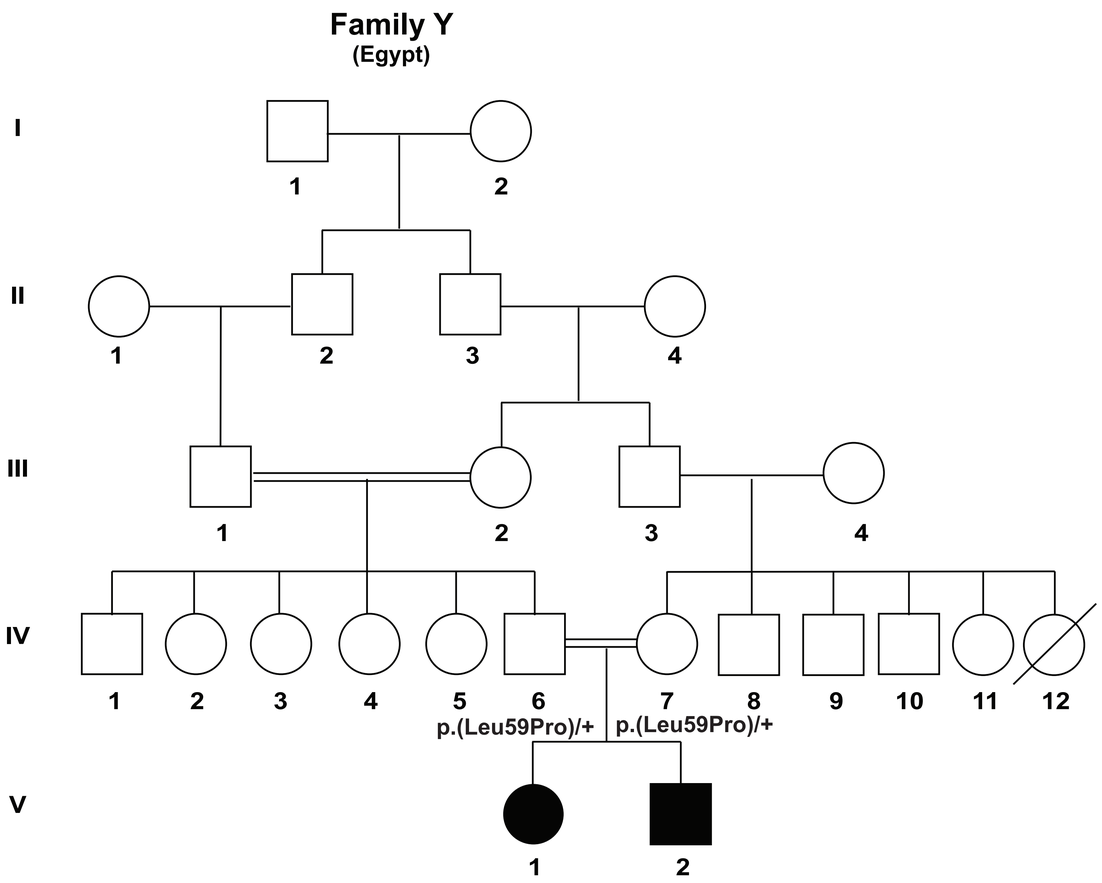

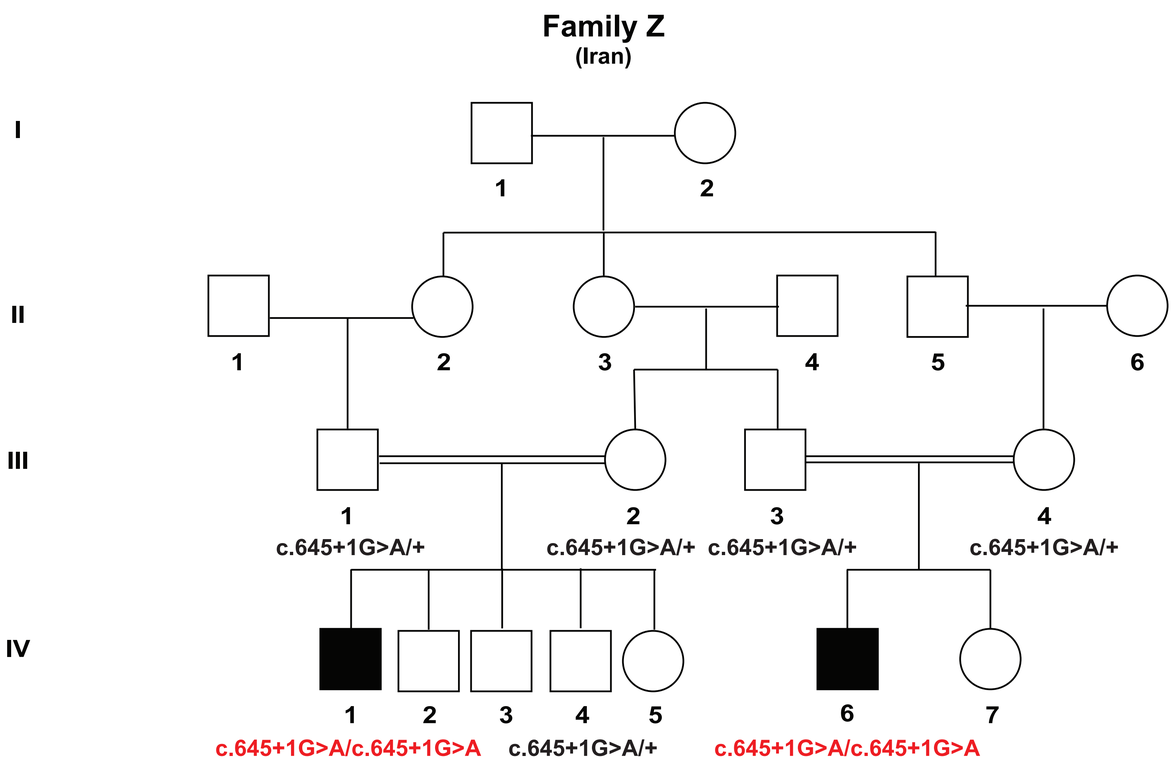

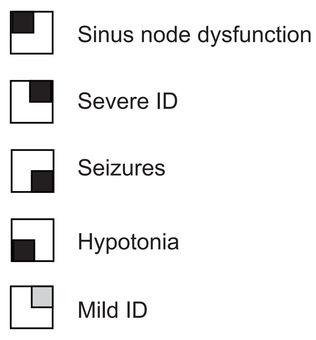

Figure S1. IDDCA and LADCI family trees. Pedigrees of the nine consanguineous families described in this study; affected individuals carry homozygous GNB5 variants inherited from heterozygous parents. Filled symbols represent individuals with severe sinus node dysfunction (top left quarter), intellectual disability (ID, top right quarter), seizures (bottom right quarter) and hypotonia (bottom left quarter). The light grey top quarter indicates the occurrence of mild ID. The affected individuals of families T, W and Y harbor novel variants which are modeled in panel A of **Figure 1**. The variants of IDDCA affected individuals are displayed in red (LoF), whereas missense LADCI variants are in blue.

Figure S2

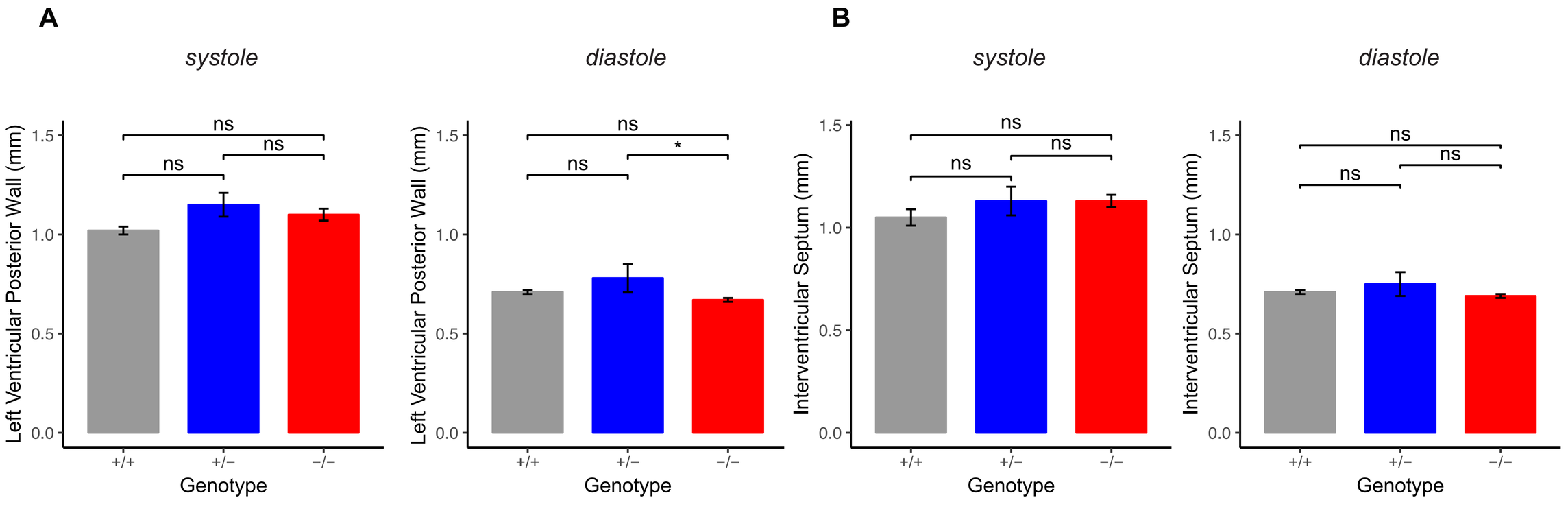

Figure S2: **Unchanged morphological parameters measured by echocardiography.** (**A**) Cardiac wall thickness in systole (right) and diasto-le (left). (**B**) Interventricular septum (at systole and diastole). (**C**) Heart rate measured in baseline condition through *in vivo* ECG. Values of knock-out (red) mice show a trend toward increased heart rate both during day and night (grey windows). (**D**) Qualitative measure of the mouse activity, consisting in displacement of the telemetric device. *Gnb5*$^{-/-}$ animals seem to be more active during the day, usually representing the sleeping phase for a mouse. (**E**) Measurements of the body temperature showing a similar trend to the activity (significance between knock-out and wild-type mice oscillating between p = 1.35E-04 and p = 0.9163 in the course of 36 daylight time points).

Figure S3

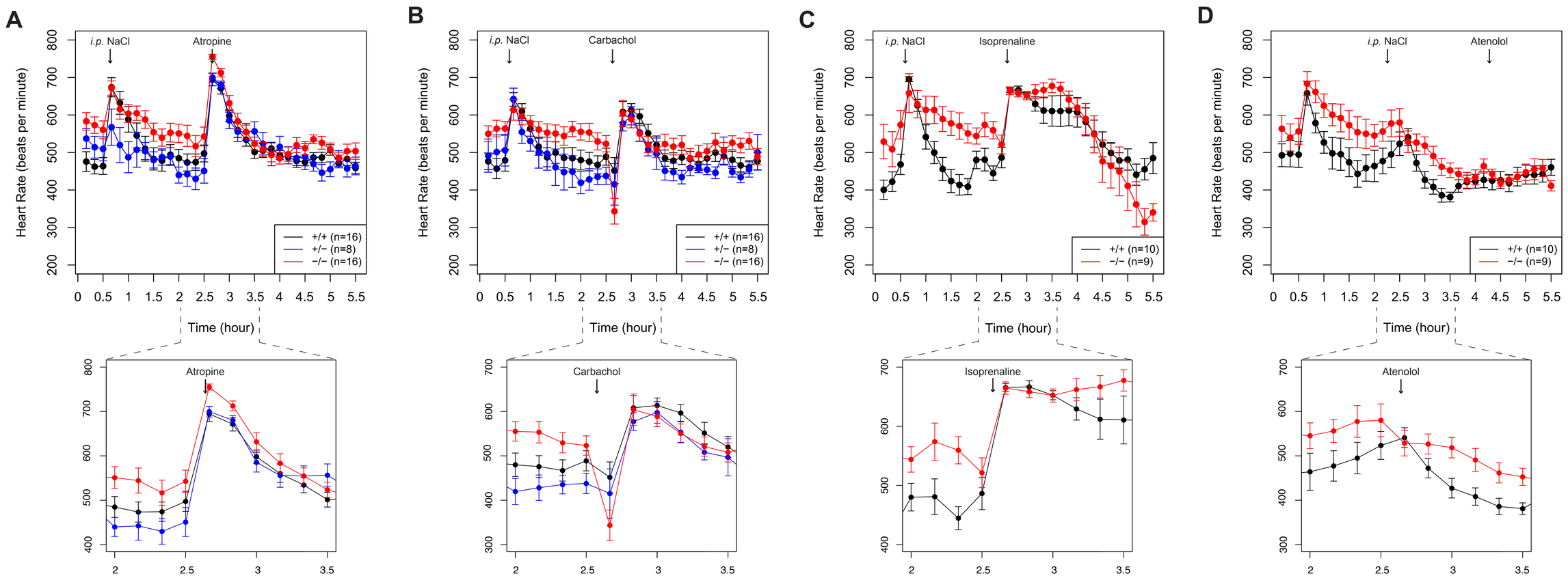

Figure S3: **Pharmacological challenges expressed in raw values.** Parasympathetyc (**A-B**) and sympathetyc (**C-D**) stimulation expressed in raw values (top). Zoom in on times ~ 2 to 3.5 hours illustrating peak and nadir heart rate differences among the genotypes (bottom).

Figure S4

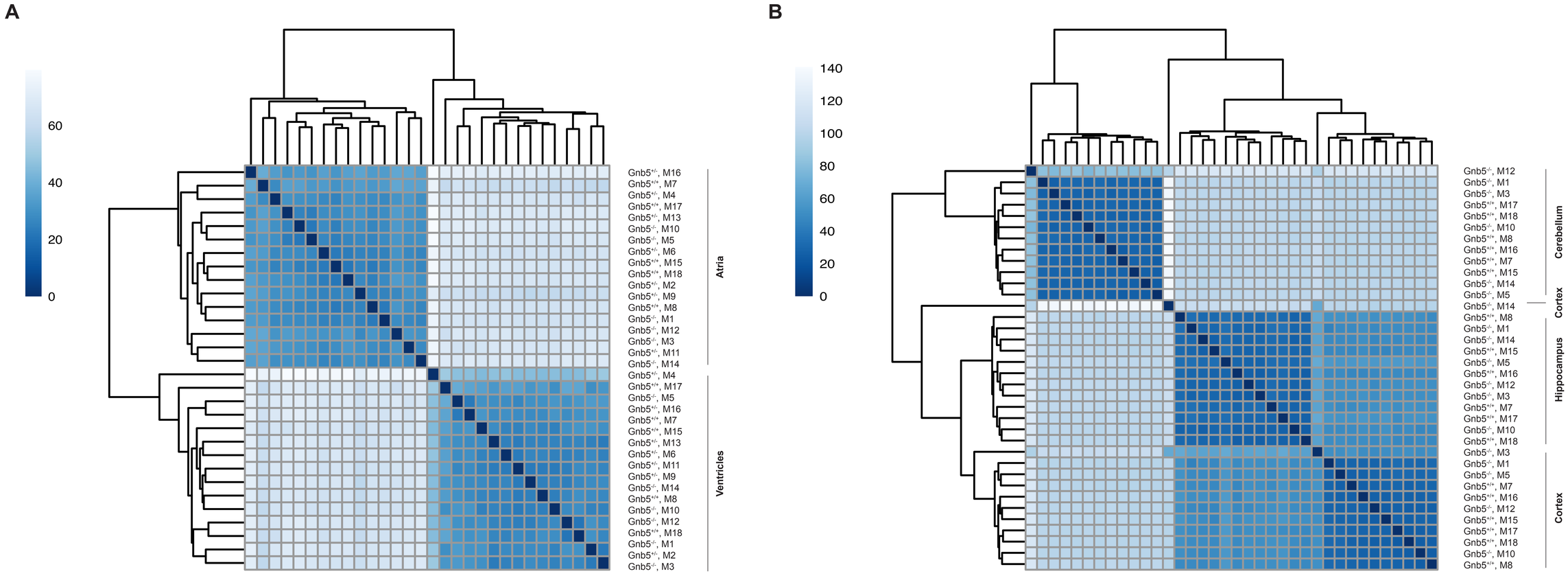

Figure S4: Samples distance of RNA samples. Heat map depicting hierarchical clustering of sample-to-sample distances for heart tissues (**A**) and brain regions (**B**) using normalized RNA-seq gene read counts. Blue color represents the nearest distance and light grey color indicates long sample-sample distance. Samples are clustered by tissue: (**A**) atria (top), and ventricles (bottom); (**B**) cerebellum (top), hippocampus (middle), and cortex (bottom). Samples M12-cerebellum, M14-cortex and M3-cortex were excluded from the analysis due to pronounced 3' mRNA degradation observed at the quality control step.

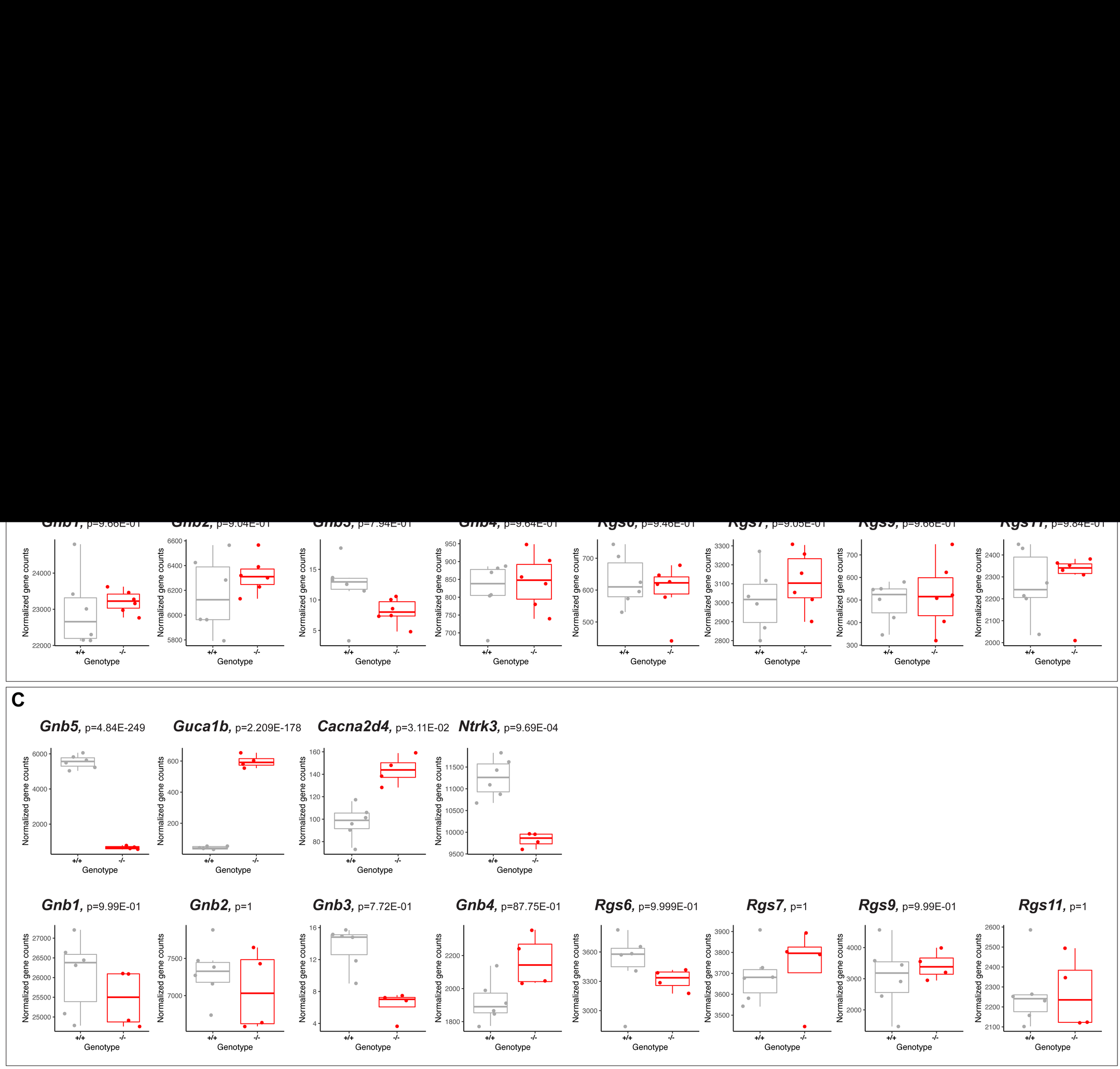

Figure S5: Expression profile of relevant genes in cerebellum, hippocampus and cerebral cortex of *Gnb5*$^{-/-}$, *vs*. *Gnb5*$^{+/+}$ mice. Expression levels of *Gnb5* (top left in each panel) and other differentially expressed genes in cerebellum (**A**, top), hippocampus (**B**, top) and cerebral cortex (**C**, top); *Gnb* and *Rgs* transcripts quantification in cerebellum (**A**, bottom), hippocampus (**B**, bottom) and cerebral cortex (**C**, bottom).

Figure S6

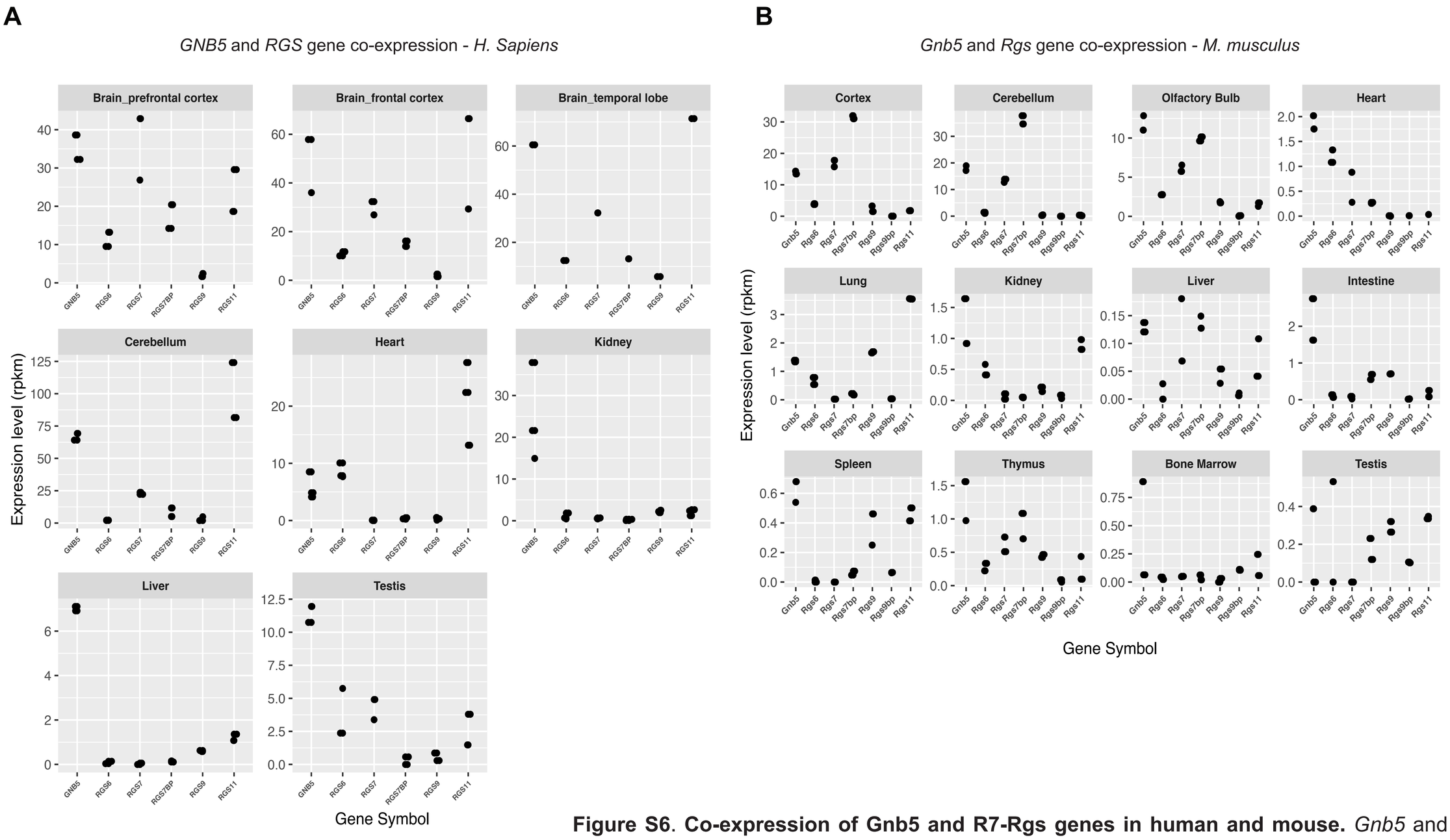

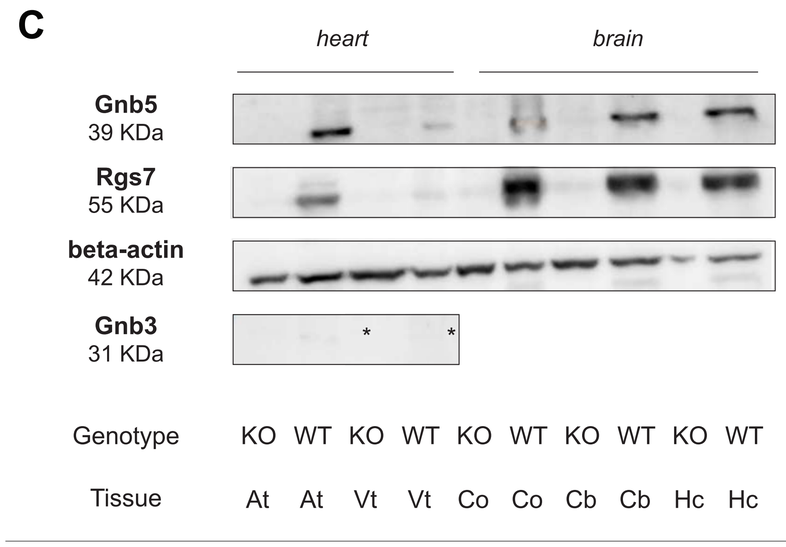

Figure S6. **Co-expression of Gnb5 and R7-Rgs genes in human and mouse.** *Gnb5* and *Rgs* genes expression was evaluated using publicly available transcritpome datasets in human (**A**) and mouse (**B**). Human data were re-trieved from (Brawand D. Nature. 2012); gene expression files for mouse tissues were obtained through the ENCODE website. Each point in the plots represents a replicate. Genes encoding for the R7 family of RGS proteins, known partners of GNB5, were inspected. In human, *GNB5* shows co-expression with *RGS7* and *RGS11* in the brain regions, while in heart co-epxression occurs between *GNB5* and *RGS6* and *RGS11*. A similar trend is observed in mouse, with *Gnb5* being co-expressed with *Rgs7* in brain, and with *Rgs6* in heart. Accordingly, *RGS9* is only expressed in eye, therefore we do not capture any co-expression profile with this subunit. (**C**) Gnb5, Rgs7, and Gnb3 protein levels across heart and brain mouse tissues by Western blotting. Beta-actin antibody was used as a loading control. ”KO” and “WT” indicate tissues harvested from *Gnb5*$^{-/-}$ and *Gnb5*$^{+/+}$ mice, respectively (At = Atria, Vt = Ventricles, Co = Cortex, Cb = Cerebellum, Hc = Hippocampi). Asterisks indicate the faint signal corresponding to Gnb3 protein expression.

Table S1. Detailed clinical features of individuals with IDDCA and LADCI syndromes

	Lodder E., De Nittis P., Koopman C. *et al.*, 2016								
	Family A		**Family B**	**Family C**		**Family D**	**Family E**		**Family F**
Individual	**1**	**2**	**3**	**4**	**5**	**6**	**7**	**8**	**9**
Gender, Age (years)	F, 22	F, 20	F, 6	F, 11	M, 9	F, 12	F, 13	M, 8	M, 23
Nucleotide change (NM_006578.3)	c.249G>A,r.249_250 ins249+1_249+25/ c.994C>T	c.249G>A,r.249_250 ins249+1_249+25/ c.994C>T	c.249+1G>T/ c.249+1G>T	c.249+3G>T/ c.249+3G>T	c.249+3G>T/ c.249+3G>T	c.906C>G/ c.906C>G	c.242C>T/ c.242C>T	c.242C>T/ c.242C>T	c.242C>T/ c.242C>T
Amino acid change (NP_006569.1)	p.Asp84Valfs*52/ p.(Arg332*)	p.Asp84Valfs*52/ p.(Arg332*)	p.Asp84Leufs*31/ p.Asp84Leufs*31	p.Asp84Valfs*31/ p.Asp84Valfs*31	p.Asp84Valfs*31/ p.Asp84Valfs*31	p.Tyr302*/ p.Tyr302*	p.(Ser81Leu)/ p.(Ser81Leu)	p.(Ser81Leu)/ p.(Ser81Leu)	p.(Ser81Leu)/ p.(Ser81Leu)
Birth weight	3580 g (50th percentile)	NA	NA	2751 g (15 th percentile)	NA	2845 g (15th percentile)	NA	NA	NA
Ethnicity	Italy	Italy	Jordan	Puerto Rico	Puerto Rico	India	Morocco	Morocco	Brazil
Consanguinity	–	–	+	+	+	–	–	–	+
Altered speech development	+	+	NR	+	+	+	+	+	NA
- Verbal understanding	NA	NA	nonverbal	unremarkable	unremarkable	NA	NA	NA	NA
- Lexical production	NA	NA	nonverbal	delayed	delayed	nonverbal	delayed	delayed	NA
Intellectual disability (ID)	+	+	+	+	+	+	mild	mild	mild
Epilepsy	+	+	+	-	-	+	-	-	-
Sinus Sick Syndrome (SSS)	+	+	+	+	+	increased PR interval (intermittent Weckenbach)	+	+	+
- Minimum heart rate	24	39	NA	paced	paced	NA	20	16	NA
- Maximum heart rate	163	192	NA	paced (27% heartbeats on Holter)	paced (20% heartbeats on Holter)	NA	176	180	NA
- Chronotropic response	NA	NA	NA	+	+	NA	unremarkable	unremarkable	NA
- Escape beats	+	+	NA	paced	paced	NA	+	+	NA
Pacemaker implantation	-	-	-	+	+	-	-	+	NA
Heart structural abnormalities	-	PFO	NA	-	-	-	-	-	NA
Hypotonia	+	+	+	+	+	+	-	impaired fine motor skills	-
Pathological gastric reflux	+	+	NA	+	+	+	-	-	NA
Nystagmus	+	+	+	+	+	+	NA	-	NA
Retinal Disease	+	NA	NA	NA	NA	+	NA	NA	NA
Metabolic work-up: - Plasma amino acids chromatography	938 µm/l (restored)	+ (restored)	NA	unremarkable	unremarkable	unremarkable	444 µm/l	unremarkable	NA
- Urine organic acids	unremarkable	unremarkable	increased excretion of 3-methyl-glutaconic acid	unremarkable	unremarkable	unremarkable	NA	NA	NA
Others	-	-	-	-	-	-	-	-	-
Dysmorphic feature(s)	-	-	-	-	-	-	-	-	-
Family history	-	-	-	-	-	-	-	-	-

	Shamseldin *et al.*, 2016					Turkdogan D. *et al.*, 2016					
	Family G					**Family H**					
Individual	**10**	**11**	**12**	**13**	**14**	**15**	**16**	**17**	**18**	**19**	**20**
Gender, Age (years)	F, 10	F, 9	F, 3	F, 5	F, 9	M, 2 (second degree cousin of pt 16)	F, 10 - pair of a monozygotic twin	F (deceased 5.5months)	M (deceased 7months)	F - pair of a monozygotic twin (deceased 8months)	M (deceased 7yo)
Nucleotide change (NM_006578.3)	c.242C>T/ c.242C>T	c.242C>T/ c.242C>T	c.242C>T/ c.242C>T	c.242C>T/ c.242C>T	c.242C>T/ c.242C>T	c.355delG/ c.355delG	c.355delG/ c.355delG	c.355delG/ c.355delG	c.355delG/ c.355delG	c.355delG/ c.355delG	c.355delG/ c.355delG
Amino acid change (NP_006569.1)	p.(Ser81Leu)/ p.(Ser81Leu)	p.(Ser81Leu)/ p.(Ser81Leu)	p.(Ser81Leu)/ p.(Ser81Leu)	p.(Ser81Leu)/ p.(Ser81Leu)	p.(Ser81Leu)/ p.(Ser81Leu)	p.Ala119Profs16/ p.Ala119Profs16*	p.Ala119Profs16/ p.Ala119Profs16*	p.Ala119Profs16/ p.Ala119Profs16*	p.Ala119Profs16/ p.Ala119Profs16*	p.Ala119Profs16/ p.Ala119Profs16*	p.Ala119Profs16/ p.Ala119Profs16*
Birth weight	50th centile	50th centile	NA	50th centile	NA	NA	1800 g (<1st)	NA	NA	NA	NA
Ethnicity	Saudi	Saudi	Saudi	Saudi	Saudi	Turkish	Turkish	Turkish	Turkish	Turkish	Turkish
Consanguinity	+	+	+	-	-	+	+	+	+	+	+
Altered speech development	+	+	+	-	-	+	+	NA	NA	NA	NA
- Verbal understanding	+	+	+	+	+	no developmental milestones	no developmental milestones	NA	NA	NA	NA
- Lexical production	delayed	delayed	delayed	delayed	delayed	no developmental milestones	no developmental milestones	NA	NA	NA	NA
Intellectual disability (ID)	normal IQ, but school performance issues	normal cognitive development	NA	normal IQ	NA	+	+	+	+	+	+
Epilepsy	NA	NA	NA	NA	NA	+	+	NA	+	+	NA
Sinus Sick Syndrome (SSS)	NA	NA	NA	NA	NA	+	+	NA	NA	NA	+
- Minimum heart rate	NA	NA	NA	NA	NA	NA	NA	NA	NA	NA	NA
- Maximum heart rate	NA	NA	NA	NA	NA	NA	NA	NA	NA	NA	NA
-Chronotropic response	NA	NA	NA	NA	NA	NA	NA	NA	NA	NA	NA
- Escape beats	NA	NA	NA	NA	NA	NA	NA	NA	NA	NA	NA

Pacemaker implantation	NA	NA	NA	NA	NA	– (suggested, but refused by parents)	– (suggested, but refused by parents)	NA	NA	NA	NA
Heart structural abnormalities	NA	NA	NA	NA	NA	–	–	NA	NA	NA	NA
Hypotonia	-	-	NA	+	NA	+	+	NA	NA	NA	NA
Pathological gastric reflux	NA	NA	NA	NA	NA	NA	NA	NA	NA	NA	NA
Nystagmus	NA	NA	NA	NA	NA	+	+ (horizontal)	NA	NA	NA	NA
Retinal Disease	NA	NA	NA	NA	NA	+	+	NA	NA	NA	NA
Metabolic work-up -Plasma amino acids chromatography	NA	NA	NA	NA	NA	NA	unremarkable	NA	NA	NA	NA
-Urine organic acids	NA	NA	NA	NA	NA	NA	unremarkable	NA	NA	NA	NA
Others	ADHD, marked hyperactivity	inattentive ype ADHD	-	motor delay	ADHD, mild motor delay	-	autistic (midline hand automatisms, lack of eye contact)	NA	NA	NA	NA
Dysmorphic feature(s)	-	-	-	-	-	-	prominent forehead, acquired micro-brachycephaly	NA	NA	NA	NA
Family history	-	-	-	-	-	-	-	NA	NA	NA	NA

	Vernon H. *et al.*, 2017	Malerba N. *et al.*, 2018	Poke G. *et al.*, 2019					Tang M. *et al.*, 2020	Yadzani S. *et al.*, 2020		Sciacca F.L *et al.*, 2020
	Family I	**Family J**	**Family K**	**Family L**	**Family M**		**Family N**	**Family O**	**Family P**		**Family Q**
Individual	**21**	**22**	**23**	**24**	**25**	**26**	**27**	**28**	**29**	**30**	**31**
Gender, Age (years)	M, 2	F, 2.5	M, 10	M, 3	F (deceased 13yo)	F, 2	F, 3	M, 6 months	M, 22	M, 18	M
Nucleotide change (NM_006578.3)	c.222_226delTAAA/ c.737G>A	c.222_226delTAAGA/ c.242C>T	c.136delG/ c.136delG	c.906C>G/ c.906C>G	c.242C>A/ c.242C>A	c.242C>A/ c.242C>A	c.906C>A/ c.906C>A	c.332G>A/ c.906C>A	c.906C>G/ c.906C>G	c.906C>G/ c.906C>G	Arr[Hg19] 15q21.2: (52385564_ 52579282)x0
Amino acid change (NP_006569.1)	p.Asp74Glufs*52/ p.(Arg246Gln)	p.Asp74Glufs* 52/ p.(Ser81Leu)	p.Glu46fs*68/ p.Glu46fs*68	p.Tyr302*/ p.Tyr302*	p.Ser81*/ p.Ser81*	p.Ser81*/ p.Ser81*	p.Tyr302*/ p.Tyr302*	p.Cys111Tyr/ p.Tyr302*	p.Tyr302*/ p.Tyr302*	p.Tyr302*/ p.Tyr302*	/
Birth weight	3,311 g (50th)	1698 g (< 1st percentile)	NA	NA	NA	NA	NA	2700 g	3000 g (15^{th}-25^{th} percentile)	2540 g (3^{rd}-15^{th} percentile)	NA
Ethnicity	European/Caucasian	European/Caucasian	Cambodia	Pakistan	Algeria	Algeria	Pakistan	China (Han)	Pakistan	Pakistan	Egypt
Consanguinity	–	-	+ (second cousins)	+ (first cousin once removed)	+ (first cousins)	+ (first cousins)	-	-	+ (first cousins)	+ (first cousins)	+ (first cousins)
Altered speech development	+	+	+	+	+	+	+	NA	+	+	+
- Verbal understanding	nonverbal	+	nonverbal	nonverbal	nonverbal	nonverbal	nonverbal	NA	+	+	+
- Lexical production	nonverbal	expressive speech delay (spoken vocabulary of ~ 12 words)	nonverbal	nonverbal	nonverbal	nonverbal	nonverbal	NA	+	+	+
Intellectual disability (ID)	+	mild	+	+	+	+	+	+	+	+	+
Epilepsy	–	-	+	+	+	+	+	+	+	-	+
Sinus Sick Syndrome (SSS)	+	+	+	+	normal ECG	+	+	+	+	+	+
- Minimum heart rate	71	36	NA	NA	NA	NA	NA	NA	NA	NA	39
- Maximum heart rate	183	176	NA	NA	NA	NA	NA	NA	NA	NA	NA
- Chronotropic response	NA	NA	NA	NA	NA	NA	NA	NA	NA	NA	NA
- Escape beats	+ (prior to pacing)	+	+	+	NA	NA	NA	NA	+	NA	NA
- Pacemaker implantation	+	+	NA	NA	NA	NA	NA	NA	+	-	-
- Heart structural abnormalities	–	-	NA	NA	NA	NA	NA	NA	NA	NA	PFO and ductus arteriosus (spontaneously closed)
Hypotonia	+	+	+ (contractures, nonambulatory, no head control)	+ nonambulatory	+ nonambulatory	+ nonambulatory	+ nonambulatory	+	+ (lost gross- and fine- motor functions)	NA	+
Pathological gastric reflux	+	-	+	NA	NA	NA	NA	+	+	+ (rare and mild)	+
Nystagmus	+	strabismus (surgically corrected at 16 mo)	NA	+	+	+	+	NA	+ (lateral gaze nystagmus), strabismus	+ (lateral gaze nystagmus), strabismus, poor eye fixation	+
Retinal Disease	+	-	+	NA	NA	+	+	NA	NA	NA	+
Metabolic work-up - Plasma amino acids chromatography	NA	NA	NA	NA	NA	NA	NA	NA	NA	NA	NA

- Urine organic acids	NA	NA	NA	NA	NA	NA	NA	NA	NA	NA	NA
Others	left-sided hearing loss, intermittent extremity hypertonia, intermittent upper extremity jerking motions - sometimes in conjunction with a stimulus, laryngomalacia hypertonia, clenched hands, high-voltage cortical activity (EEG), pain of unknown etiology thin corpus callosum (brain MRI)	bilateral tympanostomy tubes; high activity level and short attentions span compared to peers	pyloric stenosis, G-tube, scoliosis	NA	NA	NA	long posterior corpus callosum, central sleep apnea	Adams-Stokes syndrome	cerebral palsy; spasticity of upper and lower extremities, erratic sleep pattern; G-tube feeding; food allergy; intermittent urinary retention	Indication of optic nerve atrophy (small, anomalous, tilted, pale discs)	bilateral ventricular and cerebral sulci enlargement on MRI; episodic bradypnea
Dysmorphic feature(s)	NA	plagiocephaly associated with torticollis at 8 mo (solved with molding helmet therapy)	NA	microcephaly	NA	NA	NA	-	-	-	-
Family history	maternal uncle and paternal first-cousin suspected to have ASD	NA	NA	NA	NA	NA	-	-	one sibling (individual 30) with similar phenotype	-	parental couple experienced five previous miscarriages

	This study												
	Family R	**Family S**	**Family T**	**Family U**	**Family V**	**Family W**	**Family X**			**Family Y**		**Family Z**	
Individual	**32**	**33**	**34**	**35**	**36**	**37**	**38**	**39**	**40**	**41**	**42**	**43**	**44**
Gender, Age (years)	M, 8 months (deceased)	M, 15	F, 1.2	F, 4	2, M	F, 7	F, 5	M deceased (7 yo)	M, 2	F, 19	M, 16	M, 8	M, 6
Nucleotide change (NM_006578.3)	c.906C>G / c.906C>G	c.906C>G/ c.906C>G	c.644G> A/ c.644G> A	c.906C>A / c.906C>A	c.906C>G/ c.906C>G	c.242C>G/ c.242C>G	c.88_89ins CTCAA/ c.88_89ins CTCAA/	c.88_89ins CTCAA/ c.88_89ins CTCAA/	c.88_89ins CTCAA/ c.88_89ins CTCAA/	c.176T>C/ c.176T>C	c.176T>C/ c.176T>C	c.645+1G >/ c.645+1G>A	c.645+1G >/ c.645+1G>A
Amino acid change (NP_006569.1)	p.Tyr302*/ p.Tyr302*	p.Tyr302*/ p.Tyr302*	p.(Gly215Glu)/ p.(Gly215Glu)	p.Tyr302*/ p.Tyr302*	p.Tyr302*/ p.Tyr302*	p.(Ser81Trp)/ p.(Ser81Trp)	p.Argfs*26/ p.Argfs*26	p.Argfs*26/ p.Argfs*26	p.Argfs*26/ p.Argfs*26	p.(Leu59Pro)/ p.(Leu59Pro)	p.(Leu59Pro)/ p.(Leu59Pro)	p.?	p.?
Birth weight	NA	NA	NA	NA	NA	2900 g	3000 g	2800 g	2500 g	2600 g	2500 g	NA	NA
Ethnicity	Pakistan	Pakistan	Pakistan	Pakistan	Pakistan	Tunisia	Egypt	Egypt	Egypt	Egypt	Egypt	Iran	Iran
Consanguinity	+	+	+	+	+	+ (first cousins)	+ (first cousins)	+ (first cousins)	+ (first cousins)	+ (first cousins)	+ (first cousins)	+ (first cousins)	+ (first cousins)
Altered speech development	+	+	+	-	+	+	+	+	+	+	+	+	+
- Verbal understanding	+	+	no developmental milestones	unremarkable	NA	low	nonverbal	nonverbal	nonverbal	nonverbal	nonverbal	no developmental milestones	delayed
- Lexical production	+	+	no developmental milestones	unremarkable	delayed (vocalization at 1.10yo)	nonverbal	vocalized	vocalized	nonverbal	meaningless single syllable words	vocalized	nonverbal	NA
Intellectual disability (ID)	+	+	-	+	NA	+ (no neuro-psychological assessment)	+	+	+	+	+	+	+
Epilepsy	-	+	-	-	+	normal EEG	+	+	+	+	+	+	+
Sinus Sick Syndrome (SSS)	NA (inconsistent heart rate noted at Echo)	NA	+	NA	NA	+	NA	NA	NA	+	+	NA	NA
- Minimum heart rate	NA	NA	18	32	29	30	NA	NA	NA	NA	NA	NA	NA
- Maximum heart rate	NA	154	142	152	158	160	NA	NA	NA	NA	NA	NA	NA
- Chronotropic response	NA	NA	NA	NA	NA	NA	NA	NA	NA	NA	NA	NA	NA
- Escape beats	NA	-	+	NA	NA	+	NA	NA	NA	NA	+	NA	NA
Pacemaker implantation	-	-	-	-	-	-	-	-	-	-	-	-	-
Heart structural abnormalities	-	-	NA	NA	-	-	small atrial septal defect	-	small atrial septal defect secundum with minimal left to right shunt; small PDA	-	-	NA	NA
Hypotonia	+	+ (no head control)	+ (no neck holding)	+ (no neck holding)	+ (along with hyporeflexia)	+ (impaired fine motor skills)	+	+	+	+	+	+	+

Pathological gastric reflux	NA	+	-	NA	-	-	+	-	+	+	+	+	+
Nystagmus	_	+	+	no eye contact	no eye contact, convergent squint (strabismus) right eye	-	-	+	+	+ (mild)	+ (mild)	+ (strabismus, horizontal nystagmus)	+ (strabismus, horizontal nystagmus)
Retinal Disease	NA	NA	-	NA	myopia (-1.5)	-	-	+	+	+ (reduced pigmentation)	+ (reduced pigmentation)	-	-
Metabolic work-up - Plasma amino acids chromatography	NA	non specific	unremarkable	unremarkable	unremarkable	global hypoAA, High Phe (146, N: 39-77)	unremarkable	unremarkable	unremarkable	unremarkable	unremarkable	unremarkable	NA
- Urine organic acids	NA	unremarkable	NA	Fatty Acid Oxidation Disorder	unremarkable	normal	unremarkable	unremarkable	unremarkable	unremarkable	unremarkable	unremarkable	NA
Others	-	thining, hypogenesis of corpus callosum, modified hypsarrhythmia, breath holding spell, taking EPIVAL (VAP) and fits are controlled	-	cerebral Atrophy on MRI	-	unexplained coma secondary to sepsis in the context of digestive infection; one episode of pyelonephritis without complications	hypogenesis of corpus callosum on MRI	autistic behavior	prominent ventricular system on MRI; dysmyelination	thin dysplastic corpus callosum, abnormal increased cortical gyration (polymicrogyria), deep white matter lesions, defective myelination	thin dysplastic corpus callosum, abnormal increased gyration (polymicrogyria), white matter lesions, defective myelination	muscle atrophy	behavioral anomalies (laughing and hand stereptypies)
Dysmorphic feature(s)	macrocephaly	-	-	deep philtrum, micrognathia, prominent ears, disproportion of skull to face	blond hair, frontal bossing, epicanthic folds, small palpebral fissure, depressed nasal bridge, high arched palate	shorter thumbs	hypotonic face, with open mouth, downslanting palpebral fissures, low set ears	NA	prominent forehead, synophrys, downslanting palpebral fissures, depressed nasal root, low set ears	long hypotonic face, with open mouth, arched eye brows, mild ptosis, prominent nose, upturned, long philtrum, thin lips, broad chin, low set ears	long hypotonic face, with open mouth, arched eye brows, mild ptosis, prominent nose, upturned, long philtrum, thin lips, broad chin, low set ears	NA	NA
Family history	respiratory stridor	one sibling with similar phenotype died, likely due to cardiac arrest	-	-	paternal uncle with severe cognitive impairment and no language; maternal aunt and uncle are severely handicapped and no language, similar to the son of another maternal aunt	-	two cousins (individuals 40 and 41) with similar phenotype	one sibling (brother) with similar phenotype (individual 41); parental couple experienced three miscarriages	parental couple experienced three miscarriages	-	-	one sibling (individual 44) with similar phenotype	-

Abbreviations are as follows: M: male; F: female; NA: Not Available; +: clinical trait present; -: clinical trait absent; PFO: Patent Foramen Ovale; ADHD: Attention Deficit Hyperactivity Disorder; IQ: Intelligence Quotient; ASD: Autism Spectrum Disorder; ECG: Electrocardiogram; Echo: Echocardiography; EEG: Electroencephalogram, MRI: Magnetic Resonance Imaging; G-tube: gastrostomy tube, PDA: Patent Ductus Arteriosus.

Table S2. Pathogenicity prediction of three novel *GNB5* variants

	GNB5 variants		
Prediction tool	p.(Ser81Trp)	p.(Gly215Glu)	p.(Leu59Pro)
Mutation Taster	Disease causing (0.99)	Disease causing (0.99)	Disease causing (0.99)
PolyPhen-2	Probably Damaging (1)	Probably Damaging (1)	Probably Damaging (1)
SIFT	Deleterious (0.00)	Deleterious (0.00)	Deleterious (0.00)
Provean	Deleterious (-5.274)	Deleterious (-7.426)	Deleterious (-6.156)
UMD-predictor	Pathogenic (100)	Pathogenic (99)	Pathogenic (87)
FATHMM	Damaging (-6.79)	Damaging (-6.92)	-
NNSplice	-	Donor increased	-
NetGene2	-	Activation of donor splice site	-
Splicing Finder	Activation of an exonic cryptic donor site, creation of an exonic ESS site	Creation of an exonic ESS site, alteration of an exonic ESE site	-
CADD	31	29.1	5.091

Supp. Table S3. Description of the mouse samples used for transcriptome

Sample name	Gnb5 genotype	Tissue
KO_At_M1	-/-	Atria
HET_At_M2	+/-	Atria
KO_At_M3	-/-	Atria
HET_At_M4	+/-	Atria
KO_At_M5	-/-	Atria
HET_At_M6	+/-	Atria
WT_At_M7	+/+	Atria
WT_At_M8	+/+	Atria
HET_At_M9	+/-	Atria
KO_At_M10	-/-	Atria
HET_At_M11	+/-	Atria
KO_At_M12	+/-	Atria
HET_At_M13	+/-	Atria
KO_At_M14	-/-	Atria
WT_At_M15	+/+	Atria
WT_At_M16	+/+	Atria
WT_At_M17	+/+	Atria
WT_At_M18	+/+	Atria
KO_At_M1	-/-	Ventricles
HET_At_M2	+/-	Ventricles
KO_At_M3	-/-	Ventricles
HET_At_M4	+/-	Ventricles
KO_At_M5	-/-	Ventricles
HET_At_M6	+/-	Ventricles
WT_At_M7	+/+	Ventricles
WT_At_M8	+/+	Ventricles
HET_At_M9	+/-	Ventricles
KO_At_M10	-/-	Ventricles
HET_At_M11	+/-	Ventricles
KO_At_M12	+/-	Ventricles
HET_At_M13	+/-	Ventricles
KO_At_M14	-/-	Ventricles
WT_At_M15	+/+	Ventricles
WT_At_M16	+/+	Ventricles
WT_At_M17	+/+	Ventricles
WT_At_M18	+/+	Ventricles
KO_At_M1	-/-	Cerebellum
KO_At_M3	-/-	Cerebellum
KO_At_M5	-/-	Cerebellum

WT_At_M7	+/+	Cerebellum
WT_At_M8	+/+	Cerebellum
KO_At_M10	-/-	Cerebellum
KO_At_M12	+/-	Cerebellum
KO_At_M14	-/-	Cerebellum
WT_At_M15	+/+	Cerebellum
WT_At_M16	+/+	Cerebellum
WT_At_M17	+/+	Cerebellum
WT_At_M18	+/+	Cerebellum
KO_At_M1	-/-	Hippocampus
KO_At_M3	-/-	Hippocampus
KO_At_M5	-/-	Hippocampus
WT_At_M7	+/+	Hippocampus
WT_At_M8	+/+	Hippocampus
KO_At_M10	-/-	Hippocampus
KO_At_M12	+/-	Hippocampus
KO_At_M14	-/-	Hippocampus
WT_At_M15	+/+	Hippocampus
WT_At_M16	+/+	Hippocampus
WT_At_M17	+/+	Hippocampus
WT_At_M18	+/+	Hippocampus
KO_At_M1	-/-	Cerebral cortex
KO_At_M3	-/-	Cerebral cortex
KO_At_M5	-/-	Cerebral cortex
WT_At_M7	+/+	Cerebral cortex
WT_At_M8	+/+	Cerebral cortex
KO_At_M10	-/-	Cerebral cortex
KO_At_M12	+/-	Cerebral cortex
KO_At_M14	-/-	Cerebral cortex
WT_At_M15	+/+	Cerebral cortex
WT_At_M16	+/+	Cerebral cortex
WT_At_M17	+/+	Cerebral cortex
WT_At_M18	+/+	Cerebral cortex

Supp Table S4. List of Differentially Expressed genes at FDR 5% in *Gnb5-/-* mice - atria

Ensembl ID	Gene Symbol	Gene name	baseMean	log2FoldChange	lfcSE	stat	pvalue	padj
ENSMUSG00000032192	Gnb5	guanine nucleotide binding protein (G protein), beta 5	588.3942165	-3.98100257	0.125384112	-31.7504546	3.13E-221	5.47E-217
ENSMUSG00000033419	Snap91	synaptosomal-associated protein 91	593.4008865	-2.204605213	0.126013386	-17.49500813	1.56E-68	1.37E-64
ENSMUSG00000048758	Rpl29	ribosomal protein L29	199.1838179	-3.250034673	0.22769114	-14.2738741	3.18E-46	1.39E-42
ENSMUSG00000032224	Fam81a	family with sequence similarity 81, member A	292.8574685	2.572498612	0.253223883	10.15898889	3.02E-24	1.06E-20
ENSMUSG00000032179	Bmp5	bone morphogenetic protein 5	205.0671832	1.328934231	0.136737848	9.718847054	2.51E-22	7.30E-19
ENSMUSG00000033590	Myo5c	myosin VC	163.7773657	-1.49164629	0.195137706	-7.644070025	2.10E-14	5.26E-11
ENSMUSG00000023979	Guca1b	guanylate cyclase activator 1B	58.67765502	1.533209378	0.212719605	7.207654307	5.69E-13	1.24E-09
ENSMUSG00000039716	Dock3	dedicator of cyto-kinesis 3	188.3304401	-1.168897128	0.168267704	-6.94665168	3.74E-12	7.27E-09
ENSMUSG00000032184	Lysmd2	LysM, putative peptidoglycan-binding, domain containing 2	586.6508467	0.667351463	0.097089163	6.873593728	6.26E-12	1.09E-08
ENSMUSG00000023249	Parp3	poly (ADP-ribose) polymerase family, member 3	1837.440683	-0.66820649	0.10214733	-6.541595295	6.09E-11	9.68E-08
ENSMUSG00000032556	Bfsp2	beaded filament structural protein 2, phakinin	57.65614782	-2.234680029	0.347888403	-6.423554248	1.33E-10	1.94E-07
ENSMUSG00000042073	Abhd14b	abhydrolase domain containing 14b	580.8699606	-0.801977921	0.127326525	-6.298592679	3.00E-10	4.04E-07
ENSMUSG00000032579	Hemk1	HemK methyltransferase family member 1	597.5715156	0.879217891	0.141144598	6.229199738	4.69E-10	5.56E-07
ENSMUSG00000032872	Cyb5r4	cytochrome b5 reductase 4	1656.745906	-0.509974877	0.081905477	-6.226383107	4.77E-10	5.56E-07
ENSMUSG00000066456	Hmgn3	high mobility group nucleosomal binding domain 3	282.7147136	-0.762798777	0.13316698	-5.728137557	1.02E-08	1.11E-05
ENSMUSG00000031849	Comp	cartilage oligomeric matrix protein	1890.434541	0.863942512	0.156893591	5.506550687	3.66E-08	3.76E-05
ENSMUSG00000043587	Pxylp1	2-phosphoxylose phosphatase 1	553.184341	-1.06209914	0.195018224	-5.446153283	5.15E-08	5.00E-05
ENSMUSG00000032563	Mrpl3	mitochondrial ribosomal protein L3	1799.161022	-0.582173662	0.107712274	-5.404896214	6.48E-08	5.97E-05

ENSMUSG00000010057	Nprl2	NPR2 like, GATOR1 complex subunit	671.0578114	0.433311959	0.080955871	5.352446372	8.68E-08	7.23E-05
ENSMUSG00000044938	Klhl31	kelch-like 31	2434.146223	-0.686725512	0.129907316	-5.286272829	1.25E-07	9.92E-05
ENSMUSG00000029683	Lmod2	leiomodin 2 (cardiac)	11173.11087	-0.54016025	0.102389096	-5.275564196	1.32E-07	1.01E-04
ENSMUSG00000015354	Pcolce2	procollagen C-endopeptidase enhancer 2	1381.444784	0.377432306	0.072416176	5.21198893	1.87E-07	1.36E-04
ENSMUSG00000113637	Gm7049	predicted gene 7049	15.78647891	2.22274028	0.431035014	5.156751094	2.51E-07	1.76E-04
ENSMUSG00000039313	Minar1	membrane integral NOTCH2 associated receptor 1	31.93558633	1.962031653	0.383199078	5.120136678	3.05E-07	2.05E-04
ENSMUSG00000078137	Ankrd63	ankyrin repeat domain 63	231.3397505	0.742695994	0.148629054	4.99697718	5.82E-07	3.77E-04
ENSMUSG00000063564	Col23a1	collagen, type XXIII, alpha 1	520.8704226	0.624586575	0.126165837	4.950520603	7.40E-07	4.62E-04
ENSMUSG00000038156	Spon1	spondin 1, (f-spondin) extracellular matrix protein	3543.885101	0.371254886	0.075961149	4.887431184	1.02E-06	6.16E-04
ENSMUSG00000032058	Ppp2r1b	protein phosphatase 2, regulatory subunit A, beta	374.2643884	0.599231525	0.123151982	4.86578874	1.14E-06	6.65E-04
ENSMUSG00000041112	Elmo1	engulfment and cell motility 1	700.2407007	0.415448791	0.085517427	4.858059972	1.19E-06	6.69E-04
ENSMUSG00000091537	Tma7	translational machinery associated 7	483.7361455	-0.685576063	0.143465638	-4.77867782	1.76E-06	9.64E-04
ENSMUSG00000022206	Npr3	natriuretic peptide receptor 3	11899.26299	0.399734149	0.083783676	4.771026642	1.83E-06	9.71E-04
ENSMUSG00000032370	Lactb	lactamase, beta	346.157966	-0.422281978	0.09066889	-4.65740759	3.20E-06	1.65E-03
ENSMUSG00000043719	Col6a6	collagen, type VI, alpha 6	1411.565721	0.828808973	0.179039549	4.629194943	3.67E-06	1.83E-03
ENSMUSG00000026638	Irf6	interferon regulatory factor 6	354.4281902	0.612952619	0.132744643	4.61753185	3.88E-06	1.89E-03
ENSMUSG00000033453	Adamts15	a disintegrin-like and metallopeptidase (reprolysin type) with thrombospondin type 1 motif, 15	1535.603828	0.567295151	0.123255032	4.60261251	4.17E-06	1.97E-03
ENSMUSG00000032498	Mlh1	mutL homolog 1	433.7803123	-0.38578188	0.084367758	-4.572622185	4.82E-06	2.22E-03
ENSMUSG00000028476	Reck	reversion-inducing-cysteine-rich protein with kazal motifs	744.0022468	0.325339922	0.071357088	4.559321694	5.13E-06	2.30E-03

ENSMUSG00000021596	Mctp1	multiple C2 domains, transmembrane 1	179.9515026	0.502011368	0.111477268	4.5032622	6.69E-06	2.93E-03
ENSMUSG00000090626	Tex9	testis expressed gene 9	278.1642117	-0.734429387	0.163584055	-4.489614741	7.14E-06	3.04E-03
ENSMUSG00000032567	Aste1	asteroid homolog 1	192.4949534	-0.666334448	0.14938301	-4.460577198	8.17E-06	3.40E-03
ENSMUSG00000032431	Crtap	cartilage associated protein	1361.165212	0.364784746	0.082147038	4.440631755	8.97E-06	3.65E-03
ENSMUSG00000049624	Slc17a5	solute carrier family 17 (anion/sugar transporter), member 5	349.6898644	0.434839012	0.09846974	4.415965889	1.01E-05	4.00E-03
ENSMUSG00000053040	Aph1c	aph1 homolog C, gamma secretase subunit	68.79153406	-0.82659287	0.187704162	-4.403700279	1.06E-05	4.14E-03
ENSMUSG00000024806	Mlana	melan-A	1627.583495	0.52838317	0.122891802	4.299580298	1.71E-05	6.51E-03
ENSMUSG00000028132	Tmem56	transmembrane protein 56	245.5306833	-0.815298268	0.191265107	-4.262660763	2.02E-05	7.52E-03
ENSMUSG00000090215	Trim34b	tripartite motif-containing 34B	11.6973086	-2.582632252	0.607008212	-4.254690792	2.09E-05	7.63E-03
ENSMUSG00000028396	2310002L09Rik	RIKEN cDNA 2310002L09 gene	344.3905263	-0.626139305	0.147377011	-4.248554772	2.15E-05	7.68E-03
ENSMUSG00000037736	Limch1	LIM and calponin homology domains 1	5228.144385	-0.312723246	0.073777902	-4.238711583	2.25E-05	7.86E-03
ENSMUSG00000031980	Agt	angiotensinogen (serpin peptidase inhibitor, clade A, member 8)	524.2715869	-0.609713334	0.144159559	-4.229433963	2.34E-05	7.97E-03
ENSMUSG00000040848	Sft2d2	SFT2 domain containing 2	2529.424876	0.234751352	0.055536798	4.226951515	2.37E-05	7.97E-03
ENSMUSG00000068227	Il2rb	interleukin 2 receptor, beta chain	82.42680251	0.659994674	0.156469105	4.218051048	2.46E-05	8.13E-03
ENSMUSG00000074059	Fbxw18	F-box and WD-40 domain protein 18	62.68513319	3.258911738	0.774283545	4.208938393	2.57E-05	8.31E-03
ENSMUSG00000078307	AI593442	expressed sequence AI593442	39.35947148	-1.838584277	0.438071347	-4.196997335	2.70E-05	8.60E-03
ENSMUSG00000019102	Aldh3a1	aldehyde dehydrogenase family 3, subfamily A1	66.67934433	1.063561484	0.253673991	4.192631185	2.76E-05	8.61E-03
ENSMUSG00000100782	Gm28231	predicted gene 28231	22.5434237	1.248506266	0.301217727	4.144863178	3.40E-05	1.04E-02
ENSMUSG00000051855	Mest	mesoderm specific transcript	455.3390815	0.528823455	0.129171073	4.093977412	4.24E-05	1.28E-02
ENSMUSG00000045594	Glb1	galactosidase, beta 1	946.3638084	-0.476991352	0.11686762	-4.081467171	4.48E-05	1.31E-02

ENSMUSG00000053093	Myh7	myosin, heavy polypeptide 7, cardiac muscle, beta	251.3134444	-0.866946809	0.212498462	-4.079779212	4.51E-05	1.31E-02
ENSMUSG00000006941	Eif1b	eukaryotic translation initiation factor 1B	1363.496793	-0.405756831	0.100156813	-4.051215455	5.10E-05	1.40E-02
ENSMUSG00000032342	Mto1	mitochondrial tRNA translation optimization 1	741.1169021	-0.255310451	0.063047704	-4.04948058	5.13E-05	1.40E-02
ENSMUSG00000111278	Gm32743	predicted gene 32743	25.8092539	-1.363865868	0.336722402	-4.050416183	5.11E-05	1.40E-02
ENSMUSG00000050640	Tmem150c	transmembrane protein 150C	40.08771757	-1.128379631	0.279418769	-4.038310072	5.38E-05	1.45E-02
ENSMUSG00000056880	Gadl1	glutamate decarboxylase-like 1	41.12226685	-1.172852268	0.291809453	-4.019240144	5.84E-05	1.55E-02
ENSMUSG00000006587	Snai3	snail family zinc finger 3	38.46789747	-1.556170083	0.3914073	-3.975833063	7.01E-05	1.83E-02
ENSMUSG00000032860	P2ry2	purinergic receptor P2Y, G-protein coupled 2	427.8475396	-0.417060355	0.105028679	-3.970918781	7.16E-05	1.84E-02
ENSMUSG00000021622	Ckmt2	creatine kinase, mitochondrial 2	30570.15221	-0.358321877	0.09037697	-3.964747643	7.35E-05	1.86E-02
ENSMUSG00000104344	Gm38077	predicted gene 38077	110.0410307	-0.694683493	0.17726808	-3.918830127	8.90E-05	2.22E-02
ENSMUSG00000032181	Scg3	secretogranin III	41.68914485	1.290206572	0.330188439	3.907485597	9.33E-05	2.30E-02
ENSMUSG00000020253	Ppm1m	protein phosphatase 1M	612.6332904	0.364501693	0.094443251	3.859478465	1.14E-04	2.76E-02
ENSMUSG00000097088	Gm26615	predicted gene 26615	43.50706638	0.836267574	0.216957467	3.854523129	1.16E-04	2.78E-02
ENSMUSG00000010064	Slc38a3	solute carrier family 38, member 3	1610.204165	-0.651101006	0.169436841	-3.842735747	1.22E-04	2.80E-02
ENSMUSG00000031709	Tbc1d9	TBC1 domain family, member 9	542.8723027	0.411804108	0.107166775	3.842647212	1.22E-04	2.80E-02
ENSMUSG00000034533	Scn10a	sodium channel, voltage-gated, type X, alpha	703.8602467	0.70040763	0.183064182	3.826022233	1.30E-04	2.88E-02
ENSMUSG00000040875	Osbpl10	oxysterol binding protein-like 10	79.84746132	-0.766643335	0.200280981	-3.82783892	1.29E-04	2.88E-02
ENSMUSG00000101257	2310015K22Rik	RIKEN cDNA 2310015K22 gene	12.05415905	-1.633324502	0.426600907	-3.828694395	1.29E-04	2.88E-02
ENSMUSG00000019817	Plagl1	pleiomorphic adenoma gene-like 1	2018.952602	0.453482958	0.119673938	3.789320943	1.51E-04	3.29E-02
ENSMUSG00000019890	Nts	neurotensin	85.16574876	-0.855082132	0.225793704	-3.787006094	1.52E-04	3.29E-02
ENSMUSG00000030515	Tarsl2	threonyl-tRNA synthetase-like 2	1170.685678	-0.243655404	0.064511345	-3.776938834	1.59E-04	3.39E-02
ENSMUSG00000006611	Hfe	hemochromatosis	890.846647	0.435320115	0.11562911	3.764796886	1.67E-04	3.51E-02

ENSMUSG00000045967	Gpr158	G protein-coupled receptor 158	373.298715	-0.686733554	0.18272265	-3.75833841	1.71E-04	3.52E-02
ENSMUSG00000047686	Rtl3	retrotransposon Gag like 3	266.2423324	0.760639578	0.20238611	3.758358611	1.71E-04	3.52E-02
ENSMUSG00000035606	Ky	kyphoscoliosis peptidase	125.6420813	-0.986271443	0.263125553	-3.748292139	1.78E-04	3.61E-02
ENSMUSG00000074207	Adh1	alcohol dehydrogenase 1 (class I)	1168.841709	0.378713887	0.101093013	3.746192504	1.80E-04	3.61E-02
ENSMUSG00000000184	Ccnd2	cyclin D2	7244.566123	0.321075122	0.085868752	3.739138085	1.85E-04	3.67E-02
ENSMUSG00000021557	Agtpbp1	ATP/GTP binding protein 1	3779.137522	-0.28831125	0.077403559	-3.724780271	1.95E-04	3.84E-02
ENSMUSG00000021557	A230056J06Rik	RIKEN cDNA A230056J06 gene	3779.137522	-0.28831125	0.077403559	-3.724780271	1.95E-04	3.84E-02
ENSMUSG00000043795	Prr33	proline rich 33	112.7136835	-0.776040696	0.208764671	-3.717298975	2.01E-04	3.91E-02
ENSMUSG00000026604	Ptpn14	protein tyrosine phosphatase, non-receptor type 14	3680.35312	0.257384789	0.069385735	3.70947703	2.08E-04	3.99E-02
ENSMUSG00000029359	Tesc	tescalcin	181.5637758	-0.947384507	0.256043393	-3.700093552	2.16E-04	4.05E-02
ENSMUSG00000031637	Lrp2bp	Lrp2 binding protein	140.0742862	-0.59046599	0.159527357	-3.701346278	2.14E-04	4.05E-02
ENSMUSG00000021957	Tkt	transketolase	1797.82233	0.732078661	0.198124968	3.695034851	2.20E-04	4.06E-02
ENSMUSG00000061780	Cfd	complement factor D (adipsin)	904.2314372	2.994362377	0.810510725	3.694414255	2.20E-04	4.06E-02
ENSMUSG00000037887	Dusp8	dual specificity phosphatase 8	774.5163123	-0.572804466	0.155345266	-3.68729915	2.27E-04	4.13E-02
ENSMUSG00000091345	Col6a5	collagen, type VI, alpha 5	326.9932512	2.283384011	0.622617345	3.667395437	2.45E-04	4.42E-02
ENSMUSG00000060639	Hist1h4i	histone cluster 1, H4i	144.8255591	-0.691858999	0.188964427	-3.661318753	2.51E-04	4.48E-02
ENSMUSG00000064371	mt-Tt	mitochondrially encoded tRNA threonine	67.46562005	-0.989792385	0.27087529	-3.654051962	2.58E-04	4.56E-02
ENSMUSG00000034485	Uaca	uveal autoantigen with coiled-coil domains and ankyrin repeats	1707.508249	-0.254012029	0.069644209	-3.647281416	2.65E-04	4.63E-02
ENSMUSG00000059742	Kcnh7	potassium voltage-gated channel, subfamily H (eag-related), member 7	286.2843348	0.587508859	0.161412283	3.639802667	2.73E-04	4.72E-02

Supp Table S5. List of Differentially Expressed genes at FDR 5% in *Gnb5-/-* mice - ventricle

Ensembl ID	Gene Symbol	Gene name	baseMean	log2FoldChange	lfcSE	stat	pvalue	padj
ENSMUSG00000032192	Gnb5	guanine nucleotide binding protein (G protein), beta 5	313.5699776	-4.21550606	0.154170849	-27.34308137	1.31E-164	2.19E-160
ENSMUSG00000033419	Snap91	synaptosomal-associated protein 91	130.8116563	-2.993668387	0.230324744	-12.9975978	1.26E-38	1.06E-34
ENSMUSG00000048758	Rpl29	ribosomal protein L29	148.0555782	-2.768271599	0.258451771	-10.71097942	9.04E-27	5.05E-23
ENSMUSG00000032224	Fam81a	family with sequence similarity 81, member A	535.3572241	1.400193385	0.158370442	8.841254493	9.46E-19	3.96E-15
ENSMUSG00000032579	Hemk1	HemK methyltransferase family member 1	699.5483486	1.255117802	0.16788463	7.476073332	7.66E-14	2.57E-10
ENSMUSG00000113637	Gm7049	predicted gene 7049	16.81236237	2.249097307	0.306354635	7.341482876	2.11E-13	5.90E-10
ENSMUSG00000111765	Gm10635	predicted gene 10635	108.9820339	-1.98648208	0.288335345	-6.889485152	5.60E-12	1.34E-08
ENSMUSG00000066456	Hmgn3	high mobility group nucleosomal binding domain 3	80.22459437	-1.098602846	0.160705843	-6.836110138	8.14E-12	1.70E-08
ENSMUSG00000023249	Parp3	poly (ADP-ribose) polymerase family, member 3	1606.053611	-0.717032187	0.109004266	-6.578019501	4.77E-11	8.88E-08
ENSMUSG00000010057	Nprl2	NPR2 like, GATOR1 complex subunit	491.5575602	0.487515133	0.082544171	5.906112138	3.50E-09	5.34E-06
ENSMUSG00000100782	Gm28231	predicted gene 28231	48.63773997	1.405293992	0.238858846	5.883365906	4.02E-09	5.61E-06
ENSMUSG00000020902	Ntn1	netrin 1	2523.450781	0.593131025	0.102551465	5.783740167	7.31E-09	9.42E-06
ENSMUSG00000019817	Plagl1	pleiomorphic adenoma gene-like 1	76.29245071	0.819492865	0.146652951	5.587973925	2.30E-08	2.57E-05
ENSMUSG00000042073	Abhd14b	abhydrolase domain containing 14b	312.5043269	-0.742734019	0.132845695	-5.590952862	2.26E-08	2.57E-05
ENSMUSG00000038801	Scgb1c1	secretoglobin, family 1C, member 1	193.8961	1.137948154	0.205183249	5.546009029	2.92E-08	2.88E-05
ENSMUSG00000097099	Gm9917	predicted gene 9917	111.2305592	-0.971774724	0.179085224	-5.426325529	5.75E-08	5.35E-05
ENSMUSG00000107653	Gm31520	sterol-C5-desaturase pseudogene	38.9097343	1.461818509	0.276075681	5.294991955	1.19E-07	1.05E-04
ENSMUSG00000032419	Tbx18	T-box18	104.4903783	-0.654370039	0.125020141	-5.234116949	1.66E-07	1.32E-04
ENSMUSG00000020253	Ppm1m	protein phosphatase 1M	224.4754793	0.629411893	0.120929771	5.204772037	1.94E-07	1.48E-04
ENSMUSG00000032563	Mrpl3	mitochondrial ribosomal protein L3	1783.956096	-0.436886258	0.085393676	-5.116143011	3.12E-07	2.27E-04

ENSMUSG00000032261	Sh3bgrl2	SH3 domain binding glutamic acid-rich protein like 2	105.6921769	-0.653725	0.128760505	-5.077061488	3.83E-07	2.68E-04
ENSMUSG00000023979	Guca1b	guanylate cyclase activator 1B	25.91071064	1.315395153	0.259962618	5.059939622	4.19E-07	2.81E-04
ENSMUSG00000091345	Col6a5	collagen, type VI, alpha 5	29.84898234	1.907639946	0.3775694	5.052422015	4.36E-07	2.81E-04
ENSMUSG00000032359	Ctsh	cathepsin H	710.7231171	-0.623022117	0.125532066	-4.963051582	6.94E-07	4.15E-04
ENSMUSG00000022219	Cideb	cell death-inducing DNA fragmentation factor, alpha subunit-like effector B	74.13239706	0.858582759	0.175534791	4.891239831	1.00E-06	5.79E-04
ENSMUSG00000010064	Slc38a3	solute carrier family 38, member 3	2341.478262	-0.809203125	0.167037335	-4.844444656	1.27E-06	7.09E-04
ENSMUSG00000032259	Drd2	dopamine receptor D2	85.88598789	0.839883098	0.174723741	4.8069203	1.53E-06	8.28E-04
ENSMUSG00000032537	Ephb1	Eph receptor B1	585.1805641	2.398021253	0.521600636	4.597427777	4.28E-06	2.24E-03
ENSMUSG00000104344	Gm38077	predicted gene 38077	168.5348807	-0.988910029	0.216709138	-4.563305623	5.04E-06	2.56E-03
ENSMUSG00000030990	Pgap2	post-GPI attachment to proteins 2	688.9552575	0.468413015	0.104101368	4.499585592	6.81E-06	3.36E-03
ENSMUSG00000062270	Morf4l1	mortality factor 4 like 1	1196.914037	-0.415696122	0.093949616	-4.424670816	9.66E-06	4.62E-03
ENSMUSG00000062270	Morf4l1b	mortality factor 4 like 1B	1196.914037	-0.415696122	0.093949616	-4.424670816	9.66E-06	4.62E-03
ENSMUSG00000032872	Cyb5r4	cytochrome b5 reductase 4	1012.878713	-0.551302186	0.125317439	-4.399245566	1.09E-05	4.92E-03
ENSMUSG00000079355	Ackr4	atypical chemokine receptor 4	94.67720248	-0.760983138	0.172765696	-4.404712012	1.06E-05	4.92E-03
ENSMUSG00000020431	Adcy1	adenylate cyclase 1	97.1204426	0.866213531	0.197445358	4.38710508	1.15E-05	4.93E-03
ENSMUSG00000023439	Gnb3	guanine nucleotide binding protein (G protein), beta 3	256.1773659	0.925120884	0.249262978	3.711425138	2.06E-04	5.21E-03
ENSMUSG00000043587	Pxylp1	2-phosphoxylose phosphatase 1	148.4011593	-0.941500636	0.215647645	-4.365921245	1.27E-05	5.21E-03
ENSMUSG00000100410	2310020H05Rik	RIKEN cDNA 2310020H05 gene	82.70867895	-0.95306705	0.218380045	-4.364258874	1.28E-05	5.21E-03
ENSMUSG00000023262	Acy1	aminoacylase 1	275.312161	0.52627658	0.12086618	4.354208773	1.34E-05	5.28E-03
ENSMUSG00000032420	Nt5e	5' nucleotidase, ecto	531.2462273	0.575371191	0.132243883	4.35083406	1.36E-05	5.28E-03
ENSMUSG00000032342	Mto1	mitochondrial tRNA translation optimization 1	628.7435289	-0.35212118	0.081316245	-4.330268576	1.49E-05	5.54E-03

ENSMUSG00000036006	Ripor2	RHO family interacting cell polarization regulator 2	280.1521625	0.766998221	0.178845813	4.288600385	1.80E-05	6.55E-03
ENSMUSG00000032567	Aste1	asteroid homolog 1	136.4175984	-0.546329802	0.129600006	-4.215507543	2.49E-05	8.88E-03
ENSMUSG00000007033	Hspa1l	heat shock protein 1-like	313.1401892	-0.868331662	0.207647674	-4.181754823	2.89E-05	1.01E-02
ENSMUSG00000062991	Nrg1	neuregulin 1	36.63309961	1.167251298	0.281216976	4.150714202	3.31E-05	1.13E-02
ENSMUSG00000057802	Gm10030	predicted gene 10030	23.54320155	1.146733244	0.277719383	4.129107706	3.64E-05	1.22E-02
ENSMUSG00000032500	Dclk3	doublecortin-like kinase 3	16.62670461	1.320424335	0.32048356	4.120100055	3.79E-05	1.24E-02
ENSMUSG00000030592	Ryr1	ryanodine receptor 1, skeletal muscle	18.10439933	-1.213191335	0.295663089	-4.103289788	4.07E-05	1.31E-02
ENSMUSG00000034533	Scn10a	sodium channel, voltage-gated, type X, alpha	113.9830881	0.858252285	0.213468675	4.020506927	5.81E-05	1.84E-02
ENSMUSG00000031066	Usp11	ubiquitin specific peptidase 11	212.3557436	0.528925104	0.131795322	4.013231248	5.99E-05	1.86E-02
ENSMUSG00000071708	Sms	spermine synthase	825.2887178	-0.362951165	0.090642781	-4.004192737	6.22E-05	1.86E-02
ENSMUSG00000113321	Gm8775	predicted gene 8775	29.48173879	1.076447965	0.268553676	4.008315883	6.12E-05	1.86E-02
ENSMUSG00000073485	H3f3aos	H3 histone, family 3A	31.32162143	-0.946720716	0.236742268	-3.998950945	6.36E-05	1.87E-02
ENSMUSG00000026414	Tnnt2	troponin T2, cardiac	217.8533484	0.619746386	0.156123287	3.969596064	7.20E-05	2.08E-02
ENSMUSG00000031637	Lrp2bp	Lrp2 binding protein	63.26457812	-1.031672567	0.264188857	-3.90505709	9.42E-05	2.68E-02
ENSMUSG00000045594	Glb1	galactosidase, beta 1	384.1377132	-0.474925266	0.123283793	-3.852292773	1.17E-04	3.27E-02
ENSMUSG00000010051	Hyal1	hyaluronoglucosaminidase 1	122.0241169	0.64246724	0.167341124	3.839266904	1.23E-04	3.39E-02
ENSMUSG00000020534	Shmt1	serine hydroxymethyltransferase 1 (soluble)	289.1479786	0.655279666	0.171422662	3.822596498	1.32E-04	3.57E-02
ENSMUSG00000060187	Lrrc10	leucine rich repeat containing 10	2494.259676	0.407948338	0.111196436	3.668717757	2.44E-04	3.91E-02
ENSMUSG00000027313	Chac1	ChaC, cation transport regulator 1	44.4569393	-1.241707583	0.328017443	-3.785492538	1.53E-04	4.08E-02
ENSMUSG00000024145	Pigf	phosphatidylinositol glycan anchor biosynthesis, class F	53.55766273	0.70037248	0.186231311	3.760766521	1.69E-04	4.37E-02
ENSMUSG00000052485	Tmem171	transmembrane protein 171	169.2165357	0.76792289	0.204074434	3.762954896	1.68E-04	4.37E-02
ENSMUSG00000031461	Myom2	myomesin 2	39422.33605	0.551200865	0.150744712	3.65651875	2.56E-04	4.71E-02

Supp. Table S6. List of Biological Processes (BP) at FDR 5% - atria

GO ID	Description	BgRatio	pvalue	p.adjust	qvalue	geneID	Count
GO:0046184	aldehyde biosynthetic process	18/21092	5.11E-05	7.82E-02	0.075133254	Bmp5/Adh1/Tkt	3
GO:0006081	cellular aldehyde metabolic process	68/21092	1.72E-04	1.32E-01	0.126431472	Bmp5/Aldh3a1/Adh1/Tkt	4
GO:0032892	positive regulation of organic acid transport	47/21092	9.32E-04	4.20E-01	0.403462799	Agt/P2ry2/Slc38a3	3
GO:0015802	basic amino acid transport	14/21092	1.45E-03	4.20E-01	0.403462799	Agt/Slc38a3	2
GO:1903793	positive regulation of anion transport	63/21092	2.18E-03	4.20E-01	0.403462799	Agt/P2ry2/Slc38a3	3
GO:0006883	cellular sodium ion homeostasis	19/21092	2.69E-03	4.20E-01	0.403462799	Agt/Tesc	2
GO:0008015	blood circulation	466/21092	2.94E-03	4.20E-01	0.403462799	Comp/Npr3/Agt/Myh7/P2ry2/Scn10a/Nts	7
GO:0003013	circulatory system process	475/21092	3.27E-03	4.20E-01	0.403462799	Comp/Npr3/Agt/Myh7/P2ry2/Scn10a/Nts	7
GO:0032890	regulation of organic acid transport	77/21092	3.85E-03	4.20E-01	0.403462799	Agt/P2ry2/Slc38a3	3
GO:0043687	post-translational protein modification	23/21092	3.93E-03	4.20E-01	0.403462799	Crtap/Agtpbp1	2
GO:0014829	vascular smooth muscle contraction	25/21092	4.64E-03	4.20E-01	0.403462799	Comp/Agt	2
GO:0050880	regulation of blood vessel size	168/21092	4.97E-03	4.20E-01	0.403462799	Comp/Agt/P2ry2/Nts	4
GO:0035150	regulation of tube size	169/21092	5.07E-03	4.20E-01	0.403462799	Comp/Agt/P2ry2/Nts	4
GO:0032526	response to retinoic acid	86/21092	5.25E-03	4.20E-01	0.403462799	Mest/Adh1/Tesc	3
GO:0051957	positive regulation of amino acid transport	28/21092	5.80E-03	4.20E-01	0.403462799	Agt/Slc38a3	2
GO:0006936	muscle contraction	281/21092	5.87E-03	4.20E-01	0.403462799	Comp/Lmod2/Agt/Myh7/Scn10a	5
GO:0002027	regulation of heart rate	91/21092	6.14E-03	4.20E-01	0.403462799	Agt/Myh7/Scn10a	3
GO:0045652	regulation of megakaryocyte differentiation	30/21092	6.64E-03	4.20E-01	0.403462799	Tesc/Hist1h4i	2
GO:1900274	regulation of phospholipase C activity	30/21092	6.64E-03	4.20E-01	0.403462799	Snap91/Agt	2

GO:0003018	vascular process in circulatory system	193/21092	8.05E-03	4.20E-01	0.403462799	Comp/Agt/P2ry2/Nts	4
GO:0006739	NADP metabolic process	36/21092	9.46E-03	4.20E-01	0.403462799	Cyb5r4/Tkt	2
GO:0042445	hormone metabolic process	207/21092	1.02E-02	4.20E-01	0.403462799	Bmp5/Agt/Hfe/Adh1	4
GO:0031279	regulation of cyclase activity	41/21092	1.22E-02	4.20E-01	0.403462799	Guca1b/Npr3	2
GO:0044070	regulation of anion transport	117/21092	1.22E-02	4.20E-01	0.403462799	Agt/P2ry2/Slc38a3	3
GO:0051339	regulation of lyase activity	43/21092	1.33E-02	4.20E-01	0.403462799	Guca1b/Npr3	2
GO:0032007	negative regulation of TOR signaling	45/21092	1.45E-02	4.20E-01	0.403462799	Nprl2/Minar1	2
GO:0010862	positive regulation of pathway-restricted SMAD protein phosphorylation	49/21092	1.71E-02	4.20E-01	0.403462799	Bmp5/Hfe	2
GO:0050905	neuromuscular process	133/21092	1.72E-02	4.20E-01	0.403462799	Comp/Tmem150c/Agtpbp1	3
GO:0032941	secretion by tissue	50/21092	1.77E-02	4.20E-01	0.403462799	Npr3/P2ry2	2
GO:0051955	regulation of amino acid transport	50/21092	1.77E-02	4.20E-01	0.403462799	Agt/Slc38a3	2
GO:0055078	sodium ion homeostasis	50/21092	1.77E-02	4.20E-01	0.403462799	Agt/Tesc	2
GO:0002064	epithelial cell development	245/21092	1.80E-02	4.20E-01	0.403462799	Bmp5/Bfsp2/Col23a1/Agt	4
GO:0030219	megakaryocyte differentiation	51/21092	1.84E-02	4.20E-01	0.403462799	Tesc/Hist1h4i	2
GO:0051954	positive regulation of amine transport	51/21092	1.84E-02	4.20E-01	0.403462799	Agt/Slc38a3	2
GO:0001505	regulation of neurotransmitter levels	376/21092	1.88E-02	4.20E-01	0.403462799	Snap91/Mctp1/Agt/P2ry2/Agtpbp1	5
GO:0030198	extracellular matrix organization	249/21092	1.89E-02	4.20E-01	0.403462799	Comp/Col23a1/Reck/Agt	4
GO:0034308	primary alcohol metabolic process	52/21092	1.91E-02	4.20E-01	0.403462799	Bmp5/Adh1	2
GO:0003012	muscle system process	383/21092	2.02E-02	4.20E-01	0.403462799	Comp/Lmod2/Agt/Myh7/Scn10a	5
GO:0010517	regulation of phospholipase activity	54/21092	2.05E-02	4.20E-01	0.403462799	Snap91/Agt	2
GO:0050879	multicellular organismal movement	54/21092	2.05E-02	4.20E-01	0.403462799	Comp/Myh7	2
GO:0050881	musculoskeletal movement	54/21092	2.05E-02	4.20E-01	0.403462799	Comp/Myh7	2
GO:1905952	regulation of lipid localization	143/21092	2.07E-02	4.20E-01	0.403462799	Agt/Mest/P2ry2	3

GO:0006865	amino acid transport	145/21092	2.15E-02	4.20E-01	0.403462799	Slc17a5/Agt/Slc38a3	3
GO:0061337	cardiac conduction	58/21092	2.34E-02	4.20E-01	0.403462799	Agt/Scn10a	2
GO:0015807	L-amino acid transport	59/21092	2.42E-02	4.20E-01	0.403462799	Agt/Slc38a3	2
GO:0014911	positive regulation of smooth muscle cell migration	60/21092	2.50E-02	4.20E-01	0.403462799	Agt/P2ry2	2
GO:0035296	regulation of tube diameter	156/21092	2.60E-02	4.20E-01	0.403462799	Comp/Agt/P2ry2	3
GO:0097746	regulation of blood vessel diameter	156/21092	2.60E-02	4.20E-01	0.403462799	Comp/Agt/P2ry2	3
GO:2001238	positive regulation of extrinsic apoptotic signaling pathway	62/21092	2.65E-02	4.20E-01	0.403462799	Ppp2r1b/Agt	2
GO:0006801	superoxide metabolic process	63/21092	2.73E-02	4.20E-01	0.403462799	Cyb5r4/Agt	2
GO:0060393	regulation of pathway-restricted SMAD protein phosphorylation	63/21092	2.73E-02	4.20E-01	0.403462799	Bmp5/Hfe	2
GO:1901264	carbohydrate derivative transport	64/21092	2.81E-02	4.20E-01	0.403462799	Slc17a5/P2ry2	2
GO:0060389	pathway-restricted SMAD protein phosphorylation	66/21092	2.98E-02	4.20E-01	0.403462799	Bmp5/Hfe	2
GO:0030509	BMP signaling pathway	165/21092	3.00E-02	4.20E-01	0.403462799	Bmp5/Comp/Hfe	3
GO:0001885	endothelial cell development	67/21092	3.06E-02	4.20E-01	0.403462799	Col23a1/Agt	2
GO:0051604	protein maturation	291/21092	3.12E-02	4.20E-01	0.403462799	Comp/Spon1/Aph1c/Tesc	4
GO:0043062	extracellular structure organization	293/21092	3.19E-02	4.20E-01	0.403462799	Comp/Col23a1/Reck/Agt	4
GO:0046942	carboxylic acid transport	297/21092	3.33E-02	4.20E-01	0.403462799	Slc17a5/Agt/P2ry2/Slc38a3	4
GO:0008016	regulation of heart contraction	172/21092	3.33E-02	4.20E-01	0.403462799	Agt/Myh7/Scn10a	3
GO:0015849	organic acid transport	298/21092	3.36E-02	4.20E-01	0.403462799	Slc17a5/Agt/P2ry2/Slc38a3	4
GO:0042446	hormone biosynthetic process	72/21092	3.49E-02	4.20E-01	0.403462799	Bmp5/Hfe	2
GO:0071772	response to BMP	176/21092	3.53E-02	4.20E-01	0.403462799	Bmp5/Comp/Hfe	3
GO:0071773	cellular response to BMP stimulus	176/21092	3.53E-02	4.20E-01	0.403462799	Bmp5/Comp/Hfe	3
GO:0051145	smooth muscle cell differentiation	73/21092	3.58E-02	4.20E-01	0.403462799	Comp/Agt	2
GO:0060191	regulation of lipase activity	73/21092	3.58E-02	4.20E-01	0.403462799	Snap91/Agt	2
GO:0003333	amino acid transmembrane transport	74/21092	3.67E-02	4.20E-01	0.403462799	Agt/Slc38a3	2

GO:0007219	Notch signaling pathway	181/21092	3.79E-02	4.20E-01	0.403462799	Reck/Aph1c/Cfd	3
GO:0055002	striated muscle cell development	181/21092	3.79E-02	4.20E-01	0.403462799	Comp/Lmod2/Agt	3
GO:0043270	positive regulation of ion transport	310/21092	3.80E-02	4.20E-01	0.403462799	Agt/P2ry2/Slc38a3/Tesc	4
GO:0002181	cytoplasmic translation	76/21092	3.86E-02	4.20E-01	0.403462799	Rpl29/Tma7	2
GO:0034765	regulation of ion transmembrane transport	459/21092	3.96E-02	4.20E-01	0.403462799	Gnb5/Agt/Scn10a/Tesc/Kcnh7	5
GO:0030534	adult behavior	185/21092	4.00E-02	4.20E-01	0.403462799	Adh1/Ccnd2/Agtpbp1	3
GO:0006995	cellular response to nitrogen starvation	10/21092	4.00E-02	4.20E-01	0.403462799	Nprl2	1
GO:0007220	Notch receptor processing	10/21092	4.00E-02	4.20E-01	0.403462799	Aph1c	1
GO:0014883	transition between fast and slow fiber	10/21092	4.00E-02	4.20E-01	0.403462799	Myh7	1
GO:0016264	gap junction assembly	10/21092	4.00E-02	4.20E-01	0.403462799	Agt	1
GO:0030049	muscle filament sliding	10/21092	4.00E-02	4.20E-01	0.403462799	Myh7	1
GO:0030854	positive regulation of granulocyte differentiation	10/21092	4.00E-02	4.20E-01	0.403462799	Tesc	1
GO:0031282	regulation of guanylate cyclase activity	10/21092	4.00E-02	4.20E-01	0.403462799	Guca1b	1
GO:0031943	regulation of glucocorticoid metabolic process	10/21092	4.00E-02	4.20E-01	0.403462799	Bmp5	1
GO:0032342	aldosterone biosynthetic process	10/21092	4.00E-02	4.20E-01	0.403462799	Bmp5	1
GO:0043562	cellular response to nitrogen levels	10/21092	4.00E-02	4.20E-01	0.403462799	Nprl2	1
GO:0048149	behavioral response to ethanol	10/21092	4.00E-02	4.20E-01	0.403462799	Adh1	1
GO:0060710	chorio-allantoic fusion	10/21092	4.00E-02	4.20E-01	0.403462799	Bmp5	1
GO:0070142	synaptic vesicle budding	10/21092	4.00E-02	4.20E-01	0.403462799	Snap91	1
GO:0070257	positive regulation of mucus secretion	10/21092	4.00E-02	4.20E-01	0.403462799	P2ry2	1
GO:0070278	extracellular matrix constituent secretion	10/21092	4.00E-02	4.20E-01	0.403462799	Agt	1
GO:1902023	L-arginine transport	10/21092	4.00E-02	4.20E-01	0.403462799	Agt	1
GO:2000807	regulation of synaptic vesicle clustering	10/21092	4.00E-02	4.20E-01	0.403462799	Snap91	1
GO:0006942	regulation of striated muscle contraction	79/21092	4.14E-02	4.20E-01	0.403462799	Myh7/Scn10a	2
GO:0007269	neurotransmitter secretion	190/21092	4.27E-02	4.20E-01	0.403462799	Snap91/Mctp1/P2ry2	3

GO:0099643	signal release from synapse	190/21092	4.27E-02	4.20E-01	0.403462799	Snap91/Mctp 1/P2ry2	3
GO:1901888	regulation of cell junction assembly	81/21092	4.33E-02	4.20E-01	0.403462799	Limch1/Agt	2
GO:0006012	galactose metabolic process	11/21092	4.40E-02	4.20E-01	0.403462799	Glb1	1
GO:0006266	DNA ligation	11/21092	4.40E-02	4.20E-01	0.403462799	Parp3	1
GO:0006705	mineralocorticoid biosynthetic process	11/21092	4.40E-02	4.20E-01	0.403462799	Bmp5	1
GO:0006957	complement activation, alternative pathway	11/21092	4.40E-02	4.20E-01	0.403462799	Cfd	1
GO:0007128	meiotic prophase I	11/21092	4.40E-02	4.20E-01	0.403462799	Mlh1	1
GO:0010872	regulation of cholesterol esterification	11/21092	4.40E-02	4.20E-01	0.403462799	Agt	1
GO:0010958	regulation of amino acid import across plasma membrane	11/21092	4.40E-02	4.20E-01	0.403462799	Agt	1
GO:0014824	artery smooth muscle contraction	11/21092	4.40E-02	4.20E-01	0.403462799	Agt	1
GO:0019511	peptidyl-proline hydroxylation	11/21092	4.40E-02	4.20E-01	0.403462799	Crtap	1
GO:0032341	aldosterone metabolic process	11/21092	4.40E-02	4.20E-01	0.403462799	Bmp5	1
GO:0051324	prophase	11/21092	4.40E-02	4.20E-01	0.403462799	Mlh1	1
GO:0060405	regulation of penile erection	11/21092	4.40E-02	4.20E-01	0.403462799	P2ry2	1
GO:0060586	multicellular organismal iron ion homeostasis	11/21092	4.40E-02	4.20E-01	0.403462799	Hfe	1
GO:0086016	AV node cell action potential	11/21092	4.40E-02	4.20E-01	0.403462799	Scn10a	1
GO:0086027	AV node cell to bundle of His cell signaling	11/21092	4.40E-02	4.20E-01	0.403462799	Scn10a	1
GO:0097084	vascular smooth muscle cell development	11/21092	4.40E-02	4.20E-01	0.403462799	Comp	1
GO:1903867	extraembryonic membrane development	11/21092	4.40E-02	4.20E-01	0.403462799	Bmp5	1
GO:0055001	muscle cell development	195/21092	4.56E-02	4.20E-01	0.403462799	Comp/Lmod2/ Agt	3
GO:0014910	regulation of smooth muscle cell migration	85/21092	4.72E-02	4.20E-01	0.403462799	Agt/P2ry2	2
GO:0000279	M phase	12/21092	4.79E-02	4.20E-01	0.403462799	Mlh1	1
GO:0000963	mitochondrial RNA processing	12/21092	4.79E-02	4.20E-01	0.403462799	Mto1	1
GO:0001542	ovulation from ovarian follicle	12/21092	4.79E-02	4.20E-01	0.403462799	Agt	1
GO:0002016	regulation of blood volume by renin-angiotensin	12/21092	4.79E-02	4.20E-01	0.403462799	Agt	1
GO:0006098	pentose-phosphate shunt	12/21092	4.79E-02	4.20E-01	0.403462799	Tkt	1

GO:0008212	mineralocorticoid metabolic process	12/21092	4.79E-02	4.20E-01	0.403462799	Bmp5	1
GO:0015809	arginine transport	12/21092	4.79E-02	4.20E-01	0.403462799	Agt	1
GO:0030432	peristalsis	12/21092	4.79E-02	4.20E-01	0.403462799	Agt	1
GO:0032308	positive regulation of prostaglandin secretion	12/21092	4.79E-02	4.20E-01	0.403462799	P2ry2	1
GO:0032353	negative regulation of hormone biosynthetic process	12/21092	4.79E-02	4.20E-01	0.403462799	Bmp5	1
GO:0033275	actin-myosin filament sliding	12/21092	4.79E-02	4.20E-01	0.403462799	Myh7	1
GO:0034309	primary alcohol biosynthetic process	12/21092	4.79E-02	4.20E-01	0.403462799	Bmp5	1
GO:0042271	susceptibility to natural killer cell mediated cytotoxicity	12/21092	4.79E-02	4.20E-01	0.403462799	Hfe	1
GO:0048143	astrocyte activation	12/21092	4.79E-02	4.20E-01	0.403462799	Agt	1
GO:0070471	uterine smooth muscle contraction	12/21092	4.79E-02	4.20E-01	0.403462799	Agt	1
GO:0071281	cellular response to iron ion	12/21092	4.79E-02	4.20E-01	0.403462799	Hfe	1
GO:0071468	cellular response to acidic pH	12/21092	4.79E-02	4.20E-01	0.403462799	Slc38a3	1
GO:0098762	meiotic cell cycle phase	12/21092	4.79E-02	4.20E-01	0.403462799	Mlh1	1
GO:0098764	meiosis I cell cycle phase	12/21092	4.79E-02	4.20E-01	0.403462799	Mlh1	1
GO:1900244	positive regulation of synaptic vesicle endocytosis	12/21092	4.79E-02	4.20E-01	0.403462799	Snap91	1
GO:1902430	negative regulation of amyloid-beta formation	12/21092	4.79E-02	4.20E-01	0.403462799	Spon1	1
GO:1903961	positive regulation of anion transmembrane transport	12/21092	4.79E-02	4.20E-01	0.403462799	Agt	1

Supp. Table S7. List of Biological Processes (BP) at FDR 5% - ventricle

GO ID	Description	BgRatio	pvalue	p.adjust	qvalue	geneID	Count
GO:0021826	substrate-independent telencephalic tangential migration	10/21092	2.55E-04	1.52E-01	0.120425014	Drd2/Nrg1	2
GO:0021843	substrate-independent telencephalic tangential interneuron migration	10/21092	2.55E-04	1.52E-01	0.120425014	Drd2/Nrg1	2
GO:1901386	negative regulation of voltage-gated calcium channel activity	15/21092	5.90E-04	1.52E-01	0.120425014	Gnb5/Drd2	2
GO:0014706	striated muscle tissue development	441/21092	6.56E-04	1.52E-01	0.120425014	Plagl1/Tbx18/Ephb1/Ripor2/Nrg1/Ryr1	6

GO:0003161	cardiac conduction system development	16/21092	6.73E-04	1.52E-01	0.120425014	Tbx18/Nrg1	2
GO:0007409	axonogenesis	451/21092	7.38E-04	1.52E-01	0.120425014	Snap91/Ntn1/Drd2/Ephb1/Adcy1/Nrg1	6
GO:0060537	muscle tissue development	462/21092	8.36E-04	1.52E-01	0.120425014	Plagl1/Tbx18/Ephb1/Ripor2/Nrg1/Ryr1	6
GO:0061564	axon development	486/21092	1.09E-03	1.55E-01	0.122484614	Snap91/Ntn1/Drd2/Ephb1/Adcy1/Nrg1	6
GO:0007519	skeletal muscle tissue development	197/21092	1.31E-03	1.55E-01	0.122484614	Plagl1/Ephb1/Ripor2/Ryr1	4
GO:0071467	cellular response to pH	23/21092	1.40E-03	1.55E-01	0.122484614	Slc38a3/Hyal1	2
GO:0060538	skeletal muscle organ development	206/21092	1.54E-03	1.55E-01	0.122484614	Plagl1/Ephb1/Ripor2/Ryr1	4
GO:0050772	positive regulation of axonogenesis	98/21092	1.72E-03	1.55E-01	0.122484614	Snap91/Ntn1/Nrg1	3
GO:0043171	peptide catabolic process	26/21092	1.80E-03	1.55E-01	0.122484614	Ctsh/Chac1	2
GO:1901020	negative regulation of calcium ion transmembrane transporter activity	26/21092	1.80E-03	1.55E-01	0.122484614	Gnb5/Drd2	2
GO:0072522	purine-containing compound biosynthetic process	227/21092	2.20E-03	1.55E-01	0.122484614	Guca1b/Adcy1/Nt5e/Shmt1	4
GO:0042692	muscle cell differentiation	383/21092	2.28E-03	1.55E-01	0.122484614	Tbx18/Ripor2/Nrg1/Ryr1/Tnnt2	5
GO:0006506	GPI anchor biosynthetic process	31/21092	2.55E-03	1.55E-01	0.122484614	Pgap2/Pigf	2
GO:0042472	inner ear morphogenesis	113/21092	2.59E-03	1.55E-01	0.122484614	Ntn1/Tbx18/Ripor2	3
GO:0001964	startle response	32/21092	2.71E-03	1.55E-01	0.122484614	Drd2/Nrg1	2
GO:0006505	GPI anchor metabolic process	32/21092	2.71E-03	1.55E-01	0.122484614	Pgap2/Pigf	2
GO:1903170	negative regulation of calcium ion transmembrane transport	35/21092	3.24E-03	1.55E-01	0.122484614	Gnb5/Drd2	2
GO:0007517	muscle organ development	420/21092	3.38E-03	1.55E-01	0.122484614	Plagl1/Ephb1/Ripor2/Nrg1/Ryr1	5
GO:0050807	regulation of synapse organization	259/21092	3.53E-03	1.55E-01	0.122484614	Snap91/Ntn1/Drd2/Ephb1	4
GO:1901385	regulation of voltage-gated calcium channel activity	37/21092	3.62E-03	1.55E-01	0.122484614	Gnb5/Drd2	2
GO:0050808	synapse organization	427/21092	3.63E-03	1.55E-01	0.122484614	Snap91/Ntn1/Drd2/Ephb1/Nrg1	5
GO:0007616	long-term memory	38/21092	3.81E-03	1.55E-01	0.122484614	Drd2/Adcy1	2

GO:0048741	skeletal muscle fiber development	38/21092	3.81E-03	1.55E-01	0.122484614	Ripor2/Ryr1	2
GO:0060236	regulation of mitotic spindle organization	38/21092	3.81E-03	1.55E-01	0.122484614	Parp3/Ripor2	2
GO:0050803	regulation of synapse structure or activity	266/21092	3.88E-03	1.55E-01	0.122484614	Snap91/Ntn1/Drd2/Ephb1	4
GO:0009268	response to pH	40/21092	4.22E-03	1.55E-01	0.122484614	Slc38a3/Hyal1	2
GO:0042471	ear morphogenesis	135/21092	4.27E-03	1.55E-01	0.122484614	Ntn1/Tbx18/Ripor2	3
GO:0031279	regulation of cyclase activity	41/21092	4.43E-03	1.55E-01	0.122484614	Guca1b/Drd2	2
GO:2001258	negative regulation of cation channel activity	41/21092	4.43E-03	1.55E-01	0.122484614	Gnb5/Drd2	2
GO:0071496	cellular response to external stimulus	277/21092	4.48E-03	1.55E-01	0.122484614	Nprl2/Slc38a3/Ripor2/Ryr1	4
GO:0006024	glycosaminoglycan biosynthetic process	42/21092	4.64E-03	1.55E-01	0.122484614	Pxylp1/Hyal1	2
GO:0014904	myotube cell development	42/21092	4.64E-03	1.55E-01	0.122484614	Ripor2/Ryr1	2
GO:0090224	regulation of spindle organization	42/21092	4.64E-03	1.55E-01	0.122484614	Parp3/Ripor2	2
GO:0006936	muscle contraction	281/21092	4.71E-03	1.55E-01	0.122484614	Drd2/Ryr1/Scn10a/Tnnt2	4
GO:0007212	dopamine receptor signaling pathway	43/21092	4.86E-03	1.55E-01	0.122484614	Gnb5/Drd2	2
GO:0051339	regulation of lyase activity	43/21092	4.86E-03	1.55E-01	0.122484614	Guca1b/Drd2	2
GO:0098693	regulation of synaptic vesicle cycle	147/21092	5.41E-03	1.66E-01	0.131229692	Snap91/Drd2/Adcy1	3
GO:0006937	regulation of muscle contraction	148/21092	5.51E-03	1.66E-01	0.131229692	Ryr1/Scn10a/Tnnt1	3
GO:0090407	organophosphate biosynthetic process	474/21092	5.64E-03	1.66E-01	0.131229692	Guca1b/Pgap2/Adcy1/Shmt1/Pigf	5
GO:0090596	sensory organ morphogenesis	297/21092	5.73E-03	1.66E-01	0.131229692	Ntn1/Tbx18/Ephb1/Ripor2	4
GO:0051146	striated muscle cell differentiation	302/21092	6.07E-03	1.72E-01	0.136016787	Ripor2/Nrg1/Ryr1/Tnnt2	4
GO:0045927	positive regulation of growth	308/21092	6.50E-03	1.80E-01	0.141909734	Ntn1/Drd2/Nrg1/Hyal1	4
GO:0051954	positive regulation of amine transport	51/21092	6.78E-03	1.80E-01	0.141909734	Slc38a3/Drd2	2
GO:0048562	embryonic organ morphogenesis	315/21092	7.03E-03	1.80E-01	0.141909734	Ntn1/Tbx18/Ripor2/Hyal1	4
GO:0006023	aminoglycan biosynthetic process	52/21092	7.04E-03	1.80E-01	0.141909734	Pxylp1/Hyal1	2
GO:0045773	positive regulation of axon extension	52/21092	7.04E-03	1.80E-01	0.141909734	Ntn1/Nrg1	2

GO:0007416	synapse assembly	169/21092	7.94E-03	1.94E-01	0.153083885	Ntn1/Ephb1/Nrg1	3
GO:0009247	glycolipid biosynthetic process	56/21092	8.12E-03	1.94E-01	0.153083885	Pgap2/Pigf	2
GO:0006661	phosphatidylinositol biosynthetic process	59/21092	8.98E-03	1.94E-01	0.153083885	Pgap2/Pigf	2
GO:0010770	positive regulation of cell morphogenesis involved in differentiation	177/21092	9.01E-03	1.94E-01	0.153083885	Snap91/Ntn1/Nrg1	3
GO:0001764	neuron migration	181/21092	9.57E-03	1.94E-01	0.153083885	Ntn1/Drd2/Nrg1	3
GO:0048489	synaptic vesicle transport	181/21092	9.57E-03	1.94E-01	0.153083885	Snap91/Drd2/Adcy1	3
GO:0055002	striated muscle cell development	181/21092	9.57E-03	1.94E-01	0.153083885	Ripor2/Ryr1/Tnnt1	3
GO:0097480	establishment of synaptic vesicle localization	181/21092	9.57E-03	1.94E-01	0.153083885	Snap91/Drd2/Adcy1	3
GO:0051926	negative regulation of calcium ion transport	61/21092	9.58E-03	1.94E-01	0.153083885	Gnb5/Drd2	2
GO:0009988	cell-cell recognition	62/21092	9.88E-03	1.94E-01	0.153083885	Ephb1/Hspa1l	2
GO:0031669	cellular response to nutrient levels	185/21092	1.02E-02	1.94E-01	0.153083885	Nprl2/Slc38a3/Ryr1	3
GO:0042440	pigment metabolic process	63/21092	1.02E-02	1.94E-01	0.153083885	Cyb5r4/Shmt1	2
GO:0031638	zymogen activation	64/21092	1.05E-02	1.94E-01	0.153083885	Ctsh/Cideb	2
GO:0007269	neurotransmitter secretion	190/21092	1.09E-02	1.94E-01	0.153083885	Snap91/Drd2/Adcy1	3
GO:0099643	signal release from synapse	190/21092	1.09E-02	1.94E-01	0.153083885	Snap91/Drd2/Adcy1	3
GO:0032413	negative regulation of ion transmembrane transporter activity	66/21092	1.11E-02	1.94E-01	0.153083885	Gnb5/Drd2	2
GO:0097479	synaptic vesicle localization	192/21092	1.12E-02	1.94E-01	0.153083885	Snap91/Drd2/Adcy1	3
GO:0030307	positive regulation of cell growth	195/21092	1.17E-02	1.94E-01	0.153083885	Ntn1/Nrg1/Hyal1	3
GO:0055001	muscle cell development	195/21092	1.17E-02	1.94E-01	0.153083885	Ripor2/Ryr1/Tnnt1	3
GO:0022029	telencephalon cell migration	70/21092	1.25E-02	1.94E-01	0.153083885	Drd2/Nrg1	2
GO:0001505	regulation of neurotransmitter levels	376/21092	1.29E-02	1.94E-01	0.153083885	Snap91/Drd2/Adcy1/Shmt1	4
GO:0050770	regulation of axonogenesis	202/21092	1.29E-02	1.94E-01	0.153083885	Snap91/Ntn1/Nrg1	3
GO:0010822	positive regulation of mitochondrion organization	72/21092	1.32E-02	1.94E-01	0.153083885	Cideb/Hspa1l	2
GO:0021885	forebrain cell migration	73/21092	1.35E-02	1.94E-01	0.153083885	Drd2/Nrg1	2

GO:0048839	inner ear development	206/21092	1.36E-02	1.94E-01	0.153083885	Ntn1/Tbx18/Ripor2	3
GO:0003012	muscle system process	383/21092	1.37E-02	1.94E-01	0.153083885	Drd2/Ryr1/Scn10a/Tnnt2	4
GO:0060047	heart contraction	207/21092	1.37E-02	1.94E-01	0.153083885	Drd2/Scn10a/Tnnt1	3
GO:0051155	positive regulation of striated muscle cell differentiation	74/21092	1.39E-02	1.94E-01	0.153083885	Ripor2/Nrg1	2
GO:0007163	establishment or maintenance of cell polarity	208/21092	1.39E-02	1.94E-01	0.153083885	Snap91/Ephb1/Ripor2	3
GO:0032410	negative regulation of transporter activity	75/21092	1.42E-02	1.94E-01	0.153083885	Gnb5/Drd2	2
GO:0048639	positive regulation of developmental growth	210/21092	1.43E-02	1.94E-01	0.153083885	Ntn1/Drd2/Nrg1	3
GO:0048747	muscle fiber development	76/21092	1.46E-02	1.94E-01	0.153083885	Ripor2/Ryr1	2
GO:0006814	sodium ion transport	212/21092	1.46E-02	1.94E-01	0.153083885	Slc38a3/Drd2/Scn10a	3
GO:0031668	cellular response to extracellular stimulus	212/21092	1.46E-02	1.94E-01	0.153083885	Nprl2/Slc38a3/Ryr1	3
GO:0003015	heart process	215/21092	1.52E-02	1.94E-01	0.153083885	Drd2/Scn10a/Tnnt1	3
GO:0006664	glycolipid metabolic process	79/21092	1.57E-02	1.94E-01	0.153083885	Pgap2/Pigf	2
GO:0043279	response to alkaloid	79/21092	1.57E-02	1.94E-01	0.153083885	Drd2/Ryr1	2
GO:1901019	regulation of calcium ion transmembrane transporter activity	79/21092	1.57E-02	1.94E-01	0.153083885	Gnb5/Drd2	2
GO:0030073	insulin secretion	218/21092	1.58E-02	1.94E-01	0.153083885	Hmgn3/Drd2/Cyb5r4	3
GO:1903509	liposaccharide metabolic process	80/21092	1.61E-02	1.94E-01	0.153083885	Pgap2/Pigf	2
GO:0030203	glycosaminoglycan metabolic process	81/21092	1.64E-02	1.94E-01	0.153083885	Pxylp1/Hyal1	2
GO:1904063	negative regulation of cation transmembrane transport	82/21092	1.68E-02	1.94E-01	0.153083885	Gnb5/Drd2	2
GO:0099504	synaptic vesicle cycle	228/21092	1.77E-02	1.94E-01	0.153083885	Snap91/Drd2/Adcy1	3
GO:0016485	protein processing	229/21092	1.79E-02	1.94E-01	0.153083885	Ctsh/Cideb/Chac1	3
GO:0090257	regulation of muscle system process	232/21092	1.86E-02	1.94E-01	0.153083885	Ryr1/Scn10a/Tnnt1	3
GO:0021954	central nervous system neuron development	87/21092	1.88E-02	1.94E-01	0.153083885	Drd2/Ephb1	2
GO:0043583	ear development	236/21092	1.94E-02	1.94E-01	0.153083885	Ntn1/Tbx18/Ripor2	3
GO:0006497	protein lipidation	89/21092	1.96E-02	1.94E-01	0.153083885	Pgap2/Pigf	2

GO:0035914	skeletal muscle cell differentiation	89/21092	1.96E-02	1.94E-01	0.153083885	Plagl1/Ephb1	2
GO:0051149	positive regulation of muscle cell differentiation	89/21092	1.96E-02	1.94E-01	0.153083885	Ripor2/Nrg1	2
GO:0019932	second-messenger-mediated signaling	430/21092	2.00E-02	1.94E-01	0.153083885	Drd2/Ackr4/Adcy1/Nrg1	4
GO:0002027	regulation of heart rate	91/21092	2.05E-02	1.94E-01	0.153083885	Drd2/Scn10a	2
GO:0090068	positive regulation of cell cycle process	246/21092	2.16E-02	1.94E-01	0.153083885	Drd2/Ripor2/Hyal1	3
GO:0042158	lipoprotein biosynthetic process	94/21092	2.17E-02	1.94E-01	0.153083885	Pgap2/Pigf	2
GO:0099003	vesicle-mediated transport in synapse	249/21092	2.23E-02	1.94E-01	0.153083885	Snap91/Drd2/Adcy1	3
GO:0034766	negative regulation of ion transmembrane transport	98/21092	2.35E-02	1.94E-01	0.153083885	Gnb5/Drd2	2
GO:0006995	cellular response to nitrogen starvation	10/21092	2.39E-02	1.94E-01	0.153083885	Nprl2	1
GO:0007270	neuron-neuron synaptic transmission	10/21092	2.39E-02	1.94E-01	0.153083885	Drd2	1
GO:0009129	pyrimidine nucleoside monophosphate metabolic process	10/21092	2.39E-02	1.94E-01	0.153083885	Shmt1	1
GO:0009221	pyrimidine deoxyribonucleotide biosynthetic process	10/21092	2.39E-02	1.94E-01	0.153083885	Shmt1	1
GO:0014883	transition between fast and slow fiber	10/21092	2.39E-02	1.94E-01	0.153083885	Tnnt2	1
GO:0021554	optic nerve development	10/21092	2.39E-02	1.94E-01	0.153083885	Ephb1	1
GO:0031282	regulation of guanylate cyclase activity	10/21092	2.39E-02	1.94E-01	0.153083885	Guca1b	1
GO:0043562	cellular response to nitrogen levels	10/21092	2.39E-02	1.94E-01	0.153083885	Nprl2	1
GO:0046085	adenosine metabolic process	10/21092	2.39E-02	1.94E-01	0.153083885	Nt5e	1
GO:0048149	behavioral response to ethanol	10/21092	2.39E-02	1.94E-01	0.153083885	Drd2	1
GO:0051823	regulation of synapse structural plasticity	10/21092	2.39E-02	1.94E-01	0.153083885	Drd2	1
GO:0070142	synaptic vesicle budding	10/21092	2.39E-02	1.94E-01	0.153083885	Snap91	1
GO:1903749	positive regulation of establishment of protein localization to mitochondrion	10/21092	2.39E-02	1.94E-01	0.153083885	Hspa1l	1
GO:1905097	regulation of guanyl-nucleotide exchange factor activity	10/21092	2.39E-02	1.94E-01	0.153083885	Ripor2	1
GO:2000402	negative regulation of lymphocyte migration	10/21092	2.39E-02	1.94E-01	0.153083885	Ripor2	1
GO:2000807	regulation of synaptic vesicle clustering	10/21092	2.39E-02	1.94E-01	0.153083885	Snap91	1
GO:0006022	aminoglycan metabolic process	99/21092	2.40E-02	1.94E-01	0.153083885	Pxylp1/Hyal1	2
GO:0031346	positive regulation of cell projection organization	462/21092	2.53E-02	1.94E-01	0.153083885	Snap91/Ntn1/Ripor2/Nrg1	4

GO:0030336	negative regulation of cell migration	263/21092	2.57E-02	1.94E-01	0.153083885	Drd2/Ripor2/Nrg1	3
GO:0051650	establishment of vesicle localization	265/21092	2.62E-02	1.94E-01	0.153083885	Snap91/Drd2/Adcy1	3
GO:0048259	regulation of receptor-mediated endocytosis	104/21092	2.62E-02	1.94E-01	0.153083885	Snap91/Drd2	2
GO:2000300	regulation of synaptic vesicle exocytosis	104/21092	2.62E-02	1.94E-01	0.153083885	Drd2/Adcy1	2
GO:0006012	galactose metabolic process	11/21092	2.63E-02	1.94E-01	0.153083885	Glb1	1
GO:0006171	cAMP biosynthetic process	11/21092	2.63E-02	1.94E-01	0.153083885	Adcy1	1
GO:0006266	DNA ligation	11/21092	2.63E-02	1.94E-01	0.153083885	Parp3	1
GO:0009125	nucleoside monophosphate catabolic process	11/21092	2.63E-02	1.94E-01	0.153083885	Nt5e	1
GO:0021892	cerebral cortex GABAergic interneuron differentiation	11/21092	2.63E-02	1.94E-01	0.153083885	Drd2	1
GO:0034776	response to histamine	11/21092	2.63E-02	1.94E-01	0.153083885	Drd2	1
GO:0035999	tetrahydrofolate interconversion	11/21092	2.63E-02	1.94E-01	0.153083885	Shmt1	1
GO:0051967	negative regulation of synaptic transmission, glutamatergic	11/21092	2.63E-02	1.94E-01	0.153083885	Drd2	1
GO:0060159	regulation of dopamine receptor signaling pathway	11/21092	2.63E-02	1.94E-01	0.153083885	Drd2	1
GO:0060600	dichotomous subdivision of an epithelial terminal unit	11/21092	2.63E-02	1.94E-01	0.153083885	Ctsh	1
GO:0086016	AV node cell action potential	11/21092	2.63E-02	1.94E-01	0.153083885	Scn10a	1
GO:0086027	AV node cell to bundle of His cell signaling	11/21092	2.63E-02	1.94E-01	0.153083885	Scn10a	1
GO:0072521	purine-containing compound metabolic process	469/21092	2.65E-02	1.94E-01	0.153083885	Guca1b/Adcy1/Nt5e/Shmt1	4
GO:0009165	nucleotide biosynthetic process	267/21092	2.67E-02	1.94E-01	0.153083885	Guca1b/Adcy1/Shmt1	3
GO:0006986	response to unfolded protein	106/21092	2.72E-02	1.94E-01	0.153083885	Hspa1l/Chac1	2
GO:0046474	glycerophospholipid biosynthetic process	106/21092	2.72E-02	1.94E-01	0.153083885	Pgap2/Pigf	2
GO:0042752	regulation of circadian rhythm	107/21092	2.77E-02	1.94E-01	0.153083885	Drd2/Adcy1	2
GO:0051209	release of sequestered calcium ion into cytosol	107/21092	2.77E-02	1.94E-01	0.153083885	Drd2/Ryr1	2
GO:0030072	peptide hormone secretion	271/21092	2.78E-02	1.94E-01	0.153083885	Hmgn3/Drd2/Cyb5r4	3
GO:0070588	calcium ion transmembrane transport	271/21092	2.78E-02	1.94E-01	0.153083885	Gnb5/Drd2/Ryr1	3
GO:0051656	establishment of organelle localization	476/21092	2.78E-02	1.94E-01	0.153083885	Snap91/Ntn1/Drd2/Adcy1	4

GO:1902803	regulation of synaptic vesicle transport	108/21092	2.81E-02	1.94E-01	0.153083885	Drd2/Adcy1	2
GO:1901293	nucleoside phosphate biosynthetic process	274/21092	2.86E-02	1.94E-01	0.153083885	Guca1b/Adcy1/ Shmt1	3
GO:0007052	mitotic spindle organization	109/21092	2.86E-02	1.94E-01	0.153083885	Parp3/Ripor2	2
GO:0030516	regulation of axon extension	109/21092	2.86E-02	1.94E-01	0.153083885	Ntn1/Nrg1	2
GO:0051283	negative regulation of sequestering of calcium ion	109/21092	2.86E-02	1.94E-01	0.153083885	Drd2/Ryr1	2
GO:0000963	mitochondrial RNA processing	12/21092	2.86E-02	1.94E-01	0.153083885	Mto1	1
GO:0007195	adenylate cyclase-inhibiting dopamine receptor signaling pathway	12/21092	2.86E-02	1.94E-01	0.153083885	Drd2	1
GO:0009265	2'-deoxyribonucleotide biosynthetic process	12/21092	2.86E-02	1.94E-01	0.153083885	Shmt1	1
GO:0014842	regulation of skeletal muscle satellite cell proliferation	12/21092	2.86E-02	1.94E-01	0.153083885	Ephb1	1
GO:0030432	peristalsis	12/21092	2.86E-02	1.94E-01	0.153083885	Drd2	1
GO:0032488	Cdc42 protein signal transduction	12/21092	2.86E-02	1.94E-01	0.153083885	Ntn1	1
GO:0046385	deoxyribose phosphate biosynthetic process	12/21092	2.86E-02	1.94E-01	0.153083885	Shmt1	1
GO:0071318	cellular response to ATP	12/21092	2.86E-02	1.94E-01	0.153083885	Ryr1	1
GO:0071468	cellular response to acidic pH	12/21092	2.86E-02	1.94E-01	0.153083885	Slc38a3	1
GO:0090494	dopamine uptake	12/21092	2.86E-02	1.94E-01	0.153083885	Drd2	1
GO:1900244	positive regulation of synaptic vesicle endocytosis	12/21092	2.86E-02	1.94E-01	0.153083885	Snap91	1
GO:2000146	negative regulation of cell motility	277/21092	2.94E-02	1.94E-01	0.153083885	Drd2/Ripor2/Nr g1	3
GO:0051282	regulation of sequestering of calcium ion	111/21092	2.96E-02	1.94E-01	0.153083885	Drd2/Ryr1	2
GO:0051208	sequestering of calcium ion	112/21092	3.01E-02	1.94E-01	0.153083885	Drd2/Ryr1	2
GO:0048568	embryonic organ development	490/21092	3.05E-02	1.94E-01	0.153083885	Ntn1/Tbx18/Rip or2/Hyal1	4
GO:0046467	membrane lipid biosynthetic process	113/21092	3.06E-02	1.94E-01	0.153083885	Pgap2/Pigf	2
GO:0006596	polyamine biosynthetic process	13/21092	3.10E-02	1.94E-01	0.153083885	Sms	1
GO:0009071	serine family amino acid catabolic process	13/21092	3.10E-02	1.94E-01	0.153083885	Shmt1	1
GO:0009219	pyrimidine deoxyribonucleotide metabolic process	13/21092	3.10E-02	1.94E-01	0.153083885	Shmt1	1
GO:0014841	skeletal muscle satellite cell proliferation	13/21092	3.10E-02	1.94E-01	0.153083885	Ephb1	1
GO:0030213	hyaluronan biosynthetic process	13/21092	3.10E-02	1.94E-01	0.153083885	Hyal1	1

GO:0031000	response to caffeine	13/21092	3.10E-02	1.94E-01	0.153083885	Ryr1	1
GO:0035810	positive regulation of urine volume	13/21092	3.10E-02	1.94E-01	0.153083885	Drd2	1
GO:0036270	response to diuretic	13/21092	3.10E-02	1.94E-01	0.153083885	Ryr1	1
GO:0060124	positive regulation of growth hormone secretion	13/21092	3.10E-02	1.94E-01	0.153083885	Drd2	1
GO:0060272	embryonic skeletal joint morphogenesis	13/21092	3.10E-02	1.94E-01	0.153083885	Hyal1	1
GO:0086067	AV node cell to bundle of His cell communication	13/21092	3.10E-02	1.94E-01	0.153083885	Scn10a	1
GO:0090493	catecholamine uptake	13/21092	3.10E-02	1.94E-01	0.153083885	Drd2	1
GO:0097202	activation of cysteine-type endopeptidase activity	13/21092	3.10E-02	1.94E-01	0.153083885	Cideb	1
GO:2001223	negative regulation of neuron migration	13/21092	3.10E-02	1.94E-01	0.153083885	Nrg1	1
GO:0051648	vesicle localization	283/21092	3.10E-02	1.94E-01	0.153083885	Snap91/Drd2/Adcy1	3
GO:1903828	negative regulation of cellular protein localization	114/21092	3.11E-02	1.94E-01	0.153083885	Ripor2/Dclk3	2
GO:1901136	carbohydrate derivative catabolic process	115/21092	3.16E-02	1.94E-01	0.153083885	Nt5e/Hyal1	2
GO:0051963	regulation of synapse assembly	117/21092	3.26E-02	1.94E-01	0.153083885	Ntn1/Ephb1	2
GO:0009416	response to light stimulus	290/21092	3.30E-02	1.94E-01	0.153083885	Guca1b/Drd2/Hyal1	3
GO:0071214	cellular response to abiotic stimulus	290/21092	3.30E-02	1.94E-01	0.153083885	Slc38a3/Ripor2/Hyal1	3
GO:0104004	cellular response to environmental stimulus	290/21092	3.30E-02	1.94E-01	0.153083885	Slc38a3/Ripor2/Hyal1	3
GO:0051604	protein maturation	291/21092	3.33E-02	1.94E-01	0.153083885	Ctsh/Cideb/Chac1	3
GO:0001771	immunological synapse formation	14/21092	3.33E-02	1.94E-01	0.153083885	Ephb1	1
GO:0006544	glycine metabolic process	14/21092	3.33E-02	1.94E-01	0.153083885	Shmt1	1
GO:0007194	negative regulation of adenylate cyclase activity	14/21092	3.33E-02	1.94E-01	0.153083885	Drd2	1
GO:0015802	basic amino acid transport	14/21092	3.33E-02	1.94E-01	0.153083885	Slc38a3	1
GO:0021781	glial cell fate commitment	14/21092	3.33E-02	1.94E-01	0.153083885	Nrg1	1
GO:0021984	adenohypophysis development	14/21092	3.33E-02	1.94E-01	0.153083885	Drd2	1
GO:0031223	auditory behavior	14/21092	3.33E-02	1.94E-01	0.153083885	Drd2	1
GO:0031987	locomotion involved in locomotory behavior	14/21092	3.33E-02	1.94E-01	0.153083885	Drd2	1
GO:0035815	positive regulation of renal sodium excretion	14/21092	3.33E-02	1.94E-01	0.153083885	Drd2	1

GO:0046033	AMP metabolic process	14/21092	3.33E-02	1.94E-01	0.153083885	Nt5e	1
GO:0046058	cAMP metabolic process	14/21092	3.33E-02	1.94E-01	0.153083885	Adcy1	1
GO:0048755	branching morphogenesis of a nerve	14/21092	3.33E-02	1.94E-01	0.153083885	Drd2	1
GO:0086069	bundle of His cell to Purkinje myocyte communication	14/21092	3.33E-02	1.94E-01	0.153083885	Scn10a	1
GO:0097154	GABAergic neuron differentiation	14/21092	3.33E-02	1.94E-01	0.153083885	Drd2	1
GO:0051952	regulation of amine transport	119/21092	3.36E-02	1.94E-01	0.153083885	Slc38a3/Drd2	2
GO:0014902	myotube differentiation	120/21092	3.41E-02	1.94E-01	0.153083885	Ripor2/Ryr1	2
GO:0060996	dendritic spine development	120/21092	3.41E-02	1.94E-01	0.153083885	Ephb1/Nrg1	2
GO:0042157	lipoprotein metabolic process	121/21092	3.47E-02	1.94E-01	0.153083885	Pgap2/Pigf	2
GO:0051153	regulation of striated muscle cell differentiation	121/21092	3.47E-02	1.94E-01	0.153083885	Ripor2/Nrg1	2
GO:0060048	cardiac muscle contraction	121/21092	3.47E-02	1.94E-01	0.153083885	Scn10a/Tnnt2	2
GO:0060326	cell chemotaxis	298/21092	3.53E-02	1.94E-01	0.153083885	Ephb1/Ackr4/Ripor2	3
GO:0009263	deoxyribonucleotide biosynthetic process	15/21092	3.57E-02	1.94E-01	0.153083885	Shmt1	1
GO:0014733	regulation of skeletal muscle adaptation	15/21092	3.57E-02	1.94E-01	0.153083885	Tnnt2	1
GO:0014857	regulation of skeletal muscle cell proliferation	15/21092	3.57E-02	1.94E-01	0.153083885	Ephb1	1
GO:0031280	negative regulation of cyclase activity	15/21092	3.57E-02	1.94E-01	0.153083885	Drd2	1
GO:0043129	surfactant homeostasis	15/21092	3.57E-02	1.94E-01	0.153083885	Ctsh	1
GO:0051974	negative regulation of telomerase activity	15/21092	3.57E-02	1.94E-01	0.153083885	Parp3	1
GO:0060134	prepulse inhibition	15/21092	3.57E-02	1.94E-01	0.153083885	Drd2	1
GO:0060192	negative regulation of lipase activity	15/21092	3.57E-02	1.94E-01	0.153083885	Snap91	1
GO:0072189	ureter development	15/21092	3.57E-02	1.94E-01	0.153083885	Tbx18	1
GO:0072498	embryonic skeletal joint development	15/21092	3.57E-02	1.94E-01	0.153083885	Hyal1	1
GO:0098926	postsynaptic signal transduction	15/21092	3.57E-02	1.94E-01	0.153083885	Nrg1	1
GO:0099527	postsynapse to nucleus signaling pathway	15/21092	3.57E-02	1.94E-01	0.153083885	Nrg1	1
GO:1903423	positive regulation of synaptic vesicle recycling	15/21092	3.57E-02	1.94E-01	0.153083885	Snap91	1
GO:2000369	regulation of clathrin-dependent endocytosis	15/21092	3.57E-02	1.94E-01	0.153083885	Snap91	1
GO:0015837	amine transport	123/21092	3.57E-02	1.94E-01	0.153083885	Slc38a3/Drd2	2

GO:0061387	regulation of extent of cell growth	124/21092	3.62E-02	1.94E-01	0.153083885	Ntn1/Nrg1	2
GO:0009582	detection of abiotic stimulus	125/21092	3.68E-02	1.94E-01	0.153083885	Guca1b/Ephb1	2
GO:0034763	negative regulation of transmembrane transport	125/21092	3.68E-02	1.94E-01	0.153083885	Gnb5/Drd2	2
GO:0046677	response to antibiotic	303/21092	3.69E-02	1.94E-01	0.153083885	Drd2/Cyb5r4/Hyal1	3
GO:0009581	detection of external stimulus	126/21092	3.73E-02	1.94E-01	0.153083885	Guca1b/Ephb1	2
GO:0006836	neurotransmitter transport	306/21092	3.78E-02	1.94E-01	0.153083885	Snap91/Drd2/Adcy1	3
GO:0035966	response to topologically incorrect protein	127/21092	3.79E-02	1.94E-01	0.153083885	Hspa1l/Chac1	2
GO:0097553	calcium ion transmembrane import into cytosol	127/21092	3.79E-02	1.94E-01	0.153083885	Drd2/Ryr1	2
GO:0002031	G protein-coupled receptor internalization	16/21092	3.80E-02	1.94E-01	0.153083885	Drd2	1
GO:0002098	tRNA wobble uridine modification	16/21092	3.80E-02	1.94E-01	0.153083885	Mto1	1
GO:0014856	skeletal muscle cell proliferation	16/21092	3.80E-02	1.94E-01	0.153083885	Ephb1	1
GO:0043968	histone H2A acetylation	16/21092	3.80E-02	1.94E-01	0.153083885	Morf4l1	1
GO:0046112	nucleobase biosynthetic process	16/21092	3.80E-02	1.94E-01	0.153083885	Shmt1	1
GO:0072672	neutrophil extravasation	16/21092	3.80E-02	1.94E-01	0.153083885	Ripor2	1
GO:2001015	negative regulation of skeletal muscle cell differentiation	16/21092	3.80E-02	1.94E-01	0.153083885	Ephb1	1
GO:0044282	small molecule catabolic process	308/21092	3.84E-02	1.94E-01	0.153083885	Glb1/Hyal1/Shmt1	3
GO:0051271	negative regulation of cellular component movement	311/21092	3.93E-02	1.94E-01	0.153083885	Drd2/Ripor2/Nrg1	3
GO:0007189	adenylate cyclase-activating G protein-coupled receptor signaling pathway	130/21092	3.95E-02	1.94E-01	0.153083885	Drd2/Adcy1	2
GO:0008037	cell recognition	131/21092	4.00E-02	1.94E-01	0.153083885	Ephb1/Hspa1l	2
GO:1902850	microtubule cytoskeleton organization involved in mitosis	131/21092	4.00E-02	1.94E-01	0.153083885	Parp3/Ripor2	2
GO:0007638	mechanosensory behavior	17/21092	4.03E-02	1.94E-01	0.153083885	Drd2	1
GO:0009070	serine family amino acid biosynthetic process	17/21092	4.03E-02	1.94E-01	0.153083885	Shmt1	1
GO:0010224	response to UV-B	17/21092	4.03E-02	1.94E-01	0.153083885	Hyal1	1
GO:0032225	regulation of synaptic transmission, dopaminergic	17/21092	4.03E-02	1.94E-01	0.153083885	Drd2	1
GO:0042754	negative regulation of circadian rhythm	17/21092	4.03E-02	1.94E-01	0.153083885	Drd2	1
GO:0042756	drinking behavior	17/21092	4.03E-02	1.94E-01	0.153083885	Drd2	1

GO:0048875	chemical homeostasis within a tissue	17/21092	4.03E-02	1.94E-01	0.153083885	Ctsh	1
GO:0051350	negative regulation of lyase activity	17/21092	4.03E-02	1.94E-01	0.153083885	Drd2	1
GO:0097091	synaptic vesicle clustering	17/21092	4.03E-02	1.94E-01	0.153083885	Snap91	1
GO:0010821	regulation of mitochondrion organization	132/21092	4.06E-02	1.94E-01	0.153083885	Cideb/Hspa1l	2
GO:0017158	regulation of calcium ion-dependent exocytosis	132/21092	4.06E-02	1.94E-01	0.153083885	Drd2/Adcy1	2
GO:0046488	phosphatidylinositol metabolic process	133/21092	4.12E-02	1.94E-01	0.153083885	Pgap2/Pigf	2
GO:0050905	neuromuscular process	133/21092	4.12E-02	1.94E-01	0.153083885	Drd2/Nrg1	2
GO:0007204	positive regulation of cytosolic calcium ion concentration	317/21092	4.12E-02	1.94E-01	0.153083885	Drd2/Ackr4/Ryr 1	3
GO:0030010	establishment of cell polarity	134/21092	4.17E-02	1.94E-01	0.153083885	Ephb1/Ripor2	2
GO:0048675	axon extension	134/21092	4.17E-02	1.94E-01	0.153083885	Ntn1/Nrg1	2
GO:0006595	polyamine metabolic process	18/21092	4.27E-02	1.94E-01	0.153083885	Sms	1
GO:0009309	amine biosynthetic process	18/21092	4.27E-02	1.94E-01	0.153083885	Sms	1
GO:0031643	positive regulation of myelination	18/21092	4.27E-02	1.94E-01	0.153083885	Nrg1	1
GO:0033604	negative regulation of catecholamine secretion	18/21092	4.27E-02	1.94E-01	0.153083885	Drd2	1
GO:0036120	cellular response to platelet-derived growth factor stimulus	18/21092	4.27E-02	1.94E-01	0.153083885	Hyal1	1
GO:0042219	cellular modified amino acid catabolic process	18/21092	4.27E-02	1.94E-01	0.153083885	Chac1	1
GO:0042401	cellular biogenic amine biosynthetic process	18/21092	4.27E-02	1.94E-01	0.153083885	Sms	1
GO:0043278	response to morphine	18/21092	4.27E-02	1.94E-01	0.153083885	Drd2	1
GO:0048268	clathrin coat assembly	18/21092	4.27E-02	1.94E-01	0.153083885	Snap91	1
GO:0050650	chondroitin sulfate proteoglycan biosynthetic process	18/21092	4.27E-02	1.94E-01	0.153083885	Pxylp1	1
GO:0050961	detection of temperature stimulus involved in sensory perception	18/21092	4.27E-02	1.94E-01	0.153083885	Ephb1	1
GO:0050965	detection of temperature stimulus involved in sensory perception of pain	18/21092	4.27E-02	1.94E-01	0.153083885	Ephb1	1
GO:0051481	negative regulation of cytosolic calcium ion concentration	18/21092	4.27E-02	1.94E-01	0.153083885	Drd2	1
GO:0060088	auditory receptor cell stereocilium organization	18/21092	4.27E-02	1.94E-01	0.153083885	Ripor2	1
GO:0070886	positive regulation of calcineurin-NFAT signaling cascade	18/21092	4.27E-02	1.94E-01	0.153083885	Nrg1	1
GO:0106058	positive regulation of calcineurin-mediated signaling	18/21092	4.27E-02	1.94E-01	0.153083885	Nrg1	1

GO:1904424	regulation of GTP binding	18/21092	4.27E-02	1.94E-01	0.153083885	Ripor2	1
GO:0046928	regulation of neurotransmitter secretion	137/21092	4.34E-02	1.95E-01	0.153818291	Drd2/Adcy1	2
GO:0009267	cellular response to starvation	139/21092	4.46E-02	1.95E-01	0.153818291	Nprl2/Slc38a3	2
GO:0040013	negative regulation of locomotion	328/21092	4.49E-02	1.95E-01	0.153818291	Drd2/Ripor2/Nrg1	3
GO:0001975	response to amphetamine	19/21092	4.50E-02	1.95E-01	0.153818291	Drd2	1
GO:0002097	tRNA wobble base modification	19/21092	4.50E-02	1.95E-01	0.153818291	Mto1	1
GO:0006027	glycosaminoglycan catabolic process	19/21092	4.50E-02	1.95E-01	0.153818291	Hyal1	1
GO:0010447	response to acidic pH	19/21092	4.50E-02	1.95E-01	0.153818291	Slc38a3	1
GO:0010996	response to auditory stimulus	19/21092	4.50E-02	1.95E-01	0.153818291	Drd2	1
GO:0014072	response to isoquinoline alkaloid	19/21092	4.50E-02	1.95E-01	0.153818291	Drd2	1
GO:0014808	release of sequestered calcium ion into cytosol by sarcoplasmic reticulum	19/21092	4.50E-02	1.95E-01	0.153818291	Ryr1	1
GO:0036119	response to platelet-derived growth factor	19/21092	4.50E-02	1.95E-01	0.153818291	Hyal1	1
GO:0043931	ossification involved in bone maturation	19/21092	4.50E-02	1.95E-01	0.153818291	Ryr1	1
GO:1903214	regulation of protein targeting to mitochondrion	19/21092	4.50E-02	1.95E-01	0.153818291	Hspa1l	1
GO:0007613	memory	141/21092	4.57E-02	1.95E-01	0.153818291	Drd2/Adcy1	2
GO:0045017	glycerolipid biosynthetic process	141/21092	4.57E-02	1.95E-01	0.153818291	Pgap2/Pigf	2
GO:0010634	positive regulation of epithelial cell migration	142/21092	4.63E-02	1.95E-01	0.153818291	Ctsh/Hyal1	2
GO:0019233	sensory perception of pain	142/21092	4.63E-02	1.95E-01	0.153818291	Ephb1/Scn10a	2
GO:0016079	synaptic vesicle exocytosis	143/21092	4.69E-02	1.95E-01	0.153818291	Drd2/Adcy1	2
GO:0002693	positive regulation of cellular extravasation	20/21092	4.73E-02	1.95E-01	0.153818291	Ripor2	1
GO:0010560	positive regulation of glycoprotein biosynthetic process	20/21092	4.73E-02	1.95E-01	0.153818291	Pxylp1	1
GO:0014075	response to amine	20/21092	4.73E-02	1.95E-01	0.153818291	Drd2	1
GO:0042451	purine nucleoside biosynthetic process	20/21092	4.73E-02	1.95E-01	0.153818291	Nt5e	1
GO:0046129	purine ribonucleoside biosynthetic process	20/21092	4.73E-02	1.95E-01	0.153818291	Nt5e	1
GO:0046653	tetrahydrofolate metabolic process	20/21092	4.73E-02	1.95E-01	0.153818291	Shmt1	1
GO:0060123	regulation of growth hormone secretion	20/21092	4.73E-02	1.95E-01	0.153818291	Drd2	1

GO:0070977	bone maturation	20/21092	4.73E-02	1.95E-01	0.153818291	Ryr1	1
GO:1903514	release of sequestered calcium ion into cytosol by endoplasmic reticulum	20/21092	4.73E-02	1.95E-01	0.153818291	Ryr1	1
GO:2000010	positive regulation of protein localization to cell surface	20/21092	4.73E-02	1.95E-01	0.153818291	Nrg1	1
GO:2000114	regulation of establishment of cell polarity	20/21092	4.73E-02	1.95E-01	0.153818291	Ripor2	1
GO:0010769	regulation of cell morphogenesis involved in differentiation	336/21092	4.76E-02	1.96E-01	0.154394136	Snap91/Ntn1/Nrg1	3
GO:0001976	neurological system process involved in regulation of systemic arterial blood pressure	21/21092	4.96E-02	1.99E-01	0.157260746	Drd2	1
GO:0007190	activation of adenylate cyclase activity	21/21092	4.96E-02	1.99E-01	0.157260746	Adcy1	1
GO:0007625	grooming behavior	21/21092	4.96E-02	1.99E-01	0.157260746	Drd2	1
GO:0015012	heparan sulfate proteoglycan biosynthetic process	21/21092	4.96E-02	1.99E-01	0.157260746	Pxylp1	1
GO:0031290	retinal ganglion cell axon guidance	21/21092	4.96E-02	1.99E-01	0.157260746	Ephb1	1
GO:0043501	skeletal muscle adaptation	21/21092	4.96E-02	1.99E-01	0.157260746	Tnnt2	1
GO:1901673	regulation of mitotic spindle assembly	21/21092	4.96E-02	1.99E-01	0.157260746	Ripor2	1
GO:0060402	calcium ion transport into cytosol	148/21092	4.99E-02	2.00E-01	0.157614938	Drd2/Ryr1	2

Supp Table S8. List of Differentially Expressed genes at FDR 5% in *Gnb5+/-* mice - atria

Ensembl ID	Gene Symbol	Gene name	baseMean	log2FoldChange	lfcSE	stat	pvalue	padj
ENSMUSG00000032224	Fam81a	family with sequence similarity 81, member A	292.8574685	2.335882638	0.253579957	9.211621721	3.21234E-20	6.22167E-16
ENSMUSG00000032192	Gnb5	guanine nucleotide binding protein (G protein), beta 5	588.3942165	-0.927754237	0.10834755	-8.562761538	1.10196E-17	1.06714E-13
ENSMUSG00000033419	Snap91	synaptosomal-associated protein 91	593.4008865	-0.644595104	0.121995504	-5.283761128	1.26558E-07	0.00081706
ENSMUSG00000051378	Kif18b	kinesin family member 18B	20.36546888	2.054560276	0.444055668	4.626807909	3.71345E-06	0.014384406
ENSMUSG00000078137	Ankrd63	ankyrin repeat domain 63	231.3397505	0.696118485	0.148990179	4.672244111	2.97927E-06	0.014384406
ENSMUSG00000053093	Myh7	myosin, heavy polypeptide 7, cardiac muscle, beta	251.3134444	-0.96720691	0.212994578	-4.540993103	5.59899E-06	0.018073528
ENSMUSG00000023979	Guca1b	guanylate cyclase activator 1B	58.67765502	0.974404672	0.217497591	4.480071111	7.46182E-06	0.020645783

Supp Table S9. List of Differentially Expressed genes at FDR 5% in *Gnb5+/-* mice - ventricle

Ensembl ID	Gene Symbol	Gene name	baseMean	log2FoldChange	lfcSE	stat	pvalue	padj
ENSMUSG00000032192	Gnb5	guanine nucleotide binding protein (G protein), beta 5	313.5699776	-0.960435275	0.123650627	-7.767330392	8.01576E-15	1.39723E-10
ENSMUSG00000032224	Fam81a	family with sequence similarity 81, member A	535.3572241	1.099542929	0.159014957	6.914713879	4.68809E-12	4.0859E-08

Supp Table S10. List of Differentially Expressed genes at FDR 5% in *Gnb5-/-* mice - cerebellum

Ensembl ID	Gene Symbol	Gene name	baseMean	log2FoldChange	lfcSE	stat	pvalue	padj
ENSMUSG00000032192	Gnb5	guanine nucleotide binding protein (G protein), beta 5	3776.684327	-2.827640286	0.055298441	-51.13417754	0.00E+00	< 2.00E-308
ENSMUSG00000023979	Guca1b	guanylate cyclase activator 1B	437.4550876	3.711107472	0.099175263	37.41968881	1.8697E-306	1.5621E-302
ENSMUSG00000032232	Cgnl1	cingulin-like 1	5161.732469	1.318444731	0.078033577	16.89586428	4.8259E-64	2.69E-60
ENSMUSG00000048758	Rpl29	ribosomal protein L29	167.003666	-2.662526944	0.179928843	-14.79766612	1.51654E-49	6.34E-46
ENSMUSG00000032556	Bfsp2	beaded filament structural protein 2, phakinin	65.92606322	-3.710156999	0.343429245	-10.8032646	3.32179E-27	1.11E-23
ENSMUSG00000043587	Pxylp1	2-phosphoxylose phosphatase 1	2090.786713	-0.93940513	0.089637192	-10.48008205	1.06651E-25	2.97E-22
ENSMUSG00000023277	Twf2	twinfilin actin binding protein 2	931.2249327	-0.527947875	0.052457731	-10.06425304	7.94884E-24	1.90E-20
ENSMUSG00000032498	Mlh1	mutL homolog 1	668.627558	-0.704540452	0.072809837	-9.676445968	3.79686E-22	7.93E-19
ENSMUSG00000020253	Ppm1m	protein phosphatase 1M	736.854351	-0.583377557	0.062857481	-9.2809567	1.67964E-20	3.12E-17
ENSMUSG00000062270	Morf4l1	mortality factor 4 like 1	4272.079558	-0.455630844	0.050708541	-8.985288001	2.58058E-19	4.31E-16
ENSMUSG00000062270	Morf4l1b	mortality factor 4 like 1B	4272.079558	-0.455630844	0.050708541	-8.985288001	2.58058E-19	4.31E-16
ENSMUSG00000032500	Dclk3	doublecortin-like kinase 3	227.5683369	1.633993963	0.194019129	8.421818885	3.70684E-17	5.63E-14
ENSMUSG00000032563	Mrpl3	mitochondrial ribosomal protein L3	2535.527483	-0.354146675	0.043154236	-8.206533358	2.27666E-16	3.17E-13
ENSMUSG00000104282	Gm37460	predicted gene 37460	24.0513232	-3.989910368	0.490489586	-8.134546545	4.13483E-16	5.31E-13
ENSMUSG00000090626	Tex9	testis expressed gene 9	591.5495903	-0.682683678	0.084985708	-8.032923324	9.51772E-16	1.14E-12
ENSMUSG00000032567	Aste1	asteroid homolog 1	261.2643017	-0.726216234	0.103776418	-6.997892664	2.59841E-12	2.89E-09
ENSMUSG00000036545	Adamts2	a disintegrin-like and metallopeptidase (reprolysin type) with thrombospondin type 1 motif, 2	865.4646909	-0.444637534	0.063619194	-6.989046931	2.7676E-12	2.89E-09
ENSMUSG00000043719	Col6a6	collagen, type VI, alpha 6	86.23142466	1.431557776	0.205901274	6.952641647	3.58509E-12	3.52E-09

ENSMUSG00000103164	Gm38150	predicted gene 38150	75.50295187	1.856335622	0.270406058	6.864992725	6.64946E-12	6.17E-09
ENSMUSG00000104286	Gm37457	predicted gene 37457	83.69435181	-1.396799984	0.20663308	-6.759808188	1.38175E-11	1.22E-08
ENSMUSG00000032494	Tdgf1	teratocarcinoma-derived growth factor 1	88.70981041	-1.228803344	0.187927365	-6.53871426	6.20499E-11	5.18E-08
ENSMUSG00000020096	Tbata	thymus, brain and testes associated	1971.627299	0.271356344	0.041688236	6.509182673	7.55608E-11	6.01E-08
ENSMUSG00000032418	Me1	malic enzyme 1, NADP(+)-dependent, cytosolic	2486.718734	0.398420712	0.061534107	6.474794711	9.49409E-11	7.21E-08
ENSMUSG00000002020	Ltbp2	latent transforming growth factor beta binding protein 2	4421.817622	-0.490281841	0.076725482	-6.390078353	1.65801E-10	1.20E-07
ENSMUSG00000032554	Trf	transferrin	516.363827	-0.885336834	0.14025914	-6.312150725	2.75184E-10	1.92E-07
ENSMUSG00000032495	Lrrc2	leucine rich repeat containing 2	337.4958733	-0.80567915	0.129576646	-6.217780565	5.04236E-10	3.37E-07
ENSMUSG00000102225	Gm37983	predicted gene 37983	24.91169952	1.872814001	0.301640962	6.208752252	5.34069E-10	3.43E-07
ENSMUSG00000023495	Pcbp4	poly(rC) binding protein 4	9608.983245	0.438156046	0.070693682	6.197951952	5.72026E-10	3.54E-07
ENSMUSG00000111348	Gm19531	predicted gene 19531	50.79214136	-1.15586438	0.18808935	-6.145294146	7.98155E-10	4.76E-07
ENSMUSG00000032383	Ppib	peptidylprolyl isomerase B	5797.045453	0.340285278	0.056151123	6.060168681	1.35979E-09	7.84E-07
ENSMUSG00000032221	Mns1	meiosis-specific nuclear structural protein 1	56.59125716	-1.175230186	0.195568968	-6.009287647	1.8634E-09	1.00E-06
ENSMUSG00000059003	Grin2a	glutamate receptor, ionotropic, NMDA2A (epsilon 1)	4488.448054	-0.246141364	0.040933749	-6.013164469	1.81936E-09	1.00E-06
ENSMUSG00000032411	Tfdp2	transcription factor Dp 2	2502.966265	0.41235966	0.0699472	5.895299004	3.74004E-09	1.95E-06
ENSMUSG00000023345	Poc1a	POC1 centriolar protein A	91.35994109	-0.946728825	0.160973191	-5.881282596	4.07099E-09	2.06E-06
ENSMUSG00000034898	Filip1	filamin A interacting protein 1	217.3345229	1.070995942	0.185443542	5.775320789	7.68066E-09	3.77E-06
ENSMUSG00000010057	Nprl2	NPR2 like, GATOR1 complex subunit	1400.200434	0.277235707	0.048216138	5.749853009	8.93211E-09	4.15E-06
ENSMUSG00000051590	Map3k19	mitogen-activated protein kinase kinase kinase 19	151.7662179	-0.72256102	0.125662208	-5.75002643	8.92295E-09	4.15E-06
ENSMUSG00000091735	Gpr62	G protein-coupled receptor 62	313.5180019	0.686846592	0.119742794	5.736016061	9.69295E-09	4.38E-06
ENSMUSG00000040536	Necab1	N-terminal EF-hand calcium binding protein 1	1182.606983	-0.675042081	0.119629524	-5.642771587	1.67334E-08	7.36E-06
ENSMUSG00000087466	A330041J22Rik	RIKEN cDNA A330041J22 gene	74.58228965	1.434589369	0.256512536	5.592667679	2.23607E-08	9.58E-06
ENSMUSG00000044037	Als2cl	ALS2 C-terminal like	1028.642711	-0.418008066	0.075093528	-5.566499248	2.59908E-08	1.09E-05
ENSMUSG00000070469	Adamtsl3	ADAMTS-like 3	113.9892968	-0.662897133	0.122069091	-5.43050764	5.6194E-08	2.29E-05
ENSMUSG00000023868	Pde10a	phosphodiesterase 10A	6880.473669	-0.676534037	0.125581847	-5.387196095	7.15653E-08	2.85E-05

ENSMUSG00000057802	Gm10030	predicted gene 10030	21.42515066	-1.977535225	0.375457621	-5.266999825	1.38671E-07	5.39E-05
ENSMUSG00000032360	Hcrtr2	hypocretin (orexin) receptor 2	28.96765092	-1.487211303	0.285983133	-5.200346213	1.98918E-07	7.55E-05
ENSMUSG00000024403	Atp6v1g2	ATPase, H+ transporting, lysosomal V1 subunit G2	10912.75865	0.157684878	0.030688324	5.138269387	2.7728E-07	1.03E-04
ENSMUSG00000102568	Gm37040	predicted gene 37040	36.43245889	-1.278054894	0.249989747	-5.112429236	3.18042E-07	1.16E-04
ENSMUSG00000033590	Myo5c	myosin VC	265.6388649	-0.549651459	0.109058116	-5.039986752	4.65564E-07	1.66E-04
ENSMUSG00000032872	Cyb5r4	cytochrome b5 reductase 4	2148.279031	-0.43931008	0.087835518	-5.001508373	5.68835E-07	1.98E-04
ENSMUSG00000047021	Cfap65	cilia and flagella associated protein 65	28.70220643	-1.970744625	0.396179632	-4.974371384	6.54597E-07	2.23E-04
ENSMUSG00000042761	Mrap2	melanocortin 2 receptor accessory protein 2	223.3199552	1.820064844	0.366864164	4.961140998	7.00803E-07	2.34E-04
ENSMUSG00000090150	Acad11	acyl-Coenzyme A dehydrogenase family, member 11	1333.016891	-0.242690676	0.049029394	-4.949901548	7.4251E-07	2.43E-04
ENSMUSG00000056596	Trnp1	TMF1-regulated nuclear protein 1	2707.369654	0.257405668	0.052080717	4.942437138	7.7152E-07	2.48E-04
ENSMUSG00000074415	3110039I08Rik	RIKEN cDNA 3110039I08 gene	858.8892546	-0.347692944	0.071049825	-4.893649586	9.8983E-07	3.12E-04
ENSMUSG00000045414	1190002N15Rik	RIKEN cDNA 1190002N15 gene	9479.974493	0.203857188	0.041965151	4.857773243	1.18713E-06	3.67E-04
ENSMUSG00000019929	Dcn	decorin	945.0632883	-0.39965724	0.083620332	-4.77942659	1.75796E-06	5.34E-04
ENSMUSG00000018659	Pnpo	pyridoxine 5'-phosphate oxidase	1853.661258	0.24366376	0.051217163	4.757463036	1.96041E-06	5.64E-04
ENSMUSG00000021265	Slc25a29	solute carrier family 25 (mitochondrial carrier, palmitoylcarnitine transporter), member 29	1086.377437	0.293381215	0.061607831	4.762076706	1.91611E-06	5.64E-04
ENSMUSG00000041506	Rrp9	RRP9, small subunit (SSU) processome component, homolog (yeast)	633.4693325	-0.348737041	0.073351895	-4.754301764	1.99133E-06	5.64E-04
ENSMUSG00000032436	Cmtm7	CKLF-like MARVEL transmembrane domain containing 7	225.5308249	-0.784340082	0.165355327	-4.743361447	2.10201E-06	5.85E-04
ENSMUSG00000070720	Tmem200b	transmembrane protein 200B	879.3241942	0.237178838	0.050148875	4.729494708	2.25079E-06	6.17E-04
ENSMUSG00000029822	Osbpl3	oxysterol binding protein-like 3	2125.961608	-0.339350961	0.073793709	-4.598643542	4.25251E-06	1.15E-03
ENSMUSG00000010048	Ifrd2	interferon-related developmental regulator 2	562.5877885	0.365850749	0.080007846	4.572685919	4.81512E-06	1.28E-03
ENSMUSG00000045967	Gpr158	G protein-coupled receptor 158	12290.27869	-0.241962539	0.053293038	-4.540227925	5.61934E-06	1.47E-03
ENSMUSG00000032356	Rasgrf1	RAS protein-specific guanine nucleotide-releasing factor 1	15290.93068	0.499536916	0.110479983	4.521515126	6.13986E-06	1.58E-03

ENSMUSG00000036760	Kcnk9	potassium channel, subfamily K, member 9	13243.63708	-0.292027828	0.06499848	-4.492840872	7.02793E-06	1.76E-03
ENSMUSG00000049624	Slc17a5	solute carrier family 17 (anion/sugar transporter), member 5	892.3986237	-0.346728247	0.077198643	-4.491377501	7.0764E-06	1.76E-03
ENSMUSG00000032497	Lrrfip2	leucine rich repeat (in FLII) interacting protein 2	1954.49032	-0.165756146	0.037035569	-4.47559331	7.61994E-06	1.87E-03
ENSMUSG00000024830	Rps6kb2	ribosomal protein S6 kinase, polypeptide 2	2329.153627	0.177815047	0.039942537	4.451771506	8.51648E-06	2.06E-03
ENSMUSG00000042210	Abhd14a	abhydrolase domain containing 14A	685.2533565	-0.289047191	0.065636456	-4.403759862	1.06391E-05	2.50E-03
ENSMUSG00000032570	Atp2c1	ATPase, Ca++-sequestering	7634.149512	0.190293715	0.043395191	4.38513372	1.15915E-05	2.69E-03
ENSMUSG00000085564	Gm12198	predicted gene 12198	144.1003058	-0.655784624	0.1506718	-4.35240452	1.34653E-05	3.08E-03
ENSMUSG00000025189	Cnnm1	cyclin M1	9936.963016	0.171522867	0.03971572	4.318765082	1.56905E-05	3.54E-03
ENSMUSG00000026156	B3gat2	beta-1,3-glucuronyltransferase 2 (glucuronosyltransferase S)	1542.762622	0.40134508	0.093300587	4.301635111	1.69542E-05	3.78E-03
ENSMUSG00000018697	Aatf	apoptosis antagonizing transcription factor	909.2901189	0.207262888	0.048456521	4.277296095	1.89177E-05	4.11E-03
ENSMUSG00000029695	Aass	aminoadipate-semialdehyde synthase	502.5914013	-0.540371692	0.126482917	-4.272289917	1.93476E-05	4.14E-03
ENSMUSG00000032936	Camkv	CaM kinase-like vesicle-associated	155.6519028	0.645556244	0.151277644	4.267360514	1.97799E-05	4.18E-03
ENSMUSG00000031274	Col4a5	collagen, type IV, alpha 5	423.3176062	-0.339340123	0.079636924	-4.261090277	2.03432E-05	4.25E-03
ENSMUSG00000025422	Agap2	ArfGAP with GTPase domain, ankyrin repeat and PH domain 2	9075.763147	0.168987623	0.039938014	4.231247511	2.32399E-05	4.79E-03
ENSMUSG00000040929	Rfx3	regulatory factor X, 3 (influences HLA class II expression)	1948.279304	-0.227743173	0.053898976	-4.225371062	2.38547E-05	4.86E-03
ENSMUSG00000046378	Asphd1	aspartate beta-hydroxylase domain containing 1	600.4949404	0.321122754	0.076280176	4.209779938	2.5562E-05	5.15E-03
ENSMUSG00000010660	Plcd1	phospholipase C, delta 1	287.7365686	-0.438423508	0.104711926	-4.186949119	2.82729E-05	5.56E-03
ENSMUSG00000026676	Ccdc3	coiled-coil domain containing 3	194.3461266	-0.787253495	0.187973755	-4.188103256	2.81296E-05	5.56E-03
ENSMUSG00000049303	Syt12	synaptotagmin XII	4738.805298	0.171600731	0.041042568	4.181042741	2.90175E-05	5.64E-03
ENSMUSG00000007594	Hapln4	hyaluronan and proteoglycan link protein 4	7762.924373	0.20525169	0.049244469	4.168015088	3.07264E-05	5.90E-03
ENSMUSG00000053702	Nebl	nebulette	4122.080911	-0.200274445	0.048467616	-4.132129069	3.59418E-05	6.82E-03
ENSMUSG00000070866	Zfp804a	zinc finger protein 804A	529.6035357	-0.273660923	0.066470521	-4.117026906	3.83791E-05	7.14E-03
ENSMUSG00000103891	Gm37941	predicted gene 37941	90.25718563	-0.590766007	0.143506106	-4.116661118	3.84401E-05	7.14E-03

ENSMUSG00000033577	Myo6	myosin VI	7952.800259	-0.177308645	0.043222703	-4.102210917	4.09221E-05	7.51E-03
ENSMUSG00000032562	Gnai2	guanine nucleotide binding protein (G protein), alpha inhibiting 2	5695.835318	0.209104738	0.051108773	4.09136684	4.28838E-05	7.79E-03
ENSMUSG00000022548	Apod	apolipoprotein D	7327.803279	-0.302224918	0.074021475	-4.082935635	4.44703E-05	7.96E-03
ENSMUSG00000025889	Snca	synuclein, alpha	753.7428095	0.310662096	0.076126465	4.080868538	4.48677E-05	7.96E-03
ENSMUSG00000040003	Magi2	membrane associated guanylate kinase, WW and PDZ domain containing 2	3517.01469	-0.198280333	0.048611072	-4.078912966	4.52468E-05	7.96E-03
ENSMUSG00000032224	Fam81a	family with sequence similarity 81, member A	752.0267376	0.40135418	0.098857026	4.059945935	4.90841E-05	8.46E-03
ENSMUSG00000035941	Ibtk	inhibitor of Bruton agammaglobulinemia tyrosine kinase	2259.614768	-0.234174871	0.057652254	-4.061851089	4.86851E-05	8.46E-03
ENSMUSG00000053399	Adamts18	a disintegrin-like and metallopeptidase (reprolysin type) with thrombospondin type 1 motif, 18	1245.172925	-0.535900624	0.132150485	-4.055230107	5.0085E-05	8.54E-03
ENSMUSG00000031209	Heph	hephaestin	212.499617	-0.524851774	0.129709845	-4.046352637	5.20218E-05	8.78E-03
ENSMUSG00000045594	Glb1	galactosidase, beta 1	603.8171745	-0.251329503	0.062199	-4.040732209	5.32846E-05	8.90E-03
ENSMUSG00000039728	Slc6a5	solute carrier family 6 (neurotransmitter transporter, glycine), member 5	2131.525392	0.184557898	0.0457464	4.034369904	5.4749E-05	9.06E-03
ENSMUSG00000022816	Fstl1	follistatin-like 1	656.1358971	-0.313458386	0.077999396	-4.018728391	5.85131E-05	9.49E-03
ENSMUSG00000060961	Slc4a4	solute carrier family 4 (anion exchanger), member 4	26482.84028	-0.210742417	0.052420959	-4.020193892	5.81503E-05	9.49E-03
ENSMUSG00000032786	Alas1	aminolevulinic acid synthase 1	2264.965012	0.16544191	0.041256635	4.010067955	6.07013E-05	9.60E-03
ENSMUSG00000034780	B3galt1	UDP-Gal:betaGlcNAc beta 1,3-galactosyltransferase, polypeptide 1	1512.878245	-0.228990845	0.057113105	-4.009427354	6.08662E-05	9.60E-03
ENSMUSG00000042757	Tmem108	transmembrane protein 108	1743.966905	0.191530914	0.047761983	4.010112257	6.06899E-05	9.60E-03
ENSMUSG00000038540	Tmc3	transmembrane channel-like gene family 3	128.5246132	-0.635080101	0.158674431	-4.002409822	6.27006E-05	9.79E-03
ENSMUSG00000019899	Lama2	laminin, alpha 2	1767.500596	-0.307800775	0.077002817	-3.997266444	6.40782E-05	9.91E-03
ENSMUSG00000020331	Hcn2	hyperpolarization-activated, cyclic nucleotide-gated K+ 2	3684.614211	0.211210959	0.053011952	3.984213928	6.77039E-05	1.04E-02
ENSMUSG00000079470	Utp14b	UTP14B small subunit processome component	593.3329387	-0.43940743	0.110425779	-3.979210594	6.91445E-05	1.05E-02

ENSMUSG00000043873	Chil5	chitinase-like 5	569.1443709	-0.529904212	0.134141397	-3.950340648	7.804E-05	1.17E-02
ENSMUSG00000034891	Sncb	synuclein, beta	6033.619166	0.257865278	0.065369039	3.944761662	7.98794E-05	1.18E-02
ENSMUSG00000111874	Gm36539	predicted gene 36539	28.68067065	-1.151072889	0.2918086	-3.944616051	7.99279E-05	1.18E-02
ENSMUSG00000040813	Tex264	testis expressed gene 264	1627.318836	0.24003156	0.061051179	3.931644982	8.43666E-05	1.24E-02
ENSMUSG00000024145	Pigf	phosphatidylinositol glycan anchor biosynthesis, class F	527.8534165	0.269835764	0.068864084	3.918381649	8.91455E-05	1.30E-02
ENSMUSG00000056019	Zfp709	zinc finger protein 709	716.7501148	-0.221064446	0.05646221	-3.915263783	9.03054E-05	1.30E-02
ENSMUSG00000047793	Sned1	sushi, nidogen and EGF-like domains 1	5436.766785	-0.214764333	0.054903128	-3.911695799	9.16503E-05	1.31E-02
ENSMUSG00000054196	Cthrc1	collagen triple helix repeat containing 1	456.6616622	0.273577589	0.070468467	3.882269615	0.000103486	1.44E-02
ENSMUSG00000062296	Trank1	tetratricopeptide repeat and ankyrin repeat containing 1	8866.298066	-0.401596014	0.103457199	-3.881759962	0.000103703	1.44E-02
ENSMUSG00000032359	Ctsh	cathepsin H	293.9199692	-0.380690598	0.098160275	-3.878255222	0.000105208	1.45E-02
ENSMUSG00000044244	Il20rb	interleukin 20 receptor beta	4371.39349	-0.294150387	0.075956801	-3.872601062	0.00010768	1.47E-02
ENSMUSG00000022540	Rogdi	rogdi homolog	3549.588552	0.19537945	0.05061794	3.859885424	0.00011344	1.54E-02
ENSMUSG00000036875	Dna2	DNA replication helicase/nuclease 2	172.3546123	-0.491356217	0.128239542	-3.831550007	0.000127338	1.72E-02
ENSMUSG00000022131	Gpr180	G protein-coupled receptor 180	1001.298783	0.180560403	0.047197908	3.825601801	0.000130453	1.74E-02
ENSMUSG00000029304	Spp1	secreted phosphoprotein 1	314.3225449	-1.037931743	0.271691281	-3.820261514	0.00013331	1.77E-02
ENSMUSG00000032571	Pik3r4	phosphoinositide-3-kinase regulatory subunit 4	2100.770068	-0.151120322	0.039789316	-3.798012582	0.000145861	1.92E-02
ENSMUSG00000038665	Dgki	diacylglycerol kinase, iota	1078.595202	-0.375885813	0.099194535	-3.78938028	0.000151024	1.97E-02
ENSMUSG00000054976	Nyap2	neuronal tyrosine-phophorylated phosphoinositide 3-kinase adaptor 2	1169.835804	-0.298167703	0.078758509	-3.785847468	0.000153186	1.98E-02
ENSMUSG00000031865	Dctn1	dynactin 1	14438.60666	0.157031021	0.041575282	3.77702842	0.000158711	2.04E-02
ENSMUSG00000032344	Cgas	cyclic GMP-AMP synthase	20.25321073	-1.137586452	0.301649272	-3.771222276	0.00016245	2.07E-02
ENSMUSG00000085084	4930570G19Rik	RIKEN cDNA 4930570G19 gene	1161.071062	-0.278073956	0.073863903	-3.76467995	0.000166763	2.11E-02
ENSMUSG00000040138	Ndp	Norrie disease (pseudoglioma) (human)	707.6201088	0.219662722	0.058391047	3.761924736	0.000168611	2.12E-02
ENSMUSG00000055254	Ntrk2	neurotrophic tyrosine kinase, receptor, type 2	19030.20769	-0.126891755	0.033783148	-3.75606662	0.000172605	2.15E-02
ENSMUSG00000027425	Kat14	lysine acetyltransferase 14	1374.54001	0.198671813	0.053026405	3.746658187	0.000179206	2.22E-02

ENSMUSG00000002274	Metrn	meteorin, glial cell differentiation regulator	5167.733381	0.251300779	0.067293283	3.734411033	0.000188155	2.31E-02
ENSMUSG00000054555	Adam12	a disintegrin and metallopeptidase domain 12 (meltrin alpha)	250.2725205	-0.367994148	0.098586085	-3.73271897	0.000189424	2.31E-02
ENSMUSG00000020185	E2f7	E2F transcription factor 7	64.89049163	-0.647104213	0.173634674	-3.726814448	0.000193915	2.31E-02
ENSMUSG00000031558	Slit2	slit guidance ligand 2	128.0552607	-0.619583532	0.166242811	-3.726979397	0.000193788	2.31E-02
ENSMUSG00000032803	Cdv3	carnitine deficiency-associated gene expressed in ventricle 3	2963.464124	-0.225267786	0.060576528	-3.718730583	0.000200226	2.37E-02
ENSMUSG00000039033	Tasp1	taspase, threonine aspartase 1	555.9554491	0.22670657	0.061038063	3.714183568	0.000203861	2.40E-02
ENSMUSG00000032323	Cyp11a1	cytochrome P450, family 11, subfamily a, polypeptide 1	160.2036109	-0.54410811	0.146689928	-3.709239733	0.000207883	2.43E-02
ENSMUSG00000027737	Slc7a11	solute carrier family 7 (cationic amino acid transporter, y+ system), member 11	1540.871957	-0.358277877	0.0967587	-3.702797536	0.000213235	2.44E-02
ENSMUSG00000033152	Podxl2	podocalyxin-like 2	6112.985547	0.265277682	0.071596768	3.705162828	0.000211255	2.44E-02
ENSMUSG00000105230	Gm42433	predicted gene 42433	287.5596305	0.32790406	0.088599373	3.700974955	0.000214773	2.44E-02
ENSMUSG00000025780	Itih5	inter-alpha (globulin) inhibitor H5	3052.757631	-0.257421968	0.069613061	-3.697897575	0.000217393	2.45E-02
ENSMUSG00000062257	Opcml	opioid binding protein/cell adhesion molecule-like	5120.415454	0.229556926	0.062123271	3.695184118	0.000219728	2.46E-02
ENSMUSG00000002228	Ppm1j	protein phosphatase 1J	73.97859987	0.543936081	0.147487001	3.688027274	0.000225999	2.48E-02
ENSMUSG00000020467	Efemp1	epidermal growth factor-containing fibulin-like extracellular matrix protein 1	661.4773856	-0.246464103	0.066769489	-3.691268372	0.000223139	2.48E-02
ENSMUSG00000071793	2610005L07Rik	cadherin 11 pseudogene	499.0576741	-0.260764185	0.070694432	-3.688609945	0.000225483	2.48E-02
ENSMUSG00000037624	Kcnk2	potassium channel, subfamily K, member 2	546.4969263	-0.275003038	0.074638882	-3.684447469	0.000229199	2.50E-02
ENSMUSG00000032184	Lysmd2	LysM, putative peptidoglycan-binding, domain containing 2	1722.663597	0.179859137	0.048875377	3.679953949	0.000233276	2.52E-02
ENSMUSG00000053716	Dusp7	dual specificity phosphatase 7	851.3299296	-0.261817054	0.071153446	-3.67961174	0.000233589	2.52E-02
ENSMUSG00000001773	Folh1	folate hydrolase 1	417.0674349	-0.340484695	0.092777155	-3.669919545	0.000242627	2.60E-02
ENSMUSG00000058966	Fam57b	family with sequence similarity 57, member B	4089.571587	0.189611427	0.051728708	3.665497087	0.000246859	2.63E-02
ENSMUSG00000063382	Bcl9l	B cell CLL/lymphoma 9-like	2478.992746	0.160810433	0.043905694	3.662632777	0.000249636	2.64E-02
ENSMUSG00000039163	Cmc1	COX assembly mitochondrial protein 1	342.5573765	0.344219264	0.094239415	3.652603992	0.000259594	2.73E-02

ENSMUSG00000006611	Hfe	hemochromatosis	233.2512245	0.407642583	0.11167162	3.65036868	0.000261864	2.73E-02
ENSMUSG00000025666	Tmem47	transmembrane protein 47	6719.132151	-0.216149918	0.059318852	-3.643865528	0.000268574	2.79E-02
ENSMUSG00000043631	Ecm2	extracellular matrix protein 2, female organ and adipocyte specific	522.2468524	-0.450393032	0.124061234	-3.630409094	0.000282972	2.92E-02
ENSMUSG00000000168	Dlat	dihydrolipoamide S-acetyltransferase (E2 component of pyruvate dehydrogenase complex)	4583.776794	0.176427012	0.048640056	3.627195923	0.000286516	2.92E-02
ENSMUSG00000052353	Cemip	cell migration inducing protein, hyaluronan binding	1840.025575	-0.4649413	0.128287759	-3.624206261	0.00028985	2.94E-02
ENSMUSG00000010045	Tmem115	transmembrane protein 115	1344.974255	0.214213274	0.059281784	3.613475478	0.00030212	3.02E-02
ENSMUSG00000058571	Gpc6	glypican 6	1138.981461	-0.221737078	0.061346601	-3.614496551	0.000300932	3.02E-02
ENSMUSG00000021998	Lcp1	lymphocyte cytosolic protein 1	575.426901	-0.33184577	0.091996191	-3.607168583	0.000309557	3.06E-02
ENSMUSG00000099512	Gm28703	predicted gene 28703	42.47158017	-0.723172188	0.200554314	-3.605867029	0.000311112	3.06E-02
ENSMUSG00000026344	Lypd1	Ly6/Plaur domain containing 1	707.8577798	0.357304132	0.099205924	3.601641094	0.000316215	3.09E-02
ENSMUSG00000026875	Traf1	TNF receptor-associated factor 1	452.7246797	0.445913269	0.123949496	3.597539993	0.000321241	3.12E-02
ENSMUSG00000037685	Atp8a1	ATPase, aminophospholipid transporter (APLT), class I, type 8A, member 1	11419.74021	-0.152030474	0.042369287	-3.588223594	0.000332939	3.22E-02
ENSMUSG00000022551	Cyc1	cytochrome c-1	5969.488864	0.176594951	0.049237771	3.586574833	0.00033505	3.22E-02
ENSMUSG00000000881	Dlg3	discs large MAGUK scaffold protein 3	5293.782134	0.118328055	0.033009058	3.584714728	0.000337447	3.22E-02
ENSMUSG00000004187	Kifc2	kinesin family member C2	8872.227272	0.164258912	0.045857095	3.581973822	0.000341008	3.23E-02
ENSMUSG00000039252	Lgi2	leucine-rich repeat LGI family, member 2	6372.971886	0.318458404	0.088965961	3.579553376	0.000344182	3.23E-02
ENSMUSG00000046574	Prr12	proline rich 12	3312.873574	0.150871364	0.042148131	3.579550486	0.000344186	3.23E-02
ENSMUSG00000010054	Tusc2	tumor suppressor 2, mitochondrial calcium regulator	2502.522813	0.154214131	0.043214835	3.568546102	0.000358968	3.33E-02
ENSMUSG00000024777	Ppp2r5b	protein phosphatase 2, regulatory subunit B', beta	6579.099733	0.135258768	0.037954628	3.563696347	0.000365669	3.38E-02
ENSMUSG00000063428	Ddo	D-aspartate oxidase	1482.79067	-0.154868869	0.043574294	-3.554133786	0.000379226	3.48E-02
ENSMUSG00000042155	Klhl23	kelch-like 23	3422.227809	-0.108699883	0.03072909	-3.537360911	0.000404147	3.69E-02
ENSMUSG00000001227	Sema6b	sema domain, transmembrane domain (TM), and cytoplasmic domain, (semaphorin) 6B	1758.165062	0.156707228	0.044407639	3.528834961	0.000417393	3.79E-02

ENSMUSG00000037579	Kcnh3	potassium voltage-gated channel, subfamily H (eag-related), member 3	141.4872672	0.699261434	0.198678837	3.519556709	0.000432269	3.90E-02
ENSMUSG00000039838	Slc45a1	solute carrier family 45, member 1	2158.860514	0.248713208	0.070876463	3.509108621	0.000449611	4.04E-02
ENSMUSG00000029059	Fam213b	family with sequence similarity 213, member B	1756.94047	0.240099039	0.06861156	3.499396293	0.000466313	4.17E-02
ENSMUSG00000041695	Kcnj2	potassium inwardly-rectifying channel, subfamily J, member 2	142.9180509	-0.457228698	0.130737517	-3.497302913	0.000469988	4.18E-02
ENSMUSG00000018076	Med13l	mediator complex subunit 13-like	5781.01772	-0.173663194	0.049763156	-3.489794661	0.000483392	4.26E-02
ENSMUSG00000044134	Pheta1	PH domain containing endocytic trafficking adaptor 1	704.7746099	0.237777278	0.068167136	3.48815119	0.000486373	4.26E-02
ENSMUSG00000050511	Oprd1	opioid receptor, delta 1	20.04430459	-1.209406991	0.346726523	-3.488071752	0.000486517	4.26E-02
ENSMUSG00000030092	Cntn6	contactin 6	5331.154587	-0.182682189	0.052415205	-3.485289974	0.000491604	4.28E-02
ENSMUSG00000032295	Man2c1	mannosidase, alpha, class 2C, member 1	4727.558809	0.127253112	0.036673966	3.46984868	0.000520752	4.51E-02
ENSMUSG00000023764	Sfi1	Sfi1 homolog, spindle assembly associated (yeast)	1212.243325	0.224302065	0.064771647	3.462966855	0.000534254	4.59E-02
ENSMUSG00000024076	Vit	vitrin	66.44094499	-0.547881353	0.158244454	-3.462246786	0.000535686	4.59E-02
ENSMUSG00000028150	Rorc	RAR-related orphan receptor gamma	2262.687714	0.230559859	0.066619632	3.460839586	0.000538494	4.59E-02
ENSMUSG00000040651	Fam208a	family with sequence similarity 208, member A	4400.287323	-0.205270022	0.059351971	-3.458520737	0.00054315	4.61E-02
ENSMUSG00000032328	Tmem30a	transmembrane protein 30A	15615.31096	-0.114504148	0.033143918	-3.454755915	0.000550791	4.65E-02
ENSMUSG00000109724	Gm18194	predicted gene 18194	133.610084	-0.426838601	0.123598131	-3.45343896	0.000553488	4.65E-02
ENSMUSG00000033862	Cdk10	cyclin-dependent kinase 10	1241.950755	0.202461754	0.05868709	3.449851619	0.000560895	4.65E-02
ENSMUSG00000061046	Haghl	hydroxyacylglutathione hydrolase-like	3351.199806	0.194626781	0.056425654	3.449260539	0.000562124	4.65E-02
ENSMUSG00000078480	Mrpl48-ps	Mitochondrial ribosomal protein L48	27.58601781	-3.250561366	0.94190633	-3.451045249	0.00055842	4.65E-02
ENSMUSG00000032324	Tspan3	tetraspanin 3	9627.269076	0.132814628	0.03855294	3.44499351	0.000571073	4.70E-02
ENSMUSG00000023017	Asic1	acid-sensing (proton-gated) ion channel 1	5549.805749	0.176764615	0.051358748	3.441762535	0.000577937	4.73E-02
ENSMUSG00000099616	4932413F04Rik	RIKEN cDNA 4932413F04 gene	21.90064226	2.125104477	0.619335029	3.43126802	0.000600767	4.89E-02
ENSMUSG00000110945	Gm9856	predicted gene 9856	328.9491498	-0.365949833	0.106689059	-3.4300596	0.000603449	4.89E-02

Supp Table S11. List of Differentially Expressed genes at FDR 5% in *Gnb5-/-* mice - hippocampus

Ensembl ID	Gene Symbol	Gene name	baseMean	log2FoldChange	lfcSE	stat	pvalue	padj
ENSMUSG00000032192	Gnb5	guanine nucleotide binding protein (G protein), beta 5	2382.397101	-2.949092443	0.050530966	-58.36208266	0.00E+00	< 2.00E-308
ENSMUSG00000023979	Guca1b	guanylate cyclase activator 1B	267.9709549	3.578006541	0.118457105	30.20508174	2.03E-200	1.96E-196
ENSMUSG00000048758	Rpl29	ribosomal protein L29	186.1160919	-2.54505664	0.14267899	-17.83764128	3.61E-71	2.32E-67
ENSMUSG00000020253	Ppm1m	protein phosphatase 1M	677.7813768	-0.764173504	0.069114538	-11.05662471	2.04E-28	9.82E-25
ENSMUSG00000032556	Bfsp2	beaded filament structural protein 2, phakinin	72.5712779	-3.439485494	0.36690378	-9.374352839	6.96E-21	2.68E-17
ENSMUSG00000023345	Poc1a	POC1 centriolar protein A	290.9177971	-0.980344264	0.104992395	-9.337288312	9.88E-21	3.18E-17
ENSMUSG00000032221	Mns1	meiosis-specific nuclear structural protein 1	180.727792	1.133030106	0.149838879	7.56165631	3.98E-14	1.10E-10
ENSMUSG00000049624	Slc17a5	solute carrier family 17 (anion/sugar transporter), member 5	1358.227186	0.395134078	0.0552683	7.149379957	8.72E-13	2.10E-09
ENSMUSG00000032418	Me1	malic enzyme 1, NADP(+)-dependent, cytosolic	3220.61655	0.35094107	0.049212845	7.131086888	9.96E-13	2.13E-09
ENSMUSG00000032344	Cgas	cyclic GMP-AMP synthase	64.05394375	-1.297224737	0.183150018	-7.082853442	1.41E-12	2.48E-09
ENSMUSG00000087466	A330041J22Rik	RIKEN cDNA A330041J22 gene	106.9804268	1.041048682	0.146908797	7.086360423	1.38E-12	2.48E-09
ENSMUSG00000032383	Ppib	peptidylprolyl isomerase B	7246.634387	0.323390812	0.046451328	6.961928182	3.36E-12	5.39E-09
ENSMUSG00000034910	Pygo1	pygopus 1	4535.707067	0.296843044	0.042829899	6.930743563	4.19E-12	6.21E-09
ENSMUSG00000057802	Gm10030	predicted gene 10030	24.02046494	-2.238670246	0.325437036	-6.878965819	6.03E-12	8.31E-09
ENSMUSG00000103164	Gm38150	predicted gene 38150	26.51357105	1.792662303	0.27409376	6.540325124	6.14E-11	7.89E-08
ENSMUSG00000047257	Prss45	protease, serine 45	29.29370674	2.22072601	0.345290573	6.431470148	1.26E-10	1.52E-07
ENSMUSG00000042210	Abhd14a	abhydrolase domain containing 14A	1011.239637	-0.395645636	0.062995633	-6.280524786	3.37E-10	3.83E-07
ENSMUSG00000102225	Gm37983	predicted gene 37983	19.23587601	2.053502553	0.328382635	6.253383503	4.02E-10	4.30E-07
ENSMUSG00000113637	Gm7049	predicted gene 7049	22.35956108	2.599937147	0.417875517	6.221798223	4.91E-10	4.99E-07
ENSMUSG00000032498	Mlh1	mutL homolog 1	473.749797	-0.608376157	0.098140351	-6.199041977	5.68E-10	5.48E-07
ENSMUSG00000032349	Elovl5	ELOVL family member 5, elongation of long chain fatty acids (yeast)	3448.449111	0.266712933	0.043182619	6.176395514	6.56E-10	6.02E-07
ENSMUSG00000032872	Cyb5r4	cytochrome b5 reductase 4	1427.463459	-0.552583779	0.097467466	-5.669417721	1.43E-08	1.26E-05

ENSMUSG00000062270	Morf4l1	mortality factor 4 like 1	4261.150376	-0.370709156	0.066751219	-5.553593847	2.80E-08	2.35E-05
ENSMUSG00000062270	Morf4l1b	mortality factor 4 like 1B	4261.150376	-0.370709156	0.066751219	-5.553593847	2.80E-08	2.35E-05
ENSMUSG00000032232	Cgnl1	cingulin-like 1	716.6625714	-0.674264189	0.126477175	-5.331113623	9.76E-08	7.55E-05
ENSMUSG00000032563	Mrpl3	mitochondrial ribosomal protein L3	2653.667229	-0.241906517	0.045381018	-5.330566088	9.79E-08	7.55E-05
ENSMUSG00000029471	Camkk2	calcium/calmodulin-dependent protein kinase kinase 2, beta	7986.908004	0.28842287	0.055844882	5.164714513	2.41E-07	1.79E-04
ENSMUSG00000111348	Gm19531	predicted gene 19531	60.80809486	-0.967537	0.190133025	-5.088737203	3.60E-07	2.57E-04
ENSMUSG00000032363	Adamts7	a disintegrin-like and metallopeptidase (reprolysin type) with thrombospondin type 1 motif, 7	60.02830454	1.253658417	0.250364087	5.007341231	5.52E-07	3.79E-04
ENSMUSG00000034898	Filip1	filamin A interacting protein 1	818.7049445	1.116876389	0.2236231	4.994458936	5.90E-07	3.79E-04
ENSMUSG00000046186	Cd109	CD109 antigen	440.3239799	0.744000787	0.14896346	4.994518707	5.90E-07	3.79E-04
ENSMUSG00000032184	Lysmd2	LysM, putative peptidoglycan-binding, domain containing 2	1535.062665	0.192736213	0.039007063	4.941059295	7.77E-07	4.83E-04
ENSMUSG00000032567	Aste1	asteroid homolog 1	258.6818556	-0.411147502	0.08364275	-4.915518725	8.85E-07	5.34E-04
ENSMUSG00000004366	Sst	somatostatin	4564.046349	-0.619153137	0.128391349	-4.822389825	1.42E-06	8.05E-04
ENSMUSG00000086296	D030055H07Rik	RIKEN cDNA 030055H07 gene	30.05950376	1.958950704	0.408226916	4.798680896	1.60E-06	8.80E-04
ENSMUSG00000029819	Npy	neuropeptide Y	939.2650548	-0.512512486	0.107467639	-4.768993613	1.85E-06	9.92E-04
ENSMUSG00000042208	0610010F05Rik	RIKEN cDNA 0610010F05 gene	2105.523782	0.161358008	0.034019647	4.743082913	2.10E-06	1.10E-03
ENSMUSG00000042073	Abhd14b	abhydrolase domain containing 14b	680.5734956	-0.292955368	0.061980538	-4.726570277	2.28E-06	1.16E-03
ENSMUSG00000028681	Ptch2	patched 2	163.9075961	0.837619832	0.177967416	4.706590954	2.52E-06	1.21E-03
ENSMUSG00000064023	Klk8	kallikrein related-peptidase 8	472.905183	0.558842709	0.118652722	4.709902128	2.48E-06	1.21E-03
ENSMUSG00000039474	Wfs1	wolframin ER transmembrane glycoprotein	6619.822236	0.444546447	0.094628776	4.6977935	2.63E-06	1.24E-03
ENSMUSG00000021680	Crhbp	corticotropin releasing hormone binding protein	811.9965294	-0.700244123	0.150359765	-4.657124341	3.21E-06	1.47E-03
ENSMUSG00000049303	Syt12	synaptotagmin XII	1361.722132	0.338352088	0.072743355	4.651312622	3.30E-06	1.48E-03
ENSMUSG00000104586	4921539H07Rik	RIKEN cDNA 4921539H07	315.8272611	0.702883487	0.151686402	4.633793656	3.59E-06	1.57E-03
ENSMUSG00000041506	Rrp9	RRP9, small subunit (SSU) processome component, homolog (yeast)	673.6407763	-0.305170804	0.066043718	-4.620739307	3.82E-06	1.64E-03

ENSMUSG00000032420	Nt5e	5' nucleotidase, ecto	175.8655902	0.583004051	0.126570941	4.606144538	4.10E-06	1.72E-03
ENSMUSG00000023982	Guca1a	guanylate cyclase activator 1a (retina)	10.42051793	2.196823203	0.478445803	4.591582138	4.40E-06	1.81E-03
ENSMUSG00000060935	Tmem263	transmembrane protein 263	1125.137161	0.21083974	0.045978252	4.585640582	4.53E-06	1.82E-03
ENSMUSG00000010054	Tusc2	tumor suppressor 2, mitochondrial calcium regulator	2669.280548	0.150507457	0.033050594	4.553850268	5.27E-06	2.03E-03
ENSMUSG00000016942	Tmprss6	transmembrane serine protease 6	39.72576369	1.593037625	0.349843922	4.553566674	5.27E-06	2.03E-03
ENSMUSG00000030966	Trim21	tripartite motif-containing 21	113.3212122	-0.693400583	0.152836079	-4.536890679	5.71E-06	2.16E-03
ENSMUSG00000030688	Stard10	START domain containing 10	541.7897091	-0.295630626	0.065426937	-4.518484851	6.23E-06	2.31E-03
ENSMUSG00000029361	Nos1	nitric oxide synthase 1, neuronal	8256.593264	-0.261130979	0.059373749	-4.398088118	1.09E-05	3.97E-03
ENSMUSG00000063297	Luzp2	leucine zipper protein 2	6275.556935	0.268145569	0.061330761	4.372122009	1.23E-05	4.39E-03
ENSMUSG00000032570	Atp2c1	ATPase, Ca++-sequestering	10045.80105	0.188841067	0.043261344	4.365122496	1.27E-05	4.46E-03
ENSMUSG00000043719	Col6a6	collagen, type VI, alpha 6	118.7663673	1.69637505	0.390171056	4.347772659	1.38E-05	4.74E-03
ENSMUSG00000032332	Col12a1	collagen, type XII, alpha 1	629.8618523	-0.433906638	0.100352904	-4.32380748	1.53E-05	5.02E-03
ENSMUSG00000053040	Aph1c	aph1 homolog C, gamma secretase subunit	494.1347982	-0.311844717	0.072119583	-4.323995034	1.53E-05	5.02E-03
ENSMUSG00000058587	Tmod3	tropomodulin 3	1118.986474	-0.281319427	0.065066984	-4.323535703	1.54E-05	5.02E-03
ENSMUSG00000043587	Pxylp1	2-phosphoxylose phosphatase 1	545.5374077	-0.597492552	0.139927712	-4.270008748	1.95E-05	6.28E-03
ENSMUSG00000037089	Slc35b2	solute carrier family 35, member B2	868.1670288	0.238115051	0.05583839	4.264360995	2.00E-05	6.34E-03
ENSMUSG00000054204	Alkal2	ALK and LTK ligand 2	136.1426888	-0.81219183	0.191945922	-4.231357575	2.32E-05	7.23E-03
ENSMUSG00000032572	Col6a4	collagen, type VI, alpha 4	126.9727054	-2.511414656	0.595871353	-4.214692722	2.50E-05	7.66E-03
ENSMUSG00000085007	Gm11549	predicted gene 11549	231.5328462	0.4463464	0.106199532	4.202903639	2.64E-05	7.94E-03
ENSMUSG00000000805	Car4	carbonic anhydrase 4	2357.367529	0.308419263	0.073606666	4.19009963	2.79E-05	8.27E-03
ENSMUSG00000032330	Cox7a2	cytochrome c oxidase subunit 7A2	3013.00797	0.125559116	0.030057148	4.177346281	2.95E-05	8.49E-03
ENSMUSG00000110814	Gm38661	predicted gene 38661	14.96083878	-1.561989653	0.373750415	-4.179231894	2.92E-05	8.49E-03
ENSMUSG00000091345	Col6a5	collagen, type VI, alpha 5	174.2352851	1.016652505	0.244067905	4.165449379	3.11E-05	8.81E-03
ENSMUSG00000068428	Gmnc	geminin coiled-coil domain containing	264.2827313	-0.336898445	0.080973307	-4.160611156	3.17E-05	8.87E-03
ENSMUSG00000024883	Rin1	Ras and Rab interactor 1	4208.394122	0.206174191	0.049688679	4.149319198	3.33E-05	9.19E-03

ENSMUSG00000105230	Gm42433	predicted gene 42433	436.7842918	0.246770538	0.059606745	4.139976749	3.47E-05	9.44E-03
ENSMUSG00000071252	2210408I21Rik	RIKEN cDNA 2210408I21 gene	389.615445	0.264361422	0.064174253	4.119431228	3.80E-05	1.02E-02
ENSMUSG00000041923	Nol4	nucleolar protein 4	3286.050462	0.140254784	0.034100943	4.112929765	3.91E-05	1.03E-02
ENSMUSG00000019947	Arid5b	AT rich interactive domain 5B (MRF1-like)	1885.967968	-0.260157537	0.06335511	-4.106338656	4.02E-05	1.03E-02
ENSMUSG00000037104	Socs5	suppressor of cytokine signaling 5	5886.68313	0.107574506	0.026251141	4.097898351	4.17E-05	1.06E-02
ENSMUSG00000028971	Cort	cortistatin	67.60807817	-0.724694391	0.178109095	-4.068823039	4.73E-05	1.18E-02
ENSMUSG00000010057	Nprl2	NPR2 like, GATOR1 complex subunit	1429.63198	0.202997062	0.050049486	4.055927008	4.99E-05	1.23E-02
ENSMUSG00000032497	Lrrfip2	leucine rich repeat (in FLII) interacting protein 2	1294.793986	-0.201517371	0.049816198	-4.045217774	5.23E-05	1.26E-02
ENSMUSG00000040875	Osbpl10	oxysterol binding protein-like 10	644.5691274	-0.352970362	0.087207161	-4.047492849	5.18E-05	1.26E-02
ENSMUSG00000031209	Heph	hephaestin	349.4145748	-0.441492572	0.109271656	-4.040321062	5.34E-05	1.27E-02
ENSMUSG00000112441	Gm48898	predicted gene 48898	20.14550056	1.319734025	0.326804115	4.03830296	5.38E-05	1.27E-02
ENSMUSG00000014601	Strip1	striatin interacting protein 1	4618.315049	0.121491804	0.030263161	4.014511357	5.96E-05	1.37E-02
ENSMUSG00000040936	Ulk4	unc-51-like kinase 4	201.3074905	-0.524730265	0.132061386	-3.973381479	7.09E-05	1.61E-02
ENSMUSG00000038859	Baiap2l1	BAI1-associated protein 2-like 1	49.0839138	-1.306916288	0.331538163	-3.941978429	8.08E-05	1.81E-02
ENSMUSG00000016763	Scube1	signal peptide, CUB domain, EGF-like 1	1726.279322	0.426222434	0.108205935	3.93899311	8.18E-05	1.81E-02
ENSMUSG00000103133	Gm37303	predicted gene 37303	77.94310654	0.522106934	0.133550723	3.909427989	9.25E-05	2.03E-02
ENSMUSG00000004951	Hspb1	heat shock protein 1	151.4367051	-0.835319314	0.213951004	-3.904255167	9.45E-05	2.05E-02
ENSMUSG00000090877	Hspa1b	heat shock protein 1B	392.1558983	-0.763255749	0.19636514	-3.88692082	1.02E-04	2.18E-02
ENSMUSG00000029462	Vps29	VPS29 retromer complex component	3845.833264	0.14493881	0.037518194	3.863160675	1.12E-04	2.32E-02
ENSMUSG00000042444	Mindy2	MINDY lysine 48 deubiquitinase 2	3612.316289	-0.152283466	0.039398177	-3.865241432	1.11E-04	2.32E-02
ENSMUSG00000108325	NA	NA	93.73890629	0.5200387	0.134475044	3.867176279	1.10E-04	2.32E-02
ENSMUSG00000035941	Ibtk	inhibitor of Bruton agammaglobulinemia tyrosine kinase	1211.17404	-0.205862348	0.053432389	-3.852763275	1.17E-04	2.40E-02
ENSMUSG00000045327	6330549D23Rik	RIKEN cDNA 6330549D23 gene	49.6841459	-0.674934781	0.1754258	-3.847408893	1.19E-04	2.42E-02
ENSMUSG00000032012	Nectin1	nectin cell adhesion molecule 1	2017.659804	0.237274266	0.061873515	3.834827627	1.26E-04	2.52E-02

ENSMUSG00000051910	Sox6	SRY (sex determining region Y)-box 6	1109.249799	-0.210449817	0.054915382	-3.832256303	1.27E-04	2.52E-02
ENSMUSG00000033644	Piwil2	piwi-like RNA-mediated gene silencing 2	81.66252996	-0.533317618	0.139890545	-3.812392175	1.38E-04	2.71E-02
ENSMUSG00000006522	Itih3	inter-alpha trypsin inhibitor, heavy chain 3	1084.136711	-0.295092903	0.078005203	-3.782990024	1.55E-04	2.99E-02
ENSMUSG00000107092	Gm7993	predicted gene 7993	27.55659689	3.745229986	0.998444348	3.751065337	1.76E-04	3.36E-02
ENSMUSG00000038370	Pcp4l1	Purkinje cell protein 4-like 1	1329.318487	-0.232791453	0.063060501	-3.69155731	2.23E-04	4.17E-02
ENSMUSG00000048001	Hes5	hes family bHLH transcription factor 5	210.1360801	0.574406535	0.155524959	3.693339899	2.21E-04	4.17E-02
ENSMUSG00000051590	Map3k19	mitogen-activated protein kinase kinase kinase 19	332.5326268	-0.512141061	0.138814957	-3.689379518	2.25E-04	4.17E-02
ENSMUSG00000032265	Tent5a	terminal nucleotidyltransferase 5A	327.0098402	-0.714753787	0.195490594	-3.656205511	2.56E-04	4.70E-02

Supp Table S12. List of Differentially Expressed genes at FDR 5% in *Gnb5-/-* mice - cerebral cortex

Ensembl ID	Gene Symbol	Gene name	baseMean	log2FoldChange	lfcSE	stat	pvalue	padj
ENSMUSG00000032192	Gnb5	guanine nucleotide binding protein (G protein), beta 5	3593.342841	-3.062918872	0.090085387	-34.0001745	2.21E-253	4.84E-249
ENSMUSG00000023979	Guca1b	guanylate cyclase activator 1B	263.8918466	3.835511755	0.13316811	28.80202898	2.0231E-182	2.209E-178
ENSMUSG00000048758	Rpl29	ribosomal protein L29	264.164767	-2.731697404	0.15217746	-17.95073601	4.73586E-72	3.44739E-68
ENSMUSG00000020253	Ppm1m	protein phosphatase 1M	894.8693801	-1.212158437	0.086719969	-13.97784672	2.1283E-44	1.16195E-40
ENSMUSG00000032221	Mns1	meiosis-specific nuclear structural protein 1	116.3525616	1.634839206	0.147435847	11.08847841	1.42694E-28	6.23231E-25
ENSMUSG00000023345	Poc1a	POC1 centriolar protein A	386.6670779	-1.089635159	0.121899515	-8.938798156	3.93426E-19	1.43194E-15
ENSMUSG00000032332	Col12a1	collagen, type XII, alpha 1	887.9004528	-0.885695463	0.103581894	-8.550678424	1.22367E-17	3.8175E-14
ENSMUSG00000111765	Gm10635	predicted gene 10635	51.20226751	-3.314939998	0.393896818	-8.415757245	3.90365E-17	1.0656E-13
ENSMUSG00000111348	Gm19531	predicted gene 19531	101.5467041	-1.241020024	0.148741013	-8.343495822	7.2126E-17	1.7501E-13
ENSMUSG00000047257	Prss45	protease, serine 45	34.35647461	2.296734155	0.277403272	8.279405412	1.23792E-16	2.70337E-13
ENSMUSG00000042210	Abhd14a	abhydrolase domain containing 14A	1032.445648	-0.613596969	0.083391587	-7.358020052	1.86658E-13	3.70567E-10
ENSMUSG00000102225	Gm37983	predicted gene 37983	19.57885383	2.58186601	0.362084881	7.130554587	9.99653E-13	1.8192E-09
ENSMUSG00000043719	Col6a6	collagen, type VI, alpha 6	105.0713081	1.589103099	0.247685384	6.41581298	1.40073E-10	2.35302E-07

ENSMUSG00000032349	Elovl5	ELOVL family member 5, elongation of long chain fatty acids (yeast)	3648.481725	0.321846446	0.051309014	6.272707688	3.54823E-10	5.53473E-07
ENSMUSG00000032418	Me1	malic enzyme 1, NADP(+)-dependent, cytosolic	2016.009287	0.340643445	0.054688731	6.228768528	4.70116E-10	6.84426E-07
ENSMUSG00000010044	Zmynd10	zinc finger, MYND domain containing 10	228.8723475	0.730365544	0.120958409	6.038154333	1.55887E-09	1.79172E-06
ENSMUSG00000032498	Mlh1	mutL homolog 1	521.8321994	-0.490752727	0.081153472	-6.047217911	1.47368E-09	1.79172E-06
ENSMUSG00000032872	Cyb5r4	cytochrome b5 reductase 4	1413.346395	-0.564165726	0.093231634	-6.051226418	1.43747E-09	1.79172E-06
ENSMUSG00000087466	A330041J22 Rik	RIKEN cDNA A330041J22 gene	81.90474134	1.204927988	0.202332849	5.955177308	2.5979E-09	2.83665E-06
ENSMUSG00000049555	Tmie	transmembrane inner ear	241.8759334	0.63716907	0.114389213	5.570184912	2.54469E-08	2.64624E-05
ENSMUSG00000032556	Bfsp2	beaded filament structural protein 2, phakinin	85.4861346	-2.94717596	0.53990551	-5.458688424	4.79665E-08	4.63913E-05
ENSMUSG00000057802	Gm10030	predicted gene 10030	22.31636754	-1.9157509	0.351165297	-5.45541065	4.88598E-08	4.63913E-05
ENSMUSG00000062270	Morf4l1	mortality factor 4 like 1	3862.642941	-0.355532571	0.066892551	-5.314979978	1.06669E-07	9.706E-05
ENSMUSG00000062270	Morf4l1b	mortality factor 4 like 1B	3862.642941	-0.355532571	0.066892551	-5.314979978	1.06669E-07	9.706E-05
ENSMUSG00000103164	Gm38150	predicted gene 38150	23.78691025	1.84771035	0.366887132	5.036181944	4.74909E-07	0.000414843
ENSMUSG00000032383	Ppib	peptidylprolyl isomerase B	6545.594919	0.317038174	0.064051057	4.949772724	7.43002E-07	0.000624064
ENSMUSG00000059146	Ntrk3	neurotrophic tyrosine kinase, receptor, type 3	10681.1642	-0.195870941	0.040335881	-4.855997647	1.19782E-06	0.000968816
ENSMUSG00000059146	E430016F16 Rik	RIKEN cDNA E430016F16 gene	10681.1642	-0.195870941	0.040335881	-4.855997647	1.19782E-06	0.000968816
ENSMUSG00000032497	Lrrfip2	leucine rich repeat (in FLII) interacting protein 2	1541.136996	-0.220140185	0.04568305	-4.81885913	1.44381E-06	0.001126072
ENSMUSG00000109975	Gm19196	predicted gene 19196	76.97292567	-0.83775478	0.179372068	-4.670486274	3.00488E-06	0.002262775
ENSMUSG00000097099	Gm9917	predicted gene 9917	87.59711317	-0.72766991	0.158976579	-4.577214553	4.71208E-06	0.003334375
ENSMUSG00000110996	Gm36251	predicted gene, 36251	83.08922865	-2.301491121	0.502918057	-4.576274579	4.73329E-06	0.003334375
ENSMUSG00000024143	Rhoq	ras homolog family member Q	1994.563327	0.27220004	0.059757079	4.555109551	5.23583E-06	0.003573126
ENSMUSG00000055125	M5C1000l18 Rik	RIKEN cDNA M5C1000l18	169.1051477	-0.512026751	0.116302137	-4.4025567	1.06983E-05	0.007079656
ENSMUSG00000043587	Pxylp1	2-phosphoxylose phosphatase 1	541.0845473	-0.522547059	0.12057503	-4.333791642	1.46563E-05	0.009413649
ENSMUSG00000032370	Lactb	lactamase, beta	508.7191939	-0.370527801	0.086670063	-4.275153232	1.91006E-05	0.011586629
ENSMUSG00000063953	Amd2	S-adenosylmethionine decarboxylase 2	13.33707831	2.326043682	0.551895854	4.214642425	2.50174E-05	0.014765689

ENSMUSG00000041506	Rrp9	RRP9, small subunit (SSU) processome component, homolog (yeast)	741.5546544	-0.371086466	0.089204231	-4.159964852	3.18297E-05	0.018292002
ENSMUSG00000034910	Pygo1	pygopus 1	2350.941427	0.238237403	0.057597268	4.13626219	3.53009E-05	0.019766684
ENSMUSG00000033208	S100b	S100 protein, beta polypeptide, neural	4168.970089	0.202698353	0.049322006	4.109693985	3.96184E-05	0.021252459
ENSMUSG00000042073	Abhd14b	abhydrolase domain containing 14b	685.2510238	-0.305729814	0.074452684	-4.106363902	4.01936E-05	0.021252459
ENSMUSG00000091735	Gpr62	G protein-coupled receptor 62	243.7985731	0.456204569	0.111202042	4.102483748	4.08739E-05	0.021252459
ENSMUSG00000033730	Egr3	early growth response 3	6887.681122	-0.476370365	0.117456133	-4.055730036	4.9978E-05	0.025381829
ENSMUSG00000041460	Cacna2d4	calcium channel, voltage-dependent, alpha 2/delta subunit 4	115.497014	0.560303026	0.139981496	4.002693509	6.26254E-05	0.031082129
ENSMUSG00000039943	Plcb4	phospholipase C, beta 4	2966.652641	-0.243003116	0.061111924	-3.976361751	6.99776E-05	0.033959376
ENSMUSG00000032184	Lysmd2	LysM, putative peptidoglycan-binding, domain containing 2	1379.081352	0.192652009	0.049069682	3.926090417	8.63377E-05	0.04098789
ENSMUSG00000107092	Gm7993	predicted gene 7993	24.59807194	3.811634628	0.974363079	3.911924324	9.15636E-05	0.042543958
ENSMUSG00000032563	Mrpl3	mitochondrial ribosomal protein L3	2663.113172	-0.178171707	0.045609773	-3.906437045	9.3667E-05	0.042614597

Supp. Table S13. List of Biological Processes (BP) at FDR 5% - cerebellum

GO ID	Description	BgRatio	pvalue	p.adjust	qvalue	geneID	Count
GO:0042391	regulation of membrane potential	430/21092	7.30339E-05	0.164189734	0.156177167	Grin2a/Dcn/Snca/Tmem108/Hcn2/Dgki/Ntrk2/Kcnk2/Tusc2/Kcnh3/Kcnj2/Oprd1/Asic1	13
GO:0043949	regulation of cAMP-mediated signaling	64/21092	0.000200911	0.164189734	0.156177167	Gpr62/Pde10a/Mrap2/Gnai2/Cgas	5
GO:0006865	amino acid transport	145/21092	0.000227254	0.164189734	0.156177167	Slc25a29/Slc17a5/Myo6/Snca/Slc6a5/Ntrk2/Slc7a11	7
GO:0050808	synapse organization	427/21092	0.000271612	0.164189734	0.156177167	Filip1/Camkv/Col4a5/Zfp804a/Myo6/Snca/Magi2/Tmem108/Sncb/Dctn1/Ntrk2/Slc7a11	12
GO:0010039	response to iron ion	20/21092	0.000596278	0.288360066	0.274287904	Trf/Snca/Hfe	3
GO:0046928	regulation of neurotransmitter secretion	137/21092	0.001064507	0.3155174	0.300119942	Syt12/Myo6/Snca/Dgki/Ntrk2/Asic1	6
GO:0006022	aminoglycan metabolic process	99/21092	0.00148897	0.3155174	0.300119942	Pxylp1/Dcn/Chil5/Itih5/Cemip	5
GO:0043951	negative regulation of cAMP-mediated signaling	28/21092	0.001631142	0.3155174	0.300119942	Pde10a/Mrap2/Gnai2	3

GO:0050654	chondroitin sulfate proteoglycan metabolic process	29/21092	0.0018082	0.3155174	0.300119942	Pxylp1/Dcn/B3gat2	3
GO:0015800	acidic amino acid transport	63/21092	0.001941813	0.3155174	0.300119942	Myo6/Snca/Ntrk2/Slc7a11	4
GO:0015711	organic anion transport	404/21092	0.002251239	0.3155174	0.300119942	Slc25a29/Slc17a5/Myo6/Snca/Slc6a5/Slc4a4/Ntrk2/Slc7a11/Atp8a1/Tmem30a	10
GO:0006855	drug transmembrane transport	66/21092	0.002304207	0.3155174	0.300119942	Slc25a29/Slc6a5/Slc7a11/Tmem30a	4
GO:0051648	vesicle localization	283/21092	0.00275487	0.3155174	0.300119942	Myo5c/1190002N15Rik/Syt12/Myo6/Snca/Magi2/Dgki/Dctn1	8
GO:0098739	import across plasma membrane	114/21092	0.002763843	0.3155174	0.300119942	Slc6a5/Hcn2/Slc7a11/Hfe/Kcnj2	5
GO:0014047	glutamate secretion	34/21092	0.002871685	0.3155174	0.300119942	Myo6/Snca/Ntrk2	3
GO:0007612	learning	168/21092	0.002988362	0.3155174	0.300119942	Grin2a/Dgki/Ntrk2/Slc7a11/Atp8a1/Asic1	6
GO:0006826	iron ion transport	35/21092	0.003121703	0.3155174	0.300119942	Trf/Heph/Hfe	3
GO:1990089	response to nerve growth factor	35/21092	0.003121703	0.3155174	0.300119942	Magi2/Tmem108/Ntrk2	3
GO:1990090	cellular response to nerve growth factor stimulus	35/21092	0.003121703	0.3155174	0.300119942	Magi2/Tmem108/Ntrk2	3
GO:0043950	positive regulation of cAMP-mediated signaling	36/21092	0.003384682	0.3155174	0.300119942	Gpr62/Mrap2/Cgas	3
GO:1902475	L-alpha-amino acid transmembrane transport	37/21092	0.003660829	0.3155174	0.300119942	Slc25a29/Slc6a5/Slc7a11	3
GO:0042983	amyloid precursor protein biosynthetic process	11/21092	0.003664453	0.3155174	0.300119942	Necab1/Aatf	2
GO:0042984	regulation of amyloid precursor protein biosynthetic process	11/21092	0.003664453	0.3155174	0.300119942	Necab1/Aatf	2
GO:0106072	negative regulation of adenylate cyclase-activating G protein-coupled receptor signaling pathway	11/21092	0.003664453	0.3155174	0.300119942	Mrap2/Gnai2	2
GO:0014065	phosphatidylinositol 3-kinase signaling	122/21092	0.003699283	0.3155174	0.300119942	1190002N15Rik/Dcn/Agap2/Nyap2/Ntrk2	5
GO:1905475	regulation of protein localization to membrane	180/21092	0.004190431	0.3155174	0.300119942	Mrap2/Magi2/Slc7a11/Cemip/Gpc6/Lypd1	6
GO:0042762	regulation of sulfur metabolic process	12/21092	0.004373164	0.3155174	0.300119942	Snca/Slc7a11	2
GO:0071281	cellular response to iron ion	12/21092	0.004373164	0.3155174	0.300119942	Trf/Hfe	2

GO:0006836	neurotransmitter transport	306/21092	0.004413778	0.3155174	0.300119942	Syt12/Myo6/Snca/Slc6a5/Dgki/Ntrk2/Slc7a11/Asic1	8
GO:0006835	dicarboxylic acid transport	79/21092	0.004416017	0.3155174	0.300119942	Myo6/Snca/Ntrk2/Slc7a11	4
GO:0050805	negative regulation of synaptic transmission	79/21092	0.004416017	0.3155174	0.300119942	Gnai2/Snca/Dgki/Asic1	4
GO:0010559	regulation of glycoprotein biosynthetic process	40/21092	0.004570232	0.3155174	0.300119942	Pxylp1/Necab1/Aatf	3
GO:0001505	regulation of neurotransmitter levels	376/21092	0.004597278	0.3155174	0.300119942	Grin2a/Syt12/Myo6/Snca/Slc6a5/Dgki/Ntrk2/Slc7a11/Asic1	9
GO:0051588	regulation of neurotransmitter transport	184/21092	0.004661041	0.3155174	0.300119942	Syt12/Myo6/Snca/Dgki/Ntrk2/Asic1	6
GO:0030203	glycosaminoglycan metabolic process	81/21092	0.004827159	0.3155174	0.300119942	Pxylp1/Dcn/Itih5/Cemip	4
GO:0038179	neurotrophin signaling pathway	41/21092	0.004900965	0.3155174	0.300119942	Magi2/Tmem108/Ppp2r5b	3
GO:0009068	aspartate family amino acid catabolic process	13/21092	0.005139884	0.3155174	0.300119942	Aass/Ddo	2
GO:0042417	dopamine metabolic process	42/21092	0.005245786	0.3155174	0.300119942	Grin2a/Snca/Sncb	3
GO:0070838	divalent metal ion transport	457/21092	0.005365327	0.3155174	0.300119942	Gnb5/Grin2a/Atp2c1/Gnai2/Snca/Ibtk/Cemip/Kcnj2/Oprd1/Asic1	10
GO:0007269	neurotransmitter secretion	190/21092	0.005438454	0.3155174	0.300119942	Syt12/Myo6/Snca/Dgki/Ntrk2/Asic1	6
GO:0099643	signal release from synapse	190/21092	0.005438454	0.3155174	0.300119942	Syt12/Myo6/Snca/Dgki/Ntrk2/Asic1	6
GO:0060079	excitatory postsynaptic potential	84/21092	0.005490883	0.3155174	0.300119942	Grin2a/Snca/Tmem108/Dgki	4
GO:0072511	divalent inorganic cation transport	460/21092	0.005610938	0.3155174	0.300119942	Gnb5/Grin2a/Atp2c1/Gnai2/Snca/Ibtk/Cemip/Kcnj2/Oprd1/Asic1	10
GO:0060732	positive regulation of inositol phosphate biosynthetic process	14/21092	0.005963602	0.320444194	0.304806305	Plcd1/Snca	2
GO:0106070	regulation of adenylate cyclase-activating G protein-coupled receptor signaling pathway	14/21092	0.005963602	0.320444194	0.304806305	Mrap2/Gnai2	2
GO:1903018	regulation of glycoprotein metabolic process	45/21092	0.006366345	0.327535356	0.311551413	Pxylp1/Necab1/Aatf	3
GO:0050807	regulation of synapse organization	259/21092	0.006366485	0.327535356	0.311551413	Camkv/Zfp804a/Snca/Magi2/Dctn1/Ntrk2/Slc7a11	7
GO:0000041	transition metal ion transport	89/21092	0.006727861	0.328072847	0.312062675	Trf/Atp2c1/Heph/Hfe	4

GO:0010642	negative regulation of platelet-derived growth factor receptor signaling pathway	15/21092	0.006843317	0.328072847	0.312062675	Apod/Snca	2
GO:0097286	iron ion import	15/21092	0.006843317	0.328072847	0.312062675	Trf/Hfe	2
GO:0051650	establishment of vesicle localization	265/21092	0.00718333	0.328072847	0.312062675	Myo5c/1190002N15Rik/Syt12/Myo6/Snca/Dgki/Dctn1	7
GO:0001504	neurotransmitter uptake	47/21092	0.007186592	0.328072847	0.312062675	Snca/Slc6a5/Slc7a11	3
GO:0014066	regulation of phosphatidylinositol 3-kinase signaling	91/21092	0.007270244	0.328072847	0.312062675	1190002N15Rik/Dcn/Agap2/Ntrk2	4
GO:0050803	regulation of synapse structure or activity	266/21092	0.007326689	0.328072847	0.312062675	Camkv/Zfp804a/Snca/Magi2/Dctn1/Ntrk2/Slc7a11	7
GO:0098696	regulation of neurotransmitter receptor localization to postsynaptic specialization membrane	16/21092	0.007778044	0.331220927	0.315057127	Magi2/Gpc6	2
GO:0006816	calcium ion transport	409/21092	0.007827052	0.331220927	0.315057127	Gnb5/Grin2a/Atp2c1/Gnai2/Snca/Ibtk/Cemip/Oprd1/Asic1	9
GO:0048015	phosphatidylinositol-mediated signaling	146/21092	0.007844937	0.331220927	0.315057127	1190002N15Rik/Dcn/Agap2/Nyap2/Ntrk2	5
GO:0070588	calcium ion transmembrane transport	271/21092	0.008075514	0.331220927	0.315057127	Gnb5/Grin2a/Atp2c1/Snca/Ibtk/Cemip/Asic1	7
GO:0099565	chemical synaptic transmission, postsynaptic	94/21092	0.008136677	0.331220927	0.315057127	Grin2a/Snca/Tmem108/Dgki	4
GO:0046916	cellular transition metal ion homeostasis	95/21092	0.008439869	0.331220927	0.315057127	Trf/Atp2c1/Heph/Hfe	4
GO:0048017	inositol lipid-mediated signaling	149/21092	0.008525244	0.331220927	0.315057127	1190002N15Rik/Dcn/Agap2/Nyap2/Ntrk2	5
GO:0015893	drug transport	210/21092	0.008719811	0.331220927	0.315057127	Slc25a29/Syt12/Snca/Slc6a5/Slc7a11/Tmem30a	6
GO:0010919	regulation of inositol phosphate biosynthetic process	17/21092	0.008766807	0.331220927	0.315057127	Plcd1/Snca	2
GO:0051386	regulation of neurotrophin TRK receptor signaling pathway	17/21092	0.008766807	0.331220927	0.315057127	Tmem108/Ppp2r5b	2
GO:0071248	cellular response to metal ion	151/21092	0.009000841	0.334046503	0.317744812	Trf/Grin2a/Syt12/Snca/Hfe	5
GO:0007528	neuromuscular junction development	52/21092	0.009500864	0.334046503	0.317744812	Col4a5/Dctn1/Ntrk2	3

GO:0006898	receptor-mediated endocytosis	214/21092	0.009516311	0.334046503	0.317744812	Trf/Myo6/Snca/Magi2/Tmem108/Hfe	6
GO:0099072	regulation of postsynaptic membrane neurotransmitter receptor levels	99/21092	0.009726387	0.334046503	0.317744812	Myo6/Magi2/Gpc6/Dlg3	4
GO:0002710	negative regulation of T cell mediated immunity	18/21092	0.009808644	0.334046503	0.317744812	Il20rb/Hfe	2
GO:0010752	regulation of cGMP-mediated signaling	18/21092	0.009808644	0.334046503	0.317744812	Pde10a/Cgas	2
GO:0050650	chondroitin sulfate proteoglycan biosynthetic process	18/21092	0.009808644	0.334046503	0.317744812	Pxylp1/B3gat2	2
GO:0006879	cellular iron ion homeostasis	54/21092	0.010534313	0.353777329	0.336512761	Trf/Heph/Hfe	3
GO:0001975	response to amphetamine	19/21092	0.010902606	0.355799583	0.338436328	Grin2a/Asic1	2
GO:0048260	positive regulation of receptor-mediated endocytosis	55/21092	0.011074497	0.355799583	0.338436328	Trf/Magi2/Hfe	3
GO:0014075	response to amine	20/21092	0.012047753	0.355799583	0.338436328	Grin2a/Asic1	2
GO:0006584	catecholamine metabolic process	57/21092	0.012202184	0.355799583	0.338436328	Grin2a/Snca/Sncb	3
GO:0009712	catechol-containing compound metabolic process	57/21092	0.012202184	0.355799583	0.338436328	Grin2a/Snca/Sncb	3
GO:0045744	negative regulation of G protein-coupled receptor signaling pathway	57/21092	0.012202184	0.355799583	0.338436328	Mrap2/Gnai2/Snca	3
GO:1903510	mucopolysaccharide metabolic process	57/21092	0.012202184	0.355799583	0.338436328	Dcn/Itih5/Cemip	3
GO:1903539	protein localization to postsynaptic membrane	57/21092	0.012202184	0.355799583	0.338436328	Grin2a/Magi2/Gpc6	3
GO:0018958	phenol-containing compound metabolic process	106/21092	0.012271653	0.355799583	0.338436328	Grin2a/Snca/Sncb/Slc7a11	4
GO:0016311	dephosphorylation	367/21092	0.012532008	0.355799583	0.338436328	Ppm1m/Gnai2/Magi2/Ppm1j/Dusp7/Dlg3/Ppp2r5b/Sfi1	8
GO:0099504	synaptic vesicle cycle	228/21092	0.01271371	0.355799583	0.338436328	Syt12/Myo6/Snca/Magi2/Sncb/Dgki	6
GO:0046942	carboxylic acid transport	297/21092	0.012907908	0.355799583	0.338436328	Slc25a29/Slc17a5/Myo6/Snca/Slc6a5/Ntrk2/Slc7a11	7
GO:0015849	organic acid transport	298/21092	0.013127784	0.355799583	0.338436328	Slc25a29/Slc17a5/Myo6/Snca/Slc6a5/Ntrk2/Slc7a11	7

GO:0003433	chondrocyte development involved in endochondral bone morphogenesis	21/21092	0.013243161	0.355799583	0.338436328	Poc1a/Vit	2
GO:0095500	acetylcholine receptor signaling pathway	21/21092	0.013243161	0.355799583	0.338436328	Gnai2/Lypd1	2
GO:1903831	signal transduction involved in cellular response to ammonium ion	21/21092	0.013243161	0.355799583	0.338436328	Gnai2/Lypd1	2
GO:1905144	response to acetylcholine	21/21092	0.013243161	0.355799583	0.338436328	Gnai2/Lypd1	2
GO:1905145	cellular response to acetylcholine	21/21092	0.013243161	0.355799583	0.338436328	Gnai2/Lypd1	2
GO:0015807	L-amino acid transport	59/21092	0.013393424	0.355882404	0.338515107	Slc25a29/Slc6a5/Slc7a11	3
GO:0060078	regulation of postsynaptic membrane potential	111/21092	0.014328207	0.368755538	0.350760024	Grin2a/Snca/Tmem108/Dgki	4
GO:0003418	growth plate cartilage chondrocyte differentiation	22/21092	0.014487914	0.368755538	0.350760024	Poc1a/Vit	2
GO:0015874	norepinephrine transport	22/21092	0.014487914	0.368755538	0.350760024	Plcd1/Snca	2
GO:1902683	regulation of receptor localization to synapse	22/21092	0.014487914	0.368755538	0.350760024	Magi2/Gpc6	2
GO:0015672	monovalent inorganic cation transport	458/21092	0.015501344	0.378545307	0.360072046	Atp6v1g2/Kcnk9/Slc4a4/Hcn2/Kcnk2/Cyc1/Kcnh3/Kcnj2/Asic1	9
GO:1903828	negative regulation of cellular protein localization	114/21092	0.015660773	0.378545307	0.360072046	Dclk3/Mrap2/Apod/Lypd1	4
GO:1903077	negative regulation of protein localization to plasma membrane	23/21092	0.015781111	0.378545307	0.360072046	Mrap2/Lypd1	2
GO:0006801	superoxide metabolic process	63/21092	0.015968412	0.378545307	0.360072046	Cyb5r4/Aatf/Gnai2	3
GO:0030330	DNA damage response, signal transduction by p53 class mediator	63/21092	0.015968412	0.378545307	0.360072046	Pcbp4/Myo6/E2f7	3
GO:0042440	pigment metabolic process	63/21092	0.015968412	0.378545307	0.360072046	Cyb5r4/Alas1/Slc7a11	3
GO:0043113	receptor clustering	63/21092	0.015968412	0.378545307	0.360072046	Magi2/Slc7a11/Dlg3	3
GO:0031346	positive regulation of cell projection organization	462/21092	0.016310554	0.379822529	0.361286939	Twf2/Mns1/Zfp804a/Magi2/Ntrk2/Metrn/Efemp1/Ppp2r5b/Tmem30a	9
GO:0006470	protein dephosphorylation	242/21092	0.016599944	0.379822529	0.361286939	Ppm1m/Gnai2/Magi2/Ppm1j/Dusp7/Ppp2r5b	6

GO:0010640	regulation of platelet-derived growth factor receptor signaling pathway	24/21092	0.017121859	0.379822529	0.361286939	Apod/Snca	2
GO:0032928	regulation of superoxide anion generation	24/21092	0.017121859	0.379822529	0.361286939	Aatf/Gnai2	2
GO:0035384	thioester biosynthetic process	24/21092	0.017121859	0.379822529	0.361286939	Snca/Dlat	2
GO:0071616	acyl-CoA biosynthetic process	24/21092	0.017121859	0.379822529	0.361286939	Snca/Dlat	2
GO:0098810	neurotransmitter reuptake	24/21092	0.017121859	0.379822529	0.361286939	Snca/Slc6a5	2
GO:0051193	regulation of cofactor metabolic process	65/21092	0.017352887	0.381448013	0.362833097	Me1/Snca/Slc7a11	3
GO:0019933	cAMP-mediated signaling	179/21092	0.017689275	0.385339341	0.366534526	Gpr62/Pde10a/Mrap2/Gnai2/Cgas	5
GO:0099010	modification of postsynaptic structure	25/21092	0.01850928	0.38858238	0.369619302	Filip1/Camkv	2
GO:0120033	negative regulation of plasma membrane bounded cell projection assembly	25/21092	0.01850928	0.38858238	0.369619302	Slit2/Cdk10	2
GO:1902473	regulation of protein localization to synapse	25/21092	0.01850928	0.38858238	0.369619302	Magi2/Gpc6	2
GO:1904376	negative regulation of protein localization to cell periphery	25/21092	0.01850928	0.38858238	0.369619302	Mrap2/Lypd1	2
GO:0006029	proteoglycan metabolic process	67/21092	0.018802373	0.38858238	0.369619302	Pxylp1/Dcn/B3gat2	3
GO:0014068	positive regulation of phosphatidylinositol 3-kinase signaling	67/21092	0.018802373	0.38858238	0.369619302	Dcn/Agap2/Ntrk2	3
GO:0051668	localization within membrane	183/21092	0.019265243	0.394676759	0.375416272	Myo6/Magi2/Slc7a11/Gpc6/Dlg3	5
GO:0048168	regulation of neuronal synaptic plasticity	68/21092	0.019551554	0.394676759	0.375416272	Grin2a/Rasgrf1/Snca	3
GO:0010921	regulation of phosphatase activity	122/21092	0.019586936	0.394676759	0.375416272	Gnai2/Magi2/Dlg3/Sfi1	4
GO:0030212	hyaluronan metabolic process	26/21092	0.019942505	0.395253915	0.375965263	Itih5/Cemip	2
GO:0045332	phospholipid translocation	26/21092	0.019942505	0.395253915	0.375965263	Atp8a1/Tmem30a	2
GO:0031589	cell-substrate adhesion	325/21092	0.020133669	0.395798462	0.376483235	Rpl29/Tdgf1/Apod/Sned1/Spp1/Ecm2/Vit	7
GO:0010811	positive regulation of cell-substrate adhesion	125/21092	0.021202155	0.402000363	0.382382479	Tdgf1/Spp1/Ecm2/Vit	4

GO:0006026	aminoglycan catabolic process	27/21092	0.021420677	0.402000363	0.382382479	Chil5/Cemip	2
GO:0034204	lipid translocation	27/21092	0.021420677	0.402000363	0.382382479	Atp8a1/Tmem30a	2
GO:1902932	positive regulation of alcohol biosynthetic process	27/21092	0.021420677	0.402000363	0.382382479	Plcd1/Snca	2
GO:0007631	feeding behavior	126/21092	0.021758176	0.402000363	0.382382479	Hcrtr2/Mrap2/Ntrk2/Oprd1	4
GO:0050433	regulation of catecholamine secretion	71/21092	0.021897022	0.402000363	0.382382479	Plcd1/Syt12/Snca	3
GO:0097120	receptor localization to synapse	71/21092	0.021897022	0.402000363	0.382382479	Magi2/Gpc6/Dlg3	3
GO:0042177	negative regulation of protein catabolic process	127/21092	0.022323059	0.402000363	0.382382479	Grin2a/Agap2/Snca/Hfe	4
GO:0097553	calcium ion transmembrane import into cytosol	127/21092	0.022323059	0.402000363	0.382382479	Grin2a/Snca/Ibtk/Cemip	4
GO:0010959	regulation of metal ion transport	410/21092	0.022737662	0.402000363	0.382382479	Gnb5/Trf/Gnai2/Snca/Hfe/Cemip/Kcnj2/Oprd1	8
GO:0003413	chondrocyte differentiation involved in endochondral bone morphogenesis	28/21092	0.022942949	0.402000363	0.382382479	Poc1a/Vit	2
GO:0045780	positive regulation of bone resorption	28/21092	0.022942949	0.402000363	0.382382479	Trf/Spp1	2
GO:0046852	positive regulation of bone remodeling	28/21092	0.022942949	0.402000363	0.382382479	Trf/Spp1	2
GO:0089718	amino acid import across plasma membrane	28/21092	0.022942949	0.402000363	0.382382479	Slc6a5/Slc7a11	2
GO:1902668	negative regulation of axon guidance	28/21092	0.022942949	0.402000363	0.382382479	Slit2/Sema6b	2
GO:0097479	synaptic vesicle localization	192/21092	0.023141781	0.402567096	0.382921555	Syt12/Myo6/Snca/Magi2/Dgki	5
GO:0071804	cellular potassium ion transport	193/21092	0.023601378	0.40313958	0.383466102	Kcnk9/Hcn2/Kcnk2/Kcnh3/Kcnj2	5
GO:0071805	potassium ion transmembrane transport	193/21092	0.023601378	0.40313958	0.383466102	Kcnk9/Hcn2/Kcnk2/Kcnh3/Kcnj2	5
GO:0055076	transition metal ion homeostasis	130/21092	0.024071178	0.40313958	0.383466102	Trf/Atp2c1/Heph/Hfe	4
GO:0003333	amino acid transmembrane transport	74/21092	0.024389498	0.40313958	0.383466102	Slc25a29/Slc6a5/Slc7a11	3
GO:0032272	negative regulation of protein polymerization	74/21092	0.024389498	0.40313958	0.383466102	Twf2/Snca/Slit2	3
GO:0050432	catecholamine secretion	74/21092	0.024389498	0.40313958	0.383466102	Plcd1/Syt12/Snca	3

GO:0042168	heme metabolic process	29/21092	0.024508486	0.40313958	0.383466102	Cyb5r4/Alas1	2
GO:0051589	negative regulation of neurotransmitter transport	29/21092	0.024508486	0.40313958	0.383466102	Snca/Asic1	2
GO:0051881	regulation of mitochondrial membrane potential	75/21092	0.025252981	0.412579103	0.392444969	Dcn/Tusc2/Oprd1	3
GO:0043112	receptor metabolic process	198/21092	0.025987788	0.417990687	0.397592465	Myo6/Snca/Magi2/Pik3r4/Pheta1	5
GO:0010038	response to metal ion	269/21092	0.026268205	0.417990687	0.397592465	Trf/Grin2a/Plcd1/Syt12/Snca/Hfe	6
GO:0090287	regulation of cellular response to growth factor stimulus	269/21092	0.026268205	0.417990687	0.397592465	Tdgf1/Dcn/Tmem108/Slit2/Bcl9l/Ppp2r5b	6
GO:1904375	regulation of protein localization to cell periphery	134/21092	0.0265278	0.417990687	0.397592465	Mrap2/Magi2/Gpc6/Lypd1	4
GO:0044272	sulfur compound biosynthetic process	77/21092	0.027028868	0.417990687	0.397592465	Snca/Slc7a11/Dlat	3
GO:0032958	inositol phosphate biosynthetic process	31/21092	0.027766067	0.417990687	0.397592465	Plcd1/Snca	2
GO:0045920	negative regulation of exocytosis	31/21092	0.027766067	0.417990687	0.397592465	Gnai2/Snca	2
GO:0099563	modification of synaptic structure	31/21092	0.027766067	0.417990687	0.397592465	Filip1/Camkv	2
GO:0099633	protein localization to postsynaptic specialization membrane	31/21092	0.027766067	0.417990687	0.397592465	Magi2/Gpc6	2
GO:0099645	neurotransmitter receptor localization to postsynaptic specialization membrane	31/21092	0.027766067	0.417990687	0.397592465	Magi2/Gpc6	2
GO:1905476	negative regulation of protein localization to membrane	31/21092	0.027766067	0.417990687	0.397592465	Mrap2/Lypd1	2
GO:0048167	regulation of synaptic plasticity	348/21092	0.027881899	0.417990687	0.397592465	Grin2a/Rasgrf1/Syt12/Myo6/Snca/Dgki/Ntrk2	7
GO:0010923	negative regulation of phosphatase activity	78/21092	0.027941239	0.417990687	0.397592465	Gnai2/Dlg3/Sfi1	3
GO:0050770	regulation of axonogenesis	202/21092	0.028004339	0.417990687	0.397592465	Twf2/Ntrk2/Metrn/Slit2/Sema6b	5
GO:0043090	amino acid import	32/21092	0.029456493	0.434303664	0.413109358	Slc6a5/Slc7a11	2
GO:0048011	neurotrophin TRK receptor signaling pathway	32/21092	0.029456493	0.434303664	0.413109358	Tmem108/Ppp2r5b	2

GO:0098659	inorganic cation import across plasma membrane	81/21092	0.030775784	0.438771595	0.417359251	Hcn2/Hfe/Kcnj2	3
GO:0099587	inorganic ion import across plasma membrane	81/21092	0.030775784	0.438771595	0.417359251	Hcn2/Hfe/Kcnj2	3
GO:0031333	negative regulation of protein complex assembly	141/21092	0.031176982	0.438771595	0.417359251	Twf2/Snca/Slit2/Oprd1	4
GO:0090288	negative regulation of cellular response to growth factor stimulus	141/21092	0.031176982	0.438771595	0.417359251	Tdgf1/Dcn/Slit2/Bcl9l	4
GO:0032733	positive regulation of interleukin-10 production	33/21092	0.03118695	0.438771595	0.417359251	Il20rb/Tusc2	2
GO:0042554	superoxide anion generation	33/21092	0.03118695	0.438771595	0.417359251	Aatf/Gnai2	2
GO:1900181	negative regulation of protein localization to nucleus	33/21092	0.03118695	0.438771595	0.417359251	Dclk3/Apod	2
GO:0010810	regulation of cell-substrate adhesion	208/21092	0.031211214	0.438771595	0.417359251	Tdgf1/Apod/Spp1/Ecm2/Vit	5
GO:0010976	positive regulation of neuron projection development	357/21092	0.031400012	0.438874154	0.417456805	Twf2/Zfp804a/Magi2/Ntrk2/Metrn/Ppp2r5b/Tmem30a	7
GO:0007611	learning or memory	283/21092	0.032509909	0.445191004	0.423465388	Grin2a/Dgki/Ntrk2/Slc7a11/Atp8a1/Asic1	6
GO:0019935	cyclic-nucleotide-mediated signaling	211/21092	0.032897621	0.445191004	0.423465388	Gpr62/Pde10a/Mrap2/Gnai2/Cgas	5
GO:0007271	synaptic transmission, cholinergic	34/21092	0.032956654	0.445191004	0.423465388	Lama2/Lypd1	2
GO:0010737	protein kinase A signaling	34/21092	0.032956654	0.445191004	0.423465388	Pde10a/Lcp1	2
GO:0090322	regulation of superoxide metabolic process	34/21092	0.032956654	0.445191004	0.423465388	Aatf/Gnai2	2
GO:0097366	response to bronchodilator	34/21092	0.032956654	0.445191004	0.423465388	Grin2a/Asic1	2
GO:0010591	regulation of lamellipodium assembly	35/21092	0.034764833	0.459351728	0.43693506	Twf2/Slit2	2
GO:0033866	nucleoside bisphosphate biosynthetic process	35/21092	0.034764833	0.459351728	0.43693506	Snca/Dlat	2
GO:0034030	ribonucleoside bisphosphate biosynthetic process	35/21092	0.034764833	0.459351728	0.43693506	Snca/Dlat	2
GO:0034033	purine nucleoside bisphosphate biosynthetic process	35/21092	0.034764833	0.459351728	0.43693506	Snca/Dlat	2
GO:0042490	mechanoreceptor differentiation	86/21092	0.035822894	0.460779532	0.438293186	Myo6/Cthrc1/Ntrk2	3

GO:0060402	calcium ion transport into cytosol	148/21092	0.036276764	0.460779532	0.438293186	Grin2a/Snca/Ibtk/Cemip	4
GO:0071241	cellular response to inorganic substance	217/21092	0.036438489	0.460779532	0.438293186	Trf/Grin2a/Syt12/Snca/Hfe	5
GO:0003417	growth plate cartilage development	36/21092	0.036610724	0.460779532	0.438293186	Poc1a/Vit	2
GO:0006739	NADP metabolic process	36/21092	0.036610724	0.460779532	0.438293186	Me1/Cyb5r4	2
GO:0033238	regulation of cellular amine metabolic process	36/21092	0.036610724	0.460779532	0.438293186	Snca/Slc7a11	2
GO:0050919	negative chemotaxis	36/21092	0.036610724	0.460779532	0.438293186	Slit2/Sema6b	2
GO:0051181	cofactor transport	36/21092	0.036610724	0.460779532	0.438293186	Slc25a29/Slc7a11	2
GO:0072524	pyridine-containing compound metabolic process	149/21092	0.037042323	0.460779532	0.438293186	Me1/Cyb5r4/Pnpo/Dlat	4
GO:1901615	organic hydroxy compound metabolic process	453/21092	0.037758467	0.460779532	0.438293186	Grin2a/Pnpo/Plcd1/Snca/Sncb/Cyp11a1 /Slc7a11/Haghl	8
GO:0042737	drug catabolic process	150/21092	0.037817159	0.460779532	0.438293186	Aass/Snca/Chil5/Ctsh	4
GO:0035418	protein localization to synapse	88/21092	0.037953804	0.460779532	0.438293186	Grin2a/Magi2/Gpc6	3
GO:0055072	iron ion homeostasis	88/21092	0.037953804	0.460779532	0.438293186	Trf/Heph/Hfe	3
GO:0006778	porphyrin-containing compound metabolic process	37/21092	0.038493575	0.460779532	0.438293186	Cyb5r4/Alas1	2
GO:0009311	oligosaccharide metabolic process	37/21092	0.038493575	0.460779532	0.438293186	B3galt1/Man2c1	2
GO:0032620	interleukin-17 production	37/21092	0.038493575	0.460779532	0.438293186	Tusc2/Rorc	2
GO:0048169	regulation of long-term neuronal synaptic plasticity	37/21092	0.038493575	0.460779532	0.438293186	Grin2a/Snca	2
GO:0048846	axon extension involved in axon guidance	37/21092	0.038493575	0.460779532	0.438293186	Slit2/Sema6b	2
GO:1902284	neuron projection extension involved in neuron projection guidance	37/21092	0.038493575	0.460779532	0.438293186	Slit2/Sema6b	2
GO:0019318	hexose metabolic process	221/21092	0.03892471	0.462775342	0.440191599	Apod/Glb1/Dlat/Man2c1/Rorc	5
GO:0051937	catecholamine transport	89/21092	0.039043081	0.462775342	0.440191599	Plcd1/Syt12/Snca	3

GO:0042770	signal transduction in response to DNA damage	90/21092	0.040148167	0.47355253	0.450442853	Pcbp4/Myo6/E2f7	3
GO:0002686	negative regulation of leukocyte migration	38/21092	0.040412644	0.474358121	0.45120913	Apod/Slit2	2
GO:0035305	negative regulation of dephosphorylation	91/21092	0.041269006	0.482069834	0.458544507	Gnai2/Dlg3/Sfi1	3
GO:0001881	receptor recycling	39/21092	0.042367197	0.484971177	0.461304263	Snca/Pheta1	2
GO:0002823	negative regulation of adaptive immune response based on somatic recombination of immune receptors built from immunoglobulin superfamily domains	39/21092	0.042367197	0.484971177	0.461304263	Il20rb/Hfe	2
GO:0019934	cGMP-mediated signaling	39/21092	0.042367197	0.484971177	0.461304263	Pde10a/Cgas	2
GO:0045807	positive regulation of endocytosis	157/21092	0.043501024	0.484971177	0.461304263	Trf/Snca/Magi2/Hfe	4
GO:0051188	cofactor biosynthetic process	228/21092	0.043519857	0.484971177	0.461304263	Pnpo/Snca/Alas1/Slc7a11/Dlat	5
GO:0033674	positive regulation of kinase activity	467/21092	0.043822185	0.484971177	0.461304263	Tdgf1/Trf/Map3k19/Agap2/Snca/Pik3r4/Cemip/Dlg3	8
GO:1990573	potassium ion import across plasma membrane	40/21092	0.044356511	0.484971177	0.461304263	Hcn2/Kcnj2	2
GO:0009100	glycoprotein metabolic process	308/21092	0.045902873	0.484971177	0.461304263	Pxylp1/Necab1/Dcn/B3gat2/Aatf/B3galt1	6
GO:0044282	small molecule catabolic process	308/21092	0.045902873	0.484971177	0.461304263	Acad11/Aass/Glb1/Cemip/Ddo/Haghl	6
GO:0007200	phospholipase C-activating G protein-coupled receptor signaling pathway	95/21092	0.045908647	0.484971177	0.461304263	Hcrtr2/Plcd1/Oprd1	3
GO:0060359	response to ammonium ion	95/21092	0.045908647	0.484971177	0.461304263	Gnai2/Snca/Lypd1	3
GO:0060401	cytosolic calcium ion transport	160/21092	0.04607626	0.484971177	0.461304263	Grin2a/Snca/Ibtk/Cemip	4
GO:0034105	positive regulation of tissue remodeling	41/21092	0.046379872	0.484971177	0.461304263	Trf/Spp1	2
GO:0051281	positive regulation of release of sequestered calcium ion into cytosol	41/21092	0.046379872	0.484971177	0.461304263	Snca/Cemip	2
GO:0043648	dicarboxylic acid metabolic process	96/21092	0.047107301	0.484971177	0.461304263	Me1/Slc7a11/Ddo	3
GO:0006813	potassium ion transport	234/21092	0.047707806	0.484971177	0.461304263	Kcnk9/Hcn2/Kcnk2/Kcnh3/Kcnj2	5

GO:1901215	negative regulation of neuron death	234/21092	0.047707806	0.484971177	0.461304263	Agap2/Snca/Sncb/Ntrk2/Slc7a11	5
GO:0006732	coenzyme metabolic process	311/21092	0.047709981	0.484971177	0.461304263	Me1/Cyb5r4/Pnpo/Snca/Folh1/Dlat	6
GO:0051656	establishment of organelle localization	476/21092	0.048042656	0.484971177	0.461304263	Mlh1/Myo5c/1190002N15Rik/Syt12/Myo6/Snca/Dgki/Dctn1	8
GO:0006140	regulation of nucleotide metabolic process	97/21092	0.048321314	0.484971177	0.461304263	Guca1b/Me1/Snca	3
GO:0002820	negative regulation of adaptive immune response	42/21092	0.048436576	0.484971177	0.461304263	Il20rb/Hfe	2
GO:0009066	aspartate family amino acid metabolic process	42/21092	0.048436576	0.484971177	0.461304263	Aass/Ddo	2
GO:0031644	regulation of neurological system process	163/21092	0.048734935	0.484971177	0.461304263	Trf/Grin2a/Tmem108/Oprd1	4
GO:0035303	regulation of dephosphorylation	163/21092	0.048734935	0.484971177	0.461304263	Gnai2/Magi2/Dlg3/Sfi1	4
GO:0051186	cofactor metabolic process	478/21092	0.049015382	0.484971177	0.461304263	Me1/Cyb5r4/Pnpo/Snca/Alas1/Slc7a11/Folh1/Dlat	8
GO:0050772	positive regulation of axonogenesis	98/21092	0.049550611	0.484971177	0.461304263	Twf2/Ntrk2/Metrn	3

Supp. Table S14. List of Biological Processes (BP) at FDR 5% - hippocampus

GO ID	Description	BgRatio	pvalue	p.adjust	qvalue	geneID	Count
GO:0031282	regulation of guanylate cyclase activity	10/21092	7.96591E-06	0.012386993	0.011663772	Guca1b/Guca1a/Nos1	3
GO:0006140	regulation of nucleotide metabolic process	97/21092	5.08445E-05	0.03953156	0.03722349	Guca1b/Me1/Guca1a/Nos1/Cox7a2	5
GO:1900542	regulation of purine nucleotide metabolic process	93/21092	0.000596112	0.140031904	0.13185607	Guca1b/Guca1a/Nos1/Cox7a2	4
GO:0031279	regulation of cyclase activity	41/21092	0.000645175	0.140031904	0.13185607	Guca1b/Guca1a/Nos1	3
GO:0010753	positive regulation of cGMP-mediated signaling	10/21092	0.00074076	0.140031904	0.13185607	Cgas/Guca1a	2
GO:0051339	regulation of lyase activity	43/21092	0.000742487	0.140031904	0.13185607	Guca1b/Guca1a/Nos1	3
GO:0007128	meiotic prophase I	11/21092	0.000902946	0.140031904	0.13185607	Mlh1/Piwil2	2
GO:0051324	prophase	11/21092	0.000902946	0.140031904	0.13185607	Mlh1/Piwil2	2
GO:0061448	connective tissue development	274/21092	0.000953328	0.140031904	0.13185607	Poc1a/Adamts7/Col12a1/Arid5b/Sox6/Hes5	6

GO:0000279	M phase	12/21092	0.001080632	0.140031904	0.13185607	Mlh1/Piwil2	2
GO:0098762	meiotic cell cycle phase	12/21092	0.001080632	0.140031904	0.13185607	Mlh1/Piwil2	2
GO:0098764	meiosis I cell cycle phase	12/21092	0.001080632	0.140031904	0.13185607	Mlh1/Piwil2	2
GO:0045604	regulation of epidermal cell differentiation	52/21092	0.00129456	0.15112002	0.1422968	Cd109/Ptch2/Hes5	3
GO:0002062	chondrocyte differentiation	116/21092	0.001360566	0.15112002	0.1422968	Poc1a/Adamts7/Col12a1/Sox6	4
GO:0021781	glial cell fate commitment	14/21092	0.001481992	0.153633144	0.144663194	Sox6/Hes5	2
GO:0051216	cartilage development	205/21092	0.001600836	0.155581213	0.146497524	Poc1a/Adamts7/Col12a1/Sox6/Hes5	5
GO:0010752	regulation of cGMP-mediated signaling	18/21092	0.002465137	0.198716323	0.187114169	Cgas/Guca1a	2
GO:0030808	regulation of nucleotide biosynthetic process	66/21092	0.002571542	0.198716323	0.187114169	Guca1b/Guca1a/Nos1	3
GO:1900371	regulation of purine nucleotide biosynthetic process	66/21092	0.002571542	0.198716323	0.187114169	Guca1b/Guca1a/Nos1	3
GO:0062012	regulation of small molecule metabolic process	340/21092	0.002836471	0.198716323	0.187114169	Guca1b/Me1/Elovl5/Guca1a/Nos1/Cox 7a2	6
GO:0022403	cell cycle phase	20/21092	0.003044935	0.198716323	0.187114169	Mlh1/Piwil2	2
GO:0031281	positive regulation of cyclase activity	20/21092	0.003044935	0.198716323	0.187114169	Guca1a/Nos1	2
GO:0051349	positive regulation of lyase activity	20/21092	0.003044935	0.198716323	0.187114169	Guca1a/Nos1	2
GO:0007601	visual perception	145/21092	0.003067004	0.198716323	0.187114169	Guca1b/Bfsp2/Wfs1/Guca1a	4
GO:0003433	chondrocyte development involved in endochondral bone morphogenesis	21/21092	0.003356461	0.202224923	0.190417917	Poc1a/Col12a1	2
GO:0050953	sensory perception of light stimulus	149/21092	0.003381253	0.202224923	0.190417917	Guca1b/Bfsp2/Wfs1/Guca1a	4
GO:0003418	growth plate cartilage chondrocyte differentiation	22/21092	0.003682244	0.212069962	0.199688148	Poc1a/Col12a1	2
GO:0045682	regulation of epidermis development	78/21092	0.004126127	0.229147391	0.215768503	Cd109/Ptch2/Hes5	3
GO:1903035	negative regulation of response to wounding	83/21092	0.004910303	0.263293819	0.247921275	Cd109/Klk8/Tmprss6	3
GO:0001822	kidney development	274/21092	0.005544714	0.287401017	0.270620961	Pygo1/Wfs1/Aph1c/Arid5b/Hes5	5

GO:0003413	chondrocyte differentiation involved in endochondral bone morphogenesis	28/21092	0.005929656	0.28974529	0.272828363	Poc1a/Col12a1	2
GO:0000041	transition metal ion transport	89/21092	0.005962604	0.28974529	0.272828363	Atp2c1/Heph/Nectin1	3
GO:0035066	positive regulation of histone acetylation	29/21092	0.006351912	0.299309808	0.281834451	Nos1/Piwil2	2
GO:2000272	negative regulation of signaling receptor activity	30/21092	0.006787485	0.310427604	0.292303129	Crhbp/Socs5	2
GO:0046916	cellular transition metal ion homeostasis	95/21092	0.00714002	0.31256615	0.294316814	Tmprss6/Atp2c1/Heph	3
GO:0007602	phototransduction	31/21092	0.007236258	0.31256615	0.294316814	Guca1b/Guca1a	2
GO:0072001	renal system development	296/21092	0.007626354	0.317723617	0.299173161	Pygo1/Wfs1/Aph1c/Arid5b/Hes5	5
GO:0030810	positive regulation of nucleotide biosynthetic process	33/21092	0.008172955	0.317723617	0.299173161	Guca1a/Nos1	2
GO:1900373	positive regulation of purine nucleotide biosynthetic process	33/21092	0.008172955	0.317723617	0.299173161	Guca1a/Nos1	2
GO:2000758	positive regulation of peptidyl-lysine acetylation	33/21092	0.008172955	0.317723617	0.299173161	Nos1/Piwil2	2
GO:0006826	iron ion transport	35/21092	0.009161101	0.334296956	0.314778857	Heph/Nectin1	2
GO:0006986	response to unfolded protein	106/21092	0.009634673	0.334296956	0.314778857	Wfs1/Hspb1/Hspa1b	3
GO:0003417	growth plate cartilage development	36/21092	0.009674188	0.334296956	0.314778857	Poc1a/Col12a1	2
GO:0006739	NADP metabolic process	36/21092	0.009674188	0.334296956	0.314778857	Me1/Cyb5r4	2
GO:0043950	positive regulation of cAMP-mediated signaling	36/21092	0.009674188	0.334296956	0.314778857	Cgas/Nos1	2
GO:0048821	erythrocyte development	37/21092	0.010199805	0.344797769	0.324666574	Tmod3/Sox6	2
GO:0032102	negative regulation of response to external stimulus	323/21092	0.01085927	0.359280116	0.338303362	Cd109/Klk8/Nt5e/Tmprss6/Socs5	5
GO:0019934	cGMP-mediated signaling	39/21092	0.011288189	0.364902962	0.343597915	Cgas/Guca1a	2
GO:0042326	negative regulation of phosphorylation	461/21092	0.012038113	0.364902962	0.343597915	Cd109/Nos1/Socs5/Nprl2/Hspb1/Ibtk	6
GO:0051701	interaction with host	116/21092	0.012291784	0.364902962	0.343597915	Tusc2/Trim21/Nectin1	3
GO:0042220	response to cocaine	42/21092	0.013012015	0.364902962	0.343597915	Crhbp/Nos1	2

GO:0045981	positive regulation of nucleotide metabolic process	42/21092	0.013012015	0.364902962	0.343597915	Guca1a/Nos1	2
GO:1900544	positive regulation of purine nucleotide metabolic process	42/21092	0.013012015	0.364902962	0.343597915	Guca1a/Nos1	2
GO:1901985	positive regulation of protein acetylation	42/21092	0.013012015	0.364902962	0.343597915	Nos1/Piwil2	2
GO:0001655	urogenital system development	339/21092	0.013163049	0.364902962	0.343597915	Pygo1/Wfs1/Aph1c/Arid5b/Hes5	5
GO:0001709	cell fate determination	43/21092	0.013610528	0.364902962	0.343597915	Ptch2/Hes5	2
GO:0003416	endochondral bone growth	43/21092	0.013610528	0.364902962	0.343597915	Poc1a/Col12a1	2
GO:0043616	keratinocyte proliferation	43/21092	0.013610528	0.364902962	0.343597915	Cd109/Klk8	2
GO:0002063	chondrocyte development	44/21092	0.014220818	0.372266453	0.350531485	Poc1a/Col12a1	2
GO:0072522	purine-containing compound biosynthetic process	227/21092	0.014511589	0.372266453	0.350531485	Guca1b/Nt5e/Guca1a/Nos1	4
GO:0044848	biological phase	45/21092	0.014842778	0.372266453	0.350531485	Mlh1/Piwil2	2
GO:0098868	bone growth	45/21092	0.014842778	0.372266453	0.350531485	Poc1a/Col12a1	2
GO:0030218	erythrocyte differentiation	126/21092	0.015329422	0.378369072	0.3562778	Tmod3/Heph/Sox6	3
GO:0035966	response to topologically incorrect protein	127/21092	0.015654387	0.380352676	0.35814559	Wfs1/Hspb1/Hspa1b	3
GO:0055076	transition metal ion homeostasis	130/21092	0.016652558	0.389337206	0.366605554	Tmprss6/Atp2c1/Heph	3
GO:0031641	regulation of myelination	48/21092	0.016777644	0.389337206	0.366605554	Klk8/Hes5	2
GO:0032330	regulation of chondrocyte differentiation	48/21092	0.016777644	0.389337206	0.366605554	Adamts7/Sox6	2
GO:0060351	cartilage development involved in endochondral bone morphogenesis	51/21092	0.01881383	0.389337206	0.366605554	Poc1a/Col12a1	2
GO:0034101	erythrocyte homeostasis	137/21092	0.019117914	0.389337206	0.366605554	Tmod3/Heph/Sox6	3
GO:0009791	post-embryonic development	138/21092	0.01948573	0.389337206	0.366605554	Pygo1/Arid5b/Sox6	3
GO:0016573	histone acetylation	138/21092	0.01948573	0.389337206	0.366605554	Morf4l1/Nos1/Piwil2	3
GO:0009583	detection of light stimulus	52/21092	0.019514601	0.389337206	0.366605554	Guca1b/Guca1a	2
GO:0006879	cellular iron ion homeostasis	54/21092	0.020948606	0.389337206	0.366605554	Tmprss6/Heph	2

GO:0035065	regulation of histone acetylation	54/21092	0.020948606	0.389337206	0.366605554	Nos1/Piwil2	2
GO:0046718	viral entry into host cell	54/21092	0.020948606	0.389337206	0.366605554	Trim21/Nectin1	2
GO:0061077	chaperone-mediated protein folding	54/21092	0.020948606	0.389337206	0.366605554	Hspb1/Hspa1b	2
GO:0007224	smoothened signaling pathway	143/21092	0.021383537	0.389337206	0.366605554	Ptch2/Scube1/Hes5	3
GO:0018393	internal peptidyl-lysine acetylation	143/21092	0.021383537	0.389337206	0.366605554	Morf4l1/Nos1/Piwil2	3
GO:0006475	internal protein amino acid acetylation	146/21092	0.022569246	0.389337206	0.366605554	Morf4l1/Nos1/Piwil2	3
GO:0030856	regulation of epithelial cell differentiation	146/21092	0.022569246	0.389337206	0.366605554	Cd109/Ptch2/Hes5	3
GO:0062013	positive regulation of small molecule metabolic process	146/21092	0.022569246	0.389337206	0.366605554	Elovl5/Guca1a/Nos1	3
GO:0006457	protein folding	147/21092	0.022972324	0.389337206	0.366605554	Ppib/Hspb1/Hspa1b	3
GO:0030260	entry into host cell	57/21092	0.02317929	0.389337206	0.366605554	Trim21/Nectin1	2
GO:0044409	entry into host	57/21092	0.02317929	0.389337206	0.366605554	Trim21/Nectin1	2
GO:0051806	entry into cell of other organism involved in symbiotic interaction	57/21092	0.02317929	0.389337206	0.366605554	Trim21/Nectin1	2
GO:0051828	entry into other organism involved in symbiotic interaction	57/21092	0.02317929	0.389337206	0.366605554	Trim21/Nectin1	2
GO:0072347	response to anesthetic	57/21092	0.02317929	0.389337206	0.366605554	Crhbp/Nos1	2
GO:1903902	positive regulation of viral life cycle	57/21092	0.02317929	0.389337206	0.366605554	Ppib/Trim21	2
GO:0018394	peptidyl-lysine acetylation	154/21092	0.025903624	0.389337206	0.366605554	Morf4l1/Nos1/Piwil2	3
GO:0051926	negative regulation of calcium ion transport	61/21092	0.026298186	0.389337206	0.366605554	Gnb5/Nos1	2
GO:0070206	protein trimerization	61/21092	0.026298186	0.389337206	0.366605554	Trim21/Col6a4	2
GO:0006816	calcium ion transport	409/21092	0.027100618	0.389337206	0.366605554	Gnb5/Wfs1/Nos1/Atp2c1/Ibtk	5
GO:2000736	regulation of stem cell differentiation	62/21092	0.027103103	0.389337206	0.366605554	Sox6/Hes5	2
GO:2000756	regulation of peptidyl-lysine acetylation	63/21092	0.027917909	0.389337206	0.366605554	Nos1/Piwil2	2
GO:0001933	negative regulation of protein phosphorylation	414/21092	0.028355965	0.389337206	0.366605554	Cd109/Nos1/Socs5/Hspb1/Ibtk	5

GO:0043949	regulation of cAMP-mediated signaling	64/21092	0.02874251	0.389337206	0.366605554	Cgas/Nos1	2
GO:1901264	carbohydrate derivative transport	64/21092	0.02874251	0.389337206	0.366605554	Slc17a5/Slc35b2	2
GO:0061035	regulation of cartilage development	66/21092	0.030420729	0.389337206	0.366605554	Adamts7/Sox6	2
GO:0090278	negative regulation of peptide hormone secretion	66/21092	0.030420729	0.389337206	0.366605554	Crhbp/Nos1	2
GO:1903034	regulation of response to wounding	165/21092	0.030897152	0.389337206	0.366605554	Cd109/Klk8/Tmprss6	3
GO:0061045	negative regulation of wound healing	67/21092	0.031274163	0.389337206	0.366605554	Cd109/Tmprss6	2
GO:0007051	spindle organization	166/21092	0.031374485	0.389337206	0.366605554	Poc1a/Mlh1/Hspa1b	3
GO:0006163	purine nucleotide metabolic process	426/21092	0.031518336	0.389337206	0.366605554	Guca1b/Nt5e/Guca1a/Nos1/Cox7a2	5
GO:0002262	myeloid cell homeostasis	171/21092	0.033819296	0.389337206	0.366605554	Tmod3/Heph/Sox6	3
GO:0002088	lens development in camera-type eye	70/21092	0.033890674	0.389337206	0.366605554	Bfsp2/Nectin1	2
GO:0043627	response to estrogen	72/21092	0.035680958	0.389337206	0.366605554	Crhbp/Nos1	2
GO:0051851	modification by host of symbiont morphology or physiology	72/21092	0.035680958	0.389337206	0.366605554	Ppib/Tusc2	2
GO:0060271	cilium assembly	301/21092	0.03599202	0.389337206	0.366605554	Poc1a/Mns1/Gmnc/Ulk4	4
GO:0071772	response to BMP	176/21092	0.036360604	0.389337206	0.366605554	Adamts7/Tmprss6/Hes5	3
GO:0071773	cellular response to BMP stimulus	176/21092	0.036360604	0.389337206	0.366605554	Adamts7/Tmprss6/Hes5	3
GO:0060350	endochondral bone morphogenesis	73/21092	0.036589618	0.389337206	0.366605554	Poc1a/Col12a1	2
GO:0034620	cellular response to unfolded protein	74/21092	0.037507172	0.389337206	0.366605554	Wfs1/Hspa1b	2
GO:1901983	regulation of protein acetylation	74/21092	0.037507172	0.389337206	0.366605554	Nos1/Piwil2	2
GO:0061515	myeloid cell development	75/21092	0.038433534	0.389337206	0.366605554	Tmod3/Sox6	2
GO:0051702	interaction with symbiont	77/21092	0.040312336	0.389337206	0.366605554	Ppib/Tusc2	2
GO:0002118	aggressive behavior	10/21092	0.040499085	0.389337206	0.366605554	Crhbp	1
GO:0002934	desmosome organization	10/21092	0.040499085	0.389337206	0.366605554	Nectin1	1
GO:0003091	renal water homeostasis	10/21092	0.040499085	0.389337206	0.366605554	Wfs1	1

GO:0006995	cellular response to nitrogen starvation	10/21092	0.040499085	0.389337206	0.366605554	Nprl2	1
GO:0007220	Notch receptor processing	10/21092	0.040499085	0.389337206	0.366605554	Aph1c	1
GO:0010825	positive regulation of centrosome duplication	10/21092	0.040499085	0.389337206	0.366605554	Poc1a	1
GO:0043562	cellular response to nitrogen levels	10/21092	0.040499085	0.389337206	0.366605554	Nprl2	1
GO:0044154	histone H3-K14 acetylation	10/21092	0.040499085	0.389337206	0.366605554	Piwil2	1
GO:0045607	regulation of inner ear auditory receptor cell differentiation	10/21092	0.040499085	0.389337206	0.366605554	Hes5	1
GO:0045631	regulation of mechanoreceptor differentiation	10/21092	0.040499085	0.389337206	0.366605554	Hes5	1
GO:0046085	adenosine metabolic process	10/21092	0.040499085	0.389337206	0.366605554	Nt5e	1
GO:0048149	behavioral response to ethanol	10/21092	0.040499085	0.389337206	0.366605554	Crhbp	1
GO:0051458	corticotropin secretion	10/21092	0.040499085	0.389337206	0.366605554	Crhbp	1
GO:0051764	actin crosslink formation	10/21092	0.040499085	0.389337206	0.366605554	Baiap2l1	1
GO:0072070	loop of Henle development	10/21092	0.040499085	0.389337206	0.366605554	Hes5	1
GO:0072173	metanephric tubule morphogenesis	10/21092	0.040499085	0.389337206	0.366605554	Hes5	1
GO:0090343	positive regulation of cell aging	10/21092	0.040499085	0.389337206	0.366605554	Cgas	1
GO:1905456	regulation of lymphoid progenitor cell differentiation	10/21092	0.040499085	0.389337206	0.366605554	Hes5	1
GO:2000980	regulation of inner ear receptor cell differentiation	10/21092	0.040499085	0.389337206	0.366605554	Hes5	1
GO:0006473	protein acetylation	184/21092	0.040625775	0.389337206	0.366605554	Morf4l1/Nos1/Piwil2	3
GO:0070838	divalent metal ion transport	457/21092	0.040686115	0.389337206	0.366605554	Gnb5/Wfs1/Nos1/Atp2c1/Ibtk	5
GO:0071277	cellular response to calcium ion	78/21092	0.041264605	0.389337206	0.366605554	Crhbp/Syt12	2
GO:0072511	divalent inorganic cation transport	460/21092	0.041650992	0.389337206	0.366605554	Gnb5/Wfs1/Nos1/Atp2c1/Ibtk	5
GO:0043279	response to alkaloid	79/21092	0.042225339	0.389337206	0.366605554	Crhbp/Nos1	2

GO:0048708	astrocyte differentiation	79/21092	0.042225339	0.389337206	0.366605554	Sox6/Hes5	2
GO:0007218	neuropeptide signaling pathway	80/21092	0.043194454	0.389337206	0.366605554	Npy/Cort	2
GO:0008544	epidermis development	321/21092	0.04385706	0.389337206	0.366605554	Cd109/Ptch2/Atp2c1/Hes5	4
GO:0015748	organophosphate ester transport	81/21092	0.044171866	0.389337206	0.366605554	Stard10/Slc35b2	2
GO:0030203	glycosaminoglycan metabolic process	81/21092	0.044171866	0.389337206	0.366605554	Pxylp1/Itih3	2
GO:0032436	positive regulation of proteasomal ubiquitin-dependent protein catabolic process	81/21092	0.044171866	0.389337206	0.366605554	Socs5/Hspa1b	2
GO:0002756	MyD88-independent toll-like receptor signaling pathway	11/21092	0.044458699	0.389337206	0.366605554	Lrrfip2	1
GO:0006527	arginine catabolic process	11/21092	0.044458699	0.389337206	0.366605554	Nos1	1
GO:0009125	nucleoside monophosphate catabolic process	11/21092	0.044458699	0.389337206	0.366605554	Nt5e	1
GO:0048664	neuron fate determination	11/21092	0.044458699	0.389337206	0.366605554	Hes5	1
GO:0070944	neutrophil mediated killing of bacterium	11/21092	0.044458699	0.389337206	0.366605554	Tusc2	1
GO:0086103	G protein-coupled receptor signaling pathway involved in heart process	11/21092	0.044458699	0.389337206	0.366605554	Nos1	1
GO:0097264	self proteolysis	11/21092	0.044458699	0.389337206	0.366605554	Tmprss6	1
GO:2000615	regulation of histone H3-K9 acetylation	11/21092	0.044458699	0.389337206	0.366605554	Piwil2	1
GO:0072521	purine-containing compound metabolic process	469/21092	0.044628846	0.389337206	0.366605554	Guca1b/Nt5e/Guca1a/Nos1/Cox7a2	5
GO:0048524	positive regulation of viral process	82/21092	0.045157492	0.389337206	0.366605554	Ppib/Trim21	2
GO:0019058	viral life cycle	193/21092	0.045713446	0.389337206	0.366605554	Ppib/Trim21/Nectin1	3
GO:0044782	cilium organization	326/21092	0.045963204	0.389337206	0.366605554	Poc1a/Mns1/Gmnc/Ulk4	4
GO:0048469	cell maturation	194/21092	0.046297442	0.389337206	0.366605554	Bfsp2/Tusc2/Hes5	3
GO:0006862	nucleotide transport	12/21092	0.048402159	0.389337206	0.366605554	Slc35b2	1
GO:0043970	histone H3-K9 acetylation	12/21092	0.048402159	0.389337206	0.366605554	Piwil2	1

GO:0045625	regulation of T-helper 1 cell differentiation	12/21092	0.048402159	0.389337206	0.366605554	Socs5	1
GO:0070986	left/right axis specification	12/21092	0.048402159	0.389337206	0.366605554	Mns1	1
GO:2000674	regulation of type B pancreatic cell apoptotic process	12/21092	0.048402159	0.389337206	0.366605554	Wfs1	1
GO:1902115	regulation of organelle assembly	199/21092	0.049272929	0.389337206	0.366605554	Mns1/Nprl2/Hspa1b	3

Supp. Table S15. List of Biological Processes (BP) at FDR 5% - cerebral cortex

GO ID	Description	BgRatio	pvalue	p.adjust	qvalue	geneID	Count
GO:0003433	chondrocyte development involved in endochondral bone morphogenesis	21/21092	0.000615719	0.139820453	0.11902696	Poc1a/Col12a1	2
GO:0003418	growth plate cartilage chondrocyte differentiation	22/21092	0.000676543	0.139820453	0.11902696	Poc1a/Col12a1	2
GO:0120034	positive regulation of plasma membrane bounded cell projection assembly	106/21092	0.000846561	0.139820453	0.11902696	Mns1/Zmynd10/Rhoq	3
GO:0003413	chondrocyte differentiation involved in endochondral bone morphogenesis	28/21092	0.001099759	0.139820453	0.11902696	Poc1a/Col12a1	2
GO:0045724	positive regulation of cilium assembly	28/21092	0.001099759	0.139820453	0.11902696	Mns1/Zmynd10	2
GO:0070306	lens fiber cell differentiation	29/21092	0.001179919	0.139820453	0.11902696	Bfsp2/Ntrk3	2
GO:0003417	growth plate cartilage development	36/21092	0.001816821	0.154604889	0.131612719	Poc1a/Col12a1	2
GO:0006739	NADP metabolic process	36/21092	0.001816821	0.154604889	0.131612719	Me1/Cyb5r4	2
GO:0007601	visual perception	145/21092	0.002083607	0.154604889	0.131612719	Guca1b/Bfsp2/Cacna2d4	3
GO:0050953	sensory perception of light stimulus	149/21092	0.002251264	0.154604889	0.131612719	Guca1b/Bfsp2/Cacna2d4	3
GO:0003416	endochondral bone growth	43/21092	0.002584086	0.154604889	0.131612719	Poc1a/Col12a1	2
GO:0002063	chondrocyte development	44/21092	0.002704155	0.154604889	0.131612719	Poc1a/Col12a1	2
GO:0098868	bone growth	45/21092	0.002826812	0.154604889	0.131612719	Poc1a/Col12a1	2
GO:0060351	cartilage development involved in endochondral bone morphogenesis	51/21092	0.003616605	0.173279586	0.147510196	Poc1a/Col12a1	2

GO:0009583	detection of light stimulus	52/21092	0.003757129	0.173279586	0.147510196	Guca1b/Cacna2d4	2
GO:0120032	regulation of plasma membrane bounded cell projection assembly	183/21092	0.004019105	0.173279586	0.147510196	Mns1/Zmynd10/Rhoq	3
GO:0060491	regulation of cell projection assembly	185/21092	0.004143112	0.173279586	0.147510196	Mns1/Zmynd10/Rhoq	3
GO:1902017	regulation of cilium assembly	58/21092	0.004652825	0.183786586	0.156454641	Mns1/Zmynd10	2
GO:1902115	regulation of organelle assembly	199/21092	0.005076661	0.189973992	0.161721882	Mns1/Zmynd10/Ntrk3	3
GO:0060348	bone development	220/21092	0.00669866	0.22492988	0.191479282	Poc1a/Col12a1/Ppib	3
GO:0002088	lens development in camera-type eye	70/21092	0.006708555	0.22492988	0.191479282	Bfsp2/Ntrk3	2
GO:0007422	peripheral nervous system development	73/21092	0.007276213	0.22492988	0.191479282	Ntrk3/Egr3	2
GO:0060350	endochondral bone morphogenesis	73/21092	0.007276213	0.22492988	0.191479282	Poc1a/Col12a1	2
GO:1902117	positive regulation of organelle assembly	78/21092	0.008268942	0.231551969	0.197116562	Mns1/Zmynd10	2
GO:0031346	positive regulation of cell projection organization	462/21092	0.00847536	0.231551969	0.197116562	Mns1/Zmynd10/Ntrk3/Rhoq	4
GO:0120031	plasma membrane bounded cell projection assembly	493/21092	0.010583125	0.231551969	0.197116562	Mns1/Poc1a/Zmynd10/Rhoq	4
GO:0006140	regulation of nucleotide metabolic process	97/21092	0.012556103	0.231551969	0.197116562	Guca1b/Me1	2
GO:0060271	cilium assembly	301/21092	0.015630743	0.231551969	0.197116562	Mns1/Poc1a/Zmynd10	3
GO:0060349	bone morphogenesis	115/21092	0.017332275	0.231551969	0.197116562	Poc1a/Col12a1	2
GO:0010825	positive regulation of centrosome duplication	10/21092	0.017408049	0.231551969	0.197116562	Poc1a	1
GO:0031282	regulation of guanylate cyclase activity	10/21092	0.017408049	0.231551969	0.197116562	Guca1b	1
GO:0002062	chondrocyte differentiation	116/21092	0.017617071	0.231551969	0.197116562	Poc1a/Col12a1	2
GO:0002756	MyD88-independent toll-like receptor signaling pathway	11/21092	0.019132549	0.231551969	0.197116562	Lrrfip2	1
GO:0007128	meiotic prophase I	11/21092	0.019132549	0.231551969	0.197116562	Mlh1	1
GO:0019227	neuronal action potential propagation	11/21092	0.019132549	0.231551969	0.197116562	Ntrk3	1
GO:0048680	positive regulation of axon regeneration	11/21092	0.019132549	0.231551969	0.197116562	Ntrk3	1

GO:0051324	prophase	11/21092	0.019132549	0.231551969	0.197116562	Mlh1	1
GO:0098870	action potential propagation	11/21092	0.019132549	0.231551969	0.197116562	Ntrk3	1
GO:0044782	cilium organization	326/21092	0.019289759	0.231551969	0.197116562	Mns1/Poc1a/Zmynd10	3
GO:0009582	detection of abiotic stimulus	125/21092	0.020269212	0.231551969	0.197116562	Guca1b/Cacna2d4	2
GO:0034763	negative regulation of transmembrane transport	125/21092	0.020269212	0.231551969	0.197116562	Gnb5/Rhoq	2
GO:0009581	detection of external stimulus	126/21092	0.020573645	0.231551969	0.197116562	Guca1b/Cacna2d4	2
GO:0000279	M phase	12/21092	0.020854104	0.231551969	0.197116562	Mlh1	1
GO:0070572	positive regulation of neuron projection regeneration	12/21092	0.020854104	0.231551969	0.197116562	Ntrk3	1
GO:0070986	left/right axis specification	12/21092	0.020854104	0.231551969	0.197116562	Mns1	1
GO:0098762	meiotic cell cycle phase	12/21092	0.020854104	0.231551969	0.197116562	Mlh1	1
GO:0098764	meiosis I cell cycle phase	12/21092	0.020854104	0.231551969	0.197116562	Mlh1	1
GO:0062012	regulation of small molecule metabolic process	340/21092	0.02152968	0.231551969	0.197116562	Guca1b/Elovl5/Me1	3
GO:0006596	polyamine biosynthetic process	13/21092	0.022572718	0.231551969	0.197116562	Amd2	1
GO:0016446	somatic hypermutation of immunoglobulin genes	13/21092	0.022572718	0.231551969	0.197116562	Mlh1	1
GO:0042492	gamma-delta T cell differentiation	13/21092	0.022572718	0.231551969	0.197116562	Egr3	1
GO:0042761	very long-chain fatty acid biosynthetic process	13/21092	0.022572718	0.231551969	0.197116562	Elovl5	1
GO:0045141	meiotic telomere clustering	13/21092	0.022572718	0.231551969	0.197116562	Mlh1	1
GO:0002566	somatic diversification of immune receptors via somatic mutation	14/21092	0.024288398	0.231551969	0.197116562	Mlh1	1
GO:0030497	fatty acid elongation	14/21092	0.024288398	0.231551969	0.197116562	Elovl5	1
GO:0036159	inner dynein arm assembly	14/21092	0.024288398	0.231551969	0.197116562	Zmynd10	1
GO:0046607	positive regulation of centrosome cycle	14/21092	0.024288398	0.231551969	0.197116562	Poc1a	1
GO:0070307	lens fiber cell development	14/21092	0.024288398	0.231551969	0.197116562	Bfsp2	1

GO:0090220	chromosome localization to nuclear envelope involved in homologous chromosome segregation	14/21092	0.024288398	0.231551969	0.197116562	Mlh1	1
GO:0099151	regulation of postsynaptic density assembly	14/21092	0.024288398	0.231551969	0.197116562	Ntrk3	1
GO:0046496	nicotinamide nucleotide metabolic process	142/21092	0.025701212	0.231551969	0.197116562	Me1/Cyb5r4	2
GO:0033089	positive regulation of T cell differentiation in thymus	15/21092	0.026001147	0.231551969	0.197116562	Egr3	1
GO:0034397	telomere localization	15/21092	0.026001147	0.231551969	0.197116562	Mlh1	1
GO:0044827	modulation by host of viral genome replication	15/21092	0.026001147	0.231551969	0.197116562	Ppib	1
GO:0048304	positive regulation of isotype switching to IgG isotypes	15/21092	0.026001147	0.231551969	0.197116562	Mlh1	1
GO:1901386	negative regulation of voltage-gated calcium channel activity	15/21092	0.026001147	0.231551969	0.197116562	Gnb5	1
GO:0019362	pyridine nucleotide metabolic process	144/21092	0.026375309	0.231551969	0.197116562	Me1/Cyb5r4	2
GO:0042552	myelination	146/21092	0.027056585	0.231551969	0.197116562	Ntrk3/S100b	2
GO:0003414	chondrocyte morphogenesis involved in endochondral bone morphogenesis	16/21092	0.027710971	0.231551969	0.197116562	Col12a1	1
GO:0003429	growth plate cartilage chondrocyte morphogenesis	16/21092	0.027710971	0.231551969	0.197116562	Col12a1	1
GO:0043968	histone H2A acetylation	16/21092	0.027710971	0.231551969	0.197116562	Morf4l1	1
GO:0044794	positive regulation by host of viral process	16/21092	0.027710971	0.231551969	0.197116562	Ppib	1
GO:0046629	gamma-delta T cell activation	16/21092	0.027710971	0.231551969	0.197116562	Egr3	1
GO:0090171	chondrocyte morphogenesis	16/21092	0.027710971	0.231551969	0.197116562	Col12a1	1
GO:1904889	regulation of excitatory synapse assembly	16/21092	0.027710971	0.231551969	0.197116562	Ntrk3	1
GO:2001015	negative regulation of skeletal muscle cell differentiation	16/21092	0.027710971	0.231551969	0.197116562	S100b	1
GO:0007272	ensheathment of neurons	149/21092	0.028091837	0.231551969	0.197116562	Ntrk3/S100b	2

GO:0008360	regulation of cell shape	149/21092	0.028091837	0.231551969	0.197116562	Rhoq/S100b	2
GO:0008366	axon ensheathment	149/21092	0.028091837	0.231551969	0.197116562	Ntrk3/S100b	2
GO:0072524	pyridine-containing compound metabolic process	149/21092	0.028091837	0.231551969	0.197116562	Me1/Cyb5r4	2
GO:0003422	growth plate cartilage morphogenesis	17/21092	0.029417874	0.231551969	0.197116562	Col12a1	1
GO:0036158	outer dynein arm assembly	17/21092	0.029417874	0.231551969	0.197116562	Zmynd10	1
GO:1904469	positive regulation of tumor necrosis factor secretion	17/21092	0.029417874	0.231551969	0.197116562	Lrrfip2	1
GO:0000712	resolution of meiotic recombination intermediates	18/21092	0.031121862	0.231551969	0.197116562	Mlh1	1
GO:0006595	polyamine metabolic process	18/21092	0.031121862	0.231551969	0.197116562	Amd2	1
GO:0009309	amine biosynthetic process	18/21092	0.031121862	0.231551969	0.197116562	Amd2	1
GO:0031643	positive regulation of myelination	18/21092	0.031121862	0.231551969	0.197116562	S100b	1
GO:0042401	cellular biogenic amine biosynthetic process	18/21092	0.031121862	0.231551969	0.197116562	Amd2	1
GO:0048302	regulation of isotype switching to IgG isotypes	18/21092	0.031121862	0.231551969	0.197116562	Mlh1	1
GO:0048712	negative regulation of astrocyte differentiation	18/21092	0.031121862	0.231551969	0.197116562	Ntrk3	1
GO:0050650	chondroitin sulfate proteoglycan biosynthetic process	18/21092	0.031121862	0.231551969	0.197116562	Pxylp1	1
GO:0099150	regulation of postsynaptic specialization assembly	18/21092	0.031121862	0.231551969	0.197116562	Ntrk3	1
GO:0150052	regulation of postsynapse assembly	18/21092	0.031121862	0.231551969	0.197116562	Ntrk3	1
GO:0006733	oxidoreduction coenzyme metabolic process	160/21092	0.03202188	0.231551969	0.197116562	Me1/Cyb5r4	2
GO:0048291	isotype switching to IgG isotypes	19/21092	0.032822939	0.231551969	0.197116562	Mlh1	1
GO:1905874	regulation of postsynaptic density organization	19/21092	0.032822939	0.231551969	0.197116562	Ntrk3	1
GO:2000251	positive regulation of actin cytoskeleton reorganization	19/21092	0.032822939	0.231551969	0.197116562	Ntrk3	1

GO:0007051	spindle organization	166/21092	0.034252067	0.231551969	0.197116562	Poc1a/Mlh1	2
GO:0043271	negative regulation of ion transport	166/21092	0.034252067	0.231551969	0.197116562	Gnb5/Plcb4	2
GO:0002755	MyD88-dependent toll-like receptor signaling pathway	20/21092	0.034521109	0.231551969	0.197116562	Lrrfip2	1
GO:0010560	positive regulation of glycoprotein biosynthetic process	20/21092	0.034521109	0.231551969	0.197116562	Pxylp1	1
GO:0022403	cell cycle phase	20/21092	0.034521109	0.231551969	0.197116562	Mlh1	1
GO:0032148	activation of protein kinase B activity	20/21092	0.034521109	0.231551969	0.197116562	Ntrk3	1
GO:0046325	negative regulation of glucose import	20/21092	0.034521109	0.231551969	0.197116562	Rhoq	1
GO:0050908	detection of light stimulus involved in visual perception	20/21092	0.034521109	0.231551969	0.197116562	Cacna2d4	1
GO:0050962	detection of light stimulus involved in sensory perception	20/21092	0.034521109	0.231551969	0.197116562	Cacna2d4	1
GO:0015012	heparan sulfate proteoglycan biosynthetic process	21/21092	0.036216379	0.24065276	0.204863923	Pxylp1	1
GO:0000289	nuclear-transcribed mRNA poly(A) tail shortening	22/21092	0.037908752	0.24065288	0.204864026	Mlh1	1
GO:0000413	protein peptidyl-prolyl isomerization	22/21092	0.037908752	0.24065288	0.204864026	Ppib	1
GO:0045723	positive regulation of fatty acid biosynthetic process	22/21092	0.037908752	0.24065288	0.204864026	Elovl5	1
GO:0097107	postsynaptic density assembly	22/21092	0.037908752	0.24065288	0.204864026	Ntrk3	1
GO:1903020	positive regulation of glycoprotein metabolic process	22/21092	0.037908752	0.24065288	0.204864026	Pxylp1	1
GO:0060972	left/right pattern formation	23/21092	0.039598233	0.244743578	0.208346372	Mns1	1
GO:1903077	negative regulation of protein localization to plasma membrane	23/21092	0.039598233	0.244743578	0.208346372	Rhoq	1
GO:0006298	mismatch repair	25/21092	0.042968541	0.244743578	0.208346372	Mlh1	1
GO:0007289	spermatid nucleus differentiation	25/21092	0.042968541	0.244743578	0.208346372	Pygo1	1

GO:0010829	negative regulation of glucose transmembrane transport	25/21092	0.042968541	0.244743578	0.208346372	Rhoq	1
GO:0044788	modulation by host of viral process	25/21092	0.042968541	0.244743578	0.208346372	Ppib	1
GO:1904376	negative regulation of protein localization to cell periphery	25/21092	0.042968541	0.244743578	0.208346372	Rhoq	1
GO:0006312	mitotic recombination	26/21092	0.044649377	0.244743578	0.208346372	Mlh1	1
GO:0030201	heparan sulfate proteoglycan metabolic process	26/21092	0.044649377	0.244743578	0.208346372	Pxylp1	1
GO:0048642	negative regulation of skeletal muscle tissue development	26/21092	0.044649377	0.244743578	0.208346372	S100b	1
GO:0050927	positive regulation of positive chemotaxis	26/21092	0.044649377	0.244743578	0.208346372	Ntrk3	1
GO:1901020	negative regulation of calcium ion transmembrane transporter activity	26/21092	0.044649377	0.244743578	0.208346372	Gnb5	1
GO:1904861	excitatory synapse assembly	26/21092	0.044649377	0.244743578	0.208346372	Ntrk3	1
GO:0035987	endodermal cell differentiation	27/21092	0.04632734	0.244743578	0.208346372	Col12a1	1
GO:0050926	regulation of positive chemotaxis	27/21092	0.04632734	0.244743578	0.208346372	Ntrk3	1
GO:0060536	cartilage morphogenesis	27/21092	0.04632734	0.244743578	0.208346372	Col12a1	1
GO:1904467	regulation of tumor necrosis factor secretion	27/21092	0.04632734	0.244743578	0.208346372	Lrrfip2	1
GO:1990774	tumor necrosis factor secretion	27/21092	0.04632734	0.244743578	0.208346372	Lrrfip2	1
GO:0051307	meiotic chromosome separation	28/21092	0.048002435	0.244743578	0.208346372	Mlh1	1
GO:0042168	heme metabolic process	29/21092	0.049674668	0.244743578	0.208346372	Cyb5r4	1
GO:0046039	GTP metabolic process	29/21092	0.049674668	0.244743578	0.208346372	Rhoq	1
GO:0050654	chondroitin sulfate proteoglycan metabolic process	29/21092	0.049674668	0.244743578	0.208346372	Pxylp1	1
GO:0098698	postsynaptic specialization assembly	29/21092	0.049674668	0.244743578	0.208346372	Ntrk3	1

GO:0006302	double-strand break repair	204/21092	0.049694819	0.244743578	0.208346372	Mlh1/Morf4l1	2

Appendix: Consortia and networks involved in this study

The Synaptopathies and Paroxysmal Syndromes (SYNaPS) Study Group (http://neurogenetics.co.uk/synaptopathies-synaps/)

Study Group Members:

Prof Stanislav Groppa

Affiliation: Department of Neurology and Neurosurgery, Institute of Emergency Medicine, Chisinau, Republic of Moldova.

Email: sgroppa@gmail.com

Dr. Blagovesta Marinova Karashova

Affiliation: Department of Paediatrics, Medical University of Sofia, Sofia 1431, Bulgaria

Email: blagovestakarashova@gmail.com

Dr. Wolfgang Nachbauer

Affiliation: Department of Neurology, Medical University Innsbruck, Anichstrasse 35, Innsbruck 6020, Austria

Email: Wolfgang.Nachbauer@i-med.ac.at

Prof. Sylvia Boesch

Affiliation: Department of Neurology, Medical University Innsbruck, Anichstrasse 35, Innsbruck 6020, Austria

Email: sylvia.boesch@i-med.ac.at

Dr. Larissa Arning

Affiliation: Department of Human Genetics, Ruhr-University Bochum, Bochum 44801, Germany

Email: Larissa.Arning@ruhr-uni-bochum.de

Prof. Dagmar Timmann

Affiliation: Braun Neurologische Universitätsklinik Universität Essen, Hufelandstr 55, Essen D-45122, Germany

Email: Dagmar.Timmann-Braun@uni-duisburg-essen.de

Prof. Bru Cormand

Affiliation: Department of Genetics, Universitat de Barcelona, Barcelona 08007, Spain

Email: bcormand@ub.edu

Dr. Belen Pérez-Dueñas

Affiliation: Hospital Sant Joan de Deu, Esplugues de Llobregat 08950, Barcelona, Spain

Email: bperez@sjdhospitalbarcelona.org

Dr Gabriella Di Rosa, MD, PhD

Affiliation: Department of Pediatrics, University of Messina, Messina 98123, Italy

Email: gdirosa@unime.it

Prof. Jatinder S. Goraya, MD, FRCP

Affiliation: Division of Paediatric Neurology, Dayanand Medical College & Hospital, Ludhiana, Punjab 141001, India

Email: gorayajs@gmail.com

Prof. Tipu Sultan

Affiliation: Division of Paediatric Neurology, Children's Hospital of Lahore, Lahore 381-D/2, Pakistan

Email: tipusultanmalik@hotmail.com

Prof Jun Mine

Affiliation: Department of Paediatrics, Shimane University, Faculty of Medicine, Izumo, 693-8501, Japan

Email: jmine@med.shimane-u.ac.jp

Prof. Daniela Avdjieva,

Affiliation: Department of Paediatrics, Medical University of Sofia, Sofia 1431, Bulgaria

Email: davdjieva@yahoo.com

Dr. Hadil Kathom,

Affiliation: Department of Pediatrics, Medical University of Sofia, Sofia 1431, Bulgaria

Email: hadilmk@gmail.com

Prof.Dr Radka Tincheva

Affiliation: Head of Department of Clinical Genetics, University Pediatric Hospital, Sofia 1431, Bulgaria

Email: radka.tincheva@gmail.com

Prof. Selina Banu

Affiliation: Neurosciences Unit, Institute of Child Health and Shishu Shastho Foundation Hospital, Mirpur, Dhaka 1216, Bangladesh

Email: selinabanu17@gmail.com

Prof. Mercedes Pineda-Marfa

Affiliation Servei de Neurologia Pediàtrica, l'Hospital Universitari Vall d'Hebron, Barcelona 08035, Spain

Email: pineda@hsjdbcn.org

Prof. Pierangelo Veggiotti

Affiliation: Unit of Infantile Neuropsychiatry Fondazione

Istituto Neurologico "C. Mondino" IRCCS, Via Mondino 2, Pavia 27100, Italy

Email: pierangelo.veggiotti@unipv.it

Prof. Michel D. Ferrari

Affiliation: Leiden University Medical Center, Albinusdreef 2, Leiden 2333, Netherlands

Email: M.D.Ferrari@lumc.nl

Prof. Alberto Verrotti

Affiliation: University of L'Aquila, L'Aquila, Italy

Email: verrottidipianella@univaq.it

Prof Giangluigi Marseglia

Affiliation: Department of Pediatrics, University of Pavia, IRCCS Policlinico "San Matteo", Pavia 27100, Italy

Email: gl.marseglia@smatteo.pv.it

Dr. Salvatore Savasta

Affiliation: Division of Pediatric Neurology, Department of Pediatrics, University of Pavia, IRCCS Policlinico "San Matteo", Pavia 27100, Italy

Email: S.Savasta@smatteo.pv.it

Dr. Mayte García-Silva

Affiliation: Hospital Universitario 12 de Octubre, Madrid 28041, Spain

Email: mgarciasilva@salud.madrid.org

Dr. Alfons Macaya Ruiz

Affiliation: University Hospital Vall d'Hebron, Barcelona 08035, Spain

Email: amacaya@vhebron.net

Prof. Barbara Garavaglia

Affiliation: IRCCS Foundation, Neurological Institute “Carlo Besta”, Molecular Neurogenetics, 20126 Milan, Italy

Email: segr.neurogenetica@istituto-besta.it

Dr. Eugenia Borgione

Affiliation: Laboratorio di Neuropatologia Clinica, U.O.S. Malattie, Neuromuscolari Associazione OASI Maria SS. ONLUS – IRCCS, Via Conte Ruggero 73, 94018 Troina, Italy

Email: eborgione@oasi.en.it

Dr. Simona Portaro

Affiliation: IRCCS Centro Neurolesi "Bonino Pulejo", SS113, c.da Casazza, 98124 Messina, Italy

Email: simonaportaro@hotmail.it

Dr. Benigno Monteagudo Sanchez

Affiliation: Hospital Arquitecto Marcide, Avenida de la Residencia S/N, Ferrol (A Coruña), 15401 Spain

Email: benims@hotmail.com

Dr. Richard Boles

Affiliation: Courtagen Life Sciences, 12 Gill Street Suite 3700, Woburn, MA 01801 USA

Email: Richard.Boles@courtagen.com

Prof. Savvas Papacostas

Affiliation: Neurology Clinic B, The Cyprus Institute of Neurology and Genetics, 6 International Airport Road, 1683 Nicosia, Cyprus

Email: savvas@cing.ac.cy

Dr. Michail Vikelis

Affiliation: Iatreio Kefalalgias Glyfadas, 8 Lazaraki str, 3rd floor, 16675, Athens, Greece

Email: mvikelis@headaches.gr

Prof Eleni Zamba Papanicolaou

Affiliation: The Cyprus Institute of Neurology & Genetics, Nicosia, Cyprus

Email: ezamba@cing.ac.cy

Dr Efthymios Dardiotis

Affiliation: UNIVERSITY HOSPITAL OF LARISSA, NEUROLOGY Department, Greece

Email: edar@med.uth.gr

Prof Shazia Maqbool

Affiliation: Department of Developmental and Behavioral Pediatrics, CH&ICH, Lahore, Pakistan

Email: drshazimaq@yahoo.com

Prof Shahnaz Ibrahim

Affiliation: Department of Pediatrics and child health, Aga Khan University, Karachi, Pakistan

Email: shahnaz.ibrahim@aku.edu

Prof Salman Kirmani

Affiliation: Department of Paediatrics & Child Health, The Aga Khan University, Karachi , Pakistan

Email: salman.kirmani@aku.edu

Dr. Nuzhat Noureen Rana

Affiliation: Department of Paediatric Neurology, Children Hospital Complex and ICH, Multan, Pakistan

Email: drnuzhatrana@gmail.com

Dr. Osama Atawneh

Affiliation: Hilal Pediatric Hospital Hebron, Hebron West Bank, Palestine

Email: osamaat@gmail.com

Prof George Koutsis

Dr Marianthi Breza

Affiliation: Neurogenetics Unit, Neurology Department, Eginition Hospital, National and Kapodistrian University, Athens, Greece

Email: marianthibr@med.uoa.gr

Prof Salvatore Mangano

Affiliation: Unità di Neuropsichiatria Infantile, AOUP "P.Giaccone" Palermo, Italy

Email: salvatore.mangano@unipa.it

Dr Carmela Scuderi

Affiliation: Associazione Oasi Maria SS, 94018 Troina, Italy

Email: cscuderi@oasi.en.it

Dr Eugenia Borgione

Affiliation: Associazione Oasi Maria SS, 94018 Troina, Italy

Email: eborgione@oasi.en.it

Dr Giovanna Morello

Affiliation: Institute of Neurological Sciences, National Research Council, Mangone, Italy

Email: g.morello@isn.cnr.it

Dr Tanya Stojkovic

Affiliation: Institute of Myology, Hôpital La Pitié Salpêtrière, Paris, France

Email: stojkovic.tanya@aphp.fr

Prof Massimi Zollo

Affiliation: CEINGE, Biotecnologie Avanzate S.c.a.rl., Naples, Italy

Email: massimo.zollo@unina.it

Dr Gali Heimer

Affiliation: University Hospital of Tel Aviv, Tel Aviv, Israel

Email: galih.md@gmail.com

Prof Yves A. Dauvilliers

Affiliation: University Hospital Montpellier, Montpellier, France

Email: ydauvilliers@yahoo.fr

Prof Pasquale Striano

Affiliation: Institute “Giannina Gaslini”, Genova, Italy

Email: strianop@gmail.com

Dr Issam Al-Khawaja

Affiliation: Albashir University Hospital, Amman, Jordan

Email: isamkhawaja61@gmail.com

Dr Fuad Al-Mutairi

Affiliation: King Saud University, Riyadh, Saudi Arabia

Email: almutairifu@NGHA.MED.SA

Prof Hamed Sherifa

Affiliation: Assiut University Hospital, Assiut, Egypt

Email: hamed_sherifa@yahoo.com